Development of Probes for Bile Acid Transporters and Synthetic Approaches to the Core of Massadine

BY

HYUNJIN LEE

B.S., University of Illinois, Urbana, Illinois, 2012

THESIS

Submitted as partial fulfillment of the requirements
for the degree of Doctor of Philosophy of Chemistry
in the Graduated College of the
University of Illinois at Chicago, 2018

Chicago, Illinois

Defense Committee:

Daesung Lee, Advisor and Chair, Chemistry
Duncan Wardrop, Chemistry
Laura Anderson, Chemistry
Justin T. Mohr, Chemistry
Waddha Alrefai, College of Medicine

ACKNOWLEDGEMENTS

First of all, I would like to express my deepest gratitude to my advisor, Professor Daesung Lee, for his support and the opportunity to grow as a scientist for the past five years. Professor Lee has been an example of an excellent chemist and truly inspirational to me. I am sincerely grateful to join his lab working and learning under his unparalleled guidance during my Ph.D.

I would like to sincerely thank my committee members, Professor Duncan Wardrop, Professor Laura Anderson and Professor Justin T. Mohr from the Department of Chemistry, and Professor Waddah Alrefai from the Department of Medicine for their time, encouragement, advice which directed my graduate research in a right trajectory.

I am grateful for all of wonderful Lee's group members. I would like to thank all of the senior graduate students who trained me and influenced in my research positively: Dr. Phani Mamidipalli, Dr. Matthew J. O'Connor, Dr. Venkata Reddy Sabassani, Dr. Rajdip Karmakar. I especially acknowledge Dr. Venkata Reddy Sabassani for his time and help to train me in my first year. I would like to thank all of the junior members: Sourav Ghorai, Saswata Gupta, Anh Le and Siyuan Su. Thank you all for being so wonderful to work with.

I am grateful for working with the Alrefai lab, UIC College of Medicine. I would especially thank Professor Waddah Alrefai and Alexander Ticho for the remarkable collaboration. I was fortunate to have the chance to work for the probe design project which allowed me to gain a lot of bioassay backgrounds.

I would like to thank Dr. Danielle Gray from X-ray crystallography lab at UIUC for your encouragement to continue my study in chemistry and introduction to chemistry research.

I would like to thank graduate Women in Chemistry (gWiCh) board members, Dr. Victoria Helan, Mi Nguyen, Lianyan Xu and Audra Lamley and all other female graduate students who were/are involved in gWiCh team.

Also, UIC has wonderful female faculty members who serve as role models to look up to. I am grateful to Professor Laura Anderson, Professor Stephanie Cologna, Professor Laura Sanchez, Professor Leslie Fung, Dr. Alyssa Haynes for their mentorship and for their support to create an empowering community among all female graduate students in Department of Chemistry.

I would also like to thank our administrative office members, Ms. Rhonda Staudohar, Ms. Silvia Solis and Ms. Maggie Shortall for all of their support to make a chemistry department community strong.

To my family: my mom Inok Chang, my dad Kyungup Lee, my older sisters Hyunah Lee, my younger sister Hyunjung Lee, aunt Hyeonsuk Sue Boyce and uncle Robert Boyce. Thank you for your unconditional support and love.

Last but not least, I would like to thank my fiancé Eric Chen for his tremendous support throughout the years. I am looking forward to starting a new chapter and adventure with you.

HJL

2018 in Chicago

CONTRIBUTION OF AUTHORS

Chapter I represents a published paper (Ticho, A. L.; Lee, H.; Gill, R. K.; Dudeja, P. K.; Saksena, S.; Lee, D.; Alrefai, W. A. *Am. J. Physiol. Gastrointest. Liver Physiol*. **2018**, doi: 10.1152/ajpgi.00133.2018) for which I am a co-author with Alexander Ticho. Design of probes proposed by Professor Waddah Alrefai and Alexander Ticho and all synthesis has been carried out by me. The bioassay portion is completed by the Alrefai lab. This chapter contains both the published and unpublished works. Chapter III represents a published paper (Sun, C.; Lee, H.; Lee, D. *Org. Lett*. **2015**, *17*, 5348–5351) and an unpublished work. The racemic and enantioselective synthetic routes toward carbocycle core of massadine was proposed and developed by Professor Lee and Dr. Chunrui Sun. For racemic version, I repeated all reactions to acquire spectral data and optimized reaction conditions. I have played a role in the writing of the manuscript. An enantioselective synthetic route has been revised by Professor Daesung Lee and myself. I have carried out the all experiments.

DEDICATION

I dedicate this thesis to the memories of my grandmother, Jongmook Hong (February 25th 1925-August 6th 2018) who shaped my outlook on life. I am eternally grateful.

TABLE OF CONTENTS

PART I

STUDIES ON PROBE SYNTHESIS OF BILE ACID AND CHOLESTEROL TRANSPORTERS

Part II

SYNTHESIS OF THE CARBOCYCLE CORE OF MASSADINE

LIST OF SCHEMES

LIST OF SCHEMES (continued)

LIST OF FIGURES

LIST OF FIGURES (continued)

LIST OF TABLES

LIST OF ABBREVIATION

Ac	Acetyl
amF	Aminofluorescein
ASBT	Apical sodium-dependent bile acid transporter
ATP	Adenosine triphosphate
BA	Bile acid
BLI	Bioluminescence imaging
Bn	Benzyl
BOM	Benzyloxymethyl
^{13}C NMR	Carbon-13 nuclear magnetic resonance
CA	Cholic acid
Cbz	Carbobenzyloxy
CCD	Charge-coupled device
CDCA	Deoxycholic acid
CFL	Compact fluorescent lamp
CHO	Chinese hamster ovary
CT	Computed tomography
DBU	1,8-Diazabicyclo[5.4.0]undec-7-ene
DCC	Dicyclohexylcarbodiimide
DCE	Dichloroethane
DCM	Dichloromethane
DIBAL	Diisobutylaluminum hydride

DIPEA	*N,N*-Diisopropylethylamine
DMAP	4-Dimethylaminopyridine
DMDO	Dimethyldioxirane
DMF	Dimethylformamide
DMP	Dimethoxypropane
DMSO	Dimethyl sulfoxide
dr	Diastereomeric ratio
2,6-DTBP	2,6-Di-*tert*-butylphenol
EDC	1-Ethyl-3-(3-dimethylaminopropyl)carbodiimide
EI	Electron impact
EZE	Ezetimibe
FLuc	Firefly luciferase
Fmoc	9-Fluorenylmethoxycarbonyl
FXR	Farnesoid X Receptor
GLuc	Gaussia luciferase
GSH	Glutathione
HBTU	*N,N,N´,N´*-Tetramethyl-*O*-(1*H*-benzotriazol-1-yl)uronium hexafluorophosphate
HEK	Human embryonic kidney
HepG2	Liver hepatocellular cells
HMPA	Hexamethylphosphoramide
IBX	2-Iodoxybenzoic acid
IVIS	In vivo imaging system
J	Coupling constant

KHMDS	Postassium hexamethyldisilazide
K_m	Michaelis constant
KSCN	Potassium thiocyanate
LAH	Lithium aluminum hydride
LiHMDS	Lithium hexamethyldisilazide
Ms	Methanesulfonyl
NBD	4-Nitrobenzo-2-oxa-1,3-diazole
NBS	*N*-Bromosuccinimide
^{n}Bu	*n*-Butyl
NMO	*N*-Methylmorpholine *N*-oxide
NMR	Nuclear magnetic resonance
NTCP	Na^+ Taurocholate co-transporting polypeptide
OATP	Organic-anion-transporting polypeptide
PCC	Pyridinium chlorochromate
PET	Positron emission tomography
PPTS	Pyridinium *p*-toluenesulfonate
Pry	Pyridine
PTP	Protein tyrosine phosphatase
PTSA	*para*-Toluenesulfonic acid
RLuc	Renilla luciferase
rt	Room temperature
SERT	Serotonin transporter transfected
TBAF	Tetra-*n*-butylammonium fluoride

TBHP	*tert*-Butylhydroperoxide
TBS	*tert*-Butyldimethylsilyl
TCDC	Taurochenodeoxycholate
TEA	Triethylamine
TES	Triethylsilyl
TFA	Trifluoroacetic acid
THF	Tetrahydrofuran
TIPS	Triisopropylsilyl
TLC	Thin layer chromatography
TMEDA	*N,N,N′,N′*-tetramethylethylenediamine
TMS	Tetramethylsilane, and Trimethylsilyl
Ts	Toluensulfonyl
UDCA	Ursodeoxycholic acid

SUMMARY

This thesis contains two parts. The two chapters in Part I deal with the development of novel probes to study the activities of bile acid (BA) and cholesterol transporters by exploiting a self-cleavable disulfide linker and "click" chemistry. In the one chapter of Part II, the synthetic studies toward the racemic and enantioseletive versions of a carbocycle core of massadine is described wherein the application of a formal [3+2] cycloaddition of α,β-unsaturated esters and lithium(trimethylsilyl)diazomethane (LTMSD) is used as a key strategy.

Chapters I involves the design and development of a bile acid (BA) transporter probe for investigating BA transporter activity in real time. BA probes (BA-SS-Luc) containing a luciferin moiety connected via a disulfide cleavable linker were found to be useful tool to measure bile acid uptake in real time in vitro. For the future study, this quantitative approach will be applied to identify compounds that modulate BA transporter activity in vivo. In chapter II, an alkyne cholesterol probe and a photo-activatable alkyne-conjugated BA were developed to exploit the "click" chemistry between a terminal alkyne and suitable azides in biological system. The alkyne cholesterol was successfully exploited in Caco-2 cells for a sterol imaging with azide reporter. Further studies on a photo-activatable alkyne-conjugated BA and proteomic study with various cell lines are currently underway in collaboration with the Alrefai lab.

Chapter III deals with synthetic studies of a carbocycle core of massadine, which is a member of structurally complex dimeric pyrrole-imidazole alkaloids. Due to its unique structural diversity, complexity and significant biological activities, massadine, has been a highly sought-after target for total synthesis among many research groups. Our synthetic approach toward the synthesis of the core skeleton relies on the formal [3+2] cycloaddition between LTMSD and α,β-unsaturated esters followed by protonylitic N–N bond cleavage to construct α-amino-β-cyano

groups with excellent stereochemical control. These functional groups would act as a synthetic handle to construct the remaining structural features of massadine.

Part I

Studies on Probe Synthesis of Bile Acid and Cholesterol Transporters

Chapter 1

Synthesis of Bile Acid Transporter Probe

(Previously published as Ticho, A. L.; Lee, H.; Gill, R. K.; Dudeja, P. K.; Saksena, S.; Lee, D.; Alrefai, W. A. *Am. J. Physiol. Gastrointest. Liver Physiol*. **2018**, doi: 10.1152/ajpgi.00133.2018)

1.1. Introduction

Bile Acids (BAs) are important digestive surfactants that promote intestinal digestion and emulsification of a variety of substances such as absorption of fats, including fat-soluble vitamins, cholesterol and steroids.[1] They consist of a steroid core and a side chain where their hydrophobicity is determined by the number and position of hydroxyl groups on the steroid core. The synthesis of BAs occurs exclusively in the hepatocytes where the hydrophobic cholesterol is converted into a more water-soluble amphipathic compound. After conversion of cholesterol into BAs, the derivatives, called primary BAs, are transported into the gut where the microbiota modifies them into secondary BAs. BAs also play the role as signaling molecules regulating lipid, glucose, nucleic acid, and drug metabolism, facilitate the composition of gut microbiota, and modulation of the immune responses.[2,3] BAs are cytotoxic when present in abnormally high concentrations, therefore, regulating the concentration of BAs are critical. While BAs are an essential component of the gastrointestinal tract, their dysregulation has cytotoxic effects such as hypercholesterolemia and diarrhea. Additionally, disorders in BAs circulation have been related to neurodegenerative disorders such as Alzheimer's disease.[4]

1.1.1. Enterohepatic Circulation of BAs

BAs are synthesized in the perivenous hepatocyte where hydrophobic cholesterol is converted into water-soluble amphipathic derivatives (**Figure 1.1**). The synthesis of BAs provides the derivative with its characteristic structural and chemical properties. In the first step, cholesterol is hydroxylated by the cytochrome P450 and cholesterol 7α-hydroxylase (CYP7A1). After hydroxylation, the C_5–C_6 double bond is saturated followed by epimerization of the C_3-

hydroxyl group, and then the C_{25}–C_{27} carbon unit of the resultant is cleaved off. This hepatic synthesis of BAs represents 90% of total BA production in humans.[5]

Figure 1.1. Structure of BAs

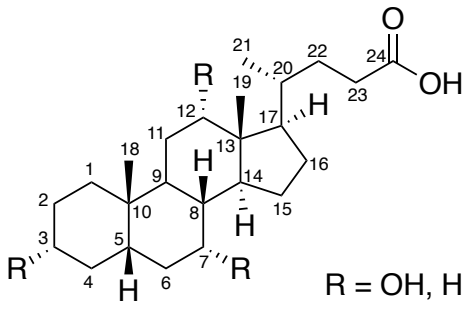

The primary derivatives of the conversion are chenodeoxycholic acid (CDCA) and cholic acid (CA). The liver cells then conjugate the primary BAs with either glycine or taurine to form, glycocholic acid, glycochenodeoxycholic acid, taurocholic acid, taurochenodeoxycholic acid. The conjugation is a critical step in the bile synthesis pathway because it imparts the primary BAs with physiologically important acid-base properties such as increased water solubility and enhanced fat emulsification. After conjugation, the BAs are transported and secreted into the small intestine via active BA transporters. In the gut, the primary BAs undergo partial dihydroxylation and deconjugation through the action of microbiota to generate secondary BAs. For instance, the CA is converted to deoxycholic acid and CDCA into lithocholic acid. The four BAs, CA, deoxycholic acid, CDCA, and lithocholic acid can undergo enterohepatic circulation (**Figure 1.2**) where the BAs are reabsorbed back into the ileum, then into the bloodstream and returned to the liver for re-secretion. This processes of synthesis, secretion, and reabsorption maintain the homeostasis of BAs.[6,7]

Figure 1.2. Enterohepatic circulation of cholesterol

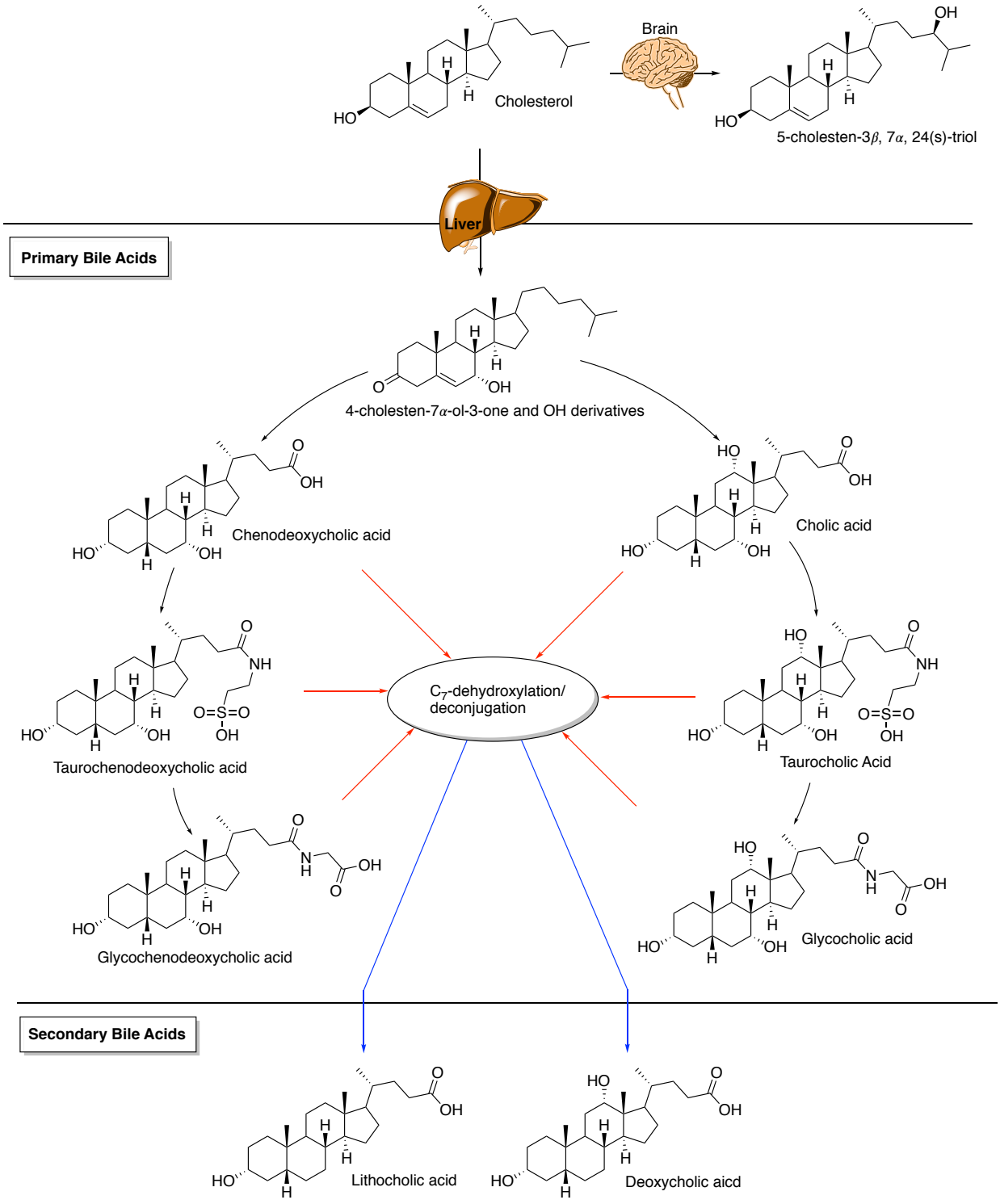

1.1.2. BA Transporters

The BAs transporters are energy-driven transport systems, which facilitate the movement of BAs across membranes of the hepatocytes and enterocytes of the enterohepatic circulation (**Figure 1.3**). In the liver, the Na^+ taurocholate co-transporting polypeptide (NTCP) with the help of sodium-dependent multi-specific organic anion transporting polypeptide transports 90% of the BAs across the hepatocytes sinusoidal membrane. At the canalicular membrane, a highly specialized transporter called the bile salt export system excretes the BAs into the bile. Following their movement with bile into the lumen of the small intestine, more than 95 % of BAs are reclaimed in the proximal small intestine, colon and the ileum by the apical sodium-dependent BA transporter (ASBT, SLC10A2).[7,8] Without the BAs transporters and hepatic enzyme-controlled mechanisms, BAs would be accumulated, which leads to primary BA diarrhea, lipid malabsorption, and steatorrhea.

Figure 1.3. Bile acid enterophepatic cycle

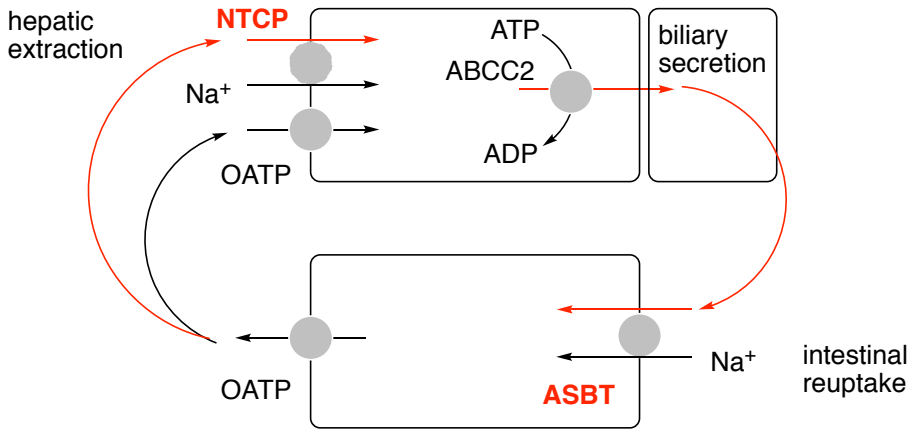

BA transporters also have an affinity for other exogenous and endogenous compounds including drugs. Moreover, the dysregulation of BAs has been linked to a number of malfunctions and diseases such gallstone disease, fatty liver disease, and liver cancer.

As such, BA transporters have been exploited as pro-drug targets and disease models with the purpose of improving drug absorption and delivery.[9]

1.1.3. Conventional Techniques to Measure BA Transporters Activity

Fluorophore-tagged and radio-labeled BAs are widely used for visualization of BA transport activity in vitro or in vivo or both. In previous studies, a number of fluorophore- and radio-labeled BAs have been synthesized and they are proven to possess similar biological properties to those of natural BAs. Versatility of these methods facilitated the early discoveries and BA transporters and characterization of their function in vitro and in vivo.[11]

1.1.3.1. Fluorophore-tagged BAs

Most well-known fluorescent dyes, aminofluorescein (amF) and 4-nitrobenzo-2-oxa-1,3-diazole (NBD) (**Figure 1.4**).[12a] These fluorescent dye-labeled BAs are employed to investigate BA uptake and distribution in cells.

Weinman and coworkers studied fluorescent probes, **CLF**, **CDC-NBD** and **C-NBD** to study BA uptake (**Figure 1.3**).[12b] All three probes mimic the natural BAs and the uptake was concentration-dependent. However, **NBD** tagged BAs, **CDC-NBD** and **C-NBD**, showed a higher affinity, lowering the Michaelis constant (k_m) value than **CLF**. Interestingly, **CLF** and **C-NBD** possess Na^+-dependent manner for the uptake but this trend was not observed with **CDC-NBD**. In other words, in the absence of Na^+, the uptake rate was decreased for **CLF** and **C-NBD** but that of **CDC-NBD** remained unchanged. This study demonstrates **C-NBD** is the most efficient tool for studying BA transporter in hepatocytes.

Figure 1.4. Structures of common fluorophores and fluorescent BA derivatives

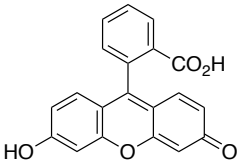

Fluorescein

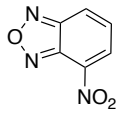

NBD

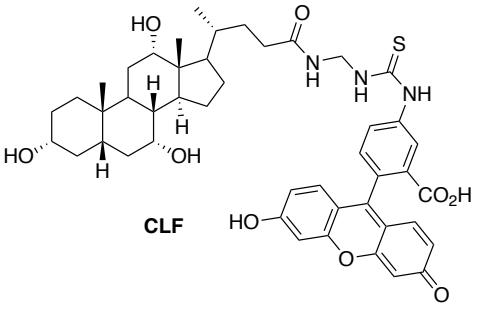

CLF

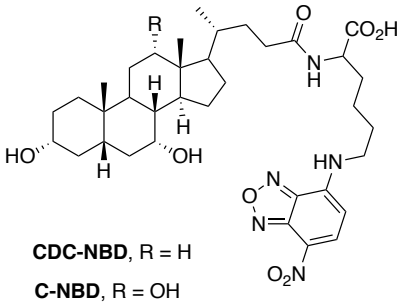

CDC-NBD, R = H

C-NBD, R = OH

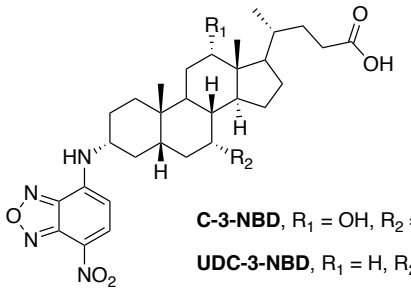

C-3-NBD, R_1 = OH, R_2 = OH

UDC-3-NBD, R_1 = H, R_2 = OH

DC-3-NBD, R_1 = OH, R_2 = H

Goto's research group evaluated the correlation of transporter substrate specificities and the chemical structures of BAs.[12c] The uptake of **NBD**-labeled BAs, **CDC-NBD** and **C-NBD**, were exanimated with BA transporters of OATP1B1- and OATP1B3-expressing HepG2 cells. Interestingly, **CDC-NBD** exhibits a higher affinity for OATP1B3 whereas **C-NBD** presents a higher affinity for OATP1B1. This discovery was interpreted as different BA transporters have their own substrate specificities for BA structures.

Gilmer and colleagues further optimized **NBD**-tagged BAs for detection of organic anion-transporting peptide-mediated processes.[12d] **NBD** group was attached to the C_3-position of BA, and C_7-OH or C_{12}-OH are preserved to differ biological properties. The uptake of **UDC-3-NBD** and **DC-3-NBD** showed highly structure-specific. For instance, **DC-3-NBD** was taken up

faster than **DC-3-NBD** in the Caco-2 cells where only C_3-α-compounds were taken up by an active transport process, but the C_3-β-compounds were not. This study implies that minor structural changes in BA probes can make a significant impact on its behavior toward BA uptake.

In conclusion, fluorophore-tagged BAs have been widely explored to investigate the molecular mechanisms and direct cellular interactions of their uptake and distribution. However, this method has a few disadvantages; this method cannot be applied to real-time in vivo analysis, and it usually shows high background signals.[12b]

1.1.3.2. Radio-labeled BAs

Radio-labeled BAs have been employed for measuring BA transporter activities in cellular models as wells as animal models. Also, many radio-labeled BAs have been used to trace BAs and protein interactions. One of the severe limitations of radio-labeled BAs, even though they can be used for in vivo studies, is the requirement of special handling, not to mention the high intra- or extra cellular background signals or both.[13]

1.1.3.3. BA Transporter Activity in Rabbit Small Intestine with ^{3}H-Labeled BAs

Kramer and co-workers disclosed Na^+-dependency of BA transporter and protein-bindings in rabbit small intestine (**Figure 1.5**).[14] [^{3}H]-Cholate or [^{3}H]-taurocholate uptake was measured in the presence and absence of Na^+ in jejunal and ileal vesicles. The [^{3}H]-cholate uptake was increased about 5-fold by Na^+, and 10-fold increase for [^{3}H]-taurocholate uptake in the ileum. In contrast, only equilibrium uptakes occur from the jejunum. In addition, photoaffinity-labeled BAs containing a diazirine moiety at C_3 or C_7 were employed to study BA-binding proteins in small intestinal vesicles. **1-1a** and **1-1e** showed identical labeling patterns

regardless of the position of a diazirine moiety, however, the unconjugated BA **1-1b** detects fewer proteins than **1-1a**. Interestingly, the α-oriented OH group at C_{12} was found to be important for optimal molecular recognition of BA transporter, therefore, **1-1b** containing a 12-β OH was not able to interact BA-binding proteins. Lastly, a cationic side chain interferes with the uptake, thus the uptake of **1-1c** did not occur with the ileal Na^+-dependent BA transporters.

Figure 1.5. ^{3}H-Labeled conjugated BA analogues

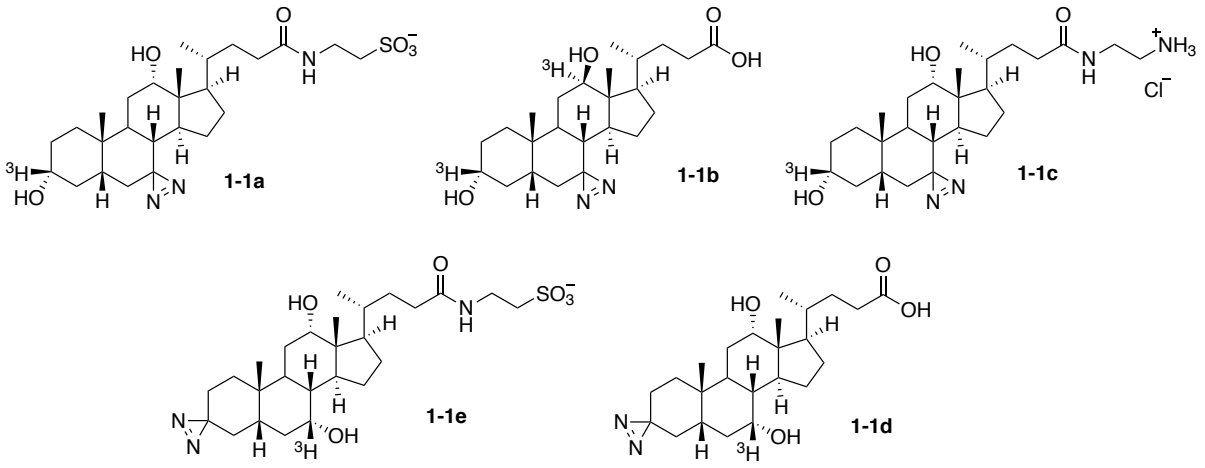

1.1.3.4. Biodistribution Study with ^{11}C-Labeled Conjugated BAs

In 2012, Frisch and co-workers developed N-^{11}C-methly taurine-conjugated BAs by methylation of the side chain with a $^{11}CH_3$ group to assess the bio-distribution of BAs in pigs by using Positron Emission Tomography (PET)/Computed Tomography (CT) scans (**Figure 1.6**).[15] Reverse phase thin layer chromatography was performed to determine the lipophilicity (indication of hydrophobicity) of these radio-labeled conjugated BAs. The study shows that all six tracers show slightly more lipophilic than their natural forms of conjugated BAs. According to PET scan data, these tracers were found in small intestine, liver, and gallbladder, which behave in a similar manner as endogenous taurine-conjugated BAs in vivo, and no radioactivity

was detected in other organs. In addition, no metabolites detection indicates that methylation on the conjugated side chain prevents BAs from deconjugation and dehydroxylation by intestinal bacteria. However, **1-2f** was found in the stomach with significantly high concentration due to gastroduodenal reflux. Therefore, possible application of this method in patients with gastroduodenal motility disorder might be limited.

Figure 1.6. ^{11}C-Labeled conjugated BA analogues

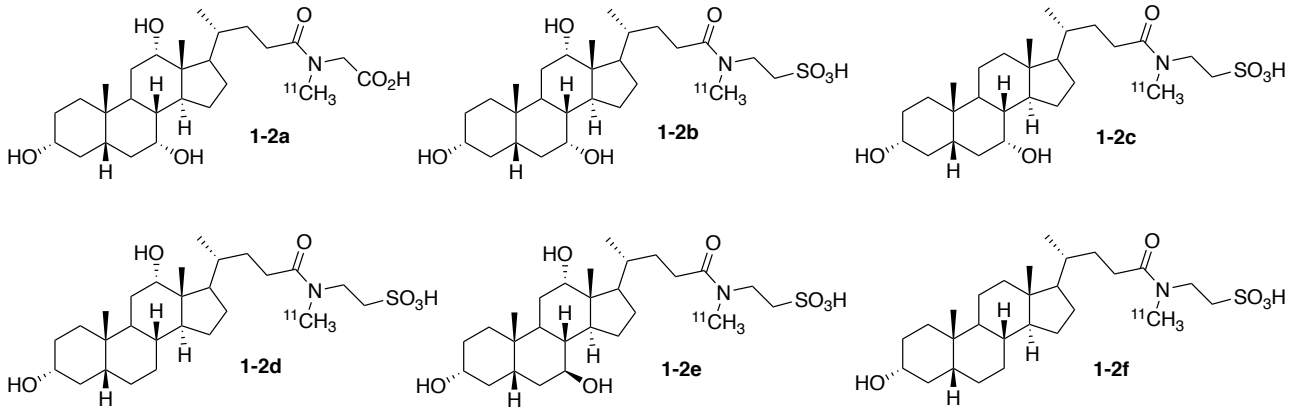

1.1.3.5. Hepatobiliary Transporter Study with ^{18}F-Labeled BAs

De Vos and coworkers investigated BAs transporter characteristics by PET imaging in vitro and in vivo with ^{18}F-labeled BA derivatives (**Figure 1.7**).[16] This new method is an alternative to overcome the short-life of ^{11}C isotope. The uptake by the BA transporters (NTCP and OATP1B1) was evaluated with transfected Chinese hamster ovary (CHO) and human embryonic kidney (HEK) cell lines. ^{18}F-Labeled BAs are evaluated in wild-type mice to monitor hepatobiliary transport by PET-scans. This study disclosed that the hepatic uptake of **1-3a**, 3α-^{18}F cholic acid is faster than **1-3d**, 3β-^{18}F cholic acid. **1-3a** has higher affinity than **1-3d**, however, CA-derived probes such as **1-3a, 1-3c, 1-3d and 1-3e** show faster uptake than chenodeoxy derivative **1-3b**. Interestingly, conjugation of CA with glycine such as in **1-3c** has no

significant difference in vivo. Since there was significantly slower rate in uptake for **1-3d**, excretion from liver occurs only 60% in gallbladder and small intestines. Scaling up of C_7- and C_{12}-fluorinated probes is synthetically challenging because of elimination reactions occurring exclusively with ^{18}F fluoride. Overall, all analogues show good binding affinity for BA transporters, NTCP and OATP1B1.

Figure 1.7. Analogues of ^{18}F-labeled BA

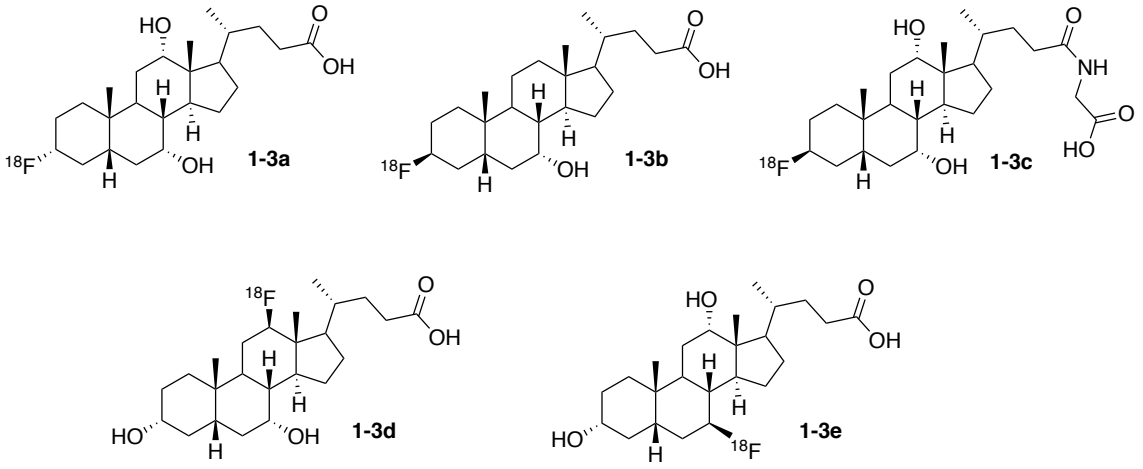

1.1.4. In Vivo Cell Tracking with Bioluminescence Imaging (BLI)

The bioluminescence imaging (BLI) is being widely used to monitor biological processes. Unlike its predecessor fluorescent proteins, BLI has high visualization, quantification, and characterization features allowing it to be used in both in vivo and in vitro.[17] Although there are many luminescent species, three bioluminescent reporters have been thoroughly studied and their enzymes have been utilized in various biomedical research: Firefly luciferase (FLuc), Gaussia luciferase (GLuc), and Renilla luciferase (RLuc) as shown in **Scheme 1.1**. In vitro cell tracking, Gluc and Rluc are commonly used because it does not require adenosine triphosphate (ATP) for activation. In vivo studies rely on the cell associated luminiferases of Fluc.

The FLuc-encoding gene is the most studied and well-characterized bioluminescent reporter. Subsequently, the FLuc-luciferin system has been adopted as the standard procedure for BLI-based in vivo cell tracking. FLuc is catalyzed by ATP to generate green luminescence with a wavelength of 562 nm. The long wavelength of FLuc is less scattered by biological tissues and absorbed by pigmented molecules is also reduced, making it more suitable for in vivo imaging. On the contrary, RLuc and GLuc display a blue-green bioluminescence without the need for ATP to emit light with a wavelength of 482 nm. The emitted light is easily absorbed by colored molecules and easily scattered by tissues, hence, limited use in in vivo imaging. With outstanding advantages of bioluminescence imaging, the imaging approach is most commonly applied to in vivo monitoring in order to assess viability of administered cells with therapeutic efficacy in preclinical small animal models.

Scheme 1.1. Major bioluminescence imaging reporters

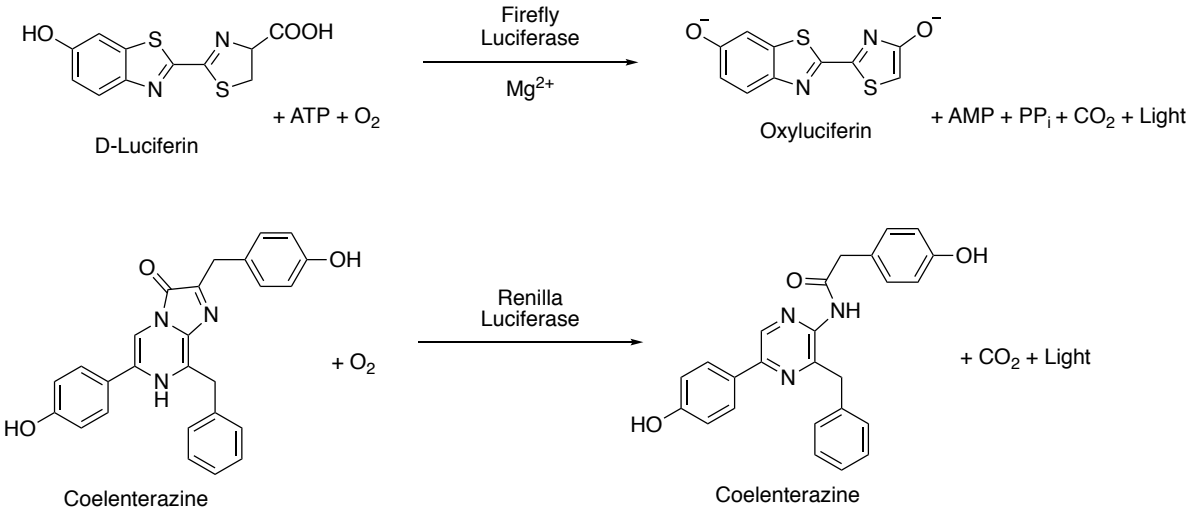

The mechanism of D-luciferin is shown in **Scheme 1.2**. D-Luciferin, a substrate for FLuc, freely diffuses across the cell membrane. FLuc emits light in the presence of D-luciferin, ATP, Mg^{2+}, and oxygen. D-Lucifierin undergoes esterification with ATP to form **1-4** luciferyl

adenylate and then generates **1-5** containing dioxetanone moiety. Emission of CO_2 to generates oxyluciferin and *hv*, which can be detected with a sensitive light-emission detecting system.

Scheme 1.2. Mechanism of D-Luciferin

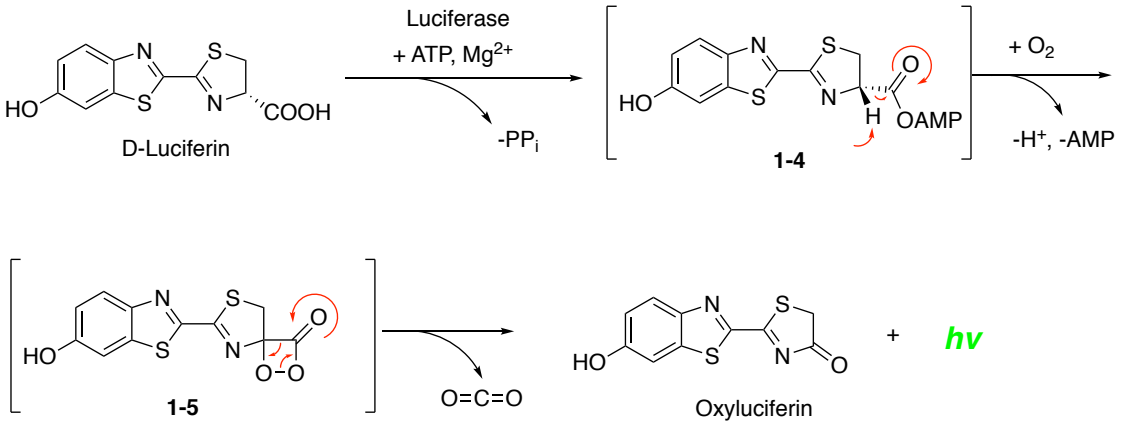

1.1.4.1. Application of Bioluminescence Imaging with Conjugated Luciferin

Wender and coworkers developed transporters to measure the uptake of transporter-conjugates and luciferin release mechanisms in real-time in cell and in animal models via a charge-coupled device (CCD) camera.[18] The mechanism of luciferin-conjugate reporter was shown in **Scheme 1.3**. D-Octaarginine was attached to D-luciferin via variety lengths of a cleavable disulfide linker that immolates by glutathione (GSH) only after cell entry. Subsequent cyclization of thiol promotes a luciferin discharge, which produces light. This study also provides quantification of transporter uptake and circumvents a synthetic difficulty of modifying luciferin conjugates by attaching a releasable linker. Three different lengths of linkers were exanimated to measure luciferin releasing rates and to extent stability of compounds. The reaction rate of linker with four carbons (n=3) shows the slowest rate for light emission due to the require seven membered ring formation of the intermediate thiol. However, the linker with two carbons (n=1) shows a significantly short half-life, 3h for carbonate, compared to three

(n=2) and four (n=3) carbon linkers, 11 h and 33 h, respectively. CCD camera was utilized to analyze the number of photons from free luciferin and demonstrates this noninvasive method can quantify transporter activity in luciferase transfected cell lines and transgenic reporter mice in real time.

Scheme 1.3. Mechanism of the luciferin-conjugate reporter

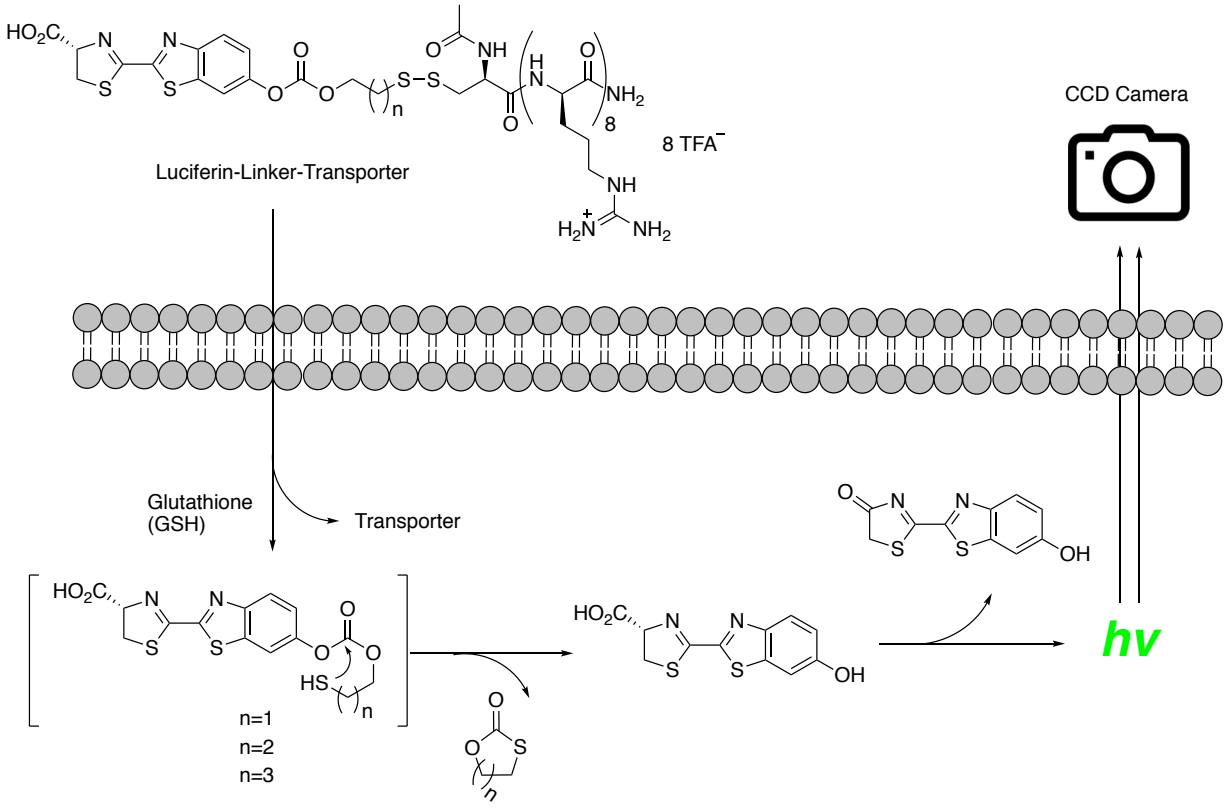

1.1.4.2. Application of Bioluminescence Imaging in Fatty Acid Uptake Study

Compared to the previous model by Wender and coworkers, Cohen research group provided an enhanced method of studying fatty acids uptake and quantifying related fluxes with the goal of understanding the physiological and pathological processes of disease models in real-

time.[19] Fatty acids and fatty acid methyl esters were conjugated via a disulfide chain containing a reporter molecule, luciferin, to provide **1-6a** and **1-6b** respectively (**Figure 1.8**). Probes **1-6a** were absorbed by several organs, including adipose tissue, liver, kidney, heart, and skeletal muscle, in animal systems and the uptake was mediated by insulin in vivo which are similar process as the distribution of natural fatty acids. However, the uptake of the control reporter **1-6b** was significantly lower than **1-6a**.

Figure 1.8. Structure of fatty acid probes

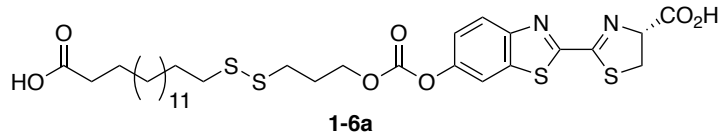

1-6a

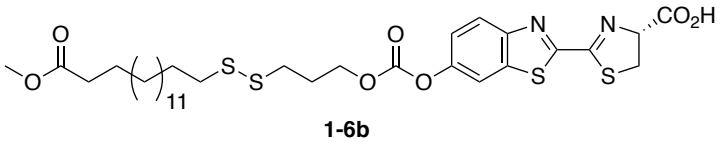

1-6b

1.2. Method of Measuring BA transport in Real Time

We have developed probes to investigate cellular uptake of BA transporters, ileal Apical Sodium Dependent BA Transporter (ASBT) and hepatic Sodium-dependent Taurocholate Co-Transporting Polypeptide (NTCP), in living cell in order to overcome disadvantages of the conventional methodologies such as delay in measurement between treatments and high radioactive and fluorescent background signals. Especially, in vivo, the delay between treatments can be a severe drawback to detect rapid post-translational regulation of ASBT or NTCP in real time. Carboxylic acid of cholic acid was modified to install a reporter molecule, luciferin, via a cleavable linker. The probe and a control model are shown in **Figure 1.9**. A bioluminescence-based method of measuring BA transporter activity in real time could provide a precise

evaluation of rapid changes in their functions. Light emitted from free luciferin was detected as well as quantified by sensitive in vivo imaging system (IVIS).

Figure 1.9. Cleavable BA transporter probe (BA-SS-Luc) and non-cleavable probe (BA-S-Luc)

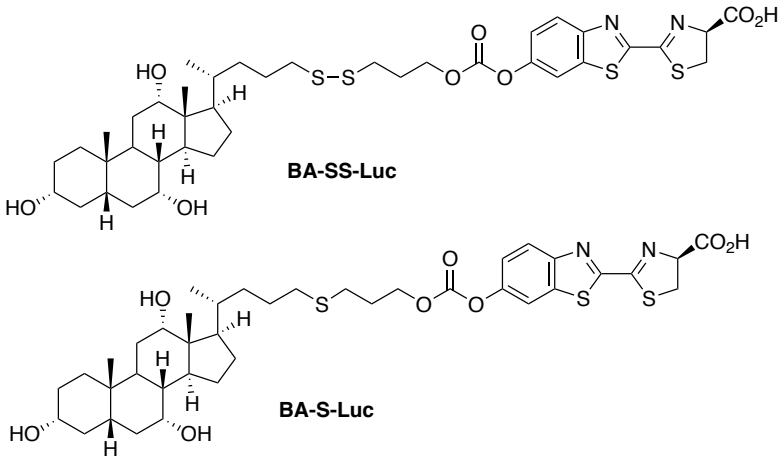

1.3. Result and Discussion

The bioluminescence probe to measure BA transporter activity is outlined in **Scheme 1.4**. The side chain of cholic acid was modified to attach a luciferin moiety via a disulfide linker. Entering into cells, intracellular glutathione initiates the process to discharge cholic acid and free luciferin. Subsequently, luciferin is catalyzed by luciferase in the cell to emit light, which can be detected by IVIS camera.

The efficacy of BA transporters can be measured in a cell culture model by using **CA-SS-Luc** probe. First, luciferase co-transfected HEK 293 cells and V5-tagged fusion ASBT were incubated with three different concentrations of the probe. Bioluminescence production was measured with IVIS camera over course of 45 minutes. The data shows the intensity of emitted light was proportional to the concentration of the probe.

Subsequently, production of luminescence in HEK 293 cells by different amounts of ASBT or NCPT was measure. The uptake was significantly higher when the cells were

transiently transfected with 750 ng/well of BA transporter, ASBT-V5 compared to the cells transfected with 250 ng/well of ASBT-V5 based on the luminescence generation from the cells. The same result was also obatined when HEK 293 cells was transfected with luciferase and NCPT but not with serotonin transporter transfected cells, SERT-V5.

In order to confirm that luminescence occurs after cell entry, the amount of bioluminescence production from CA-SS-Luc and D-luciferin was calculated. This result indicates that bioluminescence is the consequence of the cleavage of disulfide bond induced by intracellular glutathione not from decomposition of the probe outside of the cells.

In the pervious study, radio-labeled [^{3}H]-TC uptake was significantly increased by incubation with a phosphatase inhibitor PTPIII. In line with this result, ~2.5-fold enhancement of ASBT activity was observed in HEK 293 cells when incubated with PTPIII, which allows a real time monitoring of ASBT activity.

Most Interesting result from this study was the effect of natural BAs. When natural BAs are present, the probe could compete with them for a cell entry. HEK 293 cells transfected with ASBT-V5 or NTCP-V5 showed bioluminescence increase by ~1.5-fold with co-incubation with natural Bas such as taurocholate (TC). This trend was not observed in SERT-transfected HEK 293 cells. Incubation with taurochenodeoxycholate (TCDC) shows greater intensity of bioluminescence compared to TC and TCDC. This observation was in good agreement with the previous study with radio-labeled BAs.

Scheme 1.4. Scheme for measuring intercellular delivery of BA

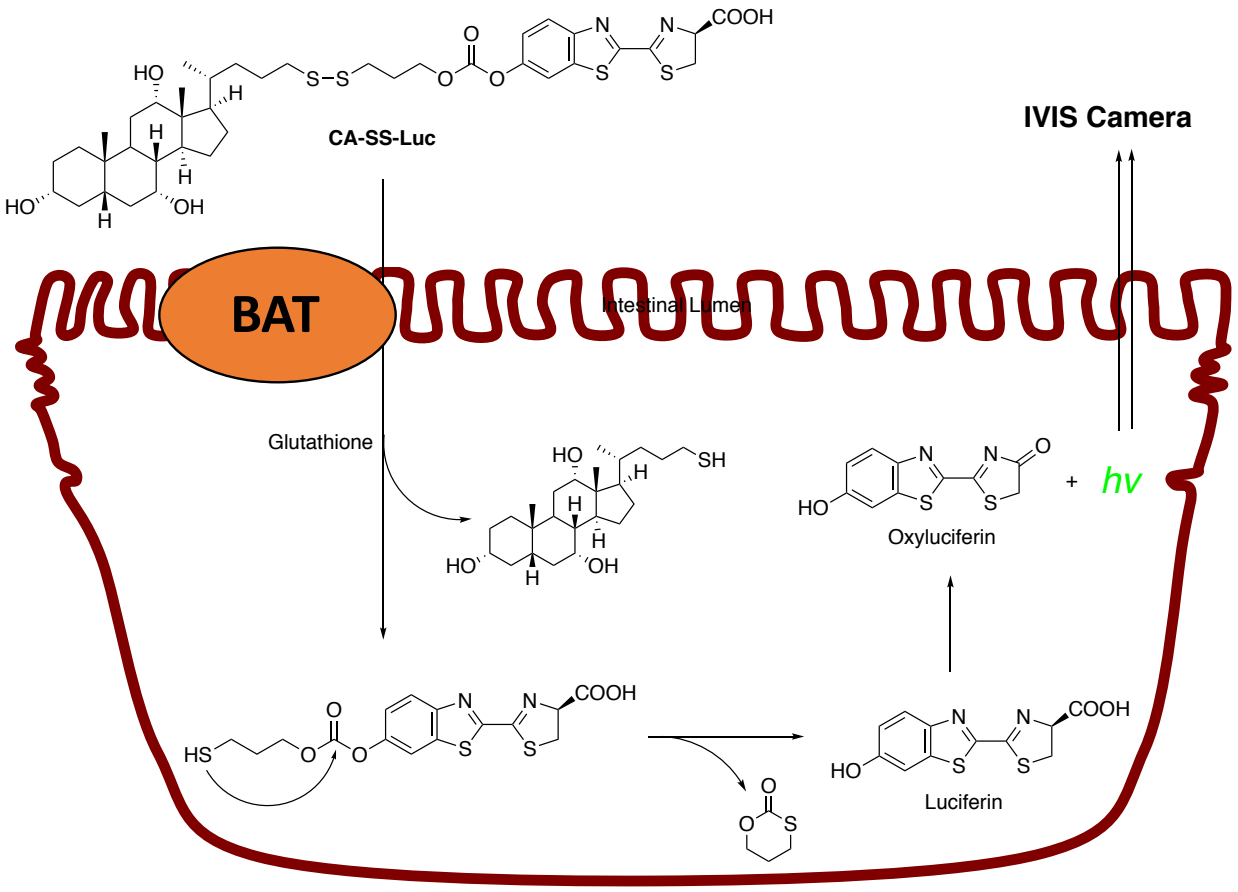

This method was also applied to native ileal enterocytes. Intestinal epithelial cells (IECs) isolated from the jejnum and ileaum of transgenic mice expressing luciferase (Luc^{Tg}) were examined for the bioluminescence assay, which showed that in the presence of Na^+, bioluminescence increased by ~2-fold in ileal but not jejunal IECs. Na^+ enhances the uptake of the probe in ileal cell whereas CA-SS-Luc uptake in HEK 293 cells was not affected by addition of Na^+. Intestinal cells and non-intestinal cells clearly display a significant difference in responding to the probe. The difference was also observed between human and mouse ASBT.

1.3.1. Synthetic Route of Probes for BA Transporters

The synthetic route for a disulfide-based probe is shown in **Scheme 1.5–1.7**. The synthesis commenced with protection of three hydroxyl groups of cholic acid with TBS groups followed by reduction of the carboxylic acid moiety to generate primary alcohol **1-8**.

Scheme 1.5. Synthesis of thiol intermediate

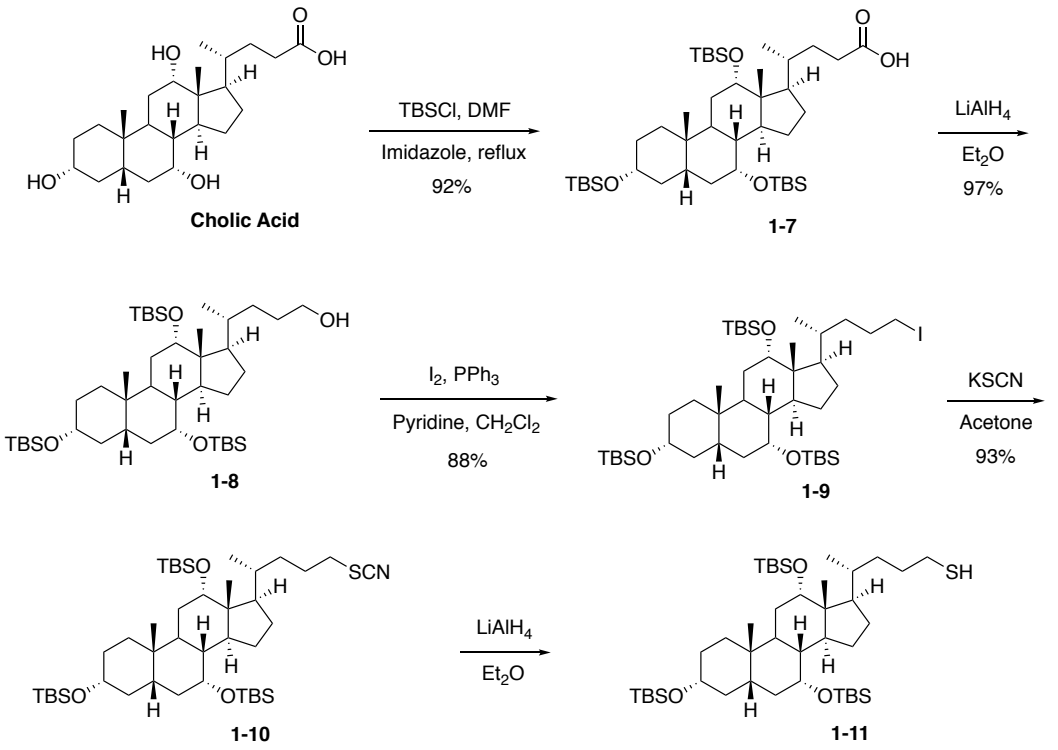

Iodination of the primary alcohol followed by substitution with KSCN and reduction of the thiocyanide moiety afforded thiol **1-11**. Hydroxy thiol **1-13** was activated with 2,2′-dithiodipyridine to generate precursor **1-14**. Disulfide **1-14** was transformed to carbonate **1-16** by treating with triphosgene followed by 2-cyano-6-hydroxybenzothiazole **1-15**.

Scheme 1.6. Synthesis of side chain **1-16**

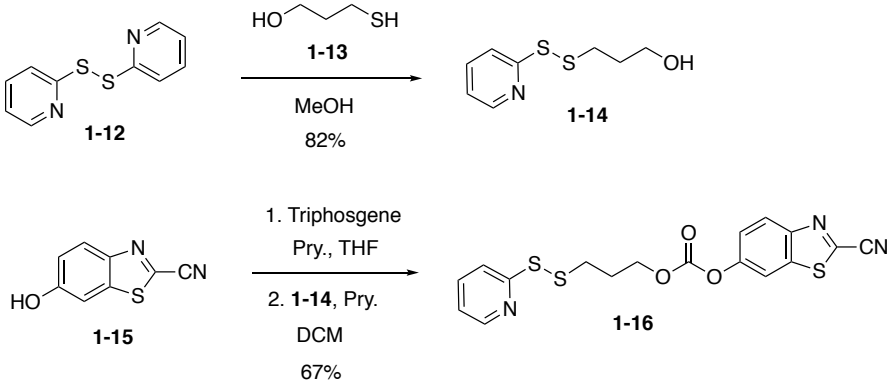

The sulfide exchange of **1-16** with thiol **1-11** proceeded smoothly to generate **1-17**. Cleavage of TBS groups by treatment with PTSA followed by treating the intermediate with D-cysteine provided probe **1-19**. A non-cleavable sulfide-based probe was synthesized and synthetic route is shown in **Scheme 1.8**. Treating compound **1-9** with 3-mercaptopropan-1-ol **1-13** and KOH to from thioether **1-20**, which was subsequently treated with triphosgene and thiopyridyl **1-16** to generate carbonate **1-21**. Deprotection of TBS groups with PTSA followed by treating with D-cystein yields a control probe **1-22**.

Scheme 1.7. Synthesis of BA transporter probe **1-19**

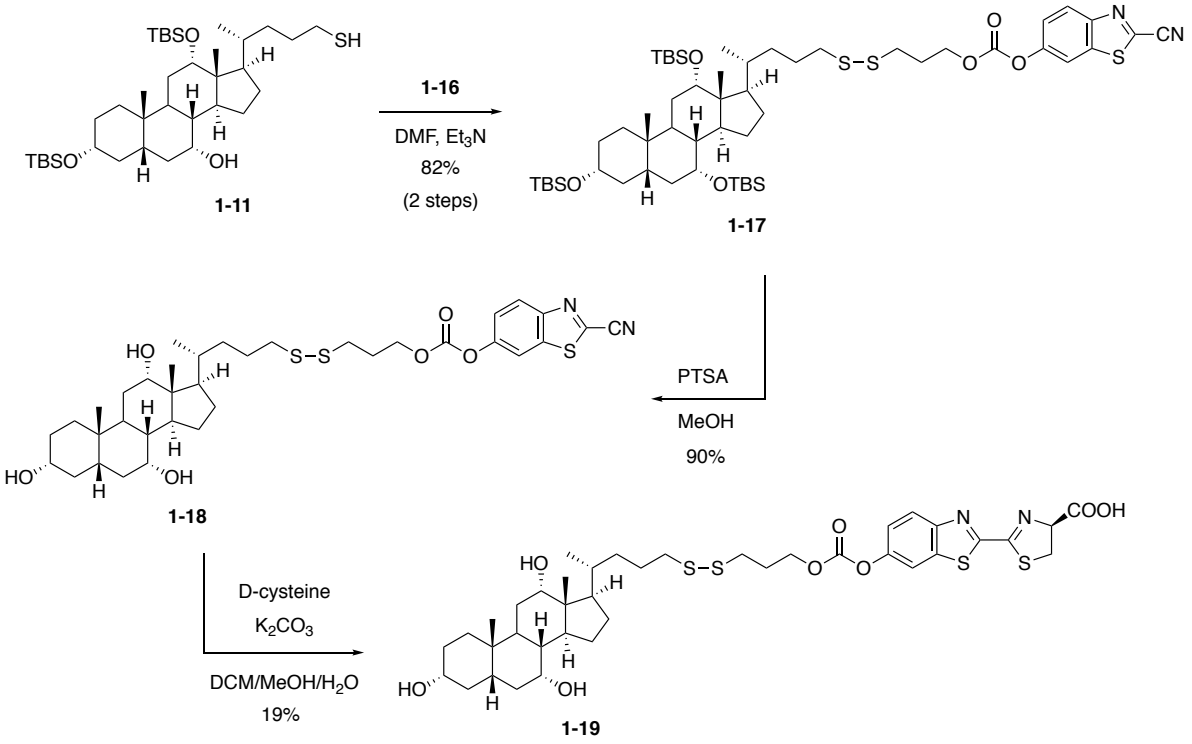

Scheme 1.8. Synthesis of a control probe for imaging

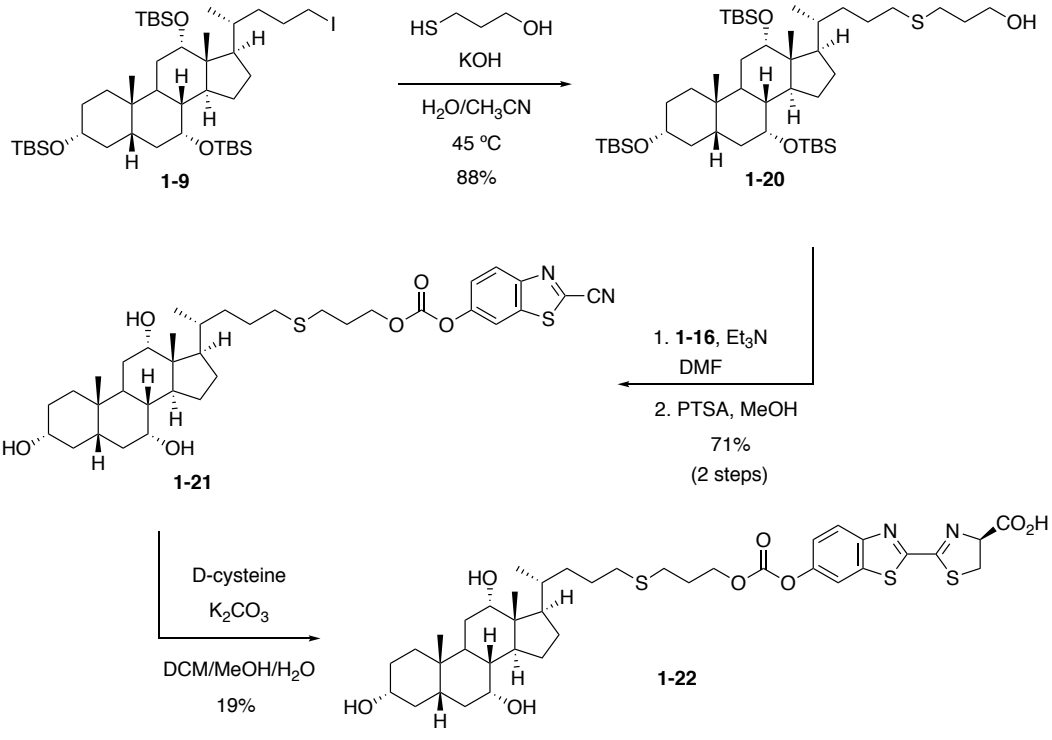

1.3.2. Bioassay Data

In HEK 293 cells expressing luciferase with either ASBT or NTCP are shown in **Figure 1**. The bioluminescence signal, which represents a velocity of the transport activity, increases linearly for ~20 minutes and then reaches a plateau, representing an equilibrium state consistent with a transporter-mediated process for CA-SS-Luc cellular entry. The intensity of emitted photons increases over time and also the signal is enhanced with the concentration of CA-SS-Luc. This result indicates that CA-SS-Luc bioluminescence is both concentration- and time-dependent. Cells were treated with three different concentrations of CA-SS-Luc at 0.01 μM (open circles), 0.1 μM (closed circles), and 1μM (open squares).

Figure 1.10. Bioluminescence generate by BA transport probe over time

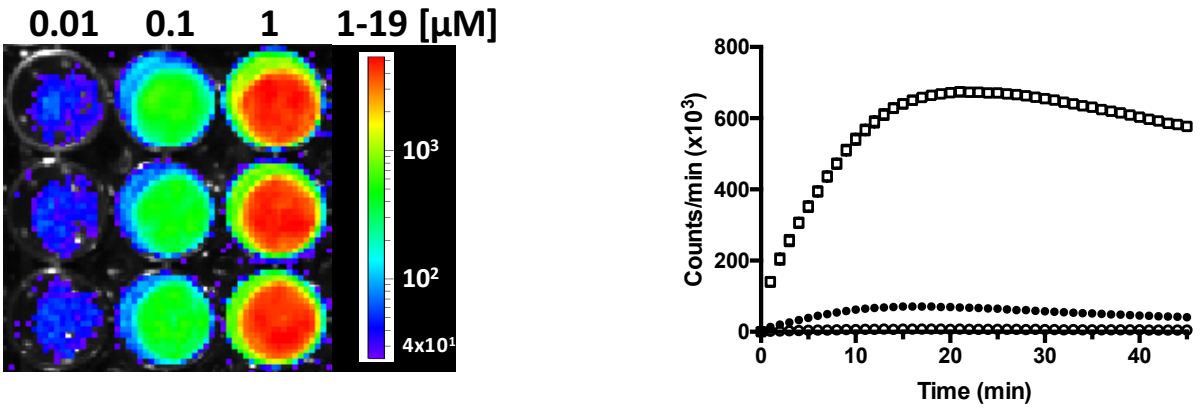

Figure 1.11. Bioluminescence production on cellular levels of ASBT

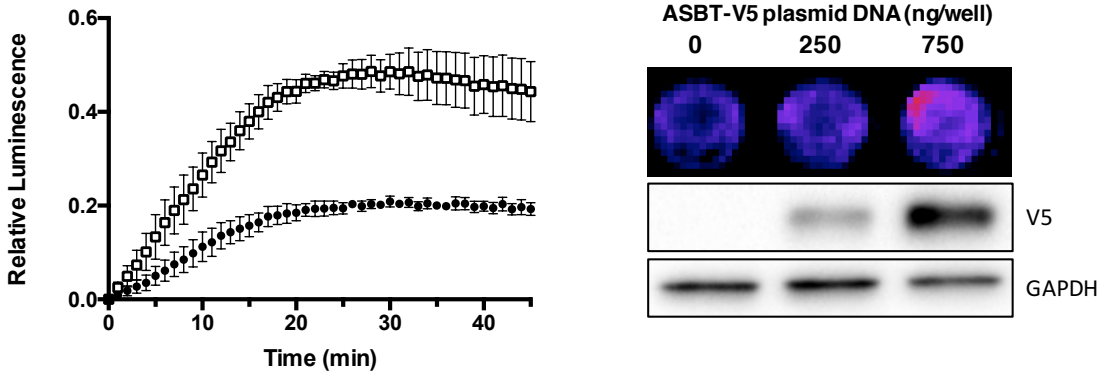

The above graph shows time course of BA transporter-dependent bioluminescence production in HEK293 transiently transfected with luciferase and 250 ng/well (closed circles) or 750 ng/well (open squares) of ASBT.

Figure 1.12. Bioluminescence production on cellular levels of NTCP

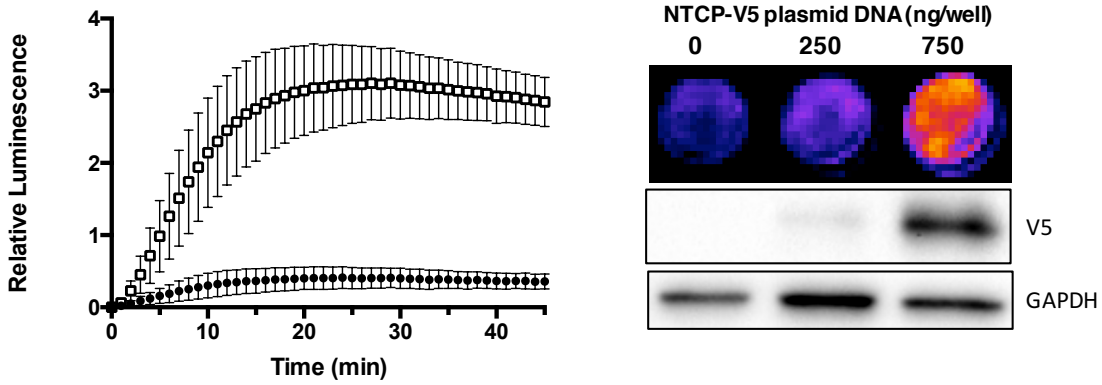

The above graph shows that time course of BA transporter-dependent bioluminescence production in HEK293 transiently transfected with luciferase and 250 ng/well (closed circles) or 750 ng/well (open squares) of NTCP. These results show that luminescence production increases with the amount of transfected BA transporters, ASBT or NTCP.

Figure 1.13. Control experiment with D-luciferin

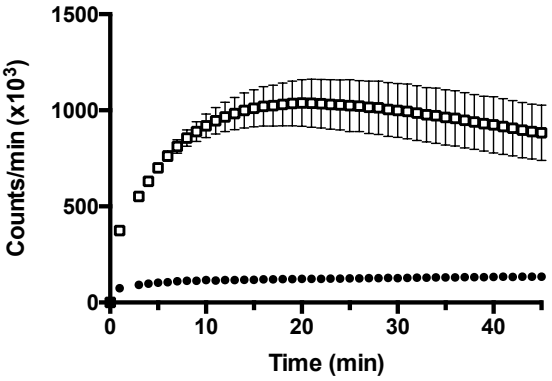

The amount of luminescence from CA-SS-Luc (open-squared) is higher than D-luciferin (closed-circled). Incubating cells with D-luciferin shows significantly less luminescence signal compared to incubating cell with CA-SS-Luc. This indicates that the emitted light is from the cell entry of the probe not from its decomposition outside of cells.

Figure 1.14. PTPIII enhances CA-SS-Luc bioluminescence production

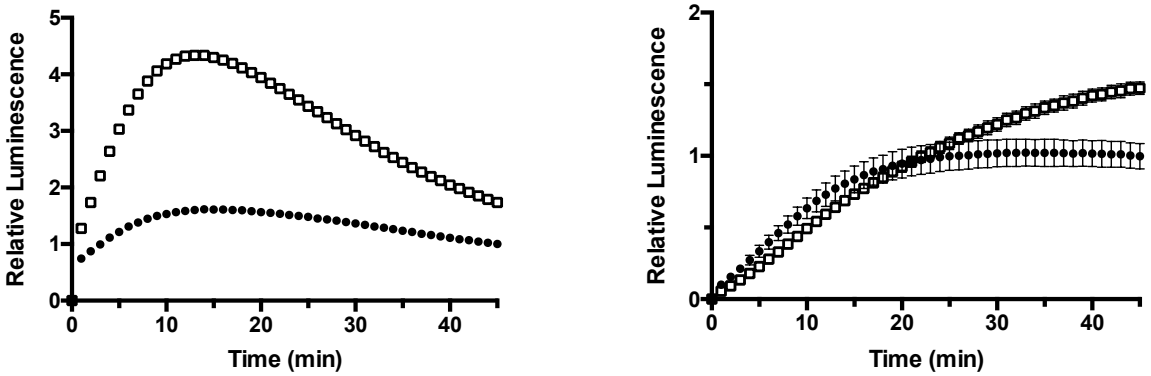

CA-SS-Luc in 2BT cells with pretreatment (the left graph) and with simultaneous treatment with 500 μM PTPIII (open squares) or DMSO (closed circles). In the presence of PTPIII, luminescence production is enhanced through the duration of the experiment. Therefore

this result provides a strong evidence that CA-SS-Luc can be used as a tool to access in rapid changes in ASBT function in real time.

Figure 1.15. Taurocholate (TC) effects on cellular uptake

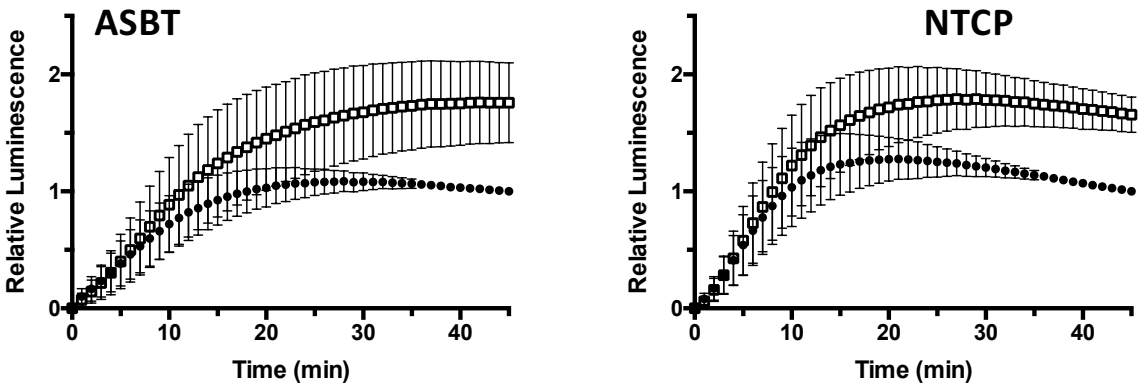

Relative bioluminescence production by CA-SS-Luc co-treated with natural BA 100 μM TC (open squares) or 0 μM TC (closed circles) in HEK cells transiently expressing ASBT (left) or NTCP (right).

Figure 1.16. Effect of Taurocholate (TCDC) concentarion on cellular uptake

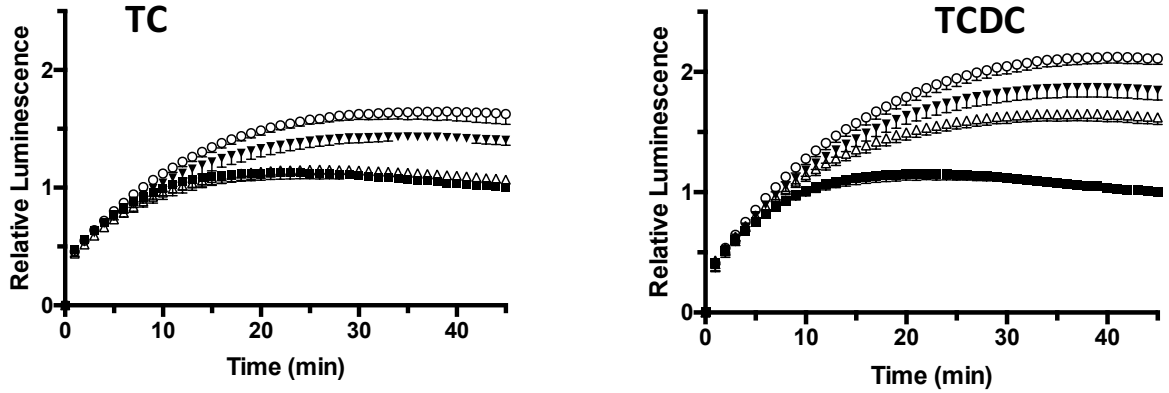

Induction of CA-SS-Luc luminescence by 0 μM (closed squares), 5 μM (open triangles), 25 μM (closed triangles), and 100 μM (open circles) with natural bile aicd TCDC in 2BT cells; n=4. In HEK 293 cells, BA-dependent luminescence induction in the presence of natural BAs, TC and TCDC, was enhanced. CA-SS-Luc uptake was enhanced to greater extend with TCDC compared to TC.

Figure 1.17. Curve fit to the Michaelis-Menten equation and k_m

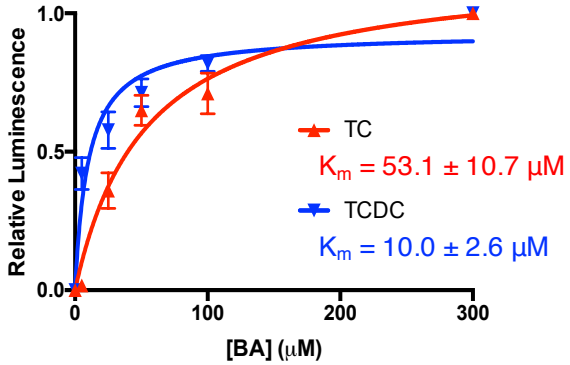

The produced luminescence was measured after 15 minutes of incubation with TC and TCDC added at concentrations of 5, 25, 50 100, and 300 μM. After fitting, the apparent k_m of TC was calculated as 53.1± 10.7 uM and the apparent k_m of TCDC was calculated as 10.0 ± 2.6 uM. The graph shows curve fit to the Michaelis-Menten equation and apparent k_m calculation by GraphPad Prism 6.0; n=4, $p < 0.05$. Lower k_m means faster velocity to reach maximum rate of reaction, which indicates a higher binding affinity. This calculation shows that TCDC shows a higher affinity.

Figure 1.18. CA-SS-Luc uptake is Na^+-dependent in intestinal epithelial cells.

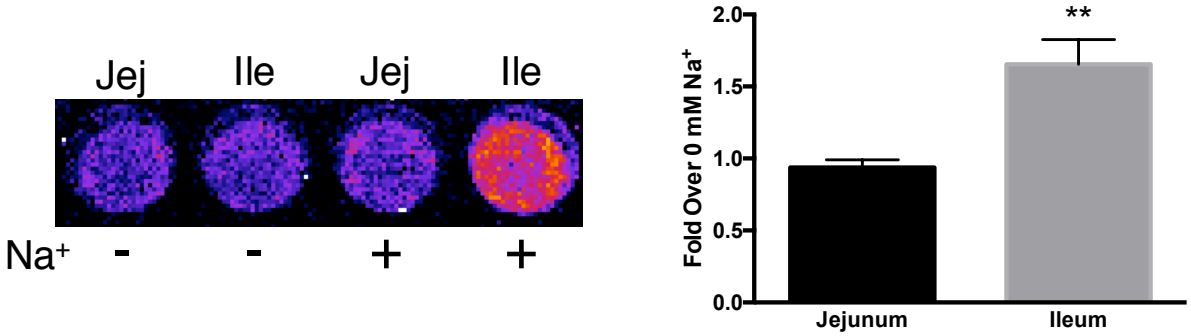

In the absence of Na^+, the bioluminescence generated by jejunal and ileal primary epithelial cells (IECs) was similar. However, in the presence of Na^+, uptake of CA-SS-Luc in ileal primary epithelial cells increases about 2-fold but not in jejunal cells. This indicates BA uptake is sodium dependent in ileal cell, which is consistent with BA localization and mechanism of uptake by ASBT.

1.4. Future Study of BA Transporter Probe

Based on the promising results from C_{27}-BA probe, we will further explore the structural specificity of the BA transporter probe including an affinity and an uptake rate. Toward this purpose, we designed C_3-luciferin probe **1-23** (**Figure 1.19**). To retain stereochemistry of at C_3, the C_3-hydroxyl group was alkylated before the luciferin was attached to C_3-position via a cleavable linker.

Figure 1.19. C_3-luciferin BA transporter probe

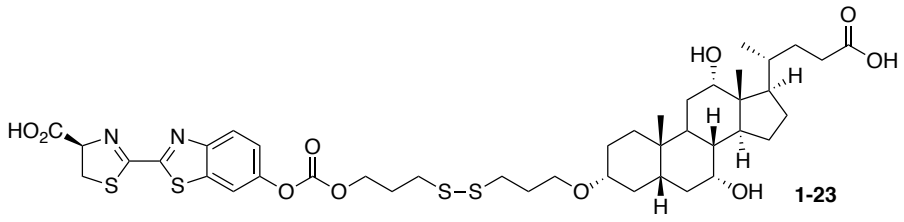

1-23

The C_3-hydroxyl group was chosen as a linker to luciferin due to the importance of a carboxylic group on the side chain and negligible effect of the C_3-hydroxyl group. The previous studies on the structure-activity relationships of BA derivatives to the ASBT and NTCP with various BA analogs demonstrated that the substituents on the steroid nucleus determine the affinity and uptake rates of the BA analogs.[22] This study showed that the activity of BA decrease when the third hydroxyl group was present. On the other hand, the C_3-α-OH, which is the characteristic feature in all naturally occurring BAs, was not critical for molecular recognition by ASBT or NTCP. Therefore, C_3-α-OH was modified for a pro-drug approach using BA transporter system.[23]

Also, BA conjugation with glycine and taurine causes different biological effects and also improves the affinity of a probe to BA transporters including ASBT and NTCP.[24] Therefore, the carboxylic group on the side chain of this new probe can be modified to have conjugation with glycine or taurine to investigate the affinity and an uptake rate in comparison with the C_{24}-luciferin probe.

Scheme 1.9. Synthesis of C_3-luciferine BA transporter probe

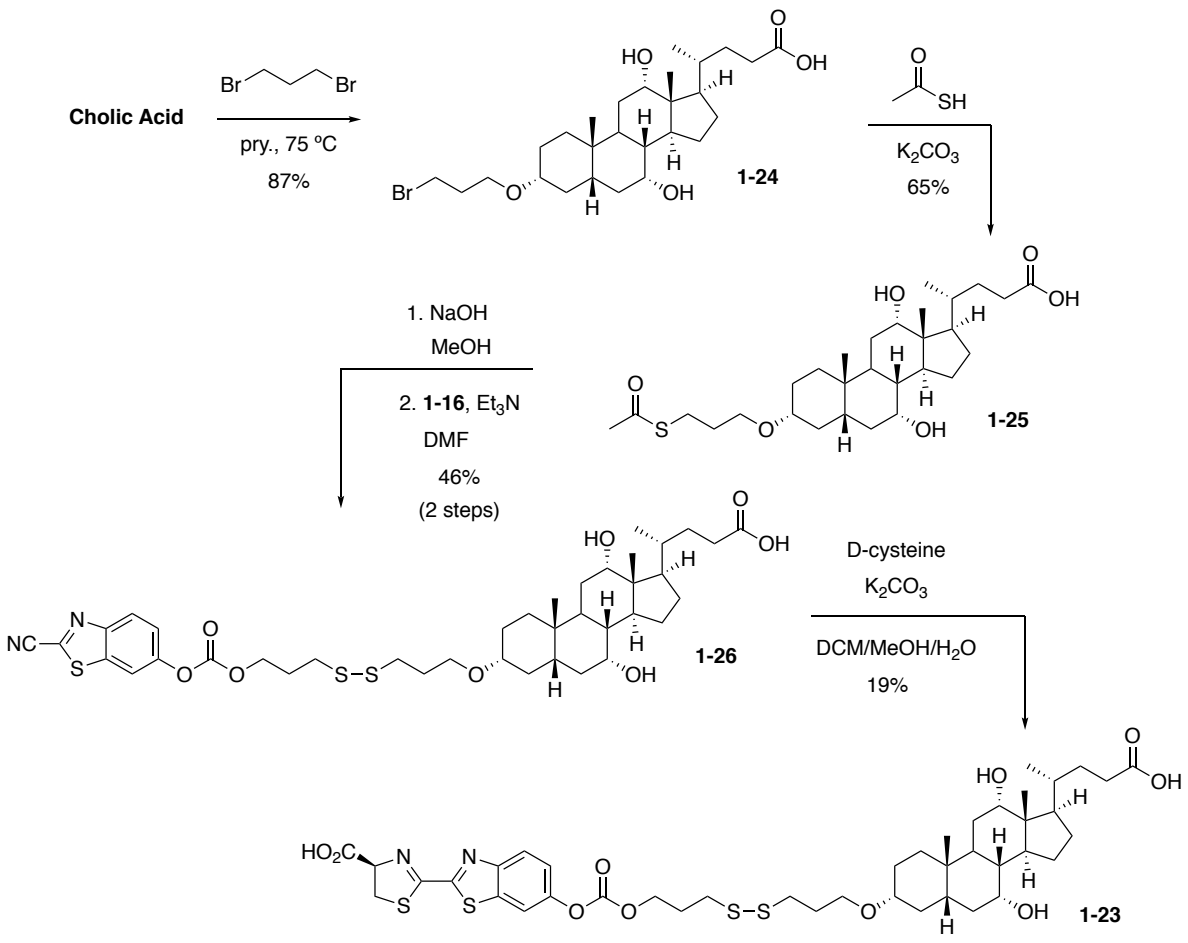

C_3-Luciferin probe (Luc-SS-CA) was designed and the general synthetic scheme is shown in **Scheme 1.9**. Regioselective alkylation of C_3 hydroxy group with 1,3-dibromopropane followed by thioester formation with thioacetic acid provided **1-24** which was treated with NaOH in MeOH followed by disulfide formation with **1-16** to provides carbonate **1-25**. Treating **1-25** with D-cysteine and K_2CO_3 delivered the desired probe **1-26**.

The C_3-luciferin probe was prepared and its bioassay is being performed in the Alrefai lab. In addition, the C_{24}-luciferin probe will directly apply to commercially available Luc^{Tg} mice to measure BA transporter function in vivo.

1.5. Conclusion

The synthesis and use of **CA-SS-Luc** probe for investigating BA transporter activity in real time has been described. This approach will be applied for further exploration of identifying BA transporter-regulating compounds and for in vivo study with animal models, which will allow for assessing BA transporter activity in other organs. Also, the cellular uptake of C_3-luciferin probe **1-26** is underway in collaboration with the Alrefai lab.

1.6. Experimental Details

1.6.1. General Information

Reactions were carried out in oven or flame-dried glassware unless otherwise noted. Compounds were purchased from Aldrich or Acros or TCI America unless otherwise noted. Toluene (C_7H_8) was distilled over calcium hydride under nitrogen atmosphere. CH_2Cl_2, THF, Et_2O were purified based on standard procedures. Tetrahydrofuran (THF) was distilled over sodium and benzophenone under nitrogen. Flash chromatography was performed using silica gel 60 Å (32−63 mesh) purchased from Silicycle Inc. Analytical thin layer chromatography (TLC) was performed on 0.25 mm E. Merck pre-coated silica gel 60 (particle size 0.040–0.063 mm). The normal phase silica-based cartridge, Strata, was purchased from Phenomenex. Yields refer to chromatographically and spectroscopically pure compounds unless otherwise stated. ^{1}H NMR and ^{13}C NMR spectra were recorded on a Bruker DR-500 spectrometer. Multiplicities are indicated by s (singlet), d (doublet), t (triplet), q (quartet), qn (quintet), sext (sextet), m (multiplet), b (broad), and app (apparent). ^{1}H NMR signals that fall within a ca. 0.3 ppm range are generally reported as a multiplet, with a single chemical shift value corresponding to the center of the peak. Coupling constants, *J*, are reported in Hz (Hertz). Electrospray ionization

(ESI) mass spectra were recorded on a Waters Micromass Q-Tof Ultima in the University of Illinois at Urbana–Champaign. Electron impact (EI) mass spectra and Chemical Ionization (CI) mass spectra were obtained using a Micromass 70-VSE in the University of Illinois at Urbana-Champaign.

1.6.2. Synthesis of BA Transporter Probe

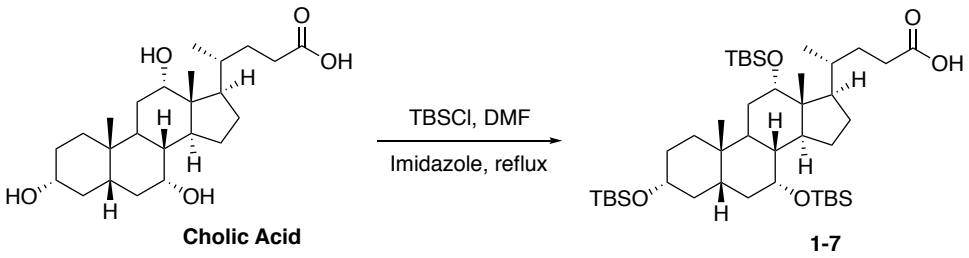

To a solution of cholic acid (1.63 g, 4 mmol) and imidazole (1.36 g, 20 mmol) in DMF (25 mL) was added TBSCl (1.9 g, 13.2 mmol) and then the reaction mixture was refluxed overnight. Saturated aqueous NH_4Cl solution was added to quench the reaction, and the resulting mixture was extracted with Et_2O. The organic layer was washed with H_2O (20 mL x 3) to remove residual DMF. The organic extract was dried over anhydrous $MgSO_4$, filtered, concentrated and purified by silica gel column chromatography (Hexanes : EtOAc = 4 : 1) to give **1-7** (2.77 g, 92%) as colorless oil.

1-7: ^{1}H NMR (500 MHz, $CDCl_3$) δ 3.97–3.96 (m, 1H), 3.80–3.79 (m, 1H), 3.36 (tt, *J* = 5.3 Hz, *J* = 10.6 Hz, 1H), 2.42–1.05 (m, 33H, steroidal skeleton H), 0.95 (d, *J* = 6.5 Hz, 3H), 0.93 (s, 9H), 0.89 (s, 9H), 0.86 (s, 3H), 0.84 (s, 9H), 0.66 (s, 3H), 0.08 (s, 6H), 0.04 (s, 6H), –0.01 (s, 6H); ^{13}C NMR (125 MHz, $CDCl_3$) δ 179.5, 175.9, 73.8, 72.1, 69.5, 47.3, 45.9, 41.9, 41.4, 40.9, 40.6, 36, 35.4, 34.8, 31.3, 30.9, 28.4, 27.7, 26.5, 26.4, 26, 25.7, 23.8, 23, 18.4, 18.3,

17.8, 12.8, -2.6, -2.8, –4.2, –4.4, –4.6, –5.4; HRMS (ESI) calcd for $C_{36}H_{69}O_5Si_2$ [M–$C_6H_{15}Si+H]^+$ 637.4684, found 637.4675.

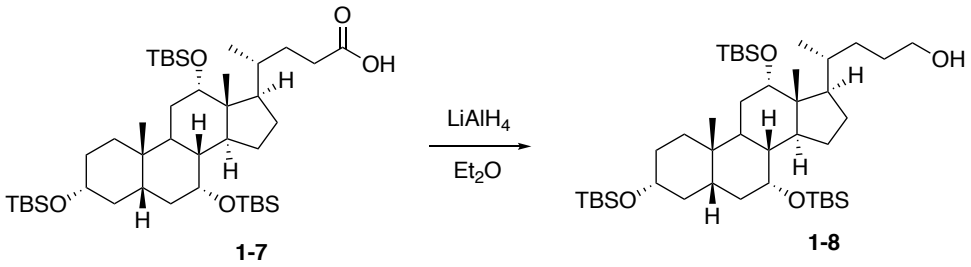

1-7 **1-8**

To a suspension of $LiAlH_4$ (190 mg, 5 mmol) in dry Et_2O (10 mL) was slowly added the TBS-protected carboxylic acid **1-7** (2.77 g, 3.68 mmol) dissolved in dry Et_2O (30 mL) under a N_2 atmosphere at 0 °C. The mixture was warmed to room temperature and stirred overnight. The mixture was carefully quenched by the sequential addition of 0.2 mL H_2O, 0.2 mL 15 w/v% aq. NaOH, 0.4 mL H_2O and was then poured into 40 mL of Et_2O and stirred for 30 min. The crude material was filtered through Celite and the solvent was removed in vacuum. The crude material was purified by silica gel column chromatography (Hexanes : EtOAc = 4 :1) to give **1-8** (2.63 g, 97%) as a colorless oil.

1-8: ^{1}H NMR (500 MHz, $CDCl_3$) δ 3.97–3.96 (m, 1H), 3.80–3.79 (m, 1H), 3.61 (t, *J* = 5.9 Hz, 2H), 3.36 (tt, *J* = 5.3 Hz, *J* = 10.6 Hz, 1H), 2.42–1.05 (m, 33H, steroidal skeleton H), 0.95 (d, *J* = 6.7 Hz, 3H), 0.93 (s, 9H), 0.89 (s, 9H), 0.86 (s, 3H), 0.84 (s, 9H), 0.66 (s, 3H), 0.08 (s, 6H) 0.04 (d, 6H) –0.01 (s, 6H); ^{13}C NMR (125 MHz, $CDCl_3$) δ 73.9, 72.1, 69.6, 63.6, 47.3, 46.4, 46.2, 46, 41.9, 41.4, 40.9, 40.6, 36.3, 35.4, 34.8, 32, 31.3, 30, 28.5, 27.9, 26.5, 26.4, 26, 25.7, 23.9, 23, 18.3, 12.8, –2.6, –2.8, –4.1, –5.4; HRMS (ESI) calcd for $C_{36}H_{71}O_4Si_2$ [M–$C_6H_{15}Si+H]^+$ 623.4891, found 623.4887.

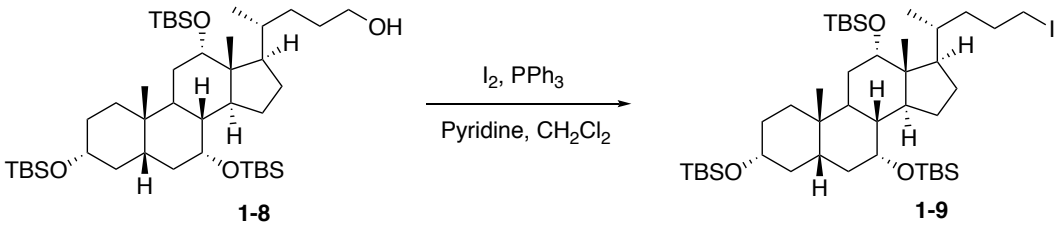

To a solution of mixture of I_2 (1.02 g, 4 mmol), triphenylphosphine (1.15 g, 4.4 mmol) and 0.88 ml anhydrous pyridine (0.32 mL, 4 mmol) in CH_2Cl_2 (18 mL) was added **1-8** (2.63 g, 3.57 mmol) dissolved in CH_2Cl_2 (15 mL) and the mixture was stirred at room temperature for 1 hour. The solvents was removed under vacuum and the residue was purified by silica gel column chromatography (Hexanes : EtOAc = 50 : 1) to give pure iodide **1-9** (2.66 g, 88% yield) as a colorless oil.

1-9: ^{1}H NMR (500 MHz, $CDCl_3$) δ 3.97–3.96 (m, 1H), 3.80–3.79 (m, 1H), 3.36 (tt, *J* = 5.3 Hz, *J* = 10.6 Hz, 1H), 3.16 (m, 2H), 2.42–1.05 (m, 33H, steroidal skeleton), 0.95 (d, *J* = 6.7 Hz, 3H), 0.94 (s, 9H), 0.90 (s, 9H), 0.86 (s, 3H), 0.84 (s, 9H), 0.66 (s, 3H), 0.08 (s, 6H), 0.04 (s, 6H), –0.01 (s, 6H); ^{13}C NMR (125 MHz, $CDCl_3$) δ 73.8, 72.1, 69.5, 47.3, 46, 41.9, 41.4, 40.9, 40.6, 36.9, 35.8, 35.4, 34.8, 31.3, 31, 28.4, 27.8, 26.5, 26.4, 26.1, 25.7, 23.9, 23, 18.3, 12.8, 7.9, –2.6, –2.8, –4.2, –4.4, –5.3; HRMS (ESI) calcd for $C_{36}H_{70}O_3Si_2I$ $[M–C_6H_{15}Si+H]^+$ 733.3908, found 733.3910.

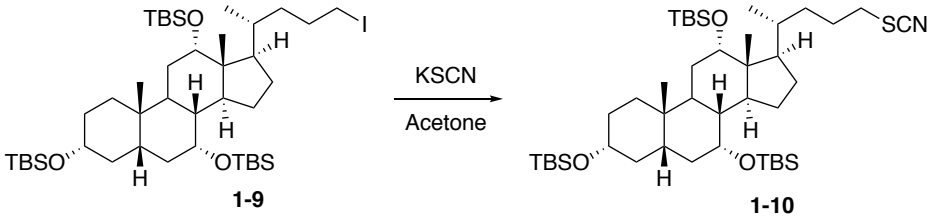

To a solution of iodine **1-9** (2.66 g, 3.14 mmol) in acetone (26 mL) was treated with KSCN (610 mg, 6.28 mmol) in one portion and the reaction was stirred at room temperature for 6 hours until

the TLC indicated the full consumption of the starting material. The solvent was removed under vacuum and the residue was purified by silica gel column chromatography (Hexanes : EtOAc = 30 : 1) to give pure thiocyanide **1-10** (2.27 g, 93% yield) as a colorless oil.

1-10: ^{1}H NMR (500 MHz, $CDCl_3$) δ 3.97 (s, 1H), 3.79 (d, *J* = 2.5 Hz, 1H), 3.36 (tt, *J* = 5.4 Hz, *J* = 10.5 Hz, 1H), 2.92 (m, 2H), 2.28 (ddd, *J* = 4.4 Hz, *J* = 10.1 Hz, *J* = 16.1 Hz, 1H), 2.27–1.05 (m, 31H, steroidal skeleton H), 0.97 (d, *J* = 6.6 Hz, 3H), 0.94 (s, 9H), 0.90 (s, 9H), 0.86 (s, 3H), 0.84 (s, 9H), 0.66 (s, 3H), 0.08 (s, 6H), 0.04 (s, 6H), –0.01 (s, 6H); ^{13}C NMR (125 MHz, $CDCl_3$) δ 73.8, 72.1, 69.5, 47.3, 46, 41.9, 41.4, 40.9, 40.6, 36.2, 35.4, 34.8, 34.6, 34.4, 31.3, 29.7, 28.4, 27.9, 27.3, 26.5, 26.4, 26, 25.7, 23.8, 22.9, 18.2, 12.8, –2.6, –2.7, –4.2, –5.4; HRMS (ESI) calcd for $C_{37}H_{70}NO_3SSi_2$ $[M–C_6H_{15}Si+H]^+$ 664.4615, found 664.4610.

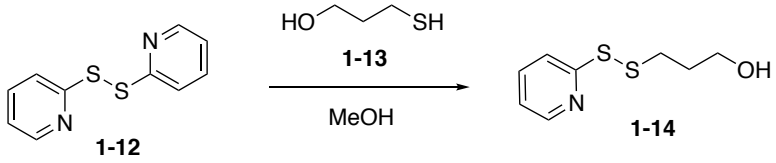

To a solution of 2'-aldrithiol **1-12** (2.64 g, 12 mmol) in MeOH (15 mL) was added 2-mercaptoethanol drop wise (0.28 mL, 4 mmol) over 10 min under nitrogen. The solution was allowed to stir for 2 hours at room temperature. The solvent was removed in vacuum and purified by silica gel column chromatography (Hexanes : EtOAc = 1 : 1) to give **1-14** (660 mg, 82%) as a pale yellow oil.

1-14: ^{1}H NMR (500 MHz, $CDCl_3$) δ; 8.43–8.40 (m, 1H), 7.66–7.59 (m, 2H), 7.09–7.05 (m, 1H), 3.77 (t, *J* = 5.9 Hz, 2H), 3.08 (s, 1H), 2.95 (t, *J* = 7.0 Hz, 1H), 1.93 (m, 1H); ^{13}C NMR (125 MHz, $CDCl_3$) δ 160.1, 149.4, 137.2, 120.8, 120.0, 60.4, 35.6, 31.5.

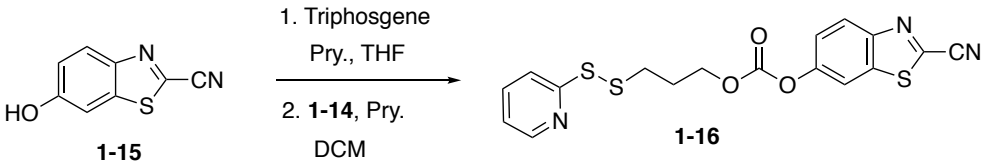

To the solution of triphosgene (593 mg, 2 mmol) in THF (3 mL) was added a solution of **1-15** (87.8 mg, 0.50 mmol) and pyridine (0.44 mL, 0.55 mmol) in THF (6 mL) was added drop wise over 30 min under nitrogen and the mixture was allowed to stir overnight at room temperature. The flask was purged into a solution of aqueous KOH for 10 min and then the solvent was evaporated under vacuum. A solution of **1-14** (100.00 mg, 0.50 mmol) and pyridine (44.18 mL, 0.55 mmol) in DCM (4 mL) was added to the flask under nitrogen and the mixture was allowed to stir for 3 hours. The solvent was evaporated under vacuum and the crude material was purified by silica gel column chromatography (Hexanes : EtOAc = 2 : 1) to give **1-16** (135 mg, 67%) as a colorless oil.

1-16: ^{1}H NMR (500 MHz, $CDCl_3$) δ 8.48 (d, J = 4.0 Hz, 1H), 8.22 (d, J = 9.0 Hz, 1H), 7.86 (d, J = 2.0 Hz, 1H), 7.67 (td, J = 7.8 Hz, J=13.6 Hz, 2H), 7.47 (dd, J = 2.2 Hz, J = 9.0 Hz, 1H), 7.27–7.24 (s, 1H), 7.12–7.09 (m, 1H), 4.42 (t, J = 6.1 Hz, 2H), 2.95 (t, J = 7.0 Hz, 2H), 2.22–2.19 (m, J = 6.6 Hz, 2H); ^{13}C NMR (125 MHz, $CDCl_3$) δ 159.7, 153.0, 151.0, 149.8, 137.0, 126.0, 122.3, 120.9, 119.9, 113.9, 112.6, 67.4, 34.7, 27.8; HRMS (ESI) calcd for $C_{17}H_{13}N_3O_3S_3$ $[C_{17}H_{13}N_3O_3S_3+H]^+$ 404.0197 found 404.0192.

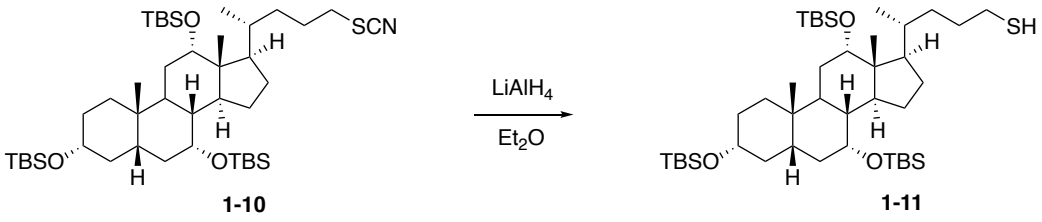

To a suspension of $LiAlH_4$ (152 mg, 5 mmol) in dry Et_2O (9 mL) was slowly added the

thiocyanide **1-10** (2.27 g, 2.92 mmol) dissolved in dry Et_2O (35 mL) under a N_2 atmosphere at 0 °C. The mixture was warmed to room temperature and stirred overnight. The mixture was carefully quenched by the sequential addition of 0.2 mL H_2O, 0.2 mL 15 w/v% aq. NaOH, 0.4 mL H_2O and was then poured into 40 mL of Et_2O and stirred for 30 min. The crude material **1-11** was filtered through Celite and the solvent was removed in vacuum. The crude material was used immediately in the next reaction without further purification.

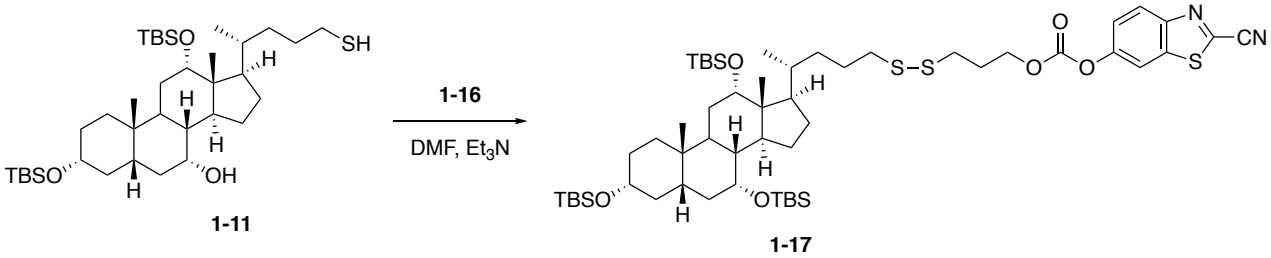

To a solution of thiol **1-11** (76.7 mg, 0.12 mmol) and **1-16** (26.0 mg, 0.09 mmol) in DMF (5 mL) was added Et_3N (0.026 mL, 0.19 mmol) and the reaction was kept at room temperature for 1 hours. Saturated aqueous NH_4Cl solution was added to quench the reaction, and the resulting mixture was extracted with Et_2O. The organic layer was washed with H_2O (3 mL x 3) to remove residual DMF. The organic extract was dried over anhydrous $MgSO_4$, filtered, concentrated, purified by silica gel column chromatography (Hexanes : EtOAc = 4 : 1) to give inseparable mixture of C_3, C_7 (49 %) and C_3, C_{12} (33 %) TBS protected alcohol **1-17** (103 mg, total 82%) as colorless oil over 2 steps.

1-17: ^{1}H NMR (500 MHz, $CDCl_3$) δ ^{13}C NMR (125 MHz, $CDCl_3$) δ 153.0, 151.1, 150.1, 136.9, 126.0, 122.3, 113.9, 112.7, 73.7, 72.9, 72.7, 72.5, 69.3, 68.5, 67.6, 47.5, 46.2, 46.0, 41.8, 41.7, 41.6, 40.7, 40.5, 40.4, 40.0, 39.5, 36.1, 35.6, 35.5, 35.3, 34.8, 34.7, 34.6, 34.5, 31.7, 30.9,

29.7, 28.4, 28.2, 28.1, 28.0, 27.5, 26.6, 26.3, 26.2, 25.9 23.6, 23.4, 23.0, 22.8, 18.2, 17.7, 12.8, 12.6, 3.5, -2.4, -2.8, -4.0, -4.5, -4.6, -5.5.

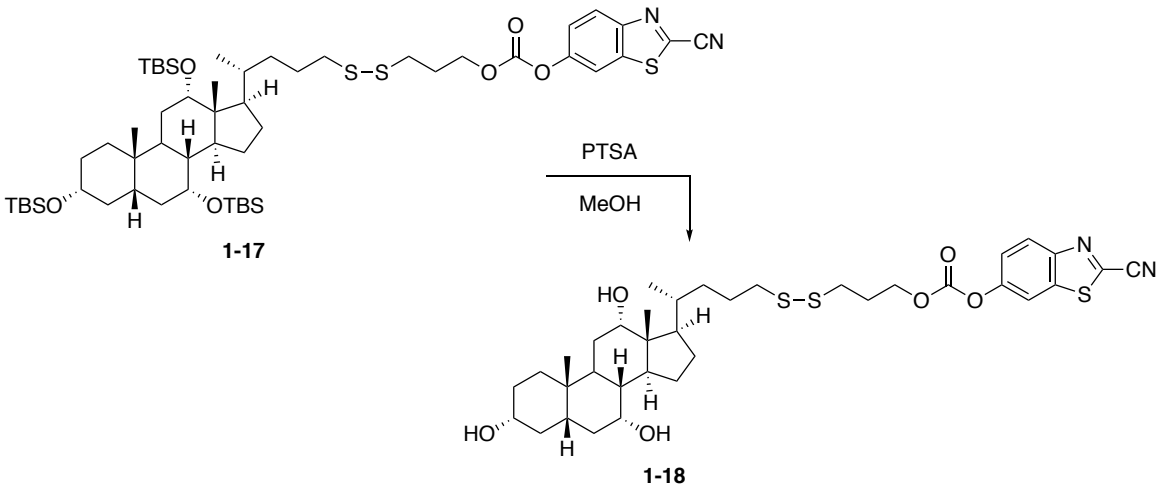

1-17 **1-18**

p-Toluenesulfonic acid (3.4 mg, 0.02 mmol) was added to disulfide compound **1-17** (103 mg, 0.098 mmol) in MeOH (4 mL). The reaction was stirred over night and the solvent was removed under vacuum. The material was extract with H_2O and EtOAc and then the extract was neutralized with 1 N NaOH to remove the residual *p*-toluenesulfonic acid. The final compound was purified in column chromatography (Hexenes : EtOAc = 1 : 5) to afford **1-18** as white solid (62 mg, 90%).

1-18: ^{1}H NMR (500 MHz, $CDCl_3$) δ 8.23 (d, *J* = 9.0 Hz, 1H), 7.88 (d, *J* = 2.2 Hz, 1H), 7.49 (dd, *J* = 2.3 Hz, *J* = 9.0 Hz, 1H), 4.42 (t, *J* = 6.2 Hz, 2H), 4.25 (t, *J* = 6.2 Hz, 2H), 3.99 (ddd, *J* = 2.7 Hz, *J* = 5.7 Hz, *J* = 8.8 Hz, 1H), 3.85 (m, 1H), 3.46 (tt, *J* = 5.3 Hz, *J* = 10.6 Hz, 1H), 2.82 (t, *J* = 7.0 Hz, 2H), 2.75 (t, *J* = 7.2 Hz, 2H), 2.66 (m, 2H), 2.42–1.05 (m, 33H, steroidal skeleton H), 1.00 (d, *J* = 6.5 Hz, 3H), 0.90 (s, 3H), 0.69 (s, 3H); ^{13}C NMR (125 MHz, $CDCl_3$) δ 125.8, 122.2, 113.8, 112.6, 110, 72.7, 71.9, 68.1, 67.2, 66.4, 47.6, 46.7, 42, 41.4, 41.1,

39.4, 35.6, 35.3, 34.8, 34.1, 30.7, 30, 29.4, 28, 27.7, 27.1, 26.2, 25.6, 23.3, 22.4, 17.8, 17.1, 12.4; HRMS (ESI) calcd for $C_{36}H_{50}N_2O_6S_3$ $[M+H]^+$703.2909, found 703.2897.

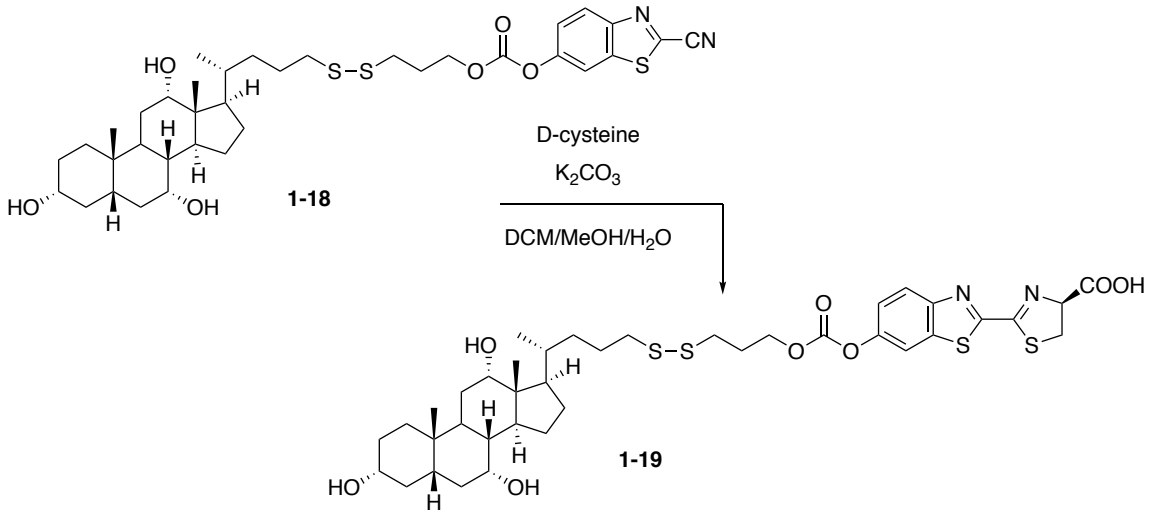

To the solution of D-cysteine hydrochloride (6.6 mg, 0.044 mmol) and **1-18** (30.9 mg, 0.044 mmol) in 4 mL of methanol/CH_2Cl_2 (v/v 1/1) was added a solution of potassium carbonate (5.78 mg, 0.044 mmol) dissolved in water (1 mL) and methanol (2 mL). The reaction was stirred for 5 min at room temperature and then the mixture was quenched with 1 M HCl for acidification. The solvents were removed in vacuum and then the crude material was washed with acetonitrile and hexanes. The extract was dried over anhydrous $MgSO_4$, filtered and concentrated in vacuum, and then the crude material was purified by a silica-based extract column (EtOAc : Methanol = 20 : 1) to give the final compound **1-19** (5.8 mg, 19%) as yellowish solid.

1-19: ^{1}H NMR (500 MHz, $CDCl_3$) δ 7.82 (d, J = 8.2 Hz, 1H), 7.47 (s, 1H), 7.32 (d, J = 7.6 Hz, 1H), 4.25 (dq, J = 2.8 Hz, J = 5.5 Hz, 1H), 4.00 (m, 1H), 3.86 (m, 1H), 3.35 (tt, J = 5.3 Hz, J = 10.6 Hz, 1H), 2.75 (tt, J = 3.2 Hz, J = 4.6 Hz, 1H), 2.42–1.05 (m, 33H, steroidal skeleton H), 1.00 (d, J = 6.4 Hz, 3H), 0.90 (s, 3H), 0.70 (s, 3H).

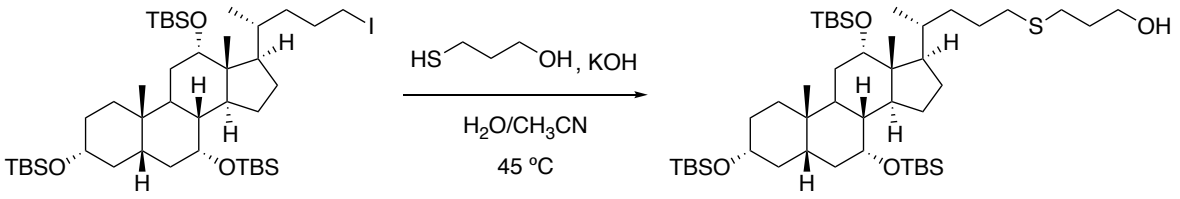

1-9 **1-20**

To a solution of iodine **1-9** (1.27 g, 1.5 mmol) and 3-mercapto-1-propanol (138 mg, 1.5 mmol) in 15 mL of DCM/CH_3CN (v/v 1/1) was treated with KOH (168 mg, 3 mmol) under N_2 and the reaction was stirred at room temperature for 7 hours until the TLC indicated the full consumption of the starting material. The solvent was removed under vacuum and the residue was purified by silica gel column chromatography (Hexanes : EtOAc = 4 : 1) to give mixture of two C_3, C_7 (53 %) and C_3, C_{12} (35 %) TBS-protected alcohol **1-20** (1.07 g, total 88%) as colorless oil.

1-20: ^{1}H NMR (500 MHz, $CDCl_3$) δ ^{1}H NMR (500 MHz, $CDCl_3$) δ 4.01–3.92 (m, 1H), 3.82–3.77 (m, 1H), 3.75 (t, *J* = 6.0 Hz, 2H), 3.42–3.34 (m, 1H), 2.62 (t, *J* = 7.0 Hz, 2H), 2.42–1.05 (m, 33H, steroidal skeleton H), 1.84 (td, *J* = 6.6 Hz, *J* = 13.0 Hz, 2H), 1.00 (d, *J* = 6.4 Hz, 3H), 0.94 (s, 9H), 0.90 (s, 9H), 0.90 (s, 3H), 0.86 (s, 3H), 0.84 (s, 9H), 0.70 (s, 3H), 0.66 (s, 3H), 0.08 (s, 6H), 0.04 (s, 6H), –0.01 (s, 6H); ^{13}C NMR (125 MHz, $CDCl_3$) δ 73.7, 73.0, 72.7, 72.5, 69.3, 68.6, 61.9, 47.5, 47.5, 46.2, 46.0, 41.8, 41.7, 41.6, 40.7, 40.5, 40.4, 40.0, 36.1d, 35.5, 35.3, 35.1, 34.9, 34.7, 34.6, 34.5, 32.6, 31.9, 31.6, 30.9, 28.9, 28.4, 28.2, 28.0, 27.5, 26.6, 26.5, 26.3, 26.3, 26.2, 25.9, 23.6, 23.4, 23.0, 22.8, 18.4, 18.4, 18.2, 17.8, 12.8, 12.6, -2.5, -2.8, -4.0, -4.4, -4.5, -4.6, -5.5.

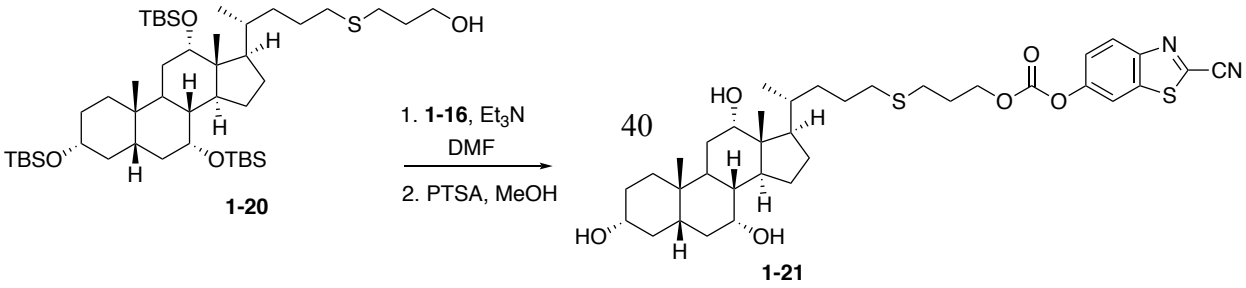

1-20 **1-21**

To a solution of **1-20** (50 mg, 0.06 mmol) and **1-16** (24.2 mg, 0.06 mmol) in DMF (4 mL) was added Et_3N (0.1 mL, 0.07 mmol) and the reaction was kept at room temperature for 1 hours. Saturated aqueous NH_4Cl solution was added to quench the reaction, and the resulting mixture was extracted with Et_2O. The organic layer was washed with H_2O (3 mL x 3) to remove residual DMF. The crude material was used immediately in the next reaction without further purification. *p*-Toluenesulfonic acid (3.4 mg, 0.02 mmol) was added to compound **7** (60.8 mg, 0.06 mmol) in MeOH (4 mL). The reaction was stirred over night and the solvent was removed under vacuum. The material was extract with H_2O and EtOAc and then the extract was neutralized with 1 N NaOH to remove the residual *p*-toluenesulfonic acid. The final compound was purified in column chromatography (Hexenes : EtOAc = 1 : 5) to afford **1-21** as white solid (28.6 mg, 71%) over 2 steps.

1-21: ^{1}H NMR (500 MHz, $CDCl_3$) δ 8.22 (d, *J* = 9.0 Hz, 1H) , 7.88 (d, *J* = 2.2 Hz, 1H) , 7.48 (dd, *J* = 2.2 Hz, *J* = 9.0 Hz, 1H) , 4.41 (t, *J* = 6.2 Hz, 2H), 3.98–3.94 (m, 1H) , 3.85–3.82 (m, 1H) , 3.76 (dd, *J* = 6.1 Hz, *J* = 12.1 Hz, 1H) , 3.46–3.43 (m, 1H) , 2.65 (td, *J* = 7.0 Hz, *J* = 14.3 Hz, 1H) , 2.53–2.50 (m, 2H) , 2.22–2.19 (m, 2H) , 2.11–1.05 (m, 33H, steroidal skeleton H), 0.98 (d, *J* = 5.7 Hz, 3H) , 0.89 (s, 3H) , 0.68 (s, 3H); ^{13}C NMR (125 MHz, $CDCl_3$) δ 126.0, 122.3, 113.9, 73.0, 72.0, 68.4, 68.0, 61.9, 47.3, 46.5, 41.9, 41.5, 39.7, 39.6, 35.4, 35.2, 35.1, 34.7, 34.6, 32.7, 32.6, 32.0, 30.5, 28.9, 28.5, 28.2, 27.6, 26.6, 26.2, 26.1, 23.2, 22.5, 17.7, 12.5.

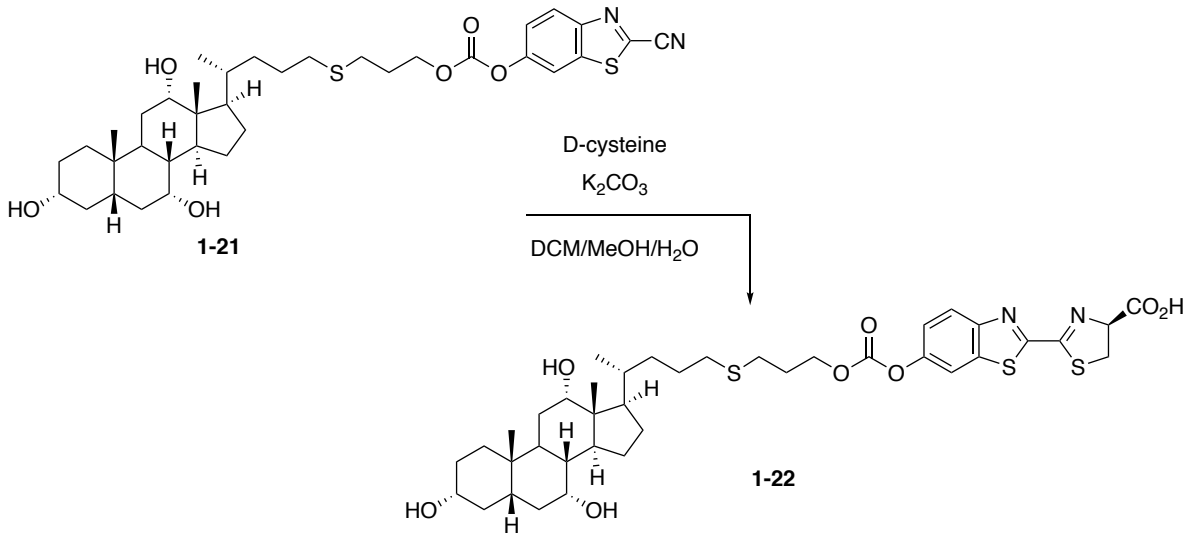

To the solution of D-cysteine hydrochloride (5.2 mg, 0.043 mmol) and **1-21** (28.6 mg, 0.043 mmol) in methanol (2 mL) and CH_2Cl_2 (2 mL) was added a solution of potassium carbonate (5.9 mg, 0.043 mmol) dissolved in water (1 mL) and methanol (2 mL). The reaction was stirred for 5 min at room temperature and then the mixture was quenched with 1 M HCl for acidification. The solvents were removed in vacuum and then the crude material was washed with acetonitrile and hexanes. The extract was dried over anhydrous $MgSO_4$, filtered and concentrated in vacuum, and then the crude material was purified by a silica-based extract column (EtOAc : Methanol = 20 : 1) to give the final compound **1-22** (6.3 mg, 19%) as a yellowish solid.

1-22: ^{1}H NMR (500 MHz, $CDCl_3$) δ 8.22 (d, J = 9.0 Hz, 1H) , 7.88 (d, J = 2.2 Hz, 1H) , 7.48 (dd, J = 2.2 Hz, J = 9.0 Hz, 1H) , 4.41 (t, J = 6.2 Hz, 2H), 3.98–3.94 (m, 1H) , 3.85–3.82 (m, 1H) , 3.76 (dd, J = 6.1 Hz, J = 12.1 Hz, 1H) , 3.46–3.43 (m, 1H) , 2.65 (td, J = 7.0 Hz, J = 14.3 Hz, 1H) , 2.53–2.50 (m, 2H) , 2.22–2.19 (m, 2H) , 2.11–1.05 (m, 33H, steroidal skeleton H), 0.98 (d, J = 5.7 Hz, 3H) , 0.89 (s, 3H) , 0.68 (s, 3H); ^{13}C NMR (125 MHz, $CDCl_3$) δ 126.0, 122.3, 113.9, 73.0, 72.0, 68.4, 68.0, 61.9, 47.3, 46.5, 41.9, 41.5, 39.7, 39.6, 35.4, 35.2, 35.1, 34.7, 34.6, 32.7, 32.6, 32.0, 30.5, 28.9, 28.5, 28.2, 27.6, 26.6, 26.2, 26.1, 23.2, 22.5, 17.7, 12.5.

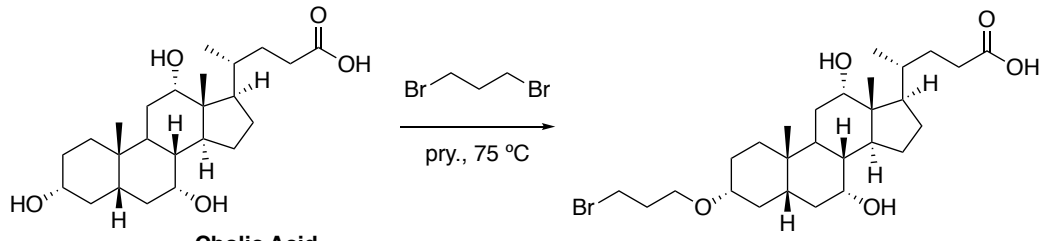

Cholic Acid **1-23**

To a solution of cholic acid (817 mg, 2 mmol) and 1,3-dibromopropane (0.21 mL, 2.1 mmol) in DMF (10 mL) was added *N,N*-diisopropylethylamine (0.73 mL, 4.2 mmol) and then the reaction mixture was stirred overnight. Saturated aqueous NH_4Cl solution was added to quench the reaction, and the resulting mixture was extracted with EtOAc. The organic layer was washed with H_2O (20 mL x 3) to remove residual DMF. The organic extract was dried over anhydrous $MgSO_4$, filtered, concentrated and purified by silica gel column chromatography (Hexanes : EtOAc = 1 : 2) to give **1-23** (921 mg, 87%) as colorless oil.

1-23: ^{1}H NMR (500 MHz, $CDCl_3$) δ 4.18 (t, *J* = 5.9 Hz, 2H), 3.94–3.92 (m, 1H), 3.82–3.80 (m, 1H), 3.44 (dd, *J* = 5.3 Hz, *J* = 11.8 Hz, 2H), 2.35 (t, *J* = 4.1 Hz, 2H), 2.45–1.05 (m, 33H, steroidal skeleton H), 0.96 (d, *J* = 5.4 Hz, 1H), 0.86 (s, 1H), 0.65 (s, 1H); ^{13}C NMR (125 MHz, $CDCl_3$) δ 174.2, 73.1, 71.8, 68.4, 62.0, 47.0, 46.4, 41.6, 41.5, 39.5, 35.3, 35.3, 34.8, 34.7, 31.7, 31.2, 30.9, 30.3, 29.5, 28.1, 27.6, 26.3, 23.2, 22.5, 17.3, 12.5; HRMS (ESI) calcd for $C_{27}H_{45}O_5Br$ $[M+H]^+$ 529.2529 found 529.2548.

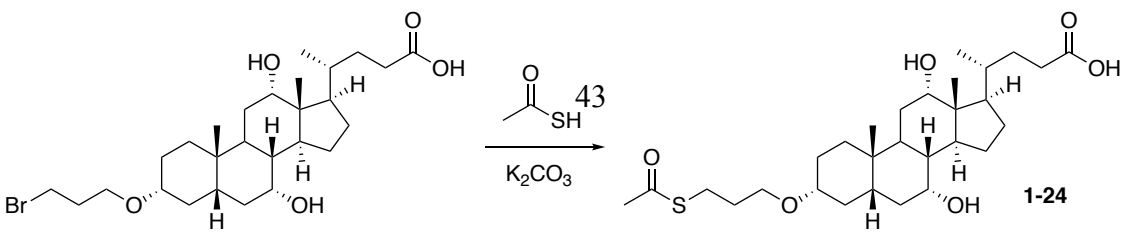

To a solution of **1-23** (530 g, 1 mmol) and thioacetic acid (0.14 mL, 2 mmol) in DMF (4 mL) was treated with K_2CO_3 (138 g, 1 mmol) and the reaction mixture was stirred at room temperature for 5 h. The mixture was diluted with EtOAc, then it was washed with 1N HCl and brine. The solution was extracted with EtOAc and the organic layer was drived over $MgSO_4$, filtered and concentrated in vacuum to afford the crude thioester. The resulting crude product was purified by silica gel column chromatography (Hexanes : EtOAc = 1 : 3) to give **1-24** (341 mg, 65%) as yellow solid.

1-24: ^{1}H NMR (500 MHz, $CDCl_3$) δ 4.08 (t, *J* = 6.1 Hz, 2H), 3.94–3.92 (m, 1H), 3.82–3.80 (m, 1H), 3.42–3.40 (m, 1H), 2.91 (t, *J* = 7.1 Hz, 2H), 2.31 (s, 1H), 2.27–1.05 (m, 33H, steroidal skeleton H), 0.96 (d, *J* = 5.1 Hz, 1H), 0.85 (s, 1H), 0.64 (s, 1H); ^{13}C NMR (125 MHz, $CDCl_3$) δ 195.6, 174.3, 73.0, 71.9, 68.4, 62.6, 47.0, 46.4, 41.7, 41.5, 39.5, 35.3, 34.8, 34.7, 31.2, 30.9, 30.6, 30.4, 28.7, 28.2, 27.5, 26.4, 25.7, 23.2, 22.5, 18.6, 17.3, 12.5; HRMS (ESI) calcd for $C_{29}H_{48}O_6S$ $[M+H]^+$ 525.3226 found 525.3236.

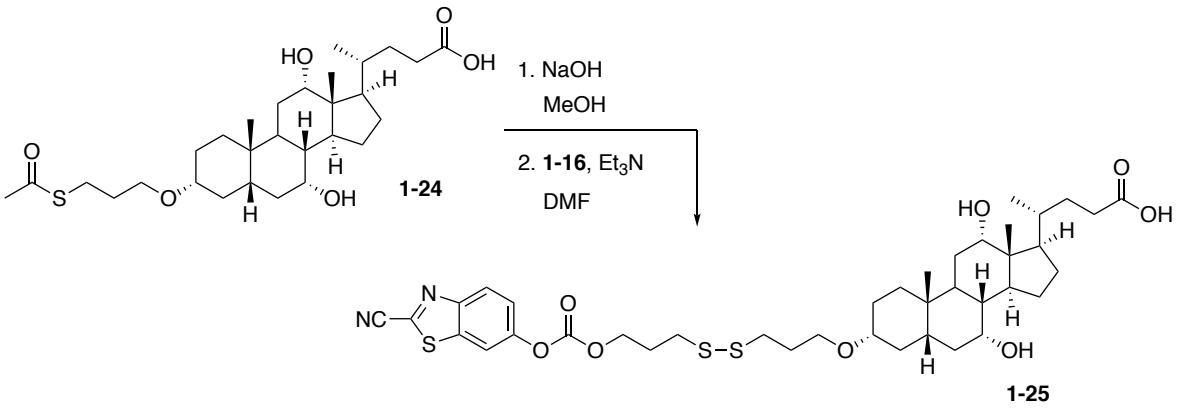

A solution of thioester **1-24** (50 mg, 0.09 mmol) in MeOH (3 mL) was treated with NaOH (7.2 mg, 0.18 mmol) and the reaction mixture was stirred until the TLC indicated the consumption of the starting material. The reaction mixture was stirred at room temperature for 12 h. The mixture was acidified with HCl (1 M) and extracted with CH_2Cl_2 (3 mL×3). The combined organic layers were dried over MgSO4, filtered and concentrated in vacuum to afford the crude thiol.
The crude material was used immediately in the next reaction without further purification.

To a solution of crude thiol (43.5 mg, 0.06 mmol) and **1-16** (24.2 mg, 0.06 mmol) in DMF (4 mL) was added Et_3N (0.1 mL, 0.07 mmol) and the reaction was kept at room temperature for 1 hours. Saturated aqueous NH_4Cl solution was added to quench the reaction, and the resulting mixture was extracted with Et_2O. The organic layer was washed with H_2O (3 mL x 3) to remove residual DMF. The organic extract was dried over anhydrous $MgSO_4$, filtered, concentrated and purified by silica gel column chromatography (EtOAc : MeOH = 10 : 1) to give **1-25** (27.7 mg, 46%) as white solid over 2 steps.

1-25: ^{1}H NMR (500 MHz, $CDCl_3$) δ 8.23 (d, *J* = 9.0 Hz, 1H), 7.88 (d, *J* = 2.1 Hz, 1H), 7.48 (dd, *J* = 2.2 Hz, *J* = 9.0 Hz, 1H), 4.42 (t, *J* = 6.2 Hz, 2H), 4.17 (t, *J* = 6.2 Hz, 2H), 3.98–3.97 (m, 1H), 3.85–3.82 (m, 1H), 3.48–3.25 (m, 1H), 2.82 (t, *J* = 7.0 Hz, 1H), 2.76 (t, *J* = 7.1 Hz, 1H), 2.37–2.34 (m, 1H), 2.27–1.05 (m, 33H, steroidal skeleton H), 0.98 (d, *J* = 6.1 Hz, 1H), 0.89 (s, 1H), 0.68 (s, 1H); ^{13}C NMR (125 MHz, $CDCl_3$) δ 174.2, 126.0, 122.3, 113.9, 113.1, 112.7, 108.9, 72.9, 71.9, 68.3, 67.5, 62.5, 47.1, 42.0, 41.4, 39.8, 39.6, 35.2, 35.1, 34.6, 34.5, 31.2, 30.9, 30.6, 28.4, 28.3, 28.0, 27.5, 26.7, 23.2, 22.6, 17.3, 12.6; HRMS (ESI) calcd for $C_{39}H_{54}N_2O_8S_3$ $[M+H]^+$ 775.3121 found 775.3099.

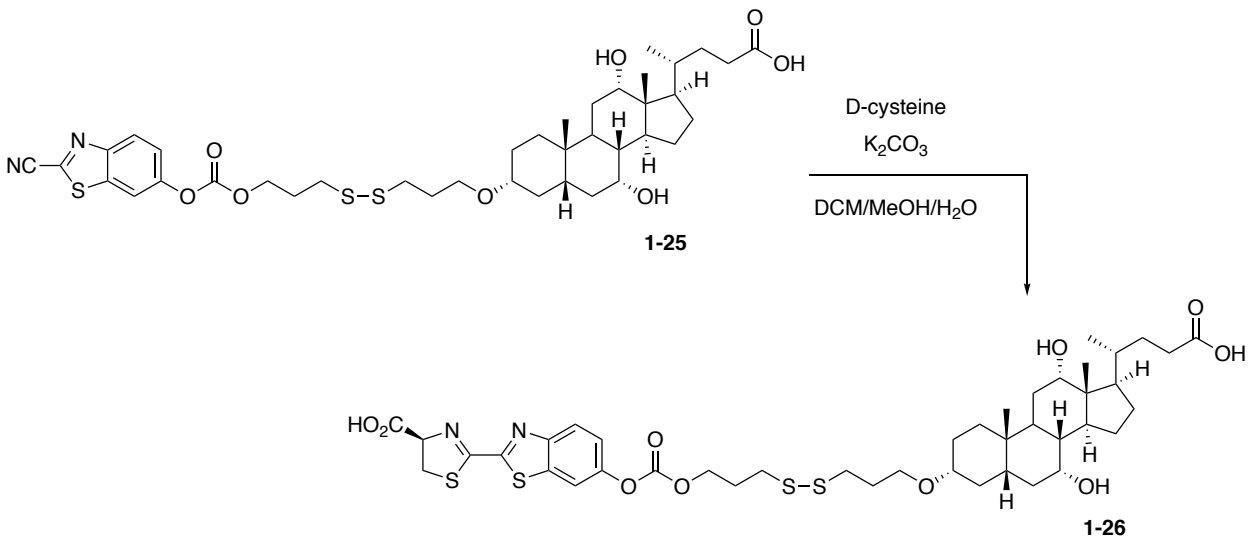

To the solution of D-cysteine hydrochloride (5.2 mg, 0.043 mmol) and **1-25** (28.6 mg, 0.043 mmol) in methanol (2 mL) and CH_2Cl_2 (2 mL) was added a solution of potassium carbonate (5.9 mg, 0.043 mmol) dissolved in water (1 mL) and methanol (2 mL). The reaction was stirred for 5 min at room temperature and then the mixture was quenched with 1 M HCl for acidification. The solvents were removed in vacuum and then the crude material was washed with acetonitrile and hexanes. The extract was dried over anhydrous $MgSO_4$, filtered and concentrated in vacuum, and then the crude material was purified by a silica-based extract column (EtOAc : Methanol = 20 : 1) to give the final compound **1-26** (6.3 mg, 19%) as a yellowish solid.

1-26: ^{1}H NMR (500 MHz, $CDCl_3$) δ 8.23 (d, J = 9.0 Hz, 1H), 7.88 (d, J = 2.1 Hz, 1H), 7.48 (dd, J = 2.2 Hz, J = 9.0 Hz, 1H), 4.42 (t, J = 6.2 Hz, 2H), 4.17 (t, J = 6.2 Hz, 2H), 3.98–3.97 (m, 1H), 3.85–3.82 (m, 1H), 3.48–3.25 (m, 1H), 2.82 (t, J = 7.0 Hz, 1H), 2.76 (t, J = 7.1 Hz, 1H), 2.37–2.34 (m, 1H), 2.27–1.05 (m, 33H, steroidal skeleton H), 0.98 (d, J = 6.1 Hz, 1H), 0.89 (s, 1H), 0.68 (s, 1H); ^{13}C NMR (125 MHz, $CDCl_3$) δ 174.2, 126.0, 122.3, 113.9, 113.1, 112.7, 108.9, 72.9, 71.9, 68.3, 67.5, 62.5, 47.1, 42.0, 41.4, 39.8, 39.6, 35.2, 35.1, 34.6, 34.5, 31.2, 30.9, 30.6, 28.4, 28.3, 28.0, 27.5, 26.7, 23.2, 22.6, 17.3, 12.6.

1.7. References

1. Chiang, J. Y. L.; *J. Lipid Res.* **2009**, *50*, 1955.
2. Thomas, C.; Pellicciari, R.; Pruzanski, M.; Auwerx, J.; Schoonjans, K. *Nat. Rev. Drug Discov*. **2008**, *7*, 678.
3. Pan, X.; Elliott, C. T.; McGuinness, B.; Passmore, P.; Kehoe, P. G.; Hölscher, C.; McClean, P. L.; Graham, S. F.; Green, B. D. *Metabolites* **2017**, *7*, 28.
4. Ackerman, H. D.; Gerhard, G. S. *Front. Aging Neurosci*. **2016**, *8*, 263.
5. Hoffmann, A. F. *Adv Intern Med*. **1976**, *21*, 501.
6. Mertens, K. L.; Kalsbeek, A.; Soeters, M. R.; Eggink, H. M. *Frontiers in Neuroscience* **2017**, *11*, 617.
7. a) Dawson, P. A; Karpen, S. J. *J. Lipid Res.* **2015**, *56*, 1085. b) Lefebvre, P.; Cariou, B.; Lien, F.; Kuipers, F.; Staels, B. *Physiol Rev.* **2009**, *89*, 147.
8. Slijepcevic, D.; van de Graaf, S. F. *J. Dig Dis.* **2017**, *35*, 251.
9. Watanabe, M.; Houten, S. M.; Mataki, C.; Christoffolete, M. A.; Kim, B. W.; Sato, H. *Nature* **2006**, *439*, 484-489.
10. Dawson, P. A.; Lan, T.; Rao, A. *J. Lipid Res*. **2009**, *50*, 2340.
11. a) Day, R. N.; Davidson, M. W. *Chem. Soc. Rev*. **2009**, *38*, 2887. b) Holzinger, F.; Schteingart, C. D.; Ton-Nu, H. T.; Eming, S. A.; Monte, M. J.; Hagey, L. R.; Hofmann, A. F. *Hepatology*. **1997**, *26*, 1263. c) Sharma, R.; Majer, F.; Peta, V. K.; Wang, J.; Keaveney, R.; Kelleher, D.; Long, A.; Gilmer, J. F. *Bioorg. Med. Chem*. **2010**, *18*, 6886. d) Wilton, J. C.; Matthews, G. M.; Burgoyne, R. D.; Mills, C. O.; Chipman, J. K.; Coleman. R. *J. Cell Biol.* **1994**, *127*, 401.

12. A) Ghosh, P.B.; Whitehouse, M.W. *Biochem. J*. **1968**, *108*, 155. b) Maglova, L. M.; Jackson, A. M.; Meng, X. J.; Carruth, M. W.; Schteingart, C. D.; Ton-Nu, H. T.; Hofmann, A. F.; Weinman, S. A. *Hepatology*. **1995**, *22*, 637. c) Yamaguchi, H.; Okada, M.; Akitaya, S.; Ohara, H.; Mikkaichi, T.; Ishikawa, H.; Sato, M.; Matsuura, M.; Saga, T.; Unno, M.; Abe, T.; Mano, N.; Hishinuma, T.; Goto J. *J. Lipid Res*. **2006**, *47*, 1196. d) Májer, F.; Salomon. J. J.; Sharma. R.; Etzbach, S. V.; Najib, M. N.; Keaveny, R.; Long, A.; Wang, J.; Ehrhardt, C.; Gilmer, J. F.; *Bioorg. Med. Chem. Lett*. **2012**, *20*, 1767.

13. Kis, E.; Rajnai, Z.; Ioja, E.; Herédi, S. K.; Nagy, T.; Méhn, D.; Krajcsi, P. *J Biomol Screen*. **2009**, *14*, 10.

14. Kramer, W.; Girbig, F.; Gutjahr, U.; Kowalewski, S.; Jouvenal, K.; Müller, G.; Tripier, D.; Wess, G. *J. Biol. Chem.* **1993**, *268*, 18035.

15. a) Frisch, K.; Jakobsen, S.; Sørensen, M. *J. Nucl. Med.* **2012**, *53*, 772. b) Schacht, A. C.; Sørensen, M.; Munk, O. L.; Frisch, K. *J. Nucl. Med.* **2016**, *57*, 628.

16. Lombaerde, S.; Kersemans, K.; Neyt, S.; Verhoeven, J.; Vanhove, C.; De Vos, F. *Contrast Media Mol. Imaging* **2018**, *2018*, 9.

17. a) Hara-Miyauchi, C.; Tsuji, O.; Hanyu, A.; Okada, S.; Yasuda, A.; Fukano, T.; Akazawa, C.; Nakamura, M.; Imamura, T.; Matsuzaki, Y.; Okano, H. J.; Miyawaki, A.; Okano, H. *Biochem. Biophys. Res. Commun*. **2012**, *419*, 188. b) Kim, J. E.; Kalimuthu, S.; Ahn, B. C. *Nucl. Med. Mol. Imaging*. **2015**, *49*, 3. c) Mezzanotte, L.; Blankevoort, V.; Löwik, C. W.; Kaijzel, E. L. *Anal. Bioanal. Chem*. **2014**, *406*, 5727. d) Dothager, R. S.; Flentie, K.; Moss, B.; Pan, M. H.; Kesarwala, A.; Piwnica-Worms, D. *Curr. Opin. Biotechnol*. **2009**, *20*, 45.

18. a) Jones, L. R.; Goun, E. A.; Shinde, R.; Rothbard, J. B.; Contag, C. H.; Wender, P. A. *J. Am. Chem. Soc.* **128**, *20*, 6526. b) Wenden, P. A.; Goun, E. A.; Jones, L. R.; Pillow, T. H.; Rothbard, J. B.; Shinde, R.; Contag, C. H. *Proc. Natl. Acad. Sci. U.S.A.* **2008**, *104*, 10340.

19. Henkin, A. H.; Cohen, A. S.; Dubikovskaya, E. A.; Park, H. M.; Nikitin, G. F.; Auzias, M. G.; Kazantzis, M.; Bertozzi, C. R.; Stahl, A. *ACS Chem. Biol*. **2012**, *7*, 1884.

20. Ticho, A. L.; Lee, H.; Gill, R.K.; Dudeja, P. K.; Saksena, S.; Lee, D.; Alrefai, W. A. *Am. J. Physiol Gastrointest Liver Physiol*. **2018**, DOI: 10.1152/ajpgi.00133.2018.

21. Hofmann, A. F.; Hagey, L. R. *Cell. Mol. Life Sci*. **2008**, *65*, 2461.

22. Kramer, W.; Stengelin, S.; Baringhaus, K.-H.; Enhsen, A.; Heuer, H.; Becker, W.; Corsiero, D.; Girbig, F.; Noll, R.; Weyland, *C. J. Lipid. Res*. **1999**, *40*, 1604.

23. Bhat, L.; Jandeleit, B.; Dias, T. M.; Moors, T. L.; Gallop, M. A. *Bioorg. Med. Chem. Lett*. **2005**, *15*, 85.

24. (a) Hofmann, A. F.; Mysels, K. J. *J. Lipid Res*. **1992**, *33*, 617. (b) Balakrishnan, A.; Polli, J. E. *Mol. Pharm*. **2006**, *3*, 223.

Chapter 2

Application of ‘Click’ Chemistry in Bioorthogonal Chemistry

2.1. Bioorthogonal Chemistry

Bioorthogonal chemistries[1] involve selective covalent tagging the biomolecule of interest with a synthetic probe as shown in **Figure 2.1**.

Figure 2.1. Overview of bioorthogonal chemistry

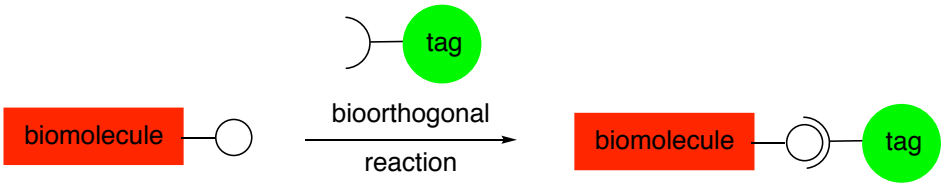

For over two decades, numerous unique transformations have developed and incorporated into the bioorthogonal toolkit. The majority of unique transformations used in the development of bioorthogonal tools are applicable to protein tagging and studies of lipids, glycans, and other biomolecules. However, the reactions differ widely in relation to their rates, selectivities, and other attributes. In bioorthogonal reaction, the reactants should be metabolically, thermodynamically, and kinetically stable and not toxic to living systems. The reaction should also produce stable covalent linkages without generating innocuous byproducts. Additionally, the bioorthogonal moieties should react selectively under suitable biological conditions such as ambient pressure and temperature, aqueous conditions, and neutral pH, without cross-reacting with the chemical functionalities in living cells.[2,3] Although it is challenging to meet the criteria for bioorthogonal reactions, numerous reactions have been exploited, which demonstrate excellent selectivity and biocompatibility in living systems. The challenges of designing suitable reactions that meet the set of criteria have motivated chemists to investigate transformations in the biological environment that match the conditions for

bioorthogonality. The bioorthogonal transformations can be categorized as either polar reactions or cycloadditions.

2.2. Bioorthogonal Chemistry Methods

2.2.1. Polar Reactions

Polar reactions involve chemical transformations between electrophiles and nucleophiles. Although there are numerous polar reactions to the form covalent bonds, only a small set of these reactions is suitable under a typical biological environment.

Figure 2.2. Ketone condensation and Staudinger ligation

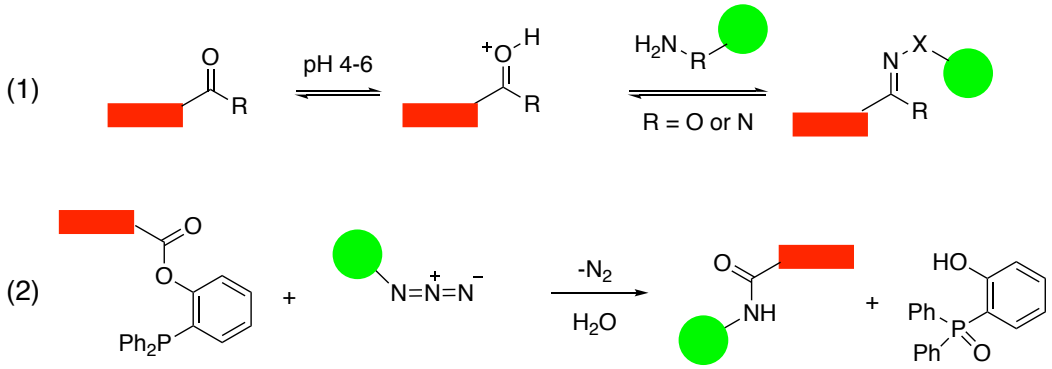

The most well-established polar reactions are aldehyde and ketone condensations (1). Aldehydes and ketones[4] are rarely presence in proteins or biopolymers, which can avoid unnecessary labeling. In order for visualization and retrieval, strong nucleophiles with an α-effect, such as hydroxylamines and hydrazines, are used under acidic conditions to generate a stable oximes and hydrazones. However, the major drawbacks of these condensations are slow kinetics[5] and low labeling efficiency, which requires high concentration of labeling reagents to

achieve good labeling effects. These disadvantages also can cause toxicity and generate high background signal. Also, it requires acidic conditions, which is difficult to obtain inside most cellular compartments.[6] Furthermore, the overall reactivity in the inside of living cells might not be optimal for these reactions, and nucleophiles may undergo side-reactions with carbonyl-bearing metabolites.

Alternatively, formation of an amide linkage via the Staudinger ligations[7] (2) drew significant attentions since the required functional groups for this transformation such as alkyl azide and triarylphosphine are not found in eukaryotes and non-toxic to biological system. However, in vivo, phosphines are prone to oxidation, which lowers the effectiveness of this method. Overall, polar reactions display slow reaction rates, thus most of them are non-optimal in biological settings.[8]

2.2.2. Cycloaddition

Recent development in bioorthogonal transformations have proven that cycloadditions such as [3+2] dipolar cycloaddition and Diels-Alder reactions are highly effective for derivatizing biomolecules. In general, cycloaddition reactions display faster reaction rates and higher selectivity towards target-labeling than polar reactions.

The copper-catalyzed azide-alkyne cycloaddition know as "click" chemistry (3),[9,10] are shown in **Figure 2.3**. In aqueous environment, treating terminal alkynes with alkyl azides in the presence of a Cu(I) catalyst affords trizole cycloadducts. The simplicity and speed of the overall process of this transformation are often exploited for biomolecule visualization, particularly in fixed cells. A "click" reaction proceeds significantly more rapid than the Staudinger ligation in biological settings even though both reactions utilize alkyl azides as a reaction counterpart.

However, a copper catalyst may toxic to the living system while reducing its concentration slows down the reaction rates considerably.[11]

Figure 2.3. Cycloadditions for bioorthogonal chemistry

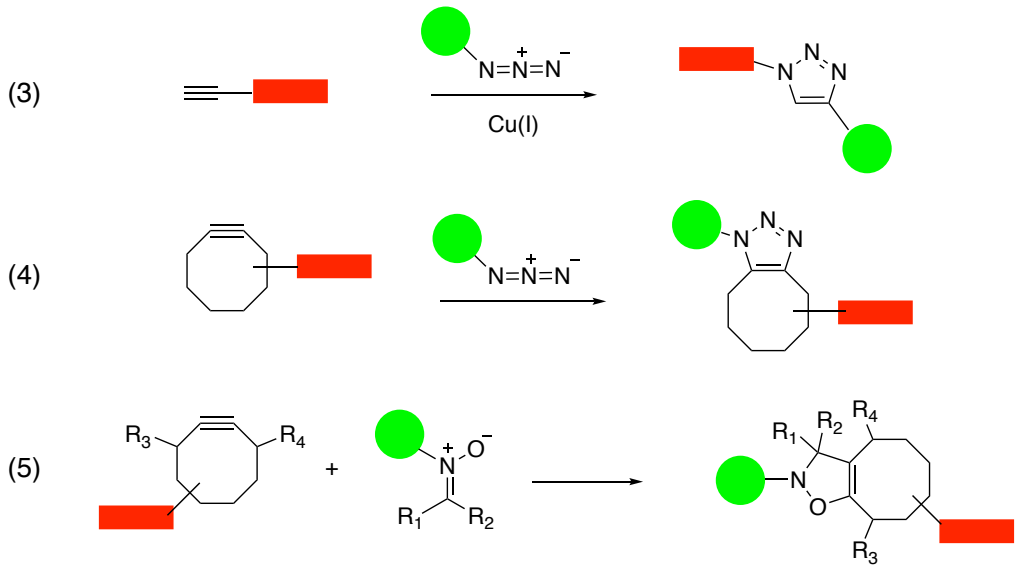

In the absence of copper catalyst, ring strained alkynes,[12,13] cyclooctynes (4), are utilized to drive the azide-alkyne reaction. When alkyne is introduced into the cyclooctane system, the linear geometry of alkyne is "bent" by 17° which induces cycloaddition with azide upon a bond breakage without a metal catalyst. Another cyclooctyne-activated [3+2] cycloaddition can be promoted by nitrones (5).[14] This reaction has been demonstrated faster reaction rates among all other azide-based cycloadditions, however, stability of nitrones in cellular environment has been questioned due to hydrolysis, and requires further studies. Overall, the high strained cyclooctyne moiety approaches are limited due to large size and hydrophobic nature of cyclooctyne that can distribution and biological properties of biomolecules.

Figure 2.4. Photo-induced cycloadditions

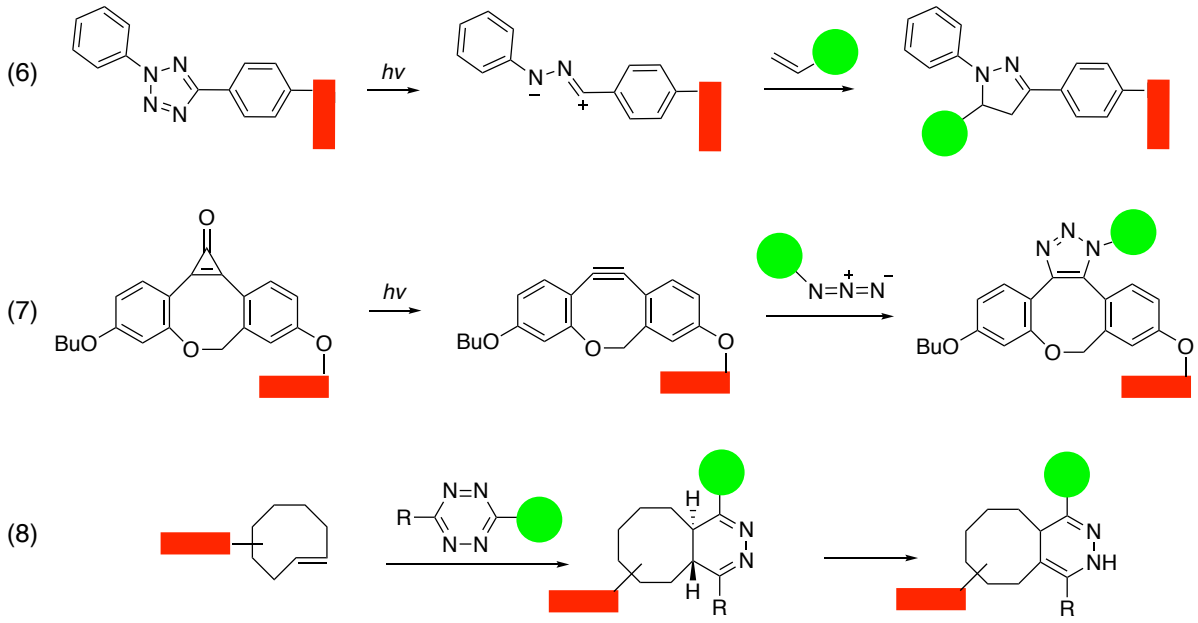

Photo-click chemistry is often described as "on-demand" based reaction in which functional groups become reactive only after being exposed to light (6).[15,16] Photo-activatable tetrazoles[17] and cyclopropenones bearing oxa-dibenzocyclooctanes[18] (7) are shown in **Figure 2.3** as representative examples. Upon being exposed to pulsed light, tetrazoles form nitrole imine intermediates, likewise cyclopropenones bearing oxa-dibenzocyclooctanes generate reactive cyclooctynes intermediates after decarbonylation. Both intermediates undergo [3+2] cycloaddition with their counterparts, terminal alkenes or azides, to generate pyrazoline and triazole, respectively. This "on-demand" tagging approach is primarily used when stability of reagents in biological environments is suspected.[19]

An inverse electron-demand Diels-Alder reactions of strained alkene such as *trans*-cyclooctene with 1,2,4,5-tetrazines (8) exhibit the fastest bioorthogonal transformations.[20] Steric and electronic modifications of tetrazines and different ring sizes of cycloalkene have been demonstrated for tuning a rate of reactions.[21,22] For instance, most tetrazines react faster with

trans-cyclooctenes than cyclopropenes, however, sterically hindered tetrazines exhibit a faster reaction rate with cyclopropenes than *trans*-cyclooctenes. Additionally, substituents added on cyclopropenes can increase their stability, thus preventing polymertization, yet they lower the reaction rate considerably. The cycloaddition of *trans*-cyclooctenes (8) has been extensively utilized in biomedical applications and in live animal imaging.

Other bioorthogonal chemistries based on a C–C bond formation, such as ruthenium-catalyzed olefin metathesis[23] and palladium-catalyzed[24] cross couplings such as Suzuki-Miyaura coupling, have been explored for their applications in biological system.

2.3. Alkyne Cholesterol

2.3.1. Cholesterol Functions in Liver and Intestine

Cholesterol is an important lipid element of eukaryotic membranes, which play significant regulatory and structural functions in eukaryotic membranes. The cellular levels of cholesterol are controlled by complex mechanisms, which regulate its uptake, synthesis, distribution, and elimination. Cholesterol has an extensive impact on numerous cellular processes and the metabolic precursor of steroid and oxysterols hormones that contain potent effects on metabolism, cell signaling, and gene expression. A subgroup of the cholesterol, sterol, plays important roles in Hedgehog (Hh) signaling, which is an approach used in numerous aspects of adult stem cell maintenance, embryonic development, and multiple human cancers.

Figure 2.5. Nomenclature of cholesterol

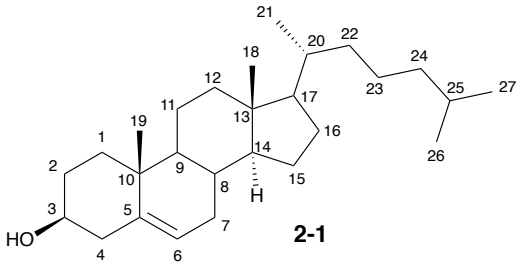

2-1

2.3.2. Fluorescent Cholesterol Probes

Numbering system for cholesterol **2-1** is shown in **Figure 2.5**. One approach used in for imaging with sterols is based on fluorescent derivatives of cholesterol (Chol) where the isooctyl tail is replaced with a fluorophore moiety (such as NBD), or the fluorophore moiety is appended to the 3β-OH group.[25] However, this approach has a limited applicability becasue the bulky fluorophores significantly modify the structural characteristics of the cholesterol framework.

Figure 2.6. Sterol imaging with dehydroergosterol **2-2** and cholestatrienol **2-3**

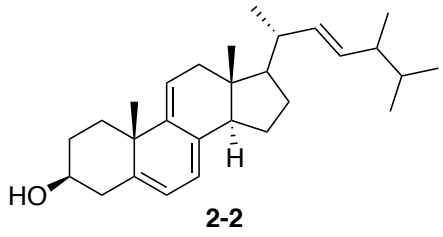

2-2

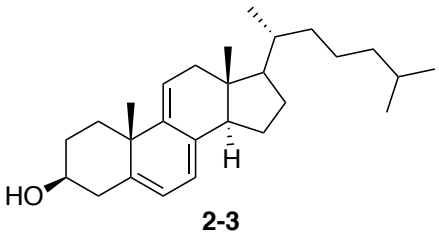

2-3

In order to minimize undesirable interactions, another approach involving dehydroergosterol **2-2** and cholestatrienol **2-3** was developed, where the conjugated double bonds on these molecules display fluorescence.[26]. These visible simulators of cholesterols mimic activity of cholesterol in cells, however, this method has a severe limitation due to the improper fluorescence properties of the molecules such as poor fluorescence characteristics and short

excitation wavelengths (high phototoxicity) that can damage the living system. An indirect visualization approach has been developed based on fluorescent polyene macrolide antibiotics that bind to cholesterol such as filipin and nystatin. This approach is vulnerable to artifacts and has distressed fluorescence properties such as poor photostability, low extinction coefficients and short excitation wavelengths. To increase photostability, fluorescent conjugates of theonellamides, which was isolated from marine scrapers, has been employed.

2.3.3. Alkyne Cholesterol Probe

In 2015, Salic and Welti reported C_{19}-ethynyl cholesterol **2-4** for sterol microscopy by using copper catalyzed cycloaddtion ('click' chemistry) with fluorescent azide (**Figure 2.7**).[27] In this approach, the C_{19}-methyl group was homologated by one carbon to form a terminal alkyne moiety. It was noted that modifying C_{19} methyl group has several advantages, including: 1) C_{19} position is easy to modify, 2) axially-oriented terminal alkyne increases accessibility for 'click' reaction, and 3) the structural similarity between this probe and the natural counterpart ensures the biological function of the probe.

Figure 2.7. C_{19}-Alkyne cholesterol

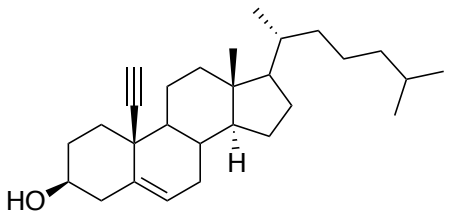

2-4

The synthesis was started with Wohl-Ziegler reaction of acetate **2-5** with NBA and $HClO_4$ followed by $Pb(OAc)_4$-mediated cyclization to give bromohydrin **2-6 (Scheme 2.1)**.

Treating **2-6** with Zn in AcOH/H_2O followed by oxidation of primary alcohol with PCC afforded aldehyde **2-7**. Wittig olefination with chloromethyltriphenylphosphonium chloride generates **2-8**, which upon treating with *n*-BuLi resulted in alkyne **2-4**.

Scheme 2.1. Synthesis of C_{19}-modified cholesterol

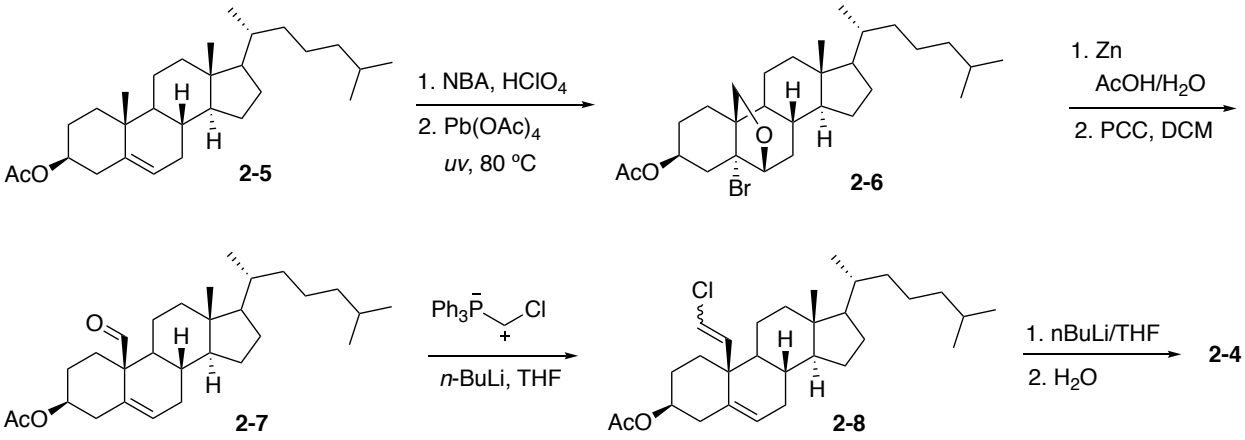

2.4. C_{27}-Alkyne Cholesterol

C_{27}-Alkyne cholesterol **2-9** was synthesized as a probe to explore the function of cholesterol in cells. We envision alkyne cholesterol containing a C_{27}-modified side chain is similar the natural cholesterol. This Probe will be also used in intestinal and liver cells to see lipid-protein interactions of cholesterol.

Figure 2.8. C_{27}-Alkyne cholesterol

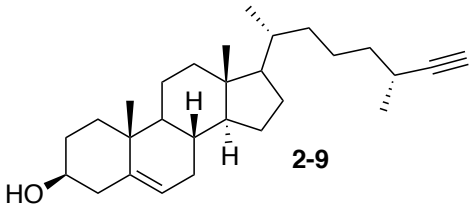

2.4.1. Synthesis of C_{27}-Alkyne Cholesterol

We synthesized the C_{27}-alkyne cholestrol to investigate sterol activity in liver and intestinal cells and the synthetic route is based on the route developed by Kurzchalia and Knölker.[28] The synthesis was commenced with Clemmensen reduction of diosgenin **2-10** with Zn and HCl to give triol **2-11**. TBS protection of two most reactive hydroxyl groups followed by mesylation of C_{12}-hydroxyl group with MsCl provides compound **2-12**. The mesylate was displaced with a hydride by using $LiAlH_4$ and subsequent deprotection of TBS ethers with catalytic amount of PPTS provides C_{27}-hydroxylcholesterol **2-13**. Regioselective oxidation of C_3-alcohol with DMP followed by homologation of one carbon with the Bestmann reagent and K_2CO_3 afford alkyne cholesterol **2-9**.

Scheme 2.2. Synthesis of C_{27}-alkyne cholesterol

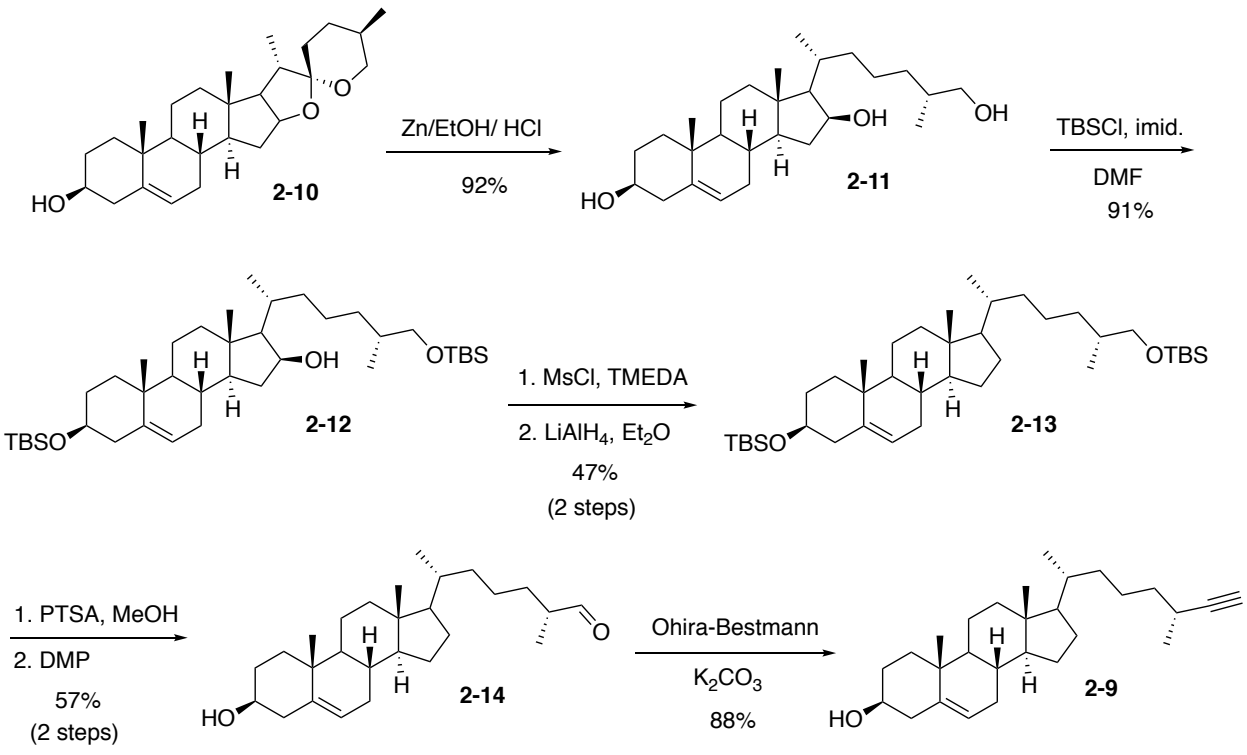

2.4.2. Bioassay of C_{27}-Alkyne Cholesterol

In order to test cholesterol functions in cells, C_{27}-alkyne cholesterol will hypothetically be transported into Caco-2 intestinal epithelial cell, which will transiently transfected with cholesterol transporter, NPC1L1. 10 μM alkyne cholesterol was prepared with mixed micelles and then cell was pretreat with 50 μM ezetimibe (EZE), inhibitor of NPC1L1, or DMSO for an 1 h. Micelles with EZE or DMSO was added in cells and then cell was incubated for 2, 4, or 6 h. Cells were harvested and lipids are extracted with methanol/chloroform. The collected lipid sample was dried, and used to perform a "click" reaction with an azide reporter, 3-azxido-7-hydroxy coumarin. The "click" reaction was initiated with $CuSO_4$ and TLC data processed in fluorescence imager. The bioassay data will not be further discussed in the following section.

2.5. Bile Acid Interaction-based Protein Mapping

2.5.1. Photo-activatable Proteome Probe

Figure 2.9. Overview of photo-activatable proteome Probe

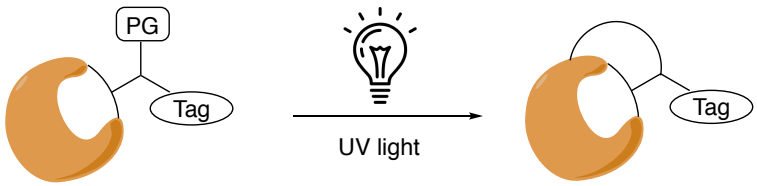

Despite improved knowledge on bile acid (BA) signaling, most therapeutic and research explorations are focused only on the plasma membrane bound G protein-coupled receptor 5 (TGR5) and the nuclear farnesoid X receptor (FXR), which are well-described BA receptors. The general scheme of photo-activatable group (PG) binding to a target protein activated by UV light is shown in **Figure 2.9**. Photo-affinity labeling is an approach of target identification that

provides an immediate proteome profiling and molecular interactions in living cells. A PG is used to create a covalent bond between the probe and targets, and a tag (receptor or analytical handle) allows visualization of probe-target interactions with alkyne cycloaddition with fluorophore-azide or biotin-azide.

2.5.2. Types of Photo-activatable Method

There are four types of photo-activatable groups, aryl azide **1-30a**, benzophenone **1-30b**, aryl diazirines **1-30c** and alkyl diazirines **1-30d**. These groups are activated by wavelengths of 260 nm, 320–360 nm and 340–380 nm, respectively (**Figure 2.10)**. Aryl azide is commonly used for crosslinking experiments because installation of azide on aromatic ring is relatively easy. Many bioactive compounds have an aromatic moiety, therefore, introduction of an azide moiety can be achieved without significant change of structures. However, the major drawbacks of aryl azide are the short activation wavelength that can damage the biological system and low crosslinking efficincy. Benzophenone has a good labeling potential and long excitation wavelength. Nevertheless, the main limitation is its bulkiness that can cause unfavorable interferences and production of non-specific background labeling due to long irradiation time. Even though a diazirine moiety shows disadvantages such as low carbene generation rate after photolysis and a subsequent crosslink reaction often competes with intramolecular rearrangement to form an alkene, it is a highly useful photo-activatable group to study protein-protein interactions. The main advantages are: activation with long wavelength minimizing the damage to biological system, stability toward acid/basic conditions, its compact size that minimize undesirable interference with labeling of native targets.

Figure 2.10. Photo-activatable groups

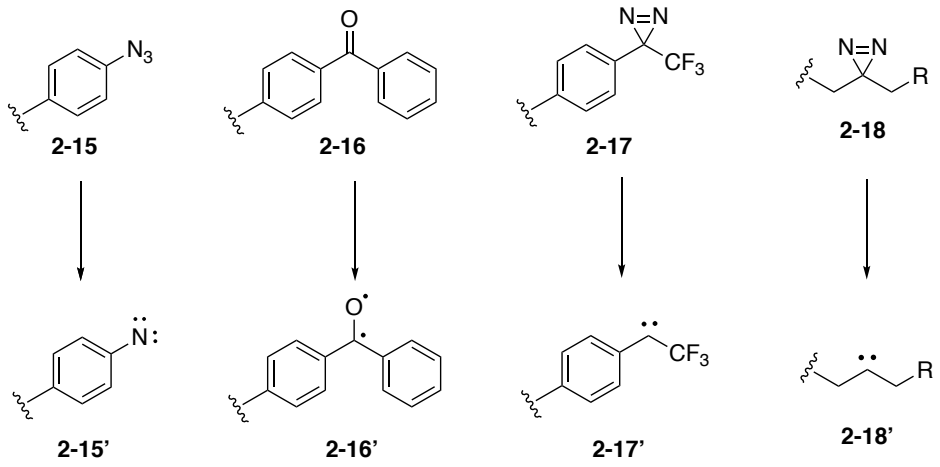

2.6. BA and Its Protein Interactions

BA receptors such as TGR5 and FXR have provided information about unique actions of BAs as signaling hormones useful in human physiological and diseases. Thus, there is a need to study novel BA-interacting proteins existing in an intestinal cell line, and if so, what are the roles of these unknown proteins and whether they can be exploited for producing BA-base remedies and drug target therapies.

2.7. Photo-reactive Alkyne BA for Protein Interaction Profiling

We synthesize photo-reactive alkyne BA to study protein-protein interactions in various cell lines including intestinal or liver cells (**Figure 2.11)**. With this approach, we can identify BA-interacting proteins and their novel functions in live cells. This may even lead to discoveries of functional pathways related to disease. Once photo-activatable probe such as **2-19** gets into the cells, it would form a covalent bond with BA-interacting proteins upon light-activation. Subsequently, under copper-catalyzed conditions, a fluorophore-azide will be reacted with the alkyne moiety of the cross-liked proteins for visualization.

Figure 2.11. Photo-reactive alkyne BA

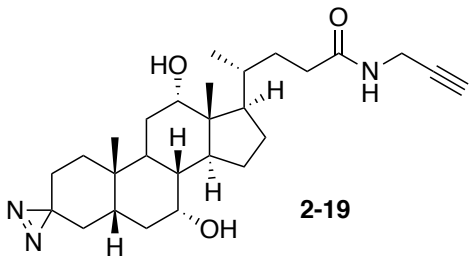

2-19

2.7.1. Synthesis of Photo-reactive Alkyne BA

The synthesis commences with protection of three hydroxyl groups of cholic acid with acetic anhydride to generate **2-20 (Scheme 2.3)**. Subsequently, esterification of the carboxylic acid moiety followed by deprotection of the C_3-OAc in acidic methanol provided ester **2-21**. The C_3-alcohol **2-20** was oxidized with DMP to yield ketone **2-22** and then subsequent diazirine formation was conducted to afford compound **2-23**. Deprotection of acetyl groups and hydrolysis of the methyl ester with NaOH in MeOH provide **2-24**. In the final step, Carboxylic acid **2-24** was conjugated with propargyl amine and HBTU to provide a final product **2-19**.

Scheme 2.3. Synthetic routes for photo-activatable alkyne-conjugated cholic acid

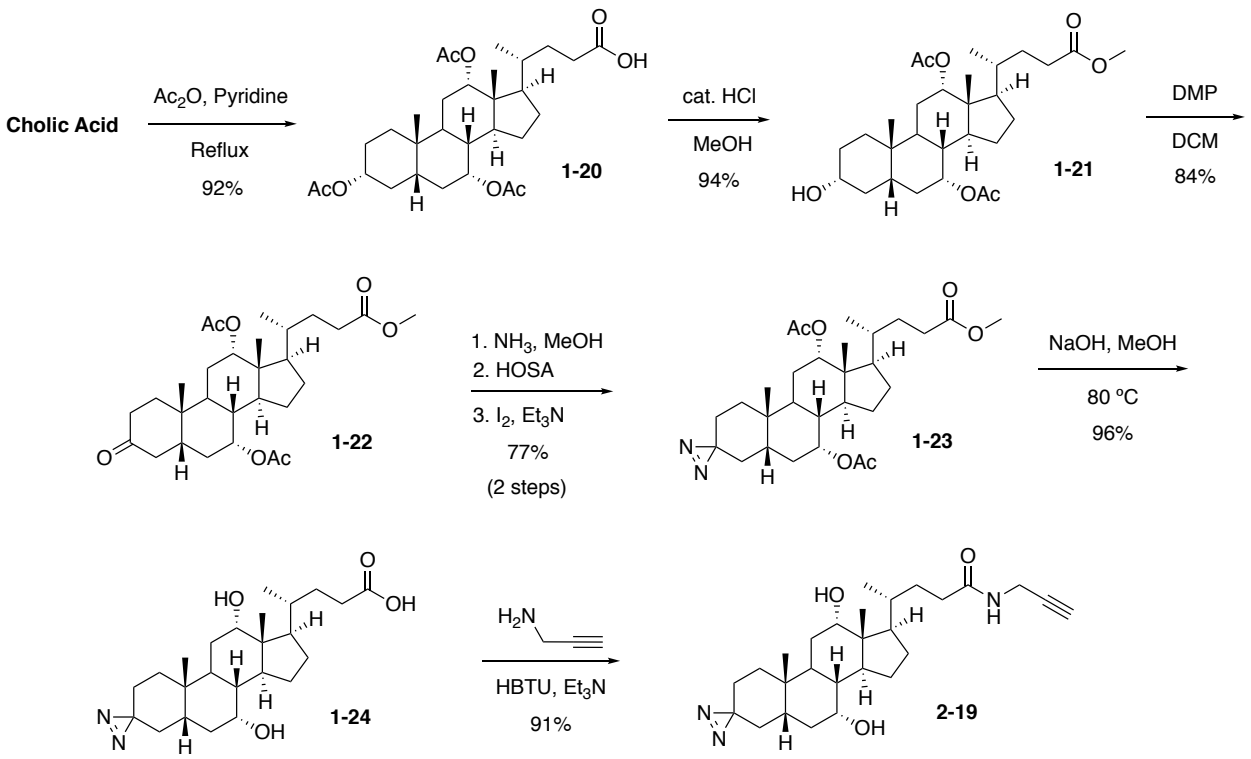

2.8. Conclusion

The cholesterol and a photo-activatable alkyne-conjugated BA probes have been developed for the application of "click" chemistry in biological system. The cholesterol transporter probe has been used for a sterol imaging with an azide reporter and 3-azxido-7-hydroxy coumarin in Caco-2 cells (data is not shown). The photo-activatable alkyne-conjugated BA probes for proteomic study have been synthesized for the investigation of protein interactions of BAs in intestinal cells and liver cells. This synthesis route is efficient and economical starting from readily available cheap cholic acid. Further investigations on the cholesterol transporter probe and proteomic study with various cell lines are currently underway in collaboration with the Alrefai lab.

2.9. Experiment Details

2.9.1. General Information

Reactions were carried out in oven or flame-dried glassware unless otherwise noted. Compounds were purchased from Aldrich or Acros or TCI America unless otherwise noted. Toluene and diethyl ether (Et_2O) was distilled over calcium hydride under nitrogen atmosphere. Tetrahydrofuran (THF) was distilled over sodium and benzophenone under nitrogen. Flash chromatography was performed using silica gel 60 Å (32−63 mesh) purchased from Silicycle Inc. Analytical thin layer chromatography (TLC) was performed on 0.25 mm E. Merck pre-coated silica gel 60 (particle size 0.040–0.063 mm). Yields refer to chromatographically and spectroscopically pure compounds unless otherwise stated. ^{1}H NMR and ^{13}C NMR spectra were recorded on a Bruker DR-500 spectrometer. Multiplicities are indicated by s (singlet), d (doublet), t (triplet), q (quartet), qn (quintet), sext (sextet), m (multiplet), b (broad), and app (apparent). ^{1}H NMR signals that fall within a ca. 0.3 ppm range are generally reported as a multiplet, with a single chemical shift value corresponding to the center of the peak. Coupling constants, *J*, are reported in Hz (Hertz). Electrospray ionization (ESI) mass spectra were recorded on a Waters Micromass Q-Tof Ultima in the University of Illinois at Urbana–Champaign. Electron impact (EI) mass spectra and Chemical Ionization (CI) mass spectra were obtained using a Micromass 70-VSE in the University of Illinois at Urbana-Champaign.

2.9.2. Synthesis of C_{27}-alkyne cholesterol

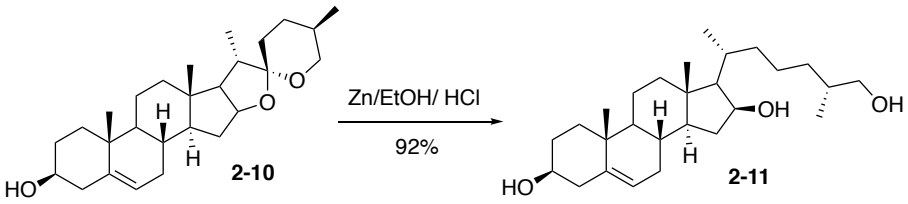

Zinc dust (90.0 g, 1.376 mol) and diosgenin **2-10** (4.5 g, 11.0 mmol) were mixed in ethanol (1 L) and the mixture was heated at reflux. Concentrated aqueous hydrochloric acid (800 mL) was added to the reaction mixture over a period of 1 h and heating was continued for a further 30 min. Unreacted zinc was removed by filtration of the hot reaction mixture. After cooling to room temperature, water (600 mL) and then EtOAc (600 mL) were added until the layers separated. The aqueous layer was extracted with EtOAc (2 x 300 mL). The combined organic layers were washed with a saturated solution of $NaHCO_3$ (100 mL) and brine (100 mL) and then dried over anhydrous $MgSO_4$, filtered, concentrated. Recrystallization of the crude product from ethanol/water (1:1) provided pure **2-11**, as a white solid (4.23g, 92%).

2-11: ^{1}H NMR (500 MHz, MeOH-d4) δ 5.34–5.32 (m, 1H), 4.31–4.28 (m, 1H), 3.41–3.39 (t, 2H), 3.34–3.31 (m, 1H), 2.22–2.19 (m, 3H), 2.42–1.05 (m, 33H, steroidal skeleton H); ^{13}C NMR (125 MHz, $CDCl_3$) δ 140.9, 120.9, 71.3, 71.0, 67.2, 61.6, 54.4, 50.3, 48.0, 47.9, 47.7, 47.5, 47.3, 42.0, 41.7, 40.0, 37.2, 36.7, 36.3, 36.0, 35.5, 33.4, 31.6, 31.5, 30.9, 29.9, 23.6, 20.6, 18.6, 17.6, 15.8, 12.2.

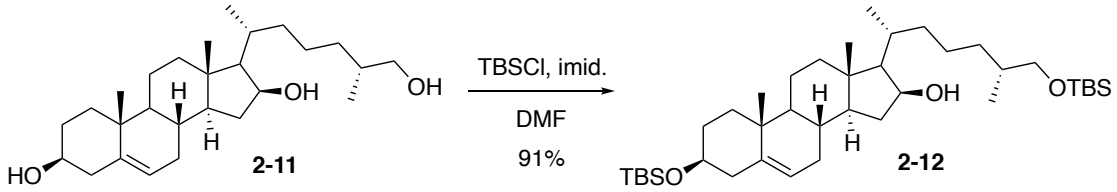

To a solution of **2-11** (1.0 g, 2.4 mmol) and imidazole (340 g, 5 mmol) in DMF (8 mL) was added TBSCl (753.6 mg, 5 mmol) and then the reaction was kept at room temperature overnight. Saturated aqueous NH_4Cl solution was added to quench the reaction, and the resulting mixture was extracted with Et_2O. The organic layer was washed with H_2O (20 mL x 3) to remove residual DMF. The organic extract was dried over anhydrous $MgSO_4$, filtered, concentrated and purified by silica gel column chromatography (Hexanes : EtOAc = 5 : 1) to give **2-12** (1.41 g, 91%) as a white solid.

2-12: ^{1}H NMR (500 MHz, $CDCl_3$) δ 5.32–5.30 (m, 1H), 4.35–4.32 (m, 1H), 3.47–3.44 (m, 2H), 3.36–3.34 (m, 1H), 2.34–1.05 (m, 33H, steroidal skeleton H), 0.89 (s, 9H), 0.88 (s, 9H), 0.05 (s, 6H), 0.03 (s, 6H); ^{13}C NMR (125 MHz, $CDCl_3$) δ 141.7, 120.9, 72.6, 72.5, 68.5, 61.4, 54.6, 50.2, 42.8, 42.2, 39.9, 37.3, 36.6, 36.5, 36.3, 35.8, 33.6, 32.1, 31.9, 31.5, 29.8, 26.0, 26.0, 23.8, 20.7, 19.4, 18.2, 16.7, 13.0, –4.6, –5.3.

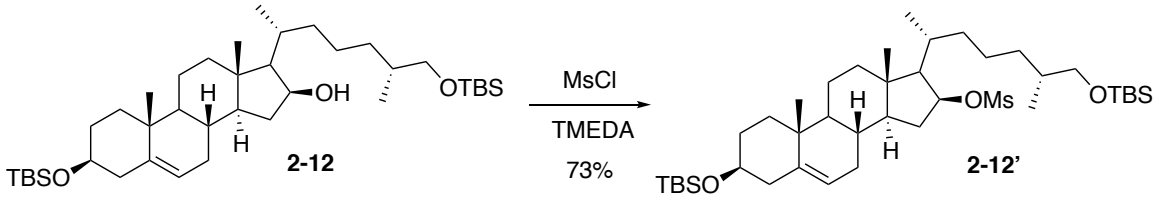

To a solution of **2-12** (1.41 g, 2.2 mmol) and TMEDA (0.99 mL, 6.6 mmol) in toluene (10 mL) was added MsCl (0.51 mL, 6.6 mmol) drop-wise at 0 °C and then the reaction was warmed to room temperature. After about 1 h, TLC indicated the consumption of the starting material. The suspension was filtered through a plug of Celite. The filtrate was concentrated and purified by

column chromatography (Hexanes : EtOAc = 8 : 1) to give the pure **2-12′** (1.16 g, 73%) as a white solid.

2-12′: ^{1}H NMR (500 MHz, $CDCl_3$) δ 5.36–5.34 (m, 1H), 5.23–5.17 (m, 1H), 3.54–3.50 (m, 1H), 3.43–3.41 (m, 1H), 2.24–2.19 (m, 1H), 2.20–1.05 (m, 33H, steroidal skeleton H), 1.01 (s, 18H), 0.91 (m, 6H), 0.68 (s, 6H); ^{13}C NMR (125 MHz, $CDCl_3$) δ 120.6, 83.3, 72.5, 68.5, 60.8, 54.8, 50.0, 42.8, 38.8, 37.3, 35.8, 35.0, 33.5, 31.6, 31.3, 30.1, 26.0, 26.0, 25.9, 24.1, 20.7, 19.4, 18.0, 16.7, 12.6, –4.6, –5.3.

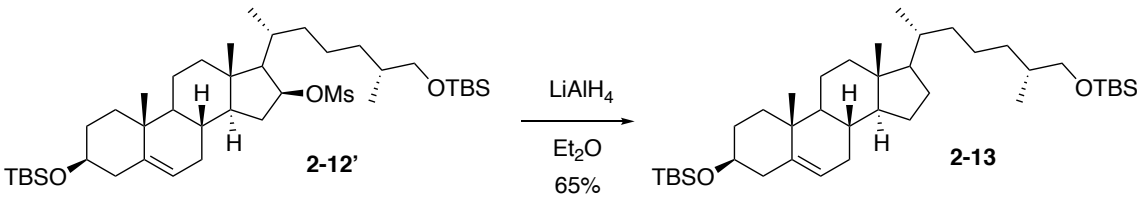

To a solution of the mesylate **2-12′** (500 mg, 0.68 mmol) in Et_2O (25 mL) was treated with lithium aluminum hydride (26 mg, 0.68 mmol) at 0 ◦C and then the resulting suspension was refluxed for 4 h under N_2. The mixture was carefully quenched by the sequential addition of H_2O (0.1 mL), 15 w/v% aq. NaOH (0.2 mL), H_2O (0.4 mL) and was then poured into 10 mL of Et_2O and stirred for 30 min. The crude material **2-13** was filtered through celite and the solvent was removed in vacuum. The filtrate was dried over anhydrous $MgSO_4$, filtered, concentrated and purified by silica gel column chromatography (Hexanes : EtOAc = 8 : 1) to give **2-13** (279 mg, 65%) as a white solid.

2-13: ^{1}H NMR (500 MHz, $CDCl_3$) δ 5.34–3.32 (m, 1H), 3.48 (dddd, J = 4.0 Hz, J = 6.3 Hz, J = 15.8 Hz, J = 20.9 Hz, 2H), 3.35–3.32 (m, 1H), 2.28–3.26 (m, 1H), 2.21–1.05 (m, 33H, steroidal skeleton H), 0.89 (s, 9H) , 0.89 (s, 9H) , 0.05 (s, 6H) , 0.03 (s, 6H); ^{13}C NMR (125

MHz, $CDCl_3$) δ 121.2, 70.1, 47.1, 42.8, 41.2, 39.8, 37.8, 35.7, 33.8, 31.9, 26.0, 22.0, 19.4, 12.1, 11.9, 9.5 -4.6, –5.3.

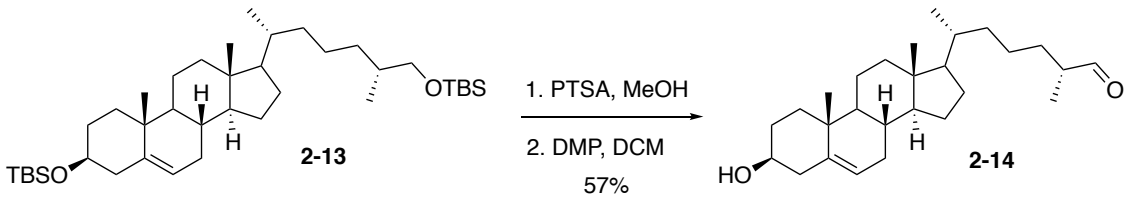

p-Toluenesulfonic acid (28 mg, 0.16 mmol) was added to compound **2-13** (50 mg, 0.08 mmol) in MeOH (3 mL). The reaction was stirred over night and the solvent was removed under vacuum. The material was extract with H_2O and EtOAc and then the extract was neutralized with 1 N NaOH to remove the residual *p*-toluenesulfonic acid. The resulting solution was concentrated and extacted with EtOAc. The crude material was used in the next reaction without further purification.

To a solution of the diol in 3 mL of dry CH_2Cl_2 was added of $NaHCO_3$ (6.8 mg, 0.08 mmol) followed by of DMP (34 mg, 0.08 mmol) at 0 °C. After 7 min, TLC indicated the formation of the product **2-14**. The suspension was filtered through a plug of celite. The filtrate was concentrated and purified by column chromatography (Hexanes : EtOAc = 4 : 1) to give the pure **2-14** (32 mg, 57%) as a white solid over 2 steps**.**

2-14: ^{1}H NMR (500 MHz, $CDCl_3$) δ 9.62 (s, 1H), 5.42–5.41 (m, 1H), 3.56–3.51 (dd, *J* = 6.0 Hz, *J* = 10.6 Hz, 1H), 2.49 (m, 2H), 2.16–0.91 (m, 33H, steroidal skeleton H), 0.91 (d, *J* = 6.7 Hz, 1H), 0.70 (s, 1H); ^{13}C NMR (125 MHz, $CDCl_3$) δ 205.4, 141.4, 121.9, 72.0, 52.8, 49.2, 48.4, 46.4, 42.2, 39.1, 37.1, 36.9, 33.1, 31.6, 31.5, 31.0, 30.8, 29.7, 25.8, 25.7, 25.0, 23.2, 23.0, 18.7, 14.7, 13.3.

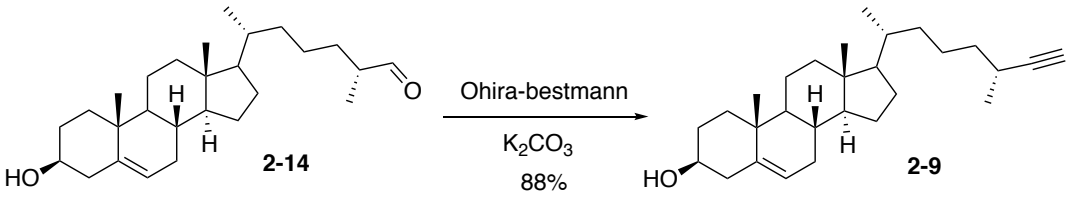

To a solution of aldehyde **2-14** (32 mg, 0.08 mmol) and K_2CO_3 (28 mg, 0.2 mmol) in MeOH (1 mL) was added Bestmann reagent (38.5 mg, 0.2 mmol) and the reaction mixture was stirred for 5 h at room temperature. The solvent was concentrated and the crude material was purified by column chromatography (Hexanes : EtOAc = 5 : 1) to give the pure **2-9** (13.9 mg, 88%) as a white solid.

2-9: ^{1}H NMR (500 MHz, $CDCl_3$) δ 5.43–5.42 (m, 1H), 3.56–3.42 (m, 1H), 2.43–3.42 (m, 1H), 2.36–0.90 (m, 33H, steroidal skeleton H); ^{13}C NMR (125 MHz, $CDCl_3$) δ 141.4, 122.0, 72.1, 68.1, 68.0, 49.2, 42.2, 39.3, 39.1, 37.2, 37.1, 33.1, 31.7, 31.5, 31.3, 31.2, 31.0, 29.7, 26.0, 25.7, 25.0, 23.3, 23.0, 21.1, 20.9, 18.7, 14.8, 14.7.

2.9.3. Synthesis of Photo-activatable BA

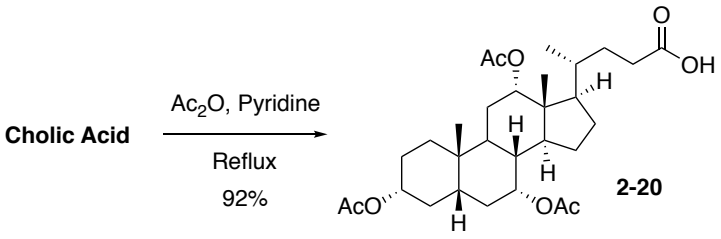

To a solution of cholic acid (1.63 g, 4 mmol) in pyridine (10 mL) was added acetic anhydride (1.42 mL, 15 mmol) and then the reaction mixture was refluxed overnight. Saturated aqueous NH_4Cl solution was added to quench the reaction, and the resulting mixture was extracted with EtOAc. The organic layer was washed with H_2O (15 mL x 3) to remove residual pyridine. The

organic extract was dried over anhydrous $MgSO_4$, filtered, concentrated and purified by silica gel column chromatography (Hexanes : EtOAc = 2 : 1) to give **2-20** (1.97 g, 92%) as a colorless oil.

2-20: ^{1}H NMR (500 MHz, $CDCl_3$) δ 5.08–5.05 (m, 1H), 4.90–4.87 (m, 1H), 3.51–3.48 (m, 1H), 2.35–1.05 (m, 33H, steroidal skeleton H), 2.11 (s, 3H), 2.07 (s, 3H), 2.03 (s, 3H), 0.89 (s, 3H), 0.80 (d, J = 5.1Hz, 1H), 0.71 (s, 3H); ^{13}C NMR (125 MHz, $CDCl_3$) δ 174.5, 170.6, 75.4, 71.7, 70.8, 60.4, 51.5, 47.4, 45.1, 43.4, 41.0, 38.7, 37.8, 34.9, 34.6, 34.3, 31.4, 30.9, 30.8, 30.5, 28.9, 27.2, 25.6, 22.8, 22.6, 21.7, 21.5, 17.5, 14.2, 12.2; HRMS (ESI) calcd for $C_{30}H_{46}O_8$ $[M+H]^+$ 535.3271 found 535.3281.

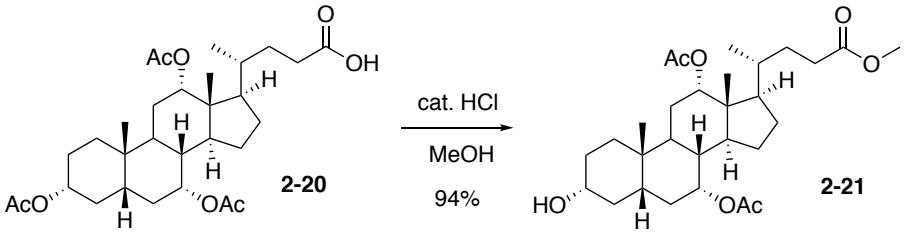

To a solution of **2-20** (1.97 g, 3.68 mmol) in MeOH (20 mL) was added 10 drops of conc. HCl and the reaction was stirred at room temperature for about 4 hours with a frequent TLC monitoring until the TLC indication of the consumption of the starting material. Saturated aqueous $NaHCO_3$ solution was added to quench the reaction, and the resulting mixture was concentrated, extracted with CH_2Cl_2 (3 x 10 mL). The combined organic extract was dried over anhydrous $MgSO_4$, filtered, concentrated and purified by silica gel column chromatography (Hexanes : EtOAc = 3 : 2) to give **2-21** (1.70 g, 94%) as a colorless oil.

2-21: ^{1}H NMR (500 MHz, $CDCl_3$) δ 5.03–5.00 (m, 1H), 4.85–4.82 (m, 1H), 3.61–3.58 (m, 1H), 2.28 (ddd, J = 4.8 Hz, J = 9.8 Hz, J = 14.8 Hz, 1H), 2.35–1.05 (m, 33H, steroidal skeleton H), 2.06 (s, 3H), 2.02 (s, 3H), 0.85 (s, 3H), 0.75 (d, J = 6.1 Hz, 3H), 0.67 (s, 3H); ^{13}C NMR (125 MHz, $CDCl_3$) δ 174.5, 170.6, 75.4, 71.6, 70.8, 51.5, 47.3, 45.0, 43.4, 41.0, 38.6, 37.7,

34.8, 34.6, 34.3, 31.3, 30.8, 30.7, 30.4, 28.9, 27.1, 25.5, 22.8, 22.5, 21.6, 21.4, 17.5, 12.2.

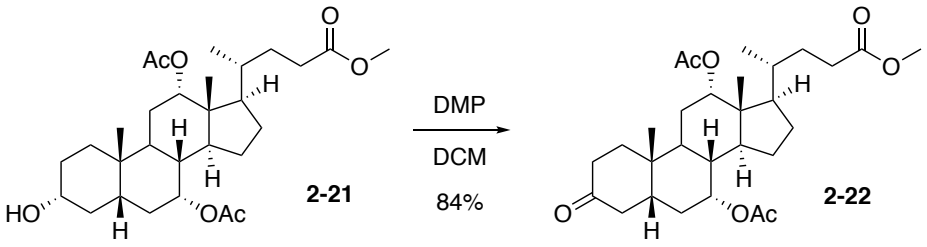

To a solution of the **2-21** (100 mg, 0.2 mmol) in 3 mL of dry CH_2Cl_2 was added of $NaHCO_3$ (25 mg, 0.3 mmol) followed by of DMP (127 mg, 0.3 mmol). After about 1 h, TLC indicated the consumption of the starting material. The suspension was filtered through a plug of Celite. The filtrate was concentrated and purified by column chromatography (Hexanes : EtOAc = 8 : 1) to give the pure **2-22** (82mg, 84%) as a colorless oil.

2-22: ^{1}H NMR (500 MHz, $CDCl_3$) δ 5.10–5.08 (m, 1H), 4.96–4.93 (m, 1H), 2.94 (t, J = 14.5 Hz, 1H), 2.35–1.05 (m, 33H, steroidal skeleton H), 2.07 (s, 3H), 2.03 (s, 3H), 0.98 (s, 3H), 0.78 (d, J = 6.4 Hz, 3H), 0.73 (s, 3H); ^{13}C NMR (125 MHz, $CDCl_3$) δ 212.0, 174.4, 170.4, 170.1, 75.2, 70.6, 60.3, 51.5, 47.4, 45.1, 44.5, 43.3, 42.1, 37.7, 36.6, 36.1, 34.6, 34.4, 30.9, 30.8, 30.7, 29.8, 27.1, 25.8, 22.8, 21.6, 21.4, 21.3, 21.0, 17.5, 14.2, 12.2; HRMS (ESI) calcd for $C_{28}H_{42}O_7$ $[M+H]^+$ 527.3009 found 527.2997.

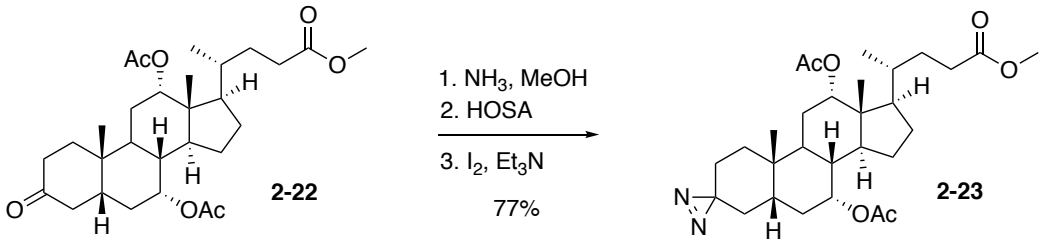

To a solution of mixture of 7 M solution of NH_3 in MeOH (6 mL) was added **2-22** (82 mg, 0.17 mmol) in MeOH (0.5 mL) and the mixture was stirred at -20 °C for 1 hour. The reaction mixture

was warmed to room temperature and the solution was stirred for another 2 h. The solution was cooled down to -20 °C and then hydroxylamine-O-sulfonic acid (65 mg × 5 times) was added every 30 mins and then, the mixture was stirred at room temperature for 14 h. The solvent and NH_3 were removed under vacuum, and the residue was dissolved in MeOH (6 mL). Then TEA (30 μL, 0.2 mmol) was added at 0 °C and subsequently I_2 (76.1 mg, 0.3 mmol) was added portion wise. The mixture was stirred at room temperature for 30 min. Sat. $Na_2S_2O_3$ solution (8 mL) was added to reduce the excess of I_2. MeOH was removed under vacuum and the mixture was extracted with CH_2Cl_2 (4 mL×3). The combined organic extract was dried over anhydrous $MgSO_4$, filtered, concentrated and purified by silica gel column chromatography (Hexanes : EtOAc = 10 : 1) to afford **2-23** (66 mg, 77%) as a white solid.

2-23: ^{1}H NMR (500 MHz, $CDCl_3$) δ 5.12–5.08 (m, 1H), 4.94–4.89 (m, 1H), 2.58 (t, J = 14.5 Hz, 1H), 2.35–1.05 (m, 33H, steroidal skeleton H), 2.14 (s, 3H), 2.05 (s, 3H), 0.98 (s, 3H), 0.78 (d, J = 6.4 Hz, 3H), 0.73 (s, 3H); ^{13}C NMR (125 MHz, $CDCl_3$) δ 174.5, 170.5, 170.2, 75.3, 70.6, 51.5, 47.4, 45.1, 43.3, 40.2, 37.7, 34.6, 34.5, 33.8, 30.9, 30.8, 28.8, 27.2, 26.5, 25.6, 22.8, 22.5, 21.6, 21.4, 17.5, 12.2.

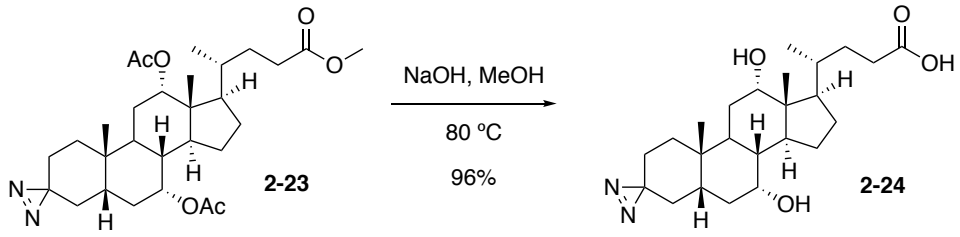

A solution of compound **2-23** (66 mg, 0.13 mmol) in MeOH (3 mL) was treated with NaOH (51 mg, 1.5 mmol) and the reaction mixture was stirred until the TLC indicated the consumption of

the starting material. The reaction mixture was stirred at room temperature for 12 h. The mixture was acidified with HCl (1 M) and extracted with CH_2Cl_2 (3 mL×3). The combined organic layers were dried over $MgSO_4$, filtered and concentrated in vacuum to afford the crude 4-50, which was purified by column chromatography (Hexanes : EtOAc = 1 : 2) to to afford the desired product **2-24** as a white solid (52 mg, 96%).

2-24: ^{1}H NMR (500 MHz, $CDCl_3$) δ 3.98–3.96 (m, 1H), 3.80–3.77 (m, 1H), 2.98 (t, *J* = 14.0 Hz, 1H), 2.33–1.05 (m, 33H, steroidal skeleton H), 2.24 (m, 1H), 1.03 (s, 3H), 1.01(s, 3H), 0.73 (s, 3H); ^{13}C NMR (125 MHz, $CDCl_3$) δ 176.8, 72.5, 67.5, 46.7, 46.1, 41.6, 41, 39.6, 35.4, 34.8, 34.6, 34.3, 33.6, 30.9, 30.6, 28.5, 28.3, 27.3, 26.3, 26, 22.8, 21.7, 16.2, 11.6.

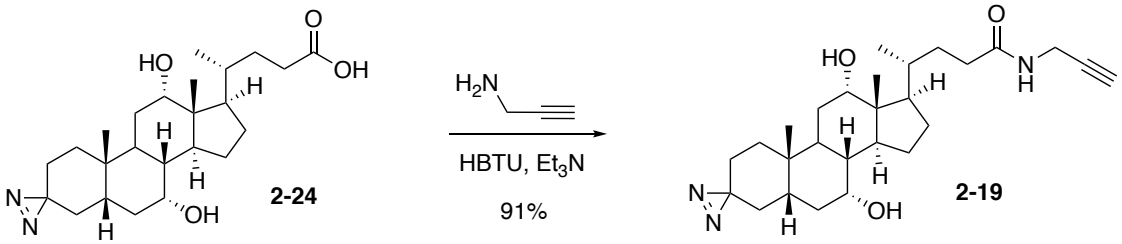

A solution of compound **2-24** (52 mg, 0.12 mmol) in anhydrous DMF (4 mL) was added HBTU (68.3 mg, 0.18 mmol). 2-Propynylamine (22 μL, 0.36 mmol) and anhydrous DIPEA (63 μL, 0.36 mmol) were added subsequently. The reaction mixture was stirred at room temperature for 20 h. Saturated aqueous NH_4Cl solution was added to quench the reaction, and EtOAc (5 mL) was added to the solution. The resulting mixture was washed with H_2O (3 mL x 3) extracted with CH_2Cl_2 (3 x 10 mL). The resulting solution was concentrated in vacuum and purified by flash chromatography (EtOAc : MeOH = 9: 1) to afford **2-19** as a white solid (49.7 mg, 91%).

2-19: ^{1}H NMR (500 MHz, $CDCl_3$) δ 5.93 (s, 1H), 4.13–4.11 (m, 1H), 4.03 (d, *J* = 2.8 Hz, 2H), 3.88–3.85 (m, 1H), 2.90 (t, *J* = 14.1 Hz, 1H), 2.42–1.05 (m, 33H, steroidal skeleton H), 1.00

(s, 3H), 0.98 (s, 3H), 0.72 (s, 3H); ^{13}C NMR (125 MHz, $CDCl_3$) δ 173.3, 73.0, 71.5, 68.2, 46.8, 46.5, 41.9, 40.6, 39.3, 35.3, 35.0, 34.7, 34.4, 33.8, 32.8, 31.2, 29.1, 28.4, 27.5, 26.4, 23.2, 22.4, 17.4, 12.5; HRMS (ESI) calcd for $C_{27}H_{41}N_3O_3$ $[M+H]^+$ 456.3226 found 456.3228.

2.10. References

1. Bioorthogonal chemistry, reviews: (a) Deane, C. *Nat. Chem. Biol.* **2017***, 13*, 1057. (b) McKay, C.; Finn. M. G. *Biochem. Cell Biol.* **2014**, 1075. (c) Patterson, D. M.; Nazarova, L. A.; Prescher, J. A. *ACS Chem. Biol*. **2014**, *9*, 592. (d) Lang, K.; Chin, J. W. *ACS Chem. Biol*. **2014**, *9*, 16. (e) Fan, X.; Li, J.; Chen, P. R. *Natl. Sci. Rev.* **2017**, *4*, 300. (f) Gong, Y.; Pan, L. *Tetrahedron Lett*. **2015**, *56*, 2123.
2. Ramil, C. P.; Lin, Q. *Chem. Commun*. **2013**, *49*, 11007.
3. (a) Prescher, J. A.; Bertozzi, C. R. *Nat. Chem. Biol*. **2005**, *1*, 13. (b) Shieh, P.; Bertozzi, C. R. *Org. Biomol. Chem*. **2014**, *12*, 9307.
4. (a) Cornish, V. W.; Hahn, K. M.; Schultz, P. G. *J. Am. Chem. Soc.* **1996**. *118*, 8150. (b) Mahal, L. K. *Science* **1997**, *276*, 1125. (c) Rideout, D. *Science* **1986**, *233*, 561. (d) Sletten, E. M.; Bertozzi, C. R. *Angew. Chem. Int. Ed.* **2009**, *48*, 6974.
5. (a) Dirksen, A.; Dirksen, S.; Hackeng, T. M.; Dawson, P.E. *J. Am. Chem. Soc.* **2006**, *128*, 15602. (b) Dirksen, A.; Hackeng, T. M.; Dawson, P.E. *Angew. Chem. Int. Ed.* **2006**, *45*, 7581. (c) Lin, F. L.; Hoyt, H. M.; van Halbeek, H.; Bergman, R. G.; Bertozzi, C. R. *J. Am. Chem. Soc.* **2005**, *127*, 2686.
6. (a) Saxon, E.; Armstrong, J. I.; Bertozzi, C. R. *Org. Lett*. **2000**, *2*, 2141. (b) Wendeler, M.; Grinberg, L.; Wang, X.; Dawson, P. E.; Baca, M. *Bioconjug. Chem*. **2014**, *25*, 93.

7. (b) Agard, N. J.; Baskin, J. M.; Prescher, J. A.; Lo, A.; Bertozzi, C. R. *ACS Chem. Biol*. **2006**, *1*, 644. (b) Saxon, E.; Armstrong, J. I.; Bertozzi, C. R. *Org. Lett*. **2000**, *2*, 2141. (c) Schilling, C. I.; Jung, N.; Biskup, M.; Schepers, U.; Brase, S. *Chem. Soc. Rev*. **2011**, *40*, 4840. (d) Speers, A. E.; Cravatt, B. F. *Chem, Biol.* **2004**, *11*, 535.

8. Baskin, J. M.; Prescher, J. A.; Laughlin, S.T.; Agard, N. J.; Chang, P. V.; Miller, I. A.; Lo, A.; Codelli, J. A.; Bertozzi, C. R. *Proc. Natl. Acad. Sci*. **2007**, *104*, 16793.

9. (a) Hein, J. E.; Fokin, V. V. *Chem. Soc. Rev*. **2010**, *39*, 1302. (b) Huisgen, R. *Angew. Chem. Int. Ed.* **1963**, *2*, 565. (c) Kolb, H. C.; Finn, M. G.; Sharpless, K. B. *Angew. Chem. Int. Ed.* **2001**, *40*, 2004.

10. (a) Rostovtsev, V. V.; Green, L. G.; Fokin, V. V.; Sharpless, K. B. *Angew. Chem. Int. Ed.* **2002**, *41*, 2596. (b) Tornøe, C. W.; Christensen, C.; Meldal, M. *J. Org. Chem*. **2002**, *67*, 3057. (c) Worrell, B. T.; Malik, J. A.; Fokin, V.V. *Science* **2013**, *340*, 457.

11. (a) Besanceney-Webler, C.; Jiang, H.; Zheng, T.; Feng, L.; Soriano del Amo, D.; Wang, W.; Klivansky, L. M.; Marlow, F. L.; Liu, Y.; Wu, P. *Angew. Chem. Int. Ed.* **2011**, *50*, 8051. (b) Brewer, G. J. *Chem. Res. Toxicol*. **2010**, *23*, 319.

12. Agard, N. J.; Prescher, J. A.; Bertozzi, C. R. *J. Am. Chem. Soc.* **2004**, *126*, 15046.

13. (a) Alder, K.; Stein, G.; Finzenhagen, H. *Justus Liebigs Ann. Chem*. **1931**, *485*, 211. (b) Alder, K.; Stein, G. *Justus Liebigs Ann. Chem*. **1933**, *501*, 1. (c) Wittig, G.; Krebs, A. *Chem. Ber*. **1961**, *94*, 3260.

14. (a) Ning, X.; Temming, R. P.; Dommerholt, J.; Guo, J.; Ania, D. B.; Debets, M. F.; Wolfert, M. A.; Boons, G. J.; van Delft, F. L. *Angew. Chem. Int. Ed.* **2010**, *49*, 3065. (b) McKay, C. S.; Moran, J.; Pezacki, J. P. *Chem. Commun*. **2010**, *46*, 931. (61) McKay, C.

S.; Blake, J. A.; Cheng, J.; Danielson, D. C.; Pezacki, J. P. *Chem. Commun*. **2011**, *47*, 10040.

15. (a) Song, W.; Wang, Y.; Yu, Z.; Vera, C. I.; Qu, J.; Lin, Q. *ACS Chem. Biol*. **2010**, *5*, 875. (b) Song, W.; Wang, Y.; Qu, J.; Madden, M. M.; Lin, Q. *Angew. Chem. Int. Ed.* **2008**, *47*, 2832.
16. (a) Adzima, B. J.; Tao, Y. H.; Kloxin, C. J.; DeForest, C. A.; Anseth, K. S.; Bowman, C. N. *Nat. Chem*. **2011**, *3*, 256. (b) Arumugam, S.; Popik, V. V. *J. Am. Chem. Soc.* **2011**, *133*, 5573. (c) Pauloehrl, T.; Delaittre, G.; Winkler, V.; Welle, A.; Bruns, M.; Borner, H. G.; Greiner, A. M.; Bastmeyer, M.; Barner-Kowollik, C. *Angew. Chem. Int. Ed.* **2012**, *51*, 1071. (d) Poloukhtine, A. A.; Mbua, N. E.; Wolfert, M. A.; Boons, G. J.; Popik, V. V. *J. Am. Chem. Soc.* **2009**, *131*, 15769. (d) Riggsbee, C. W.; Deiters, A. *Trends Biotechnol*. **2010**, *28*, 468.
17. (a) Song, W.; Wang, Y.; Qu, J.; Madden, M. M.; Lin, Q. *Angew. Chem. Int. Ed.* **2008**, *47*, 2832. (b) Wang, Y.; Song, W.; Hu, W. J.; Lin, Q. *Angew. Chem. Int. Ed.* **2009**, *48*, 5330.
18. McNitt, C. D.; Popik, V. V. *Org. Biomol. Chem*. **2012**, *10*, 8200.
19. Wang, F.; Zhang, Y.; Du, Zhi.; Ren, J.; Qu, X. *Nat. Commun*. **2018**. *9*, 1209.
20. (a) Blackman, M. L.; Royzen, M.; Fox, J. M. J. *Am. Chem. Soc.* **2008**, *130*, 13518. (b) Devaraj, N. K.; Weissleder, R.; Hilderbr, S. A. *Bioconjugate Chem*. **2008**, *19*, 2297. (c) Taylor, M. T.; Blackman, M. L.; Dmitrenko, O.; Fox, J. M. *J. Am. Chem. Soc.* **2011**, *133*, 9646.
21. (a) Lang, K.; Davis, L.; Wallace, S.; Mahesh, M.; Cox, D. J.; Blackman, M. L.; Fox, J. M.; Chin, J. W. *J. Am. Chem. Soc.* **2012**, *134*, 10317. (b) Seitchik, J. L.; Peeler, J. C.;

Taylor, M. T.; Blackman, M. L.; Rhoads, T. W.; Cooley, R. B.; Refakis, C.; Fox, J. M.; Mehl, R. A. *J. Am. Chem. Soc.* **2012**, *134*, 2898.

22. (a) Patterson, D. M.; Nazarova, L. A.; Xie, B.; Kamber, D. N.; Prescher, J. A. *J. Am. Chem. Soc.* **2012**, *134*, 18638. (b) Yang, J.; Seckute, J.; Cole, C. M.; Devaraj, N. K. *Angew. Chem. Int. Ed.* **2012**, *51*, 7476.

23. (a) Ho, C. M.; Zhang, J. L.; Zhou, C. Y.; Chan, O. Y.; Yan, J. J.; Zhang, F. Y.; Huang, J. S.; Che, C. M. *J. Am. Chem. Soc.* **2010**, *132*, 1886. (b) Skowerski, K.; Szczepaniak, G.; Wierzbicka, C.; Gulajski, L.; Bieniek, M.; Grela, K. *Catal. Sci. Technol.* **2012**, *2*, 2424. (c) Tomasek, J.; Schatz, *J. Green Chem*. **2013**, *15*, 2317.

24. (a) Chalker, J. M.; Wood, C. S.; Davis, B. G. *J. Am. Chem. Soc.* **2009**, *131*, 16346. (b) Li, N.; Lim, R. K.; Edwardraja, S.; Lin, Q. *J. Am. Chem. Soc.* **2011**, *133*, 15316. (c) Spicer, C. D.; Triemer, T.; Davis, B. G. *J. Am. Chem. Soc.* **2012**, *134*, 800. (d) Tilley, S. D.; Francis, M. B. *J. Am. Chem. Soc.* **2006**, *128*, 1080. (e) Vilaro, M.; Arsequell, G.; Valencia, G.; Ballesteros, A.; Barluenga, J. *Org. Lett*. **2008**, *10*, 3243. (f) Yusop, R. M.; Unciti-Broceta, A.; Johansson, E. M.; Sanchez-Martin, R. M.; Bradley, M. *Nat. Chem*. **2011**, *3*, 239.

25. (a) Chaudhuri, A.; Anand, D. **2017**, *6*, 1. (b) Maxfield, F. R.; Wüstner, D. *Methods Cell Biol.* **2012**, *108*, 367. (c) Solanko, K. A.; Modzel, M.; Solanko, L. M.; Wüstner, D. *Lipid Insights* **2015**, *8*, 95.

26. (a) Robalo, J. R.; Canto, A. M. T.; Carvalho, A.; Ramalho, P.; Loura, M. S. *J. Phys. Chem.* **2013**, *117*, 5806. (b) McIntosh, A. L.; Atshaves, B. P.; Huang, H.; Gallegos, A. M.; Kier, A. B.; Schroeder, F. *Lipids* **2008**, *43*, 1185.

27. Jao, C. Y.; Nedelcu, D.; Lopez, L. V.; Samarakoon, T. N.; Welti, R.; Salic, A. *ChemBioChem*. **2015**, *16*, 611.

28. Martin, R.; Schmidt, A. W.; Theumer, G.; Entchev, T. K.; Kurzchalia, T. W.; Knölker. H. *Org. Biomol. Chem*. **2009**, *7*, 909.

Part II

Synthesis of the Carbocycle Core of Massadine

Chapter 3

Synthesis of the Carbocyclic Core of Massadine

(Previously published as Sun, C.; Lee, H.; Lee, D. *Org. Lett*. **2015**, *17*, 5348–5351)

3.1. Pyrrole–Imidazole Alkaloids

A family of pyrrole–imidazole alkaloids, oroidin **(3-1a)**-derived natural products, were isolated exclusively from marine sponge cultures.[1] Over 150 members of these marine alkaloids have been discovered, and due to their architecturally complex structures with a variety of biological profiles, such as antibacterial,[2a] antitumor,[2b–2d] immunosuppressive and adrenoceptor agonist activities,[2e] attract attention from synthetic chemists and biochemists. For nearly 50 years, isolation and structural elucidation of these marine alkaloids have been extensively pursued. The parent oroidin **3-1a** was isolated from *Algelas oroides* in 1971[3] along with its derivatives, such as hymenidin **3-1b** and clathrodin **3-1c** and other pyrrole–imidazole alkaloid representatives (**Figure 3.1**).[4]

Figure 3.1. Structure of parent, monomeric and simple dimeric pyrrole–imidazole alkaloids

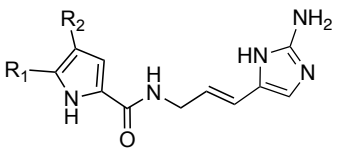

3-1a, Oroidin, R_1, R_2 = Br
3-1b, Hymenidin, R_1 = H, R_2 = Br
3-1b, Clathrodin, R_1, R_2 = H

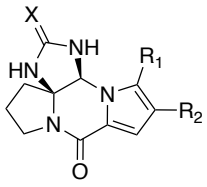

3-2a, Phakellin (X = NH, R_1 = H, R_2 = H)
3-2b, Bromophakellin (X = NH, R_1 = Br, R_2 = H)
3-2c, Dibromophakelin (X = NH, R_1 = Br, R_2 = Br)
3-2d, Phakellstatin (X = O, R_1 = H, R_2 = H)
3-2e, Dibromophakellstatin (X = O, R_1 = Br, R_2 = Br)

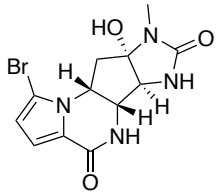

3-3, Agelastatin A

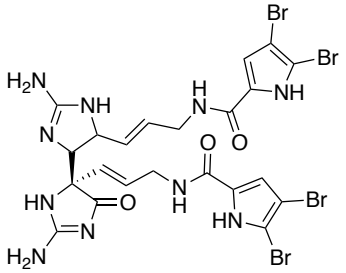

3-4, Mauritiamine

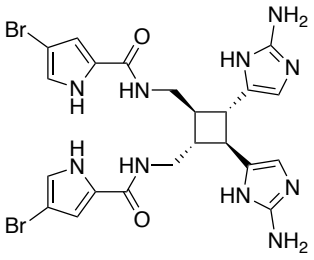

3-5, (–)-Sceptrin

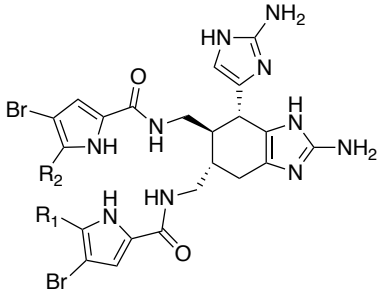

3-6a, Ageliferin (R_1 = H, R_2 = H)
3-6b, Bromoageliferin (R_1 = Br, R_2 = H)
3-6c, Dibromoageliferin (R_1 = Br, R_2 = Br)

Further degrees of complexity have been discovered including monomeric, dimeric and even tetrameric cyclized pyrrole–imidazole alkaloids, which include phakellin (**3-2a**–**3-2c**), phakellstatin (**3-2d**, **3-2e**) and agelastatin A (**3-3**) isolated from *Phakellia mauritiana* and *Agelas dendromorpha* respectively.[5] These cyclic monomers also have different levels of bromination on the pyrrole moiety. Cyclic dimer (–)-sceptrin (**3-5**) was isolated from *Agelas sceptrum* by Faylker and Clardy in 1981.[6] Subsequently, (–)-ageliferin (**3-6a**) and racemic mauritiamine (**3-4**) were isolated from the sponge *Agelas conifera*. Biogenetically, **3-5** and **3-6a** were hypothesized to undergo formal [2+2] and [4+2] cycloaddition from the dimer of oroidin, while maruitiamine possess a head-to-head dimer connectivity via a single bond of two oroidins.

Architecturally more complex dimeric congeners have been isolated (**Figure 3.2**), which include massadines (**3-7a**–**3-7b**), axinellamines (**3-8a**–**3-d**), palau'amines (**3-9a**–**3-9c**), donnazoles (**3-10a**–**3-10b**), konbu'acidins (**3-11a**–**3-11b)** and styloguanidines (**3-12a**–**3-12b**). Massadines, axinellamines, donnazoles and palaua'amines possess a fully substituted cyclopentane core, and the hexacyclic system of palau'amine is known as the most architecturally complicated dimer. In addition, structural modifications including bromination on the pyrrole moiety and the loss of the pyrrole-2-carboxamide fragment increase the diversity of oroidin dimers. In 2006, the first tetrameric oroidin, stylissadine A (**3-13**) was isolated from *Stylissa* and its structure was determined by Köck and Grube.[7] The mechanisms of biosynthesis of these complex marine alkaloids have not been fully understood.[8]

Efficient synthetic routes of all monomeric alkaloids have been reported by many research groups, however, dimeric alkaloids are still an outstanding challenge to synthetic chemists, thus only seven total syntheses of three complex alkaloids, massadine, axinellamin and palau'amine, have been reported so far.

Figure 3.2. Structure of complex dimeric and tetrameric pyrrole–imidazole alkaloids

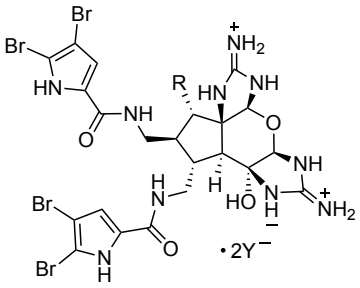

3-7a, Massadine (R = OH)
3-7b, Massadine chloride (R = Cl)

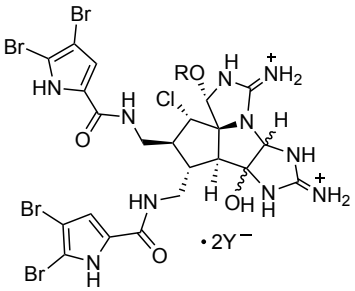

3-8a, (–)-Axinellamine A (R = H, OH, H = β)
3-8b, (–)-Axinellamine B (R = H, OH, H = α)
3-8c, Axinellamine C (R = Me, OH, H = β)
3-8d, Axinellamine D (R = Me,OH, H = α)

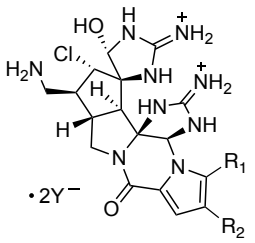

3-9a, (–)-Palau'amine (R_1, R_2 = H)
3-9b, Bromopalau'amine (R_1 = H, R_2 = Br)
3-9c, Dibromopalau'amine (R_1, R_2 = Br)

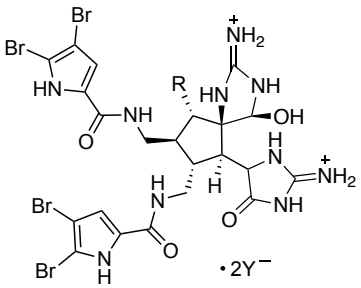

3-10a, Donnazole A (R = OH)
3-10b, Donnazole B (R = Cl)

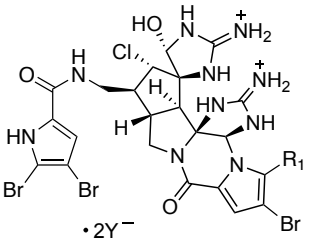

3-11a, Konbu'acidin A (R_1 = H)
3-11b, Konbu'acidin B (R_1 = Br)

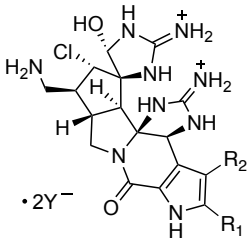

3-12a, Styloguanidine (R_1, R_2 = H)
3-12b, Bromostyloguanidine (R_1 = H, R_2 = Br)
3-12c, Styloguanidine (R_1, R_2 = Br)

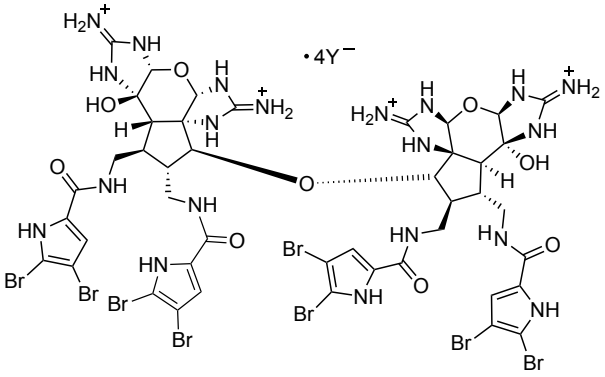

3-13, Stylissadine A

3.2. Biosynthesis of Pyrrole–imidazole Alkaloids

3.2.1. The First Biosynthetic Hypothesis

The structural interrelationship of the whole family of pyrrole–imidazole alkaloids is

assumed to originate from the simple metabolites such as oroidin (**1-1a**), clathrodin (**1-1b**) and hymenidin (**1-1c**).[9] Possible biosynthesis pathways of dimers of these metabolites have been proposed and discussed extensively, however, reported mechanistic studies have not fully proven the biosynthesis of the higher pyrrole–imidazole alkaloids such as axinellamins, massadines or palau'amines.

Scheme 3.1. The first biosynthetic hypothesis for palau'amine

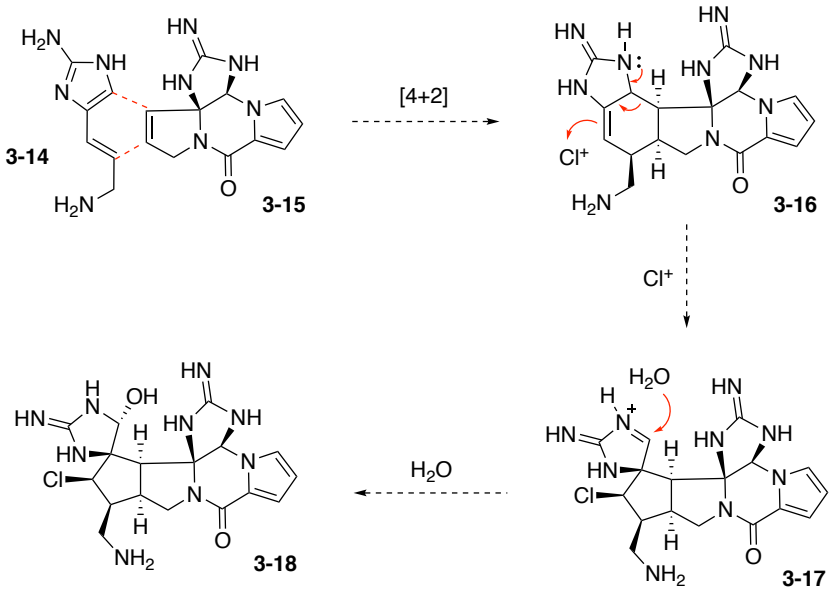

The first biosynthesis pathway was proposed by Kinnel and Scheuer in 1998 (**Scheme 3.1**).[10] Aminoimidazolyl propeneamine **3-14** and a hypothetical 'dihyrophakellin' dienophile **3-15** undergo *endo*-[4+2] cycloaddition to provide 5,6-*cis*-fused intermediate **3.16**. Subsequent ring contraction is initiated by chloroperoxidase for chloronium-induced 1,2 C–C bond shift to furnish the hexacyclic skeleton of the originally assigned structure of palau'amine (**3-18**). However, the originally assigned stereochemistry of palau'amine was revised to 5,5-*trans*-[3.3.0]bicyclic ring system as the correct structure of palau'amine (**3-9a)** in 2007.[11]

3.2.2. Revised Biosynthetic Routes for Dimers

It was suggested by Baran that all dimeric alkaloids are synthesized via a general pathway which begins with the enantioselective [4+2] cycloaddition of two oroidins (**3-14**) followed by functionalization and ring contraction to furnish the aminoimidazole ring **3-19** (**Scheme 3.2**).[12]

Scheme 3.2. Revised biosynthetic routes

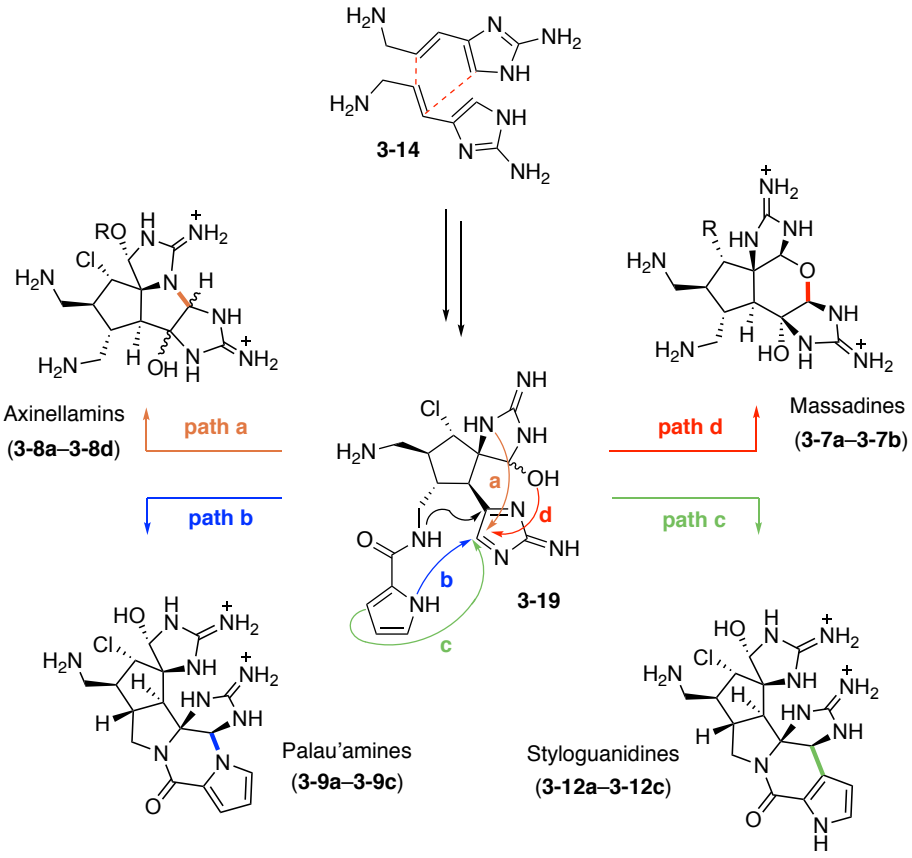

This cascade rearrangement is described in the previous biosynthetic mechanism proposed by Scheuer[13,14] which presented in **Scheme 3.1**. When **3-19** undergoes *N*-oxidative cyclization, it forms axillelamines (path a). Generation of palau'amines commences with ring closure of the nitrogen on the aminoimidazole followed by bond formation between pyrrole and the electrophilic aminoimidazole ring (path b). Via the C–C bond formation between the carbon

of the pyrrole and aminoimidazole ring generate styloguanidines (path c). If the aminoimidazole ring is connected with the hemiaminal oxygen, massadines are produced after addition of water molecule (path d).

3.2.3. A Radical Mechanism of Biosynthesis for Dimers

In 2012, Molinski and Romo proposed an enzyme-catalyzed single-electron transfer (SET)-based biosynthesis mechanism for complex [2+2] dimers of sceptrin.[9] In 2014, Baran and Chen also proposed possible pathways for [2+2], [3+2] and [4+2] oroidin dimers (**Scheme 3.3**).[12]

Scheme 3.3. A radical-based biosynthetic mechanism

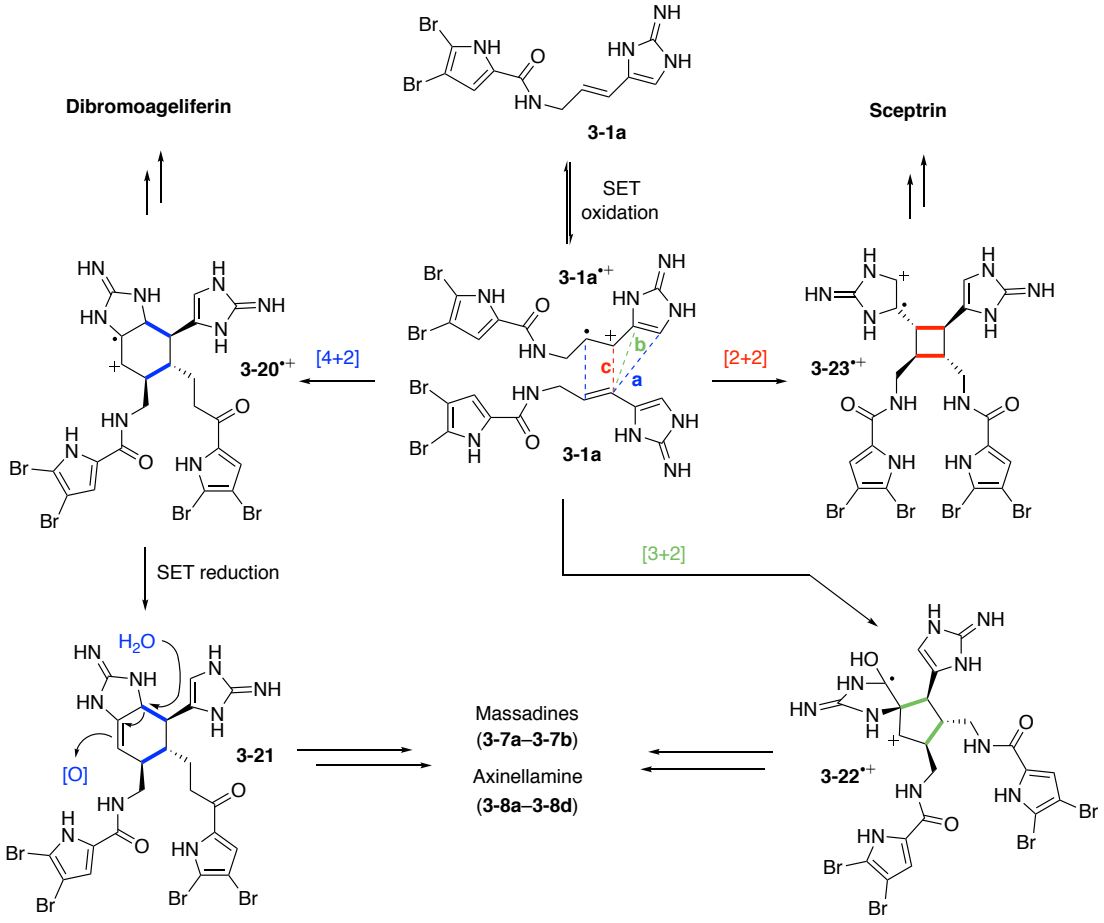

A SET-based oxidation of **3-1a** gives a radical cation **3-1a**$^{\bullet+}$, which undergoes [2+2] and

[4+2] cycloaddition reactions with a counterpart **3-1a** to afford **3-23**$^{\bullet+}$ and **3-20**$^{\bullet+}$, respectively. SET-mediated reduction of **3-20**$^{\bullet+}$ followed by an oxidative rearrangement as proposed by Scheuer provides [3+2] cycloaddition product **3-22**$^{\bullet+}$. Axinellamines and massadines are derived from **3-22**$^{\bullet+}$ after hydration.

3.3. Synthetic Efforts toward the Pyrrole–imidazole Alkaloids

The supply of marine alkaloids to fulfill the need of their interests in biochemistry and pro-drug investigations can be problematic due to the limitation of the collection of marine sponges.[20] Because of abundant interests toward marine alkaloids, the efforts on the total synthesis of these marine alkaloids have been intensely studied. The synthetic routes for monomeric oroidin are well established so far but efficient synthesis for complex dimeric compounds are still under vigorous investigation.[21]

3.3.1. Total Synthesis of Sceptrin

In 2004, the Birman[15] and Baran[16] groups reported independent routes for the first total synthesis of *rac*-sceptrin. Two years later, the first enantioselective total synthesis of (–)-sceptrin was disclosed by Baran and coworkers (**Scheme 3.4**), which led to the synthesis of naturally occurring (–)-ageliferin (**3-6a**).[17] The transformation of vinylcyclobutane moiety in **3-5a** to the corresponding cyclohexene moiety in **3-6a** may implies the same rearrangement is involved in the biosynthetic pathway.

Scheme 3.4. Enantioselective synthesis of (–)-ageliferin from (–)-sceptrin

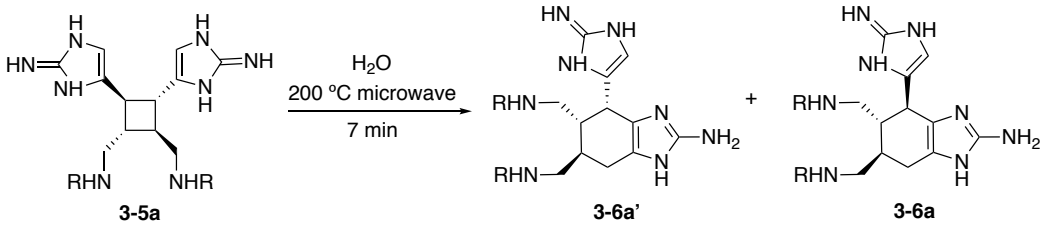

The most recent total synthesis of sceptrin by the Chen group was published in 2015 by utilizing photoredox catalyzed intramolecular [2+2] cycloaddition as the key transformation (**Scheme 3.5**). This biomimetic synthesis impacted on reassigning the stereochemistry of sceptrin and its analogues. The synthesis commences with the Julia–Kocienski olefination of aldehyde **3-24** followed by subsequent deprotection of the TBS group to generate allylic alcohol **3-25**. After coupling between **3-25** and 2,3-dihydrofuran **3-26**, oxidative deselenylation and reaction of the azido moiety with triphenylphosphine provided the precursor **3-27**. The following SET-mediated [2+2] cycloaddition of **3-27** with visible light in the presence of $Ir(ppy)_3$ yielded the desired caged tricycle (**3-28**) as a mixture of epimers (9:5 *dr*). It was recognized that the cyclization occurred only after conversion of the azido group to the iminophosporane due to the high oxidative potential of vinylazidoimidazole. Treating cycloadduct **3-28** with $TiCl_4$ provided the desired cyclobutyl-1,3-dithiane **3-29** which was converted smoothly to diols **3-30** through a 5-step sequence. Treating triol **3-30** with MsCl followed by replacement of the primary hydroxyl groups with the corresponding azide afforded **3-31** after TIPS deprotection. Oxidation of the hydroxyl group followed by condensation with Boc-guanidine formed the second aminoimidazole moiety. The resulting diazide product was reduced to **3-32** and then a coupling reaction with **3-33** gave (–)-sceptrin (**3-5**).

Scheme 3.5. Total synthesis of (–)-sceptrin by the Chen group

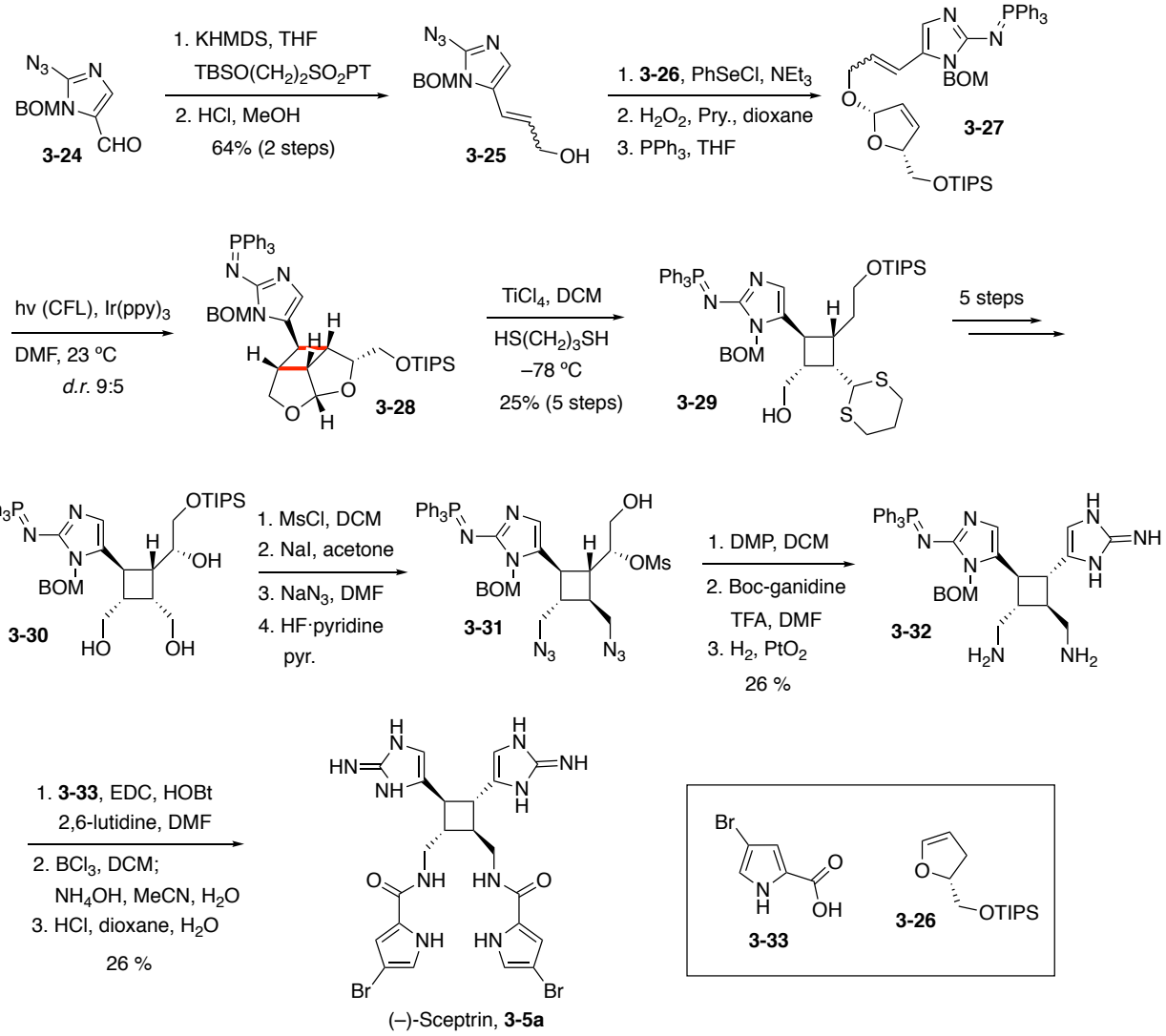

3.3.2. Total Synthesis of Axinellamines

3.3.2.1. Baran's Strategy

In 2008, the Baran group reported the first and only synthesis of a [3+2] oroidin dimer, *rac*-axinellamine A and B,[18] featuring a [4+2] Diels–Alder reaction diene **3-34** and dienophile **3-35** to obtain cyclohexene **3-36** (**Scheme 3.6**).

Scheme 3.6. The first generation of racemic total synthesis of axinellamine

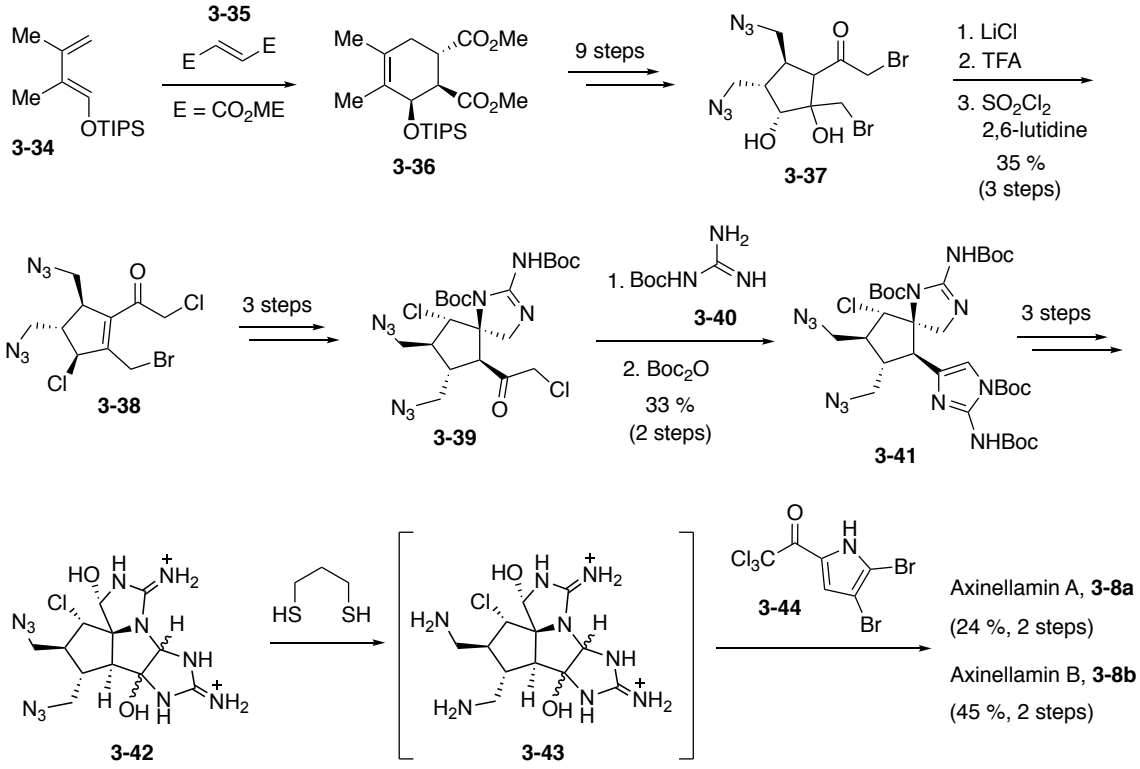

Ozonolysis of **3-36** followed by an 8-step transformation including an intramolecular aldol reaction provided the fully substituted dibromo cyclopentane core **3-37**. Treating **3-37** with LiCl to form a chloro ketone followed by elimination of the tertiary hydroxyl group and replacement of the secondary alcohol in one-pot yielded **3-38**. Through a 3-step sequence, installation of spirocyclic guanidine afforded **3-39**. The second cyclic guanidine was installed to give **3-41**, which underwent oxidative ring closure to obtain **3-42** in 5 steps. To complete the synthesis from **3-42**, two aminoimidazoles were installed after reduction of the two azide moieties with propane-1,3-dithiol to **3-43**, which affords axinellamine A (**3-8a**) and B (**3-8b**).

Scheme 3.7. The second-generation synthesis of axinellamin A and B

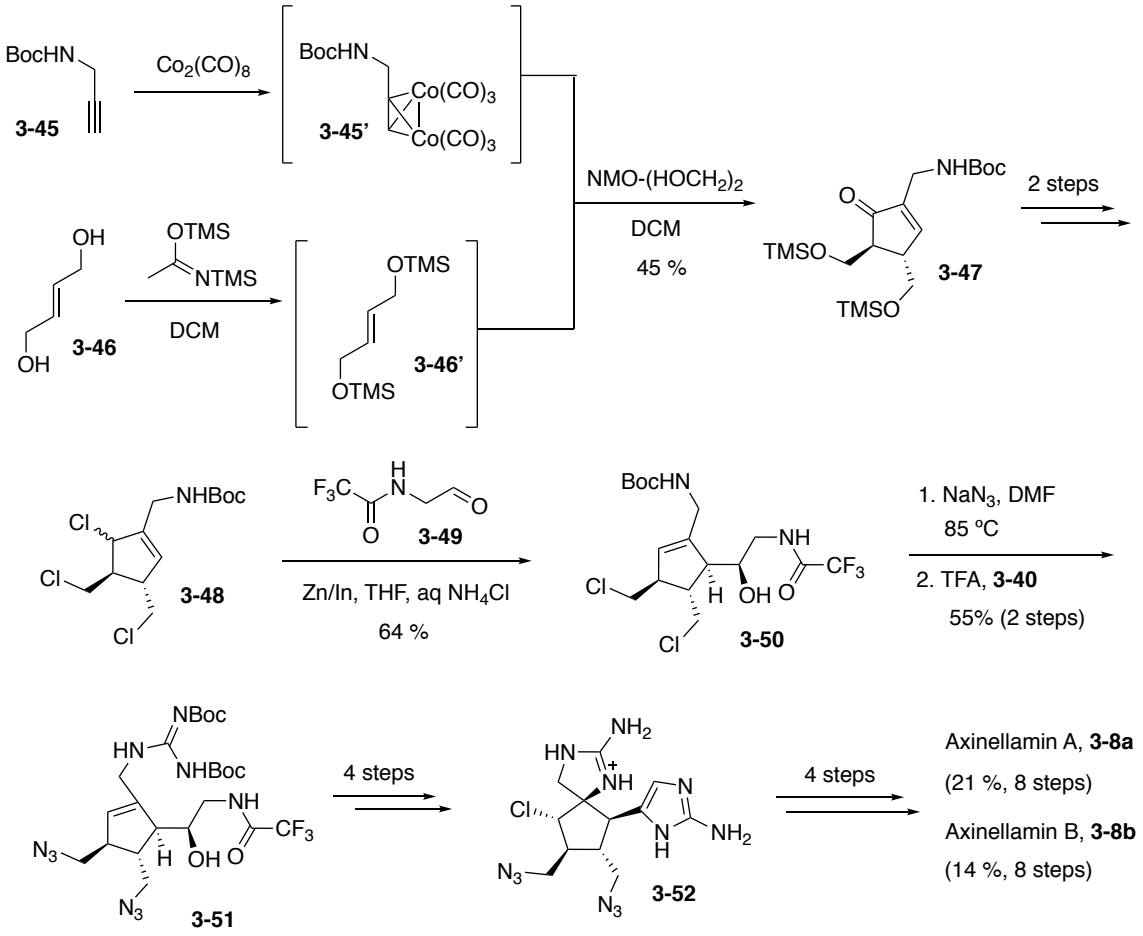

A second-generation racemic synthesis of axinellamin A[19] and its biological activity as antibacterial[20] were presented by Baran and coworkers (**Scheme 3.7**). In their second-generation synthesis, a Pauson–Khand reaction was employed to construct the required cyclopentenone core **3-47** in 45% yield from cobalt complex **3-45′** from alkyne **3-45** and silylbutene diol **3-46′** in the presence of diethylene glycol-NMO. Formation of allylic chloride **3-48** over 2 steps from **3-47** followed by a Zn/In-mediated Barbier reaction with **3-49** yielded chlorocylopentene **3-50** with good diastereoselectivity. Replacing both the primary chloride with an azide followed by treatment with the Goodman's reagent **3-40** afforded **3-51**. Efficient diastereoselective chloro spirocyclization of **3-51** provided a spirocyclic guanidine moiety, which then further elaborated to an aminoimidazole moiety-containing intermediate **3-52** via a 4-step sequence. Through an

additional 4 steps, which are the same sequence as the first-generation synthesis, were employed to cyclize and furnish all required functional groups and installation of two dibromopyrrolyl moieties. The second-generation synthesis that involves 15 longest linear steps is more efficient compared to the first-generation synthesis.

3.3.2.2. Chen's Strategy

The Chen group accomplished an enantioselective synthesis of (–)-axinellamine A[21] (**3-6a**) from the common building block **3-56**, which was employed in their synthesis of ageliferin (**Scheme 3.8**).[22] Lactone **3-55** was prepared from **3-53** and (*S*)-Garner's aldehyde-derived compound **3-54** via Mn(OAc)-based oxidation. Further modification of functional groups and epimerization provided **3-56** in 4 steps. Intermediate **3-57** was obtained via a 5-step sequence highlighting a regioselective Staudinger reduction, diastereoselective reduction of the ketone and epimerization, furnishing the required stereogenic centers. From **3-57**, an oxidative ring contraction known as the Shuer rearrangement[23] was carried out with TBHP and $Ti(Oi\text{-}Pr)_4$ to generate spiroglycocyamidine **3-58**. Stereoretentive replacement of the hydroxyl group with chloride followed by liberation of two primary amino groups provided **3-59**. After installation of dibromopyrrols, the 2-aminoimidazole moiety was introduced to generate aminoimidazole **3-60**.

Scheme 3.8. Chen's total synthesis of axinellamine

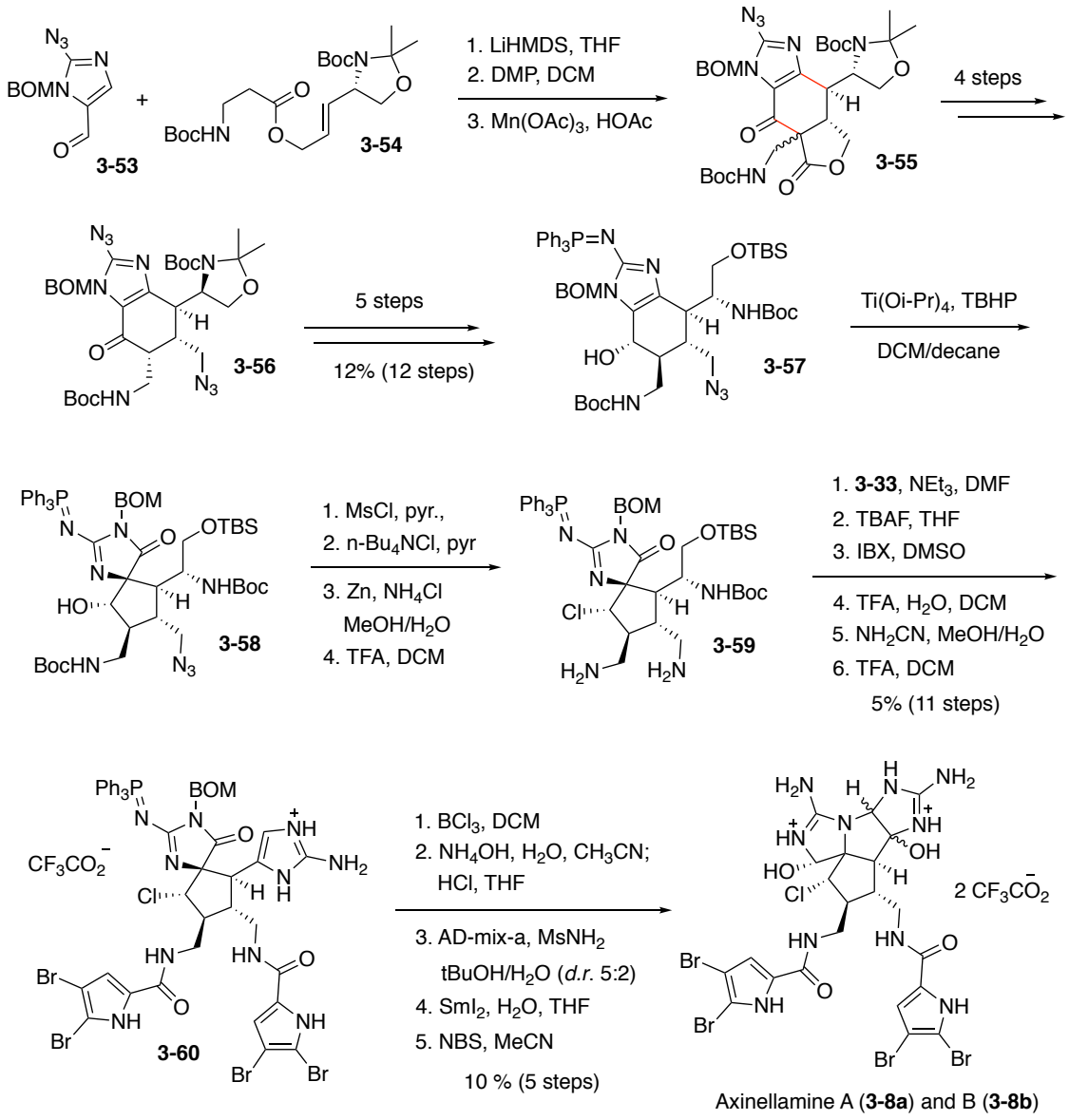

In the final stage manipulations, it was found that treating **3-60** with reducing reagents such as $CaBH_4$ and $LiAlH_4$ resulted in decomposition of the starting material instead of reduction of the carbonyl group of the spiroglycocyamidine portion. Reaction with $LiHBEt_3$ led to loss of the chloride. Therefore, the sequence was altered where the BOM group was removed first and the iminophosphorane was hydrolyzed. Oxidative cyclization induced by dihydroxylation with AD-mix-α and AD-mix-β gave the same diastereoselectivity of the axinellamine skeleton (2:1–

3:1 *dr*), which was then subjected to a condition for carbonyl group reduction using SmI_2 in THF/H_2O. Although this reaction successfully reduced the carbonyl group, 5-bromo substituents on the pyrrole moiety was also reduced. Thus, reinstallation of the bromide with NBS led to the total synthesis of (–)-axinellamine B (**3-8a**) together with (–)-axinellamine A (**3-8b**).

3.3.3. Synthesis of Palau'amine

The first racemic total synthesis of palau'amine was accomplished by the Baran group in 2010[24] and then a year later, Baran and coworkers accomplished the first enantioselective synthesis of (–)-palau'amine.[25] In 2015, the Tanino group completed the second racemic total synthesis of palau'amine.[26]

3.3.3.1. Tanino's Strategy

The total synthesis was commenced with piperazine **3-62** which was prepared from 2-cyclopentenone **3-61** in which vinyl group was successfully installed via $Hg(OTf)_2$-catalyzed cyclization over 6 steps (**Scheme 3.9**). The three consecutive stereogenic centers of the cyclopentane core of **3-63** was furnished via Baylis-Hilman reactions and ketone reduction of cyclopentanol moiety of **3-62** in 6 steps. Another 6 additional steps of functional group modifications yielded the α-brominated tetrahydropyridazin-3(2*H*)-one **3-64** which subsequently undergoes a ring contraction upon methnolysis of the hydrazine to generate **3-65**. The author stated that the steric hindrance from a vinyl group at the bridgehead led to SN_2 intramolecular ring closure induced by the amine anion **3-64′** occurred from the top face of bromine, a concave side of the ring, and then the ring-closure product was readily epimerized to **3-65** to circumvent steric repulsions. The pyrrolylcarbonyl unit was introduced to give **3-66** which is a precursor for

the key transformation. The N–N bond cleavage by treating **3-66** with LiHMDS and subsequent ring-closure by the pyrrole anion on intermediate **3-66′** containing a *trans*-bicyclo[3.3.0]octane skeleton led to **3-67**.

Scheme 3.9. Synthesis of palau'amins tetracyclic core

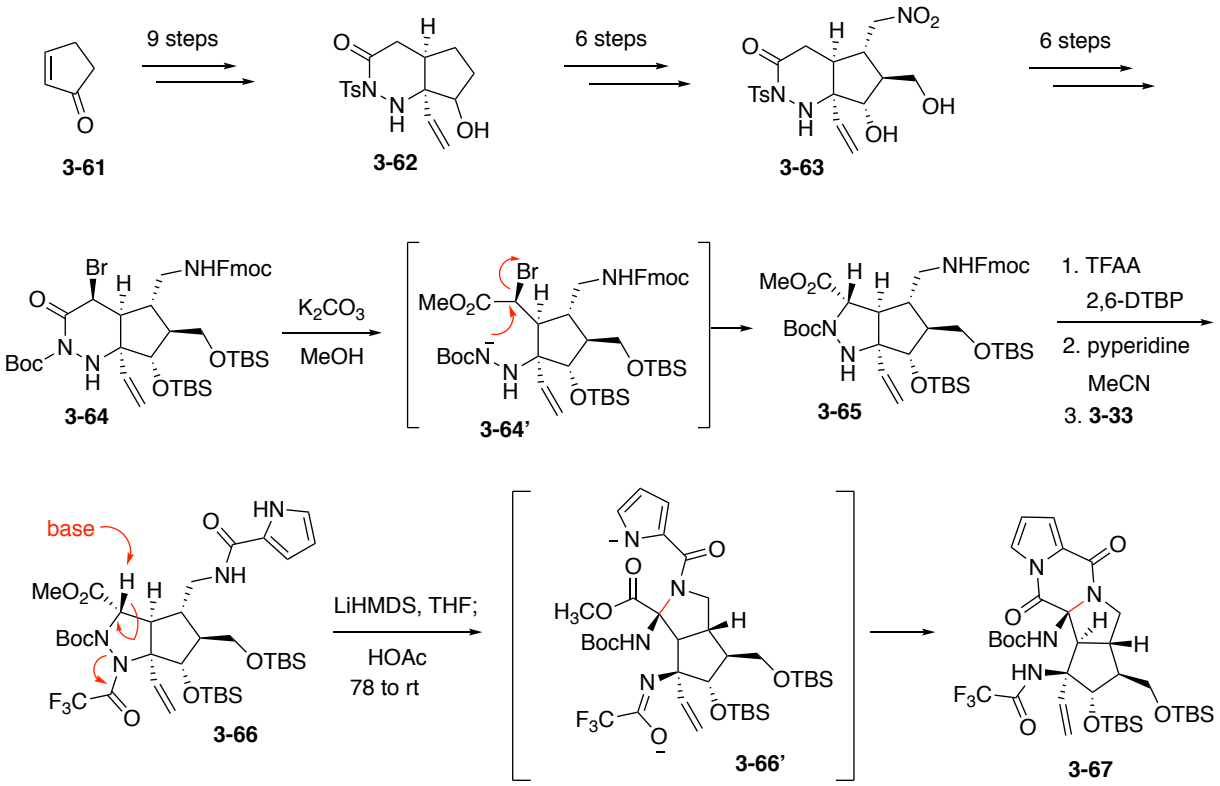

Following the sequence developed by Romo for the synthesis of dibromophakellstatin, a thiourea moiety was installed on **3-67** and one of the carbonyl group was reduced to generate hemiaminal **3-68** (**Scheme 3.10**). Cyclization of the thiourea moiety along with the pyrrole-*N,O*-hemiketal yielded pentacyclic core **3-69**. Through an additional 6 steps including dihydroxylation of the vinyl group and glycol cleavage, the hexacyclic skeleton **3-70** containing the second *bis*-protected guanidine moiety was generated. Converting the methylthio group to an amino group and further functional group modifications through a 5-step sequence led to a total

synthesis of *rac*-palau'amine in total 47 longest linear steps.

Scheme 3.10. The endgame to *rac*-palau'amine

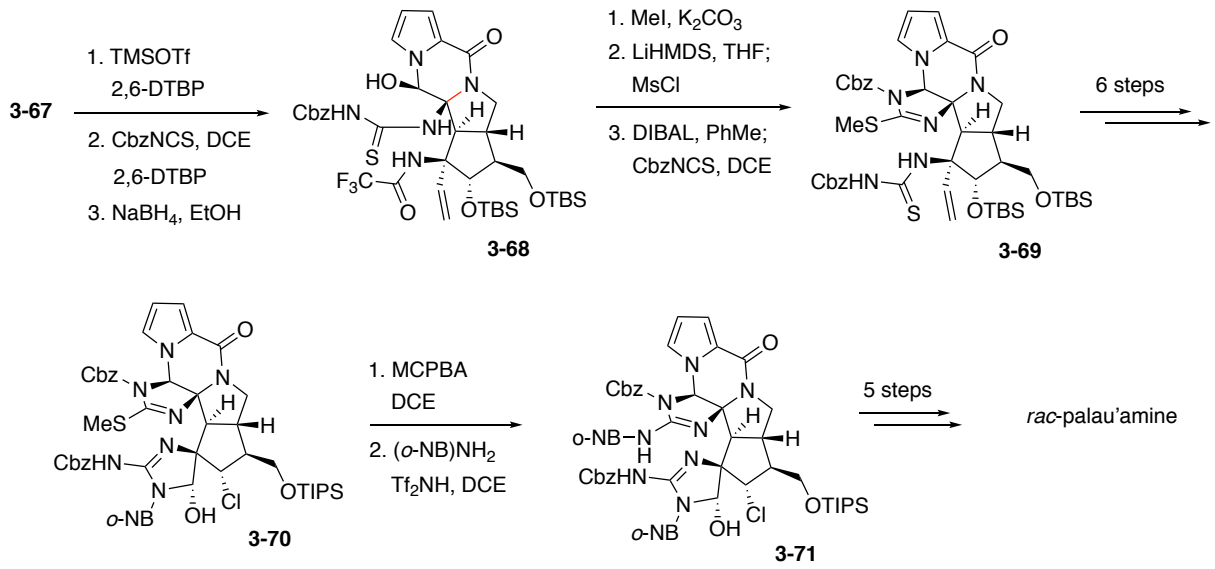

3.3.4. Synthetic Studies of Massadine

3.3.4.1. Carreira's Synthesis of the Massadine Core

The Carreira group disclosed the synthesis of a fully functionalized massadine core as a potential precursor of (–)-massadine in 2011 (**Scheme 3.11**).[27] The synthesis was started with a diastereoselective Diels–Alder reaction between TMS-cyclopentadiene **3-72** and di-(–)-menthyl fumarate **3-73** to afford cycloadduct **3-74**. Treating **3-74** with bromine provided bromolactone **3-73** which underwent a Fleming rearrangement in the presence of $AgNO_3$. The TMS group was eliminated by MeOH followed by methanolysis of the lactone moiety of **3-75′** to generate bicyclo[2.2.1]hept-2-ene **3-76**, which was subjected to aminocyanation through Ugi-4-component coupling reaction, resulting in **3-78** through a 7-step sequence.

Scheme 3.11. Massadine core synthesis by Carreira and coworkers

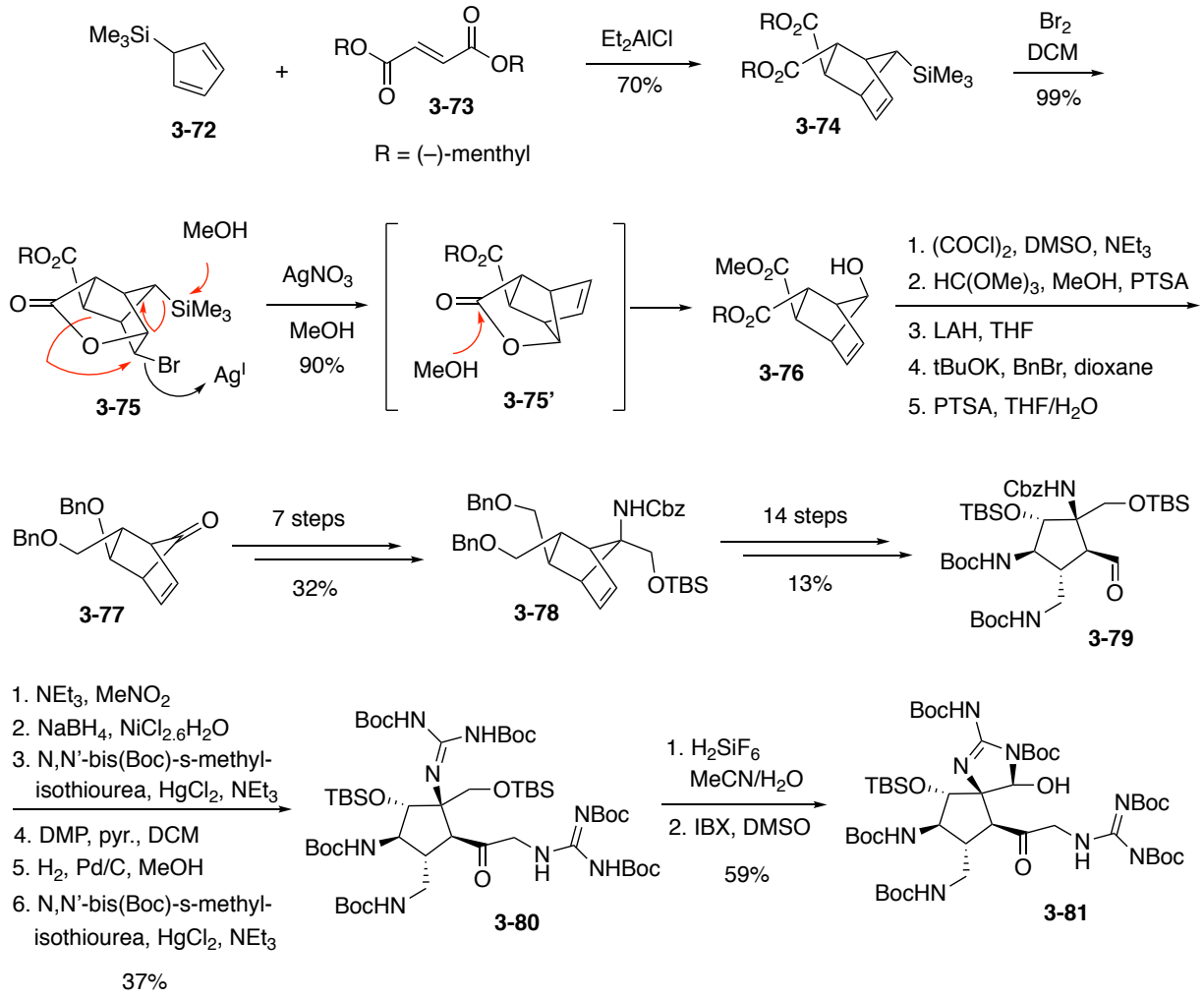

The ozonolysis of **3-78** followed by a 14-step elaboration afforded the fully substituted cyclopentane aldehyde **3-79**, which was subjected to a Henry reaction with nitromethane. The nitro group was reduced to the corresponding amine with $NaBH_4$ and the intermediate was treated with *N*,*N*′-bis(Boc)-*S*-methyl-isothiourea in the presence of $HgCl_2$ to afford the first guanidine moiety. DMP oxidation followed by removal of the Cbz group yielded the aminoketone, which was subjected to the conditions for the construction of the second guanidine moiety in **3-80**. Deprotection of the primary alcohol on **3-80** with H_2SiF_6 in $MeCN/H_2O$ followed by oxidation with IBX provided **3-81** in 38 steps from TMS-cyclopentadiene.

3.3.4.2. Baran's Total Synthesis of Massadine

The Baran's group reported the total synthesis of massadine chloride and massadine along with axinellamine and palau'amine (**Scheme 3.12**).[25] Completion of the total synthesis started with common precursor **3-52**, which was treated with silver(II) picolinate to install the hemiaminal moiety in spiroguanidine **3-79**.

Scheme 3.12. The endgame to (–)-massadine (**3-7a**) and (–)-massadine chloride (**3-7b**)

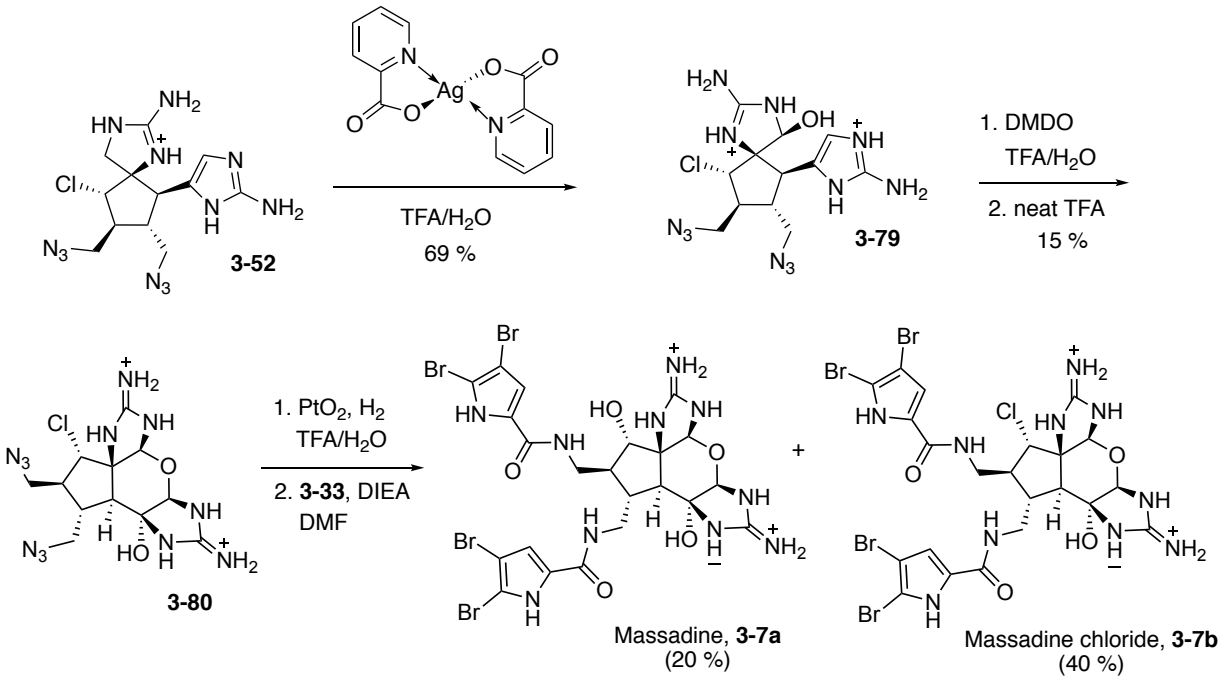

The double bond of the 2-aminoimidazole moiety was oxidized with DMDO. In the presence of TFA, the hemiaminal hydroxyl group is engaged in the ring closure reaction to form tetrahydro-*2H*-pyran moiety **3-80**. Subsequent reduction of the two azide groups with PtO_2 and the following coupling reaction with the dibromopyrrole completed the enantioselective total synthesis of (–)-massadine (**3-7a**) and (–)-massadine chloride (**3-7b**).

3.3.4.3. Chen's Synthesis of Massadine

The Chen group revealed their total synthesis of (–)-massadine in 2014 by employing the advanced intermediate **3-56**, which is the same intermediate in their synthesis of axinellamine

(**Scheme 3.13**).[12a]

Scheme 3.13. Total synthesis of (–)-massadine by Chen and coworkers

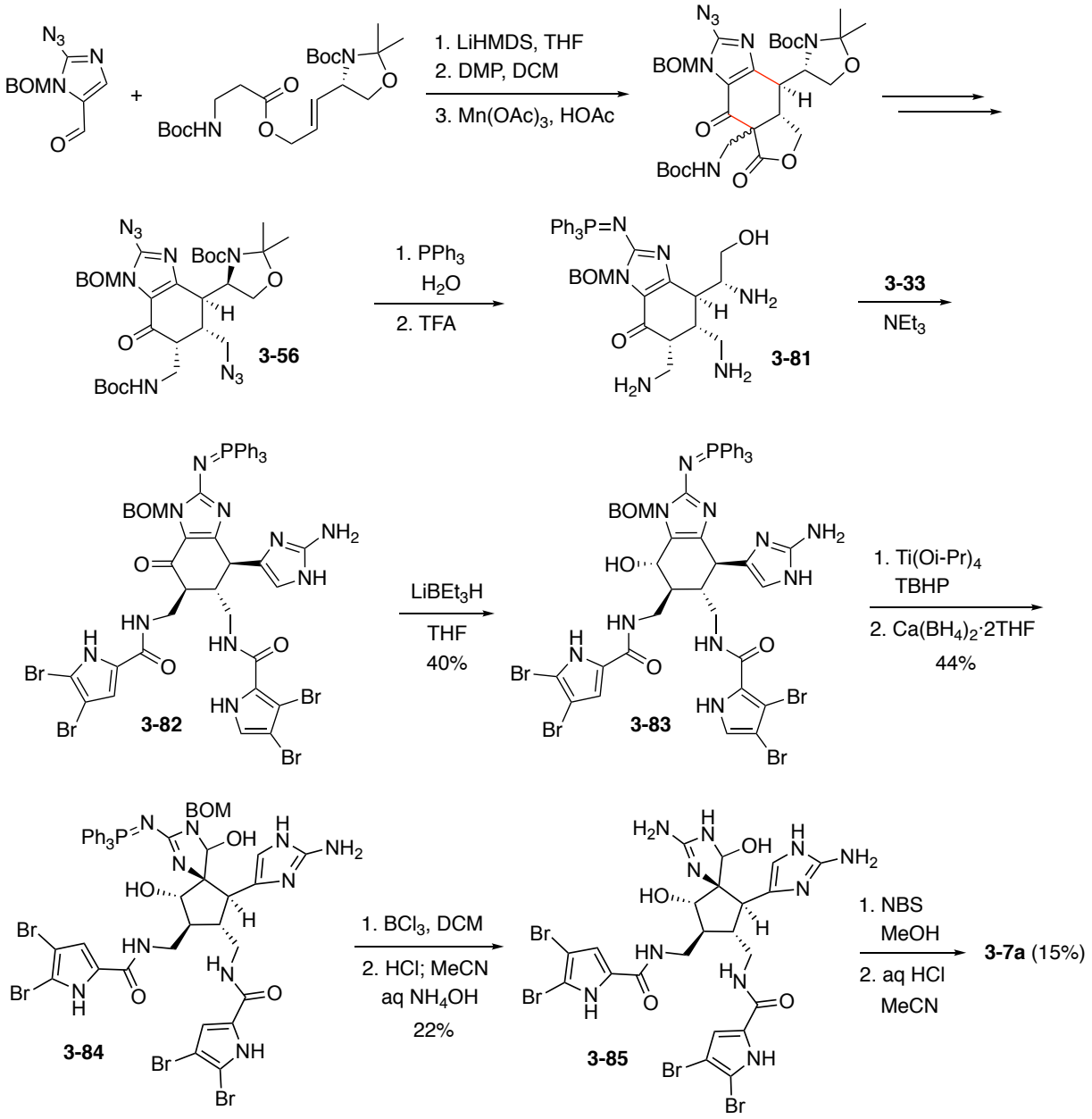

The synthesis was commenced with a Staudinger reaction of **3-56** followed by removal of acetonide and Boc group to give triamine **3-81**. Diastereoselective reduction of **3-82** with $LiBEt_3H$ generated the secondary alcohol **3-83**. Regioselective oxidation with $Ti(Oi\text{-}Pr)_4$ and

TBHP leads to the ring contracted spiroglycocyamidine, which was reduced with $Ca(BH_4)_2$ to afford the *N,O*-hemiacetal **3-84**. Deprotection of the BOM group on **3-84** with boron trichloride (BCl_3) followed by hydrolysis of iminophosphorane led to "pre-massadine" **3-85,** which underwent oxidative cyclization in the presence of NBS followed by treating with aqueous HCl generated (–)-massadine (**3-7a**) in 15% yield and 3,7-epi-massadine in 29% yield as a byproduct.

3.4. Racemic Synthesis of the Carbocyclic Core of Massadine

3.4.1. Retrosynthetic Analysis

As outlined above, the main synthetic challenges in massadine are the construction of the fully functionalized cyclopentane core as well as the elaboration of the guanidine moieties. Many synthetic efforts led to the development of efficient synthetic routes of axinellamines (**3-8a**–**3-8d**), massadines (**3-7a**–**3-7b**) and palau'amine (**3-9a**–**3-9c**). In particular, synthesis of the bioactive fully functionalized cyclopentane has received a great deal of attention in the past two decades as an attractive synthetic target.[1] In this chapter, trimethylsilyldiazomethane (TMSD)-mediate formal [3+2] cycloaddition with α,β-unsaturated carbonyl compounds followed by protonolytic N–N bond cleavage to the corresponding α-amination-β-cyano moieties is highlighted as the main subject. This formal α-amino-β-cyanation strategy has been successfully engaged in the synthesis of amathaspiramides by Lee and coworkers.[28]

Scheme 3.14. Retrosynthetic analysis

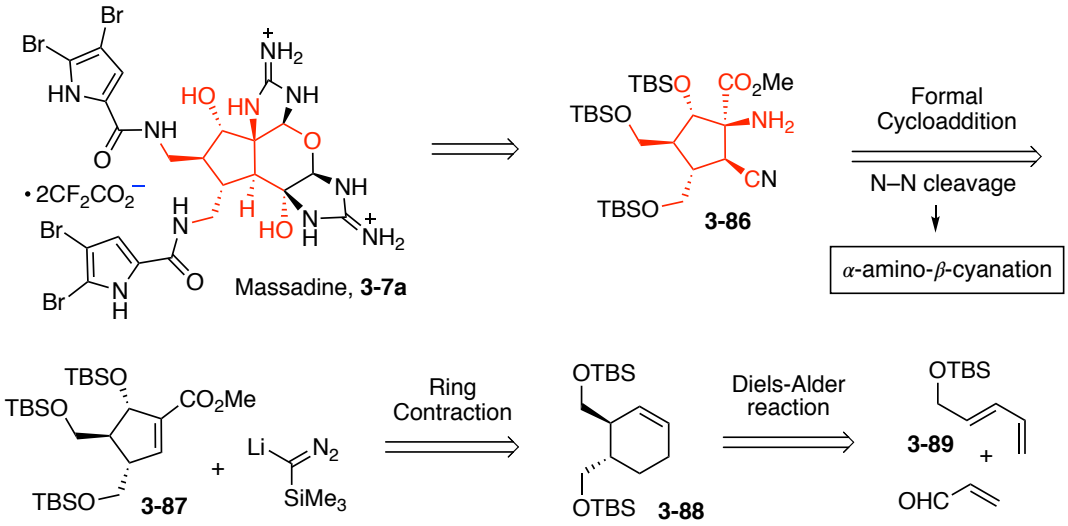

Our synthetic approach to the racemic hexasubstituted cyclopentane core of massadine is outlined in **Scheme 3.14**. We envisioned that massadine **3-7a** can be generated by the installation of the two cyclic guanidine moieties and two bromoimidazole units on the fully functionalized pentacyclic core **3-86**. The synthesis of **3-86** commenced with the construction of *cis*-oriented α-amino-β-cyano groups via formal [3+2] cycloaddition of α,β-unsaturated methyl ester **3-87** with lithium(trimethylsilyl)diazomethane (LTMSD) followed by N–N bond cleavage. In turn, cyclopentene carboxylate **3-87** can be derived from ring contraction of cyclohexene **3-88** and *trans*-**3-88** will be generated from a Diels–Alder reaction between the diene **3-89** and acrolein followed by epimerization. Finally, the diene **3-89** could be readily synthesized from commercially available malonic acid. Our strategy provides a unique entry to the installation of a tertiary amino group and the secondary cyano group in a *cis*-relationship via a short sequence compared to other reported approaches where relatively long synthetic sequences of functional group interconversion were required.

3.4.2. Key Transformation

Lee and coworkers explored synthetic applications of LTMSD toward 1,4-addition onto cyclic α,β-unsaturated ketones followed by protonolytic N–N bond cleavage (**Scheme 3.15**). In general, enones **3-90**/**3-91** undergo 1,4-addition followed by cyclization to form Δ^2-pyrazoline **3-92**/**3-93**, which afford product **3-94**/**3-95** after protonation.

Scheme 3.15. 1,4-Addition of LTMSD with cyclic ketones

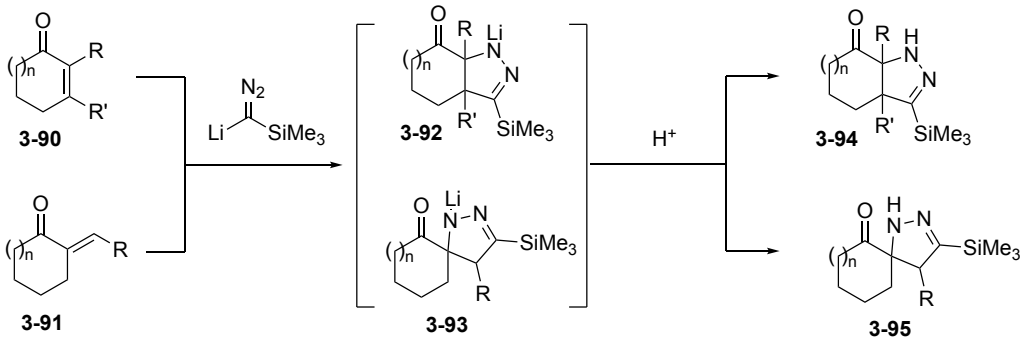

The mechanistic hypothesis of the reaction between cyclic α,β-unsaturated ketones and LTMSD followed by N–N bond cleavage was proposed by Lee and coworkers (**Scheme 3.16**).[29] First, LTMSD reacts directly with the β-carbon of α,β-unsaturated ketones **3-90** affording 1,4-adduct **3-98**, which undergoes endo-mode ring closure to generate lithiated Δ^2-pyrazoline **3-97**. Protonation of **3-97** yields Δ^2-pyrazoline **3-94** which can be treated with Brønsted acid for N–N bond cleavage. The protonolytic cleavage of the N–N bond can be initiated by the formation of ammonium intermediate **3-95**, which then subsequently attacked by the conjugate base on the silyl group to induce C–TMS and N–N bond cleavage, generating α-amino β-cyano ketone **3-96**.

Scheme 3.16. Mechanism of formal *cis*-1,2-aminocyanation of cyclic ketones

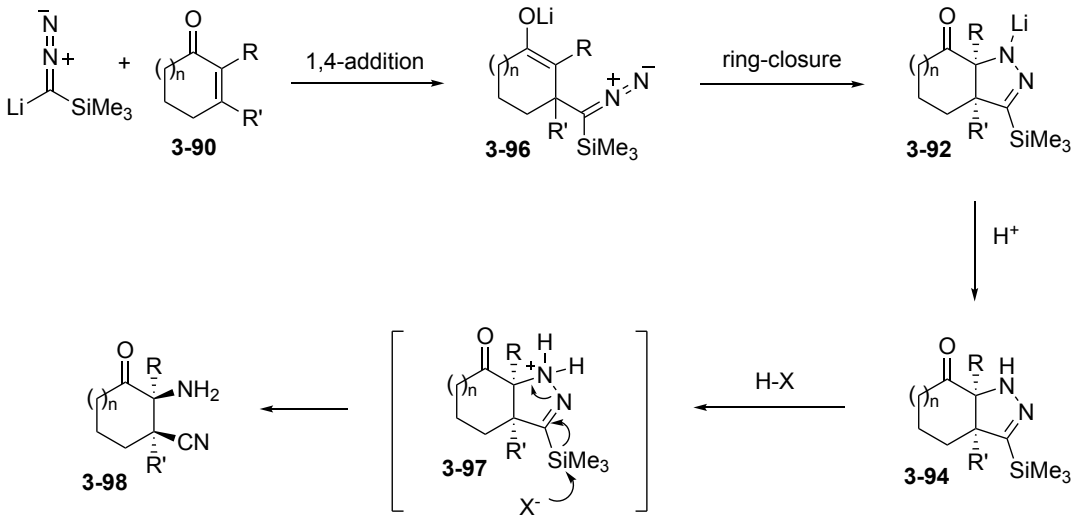

3.4.3. Construction of the Cyclopentene Carboxylate

3.4.3.1. Synthesis of Cyclopentene Carboxaldehyde

The precursor of *E*-1,3-diene was prepared from the reaction between malonic acid and acrolein in the presence of pyridine.[30] The subsequent reduction with LAH followed by TBS protection provided the desired diene **3-89** (**Scheme 3.17**).

Scheme 3.17. Synthesis of diene **3-89**

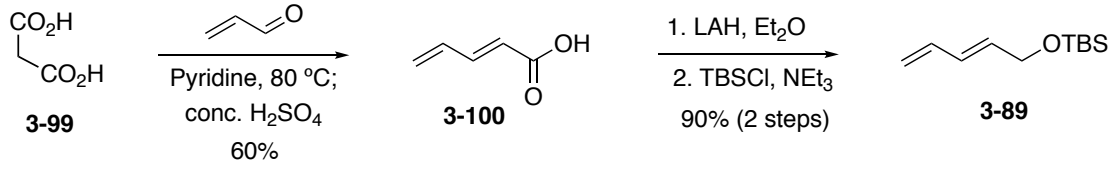

Dimethylaluminum chloride-mediated Diels–Alder reaction[31] gave *endo*-selective product *cis*-**3-102** in 88% yield (10:1*dr*), which underwent epimerization in the presence of DBU to provide the thermodynamically more stable *trans*-isomer **3-102** in an 8:1 ratio (**Scheme 3.18**). Treating aldehyde *trans*-**3-102** with $NaBH_4$ followed by primary alcohol protection with TBSCl generated cyclohexene **3-88** in 90% two-step yield.

Scheme 3.18. Preparation of a diol intermediate

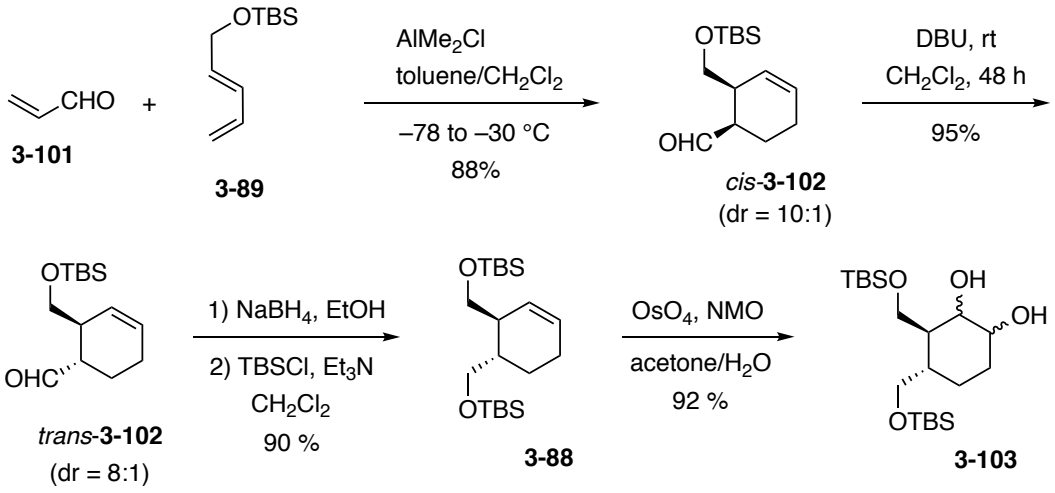

Dihydroxylation of **3-88** (cat. OsO_4, NMO) followed by the oxidative cleavage of the resulting diol **3-103** ($NaIO_4$, aq THF, pH 7 buffer) afforded dialdehyde **3-104 (Table 3.1)**. Dialdehyde **3-104** is extremely sensitive and decomposes on silica gel. In addition, it was recognized that ozonolysis of **3-88** directly to generate the dialdehyde failed. Therefore, **3-104** was used for the next step without further purification. Several aldol condensation conditions were screened, including *trans*-3-hydroxy-L-proline and piperidine/acetic acid, which gave the desired product **3-105** in 50% and 83% yield, respectively (entries 1 and 2). It was discovered that treating **3-104** with a catalytic amount of dibenzylammonium trifluoroacetate[32] provided cyclopentene carboxaldehyde **3-105** in 92% yield (entry 3).

Table 3.1. Intramolecular aldol condensation

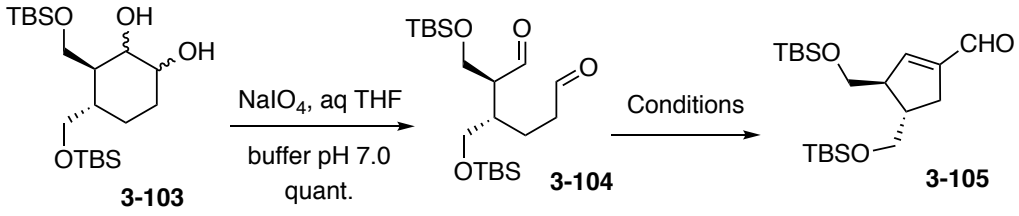

Entry	Conditions	yield (%)
1	*trans*-OH-L-proline DMSO, rt	50
2	Piperidine, Acetic acid DCM, 65 °C	83
3	$(Bn)_2N^+H_2\ ^-O_2CCH_3F_3$ Benzene, rt	92

3.4.3.2. Installation of an Allylic Alcohol

After converting the resulting α,β-unsaturated aldehyde to the corresponding methyl ester by employing Corey–Ganam oxidation, we first attempted to prepare epoxyester **3-108** and then open the epoxide with a base to achieve the corresponding allylic alcohol (**Scheme 3.19**). However, direct construction of the epoxy moiety turned out to be challenging with electron-deficient epoxidizing agents such as mCPBA. Therefore, a suitable nucleophilic epoxydizing condition, including H_2O_2/NaOH, *t*BuOOH/DBU, *t*BuOOH/KO*t*Bu were attempted, but none of these reaction conditions gave the desired product **3-87**. Fortunately, *t*BuOOH with NaHMDS generated epoxide **3-108**, although with a low yield. For a more efficient epoxidation, aldehyde **3-105** was reduced to alcohol ($NaBH_4$, EtOH) and then mCPBA was employed to generate epoxy alcohol **3-106** in 82% yield (9:1 *dr*). Treating the resulting alcohol with $RuCl_3$ and $NaIO_4$ followed by esterification with TMS-diazomethane in MeOH generated epoxy ester **3-108**.[33,34] Unfortunately, none of the attempts with various conditions to open the epoxide. After unsuccessful attempts to open the epoxide, conversion of **3-106** to epoxyaldehyde **3-109** with

DMP proceeded to generate **3-109**, which was treated with PhSH/$AlMe_3$ to afford a phenylthio aldehyde **3-110** in 70% (6:1 *dr*). The secondary hydroxyl group was protected with the TBS ether to provide **3-111** in 85% yield.

Scheme 3.19. Installation of an allylic alcohol on cyclopentene carboxylate

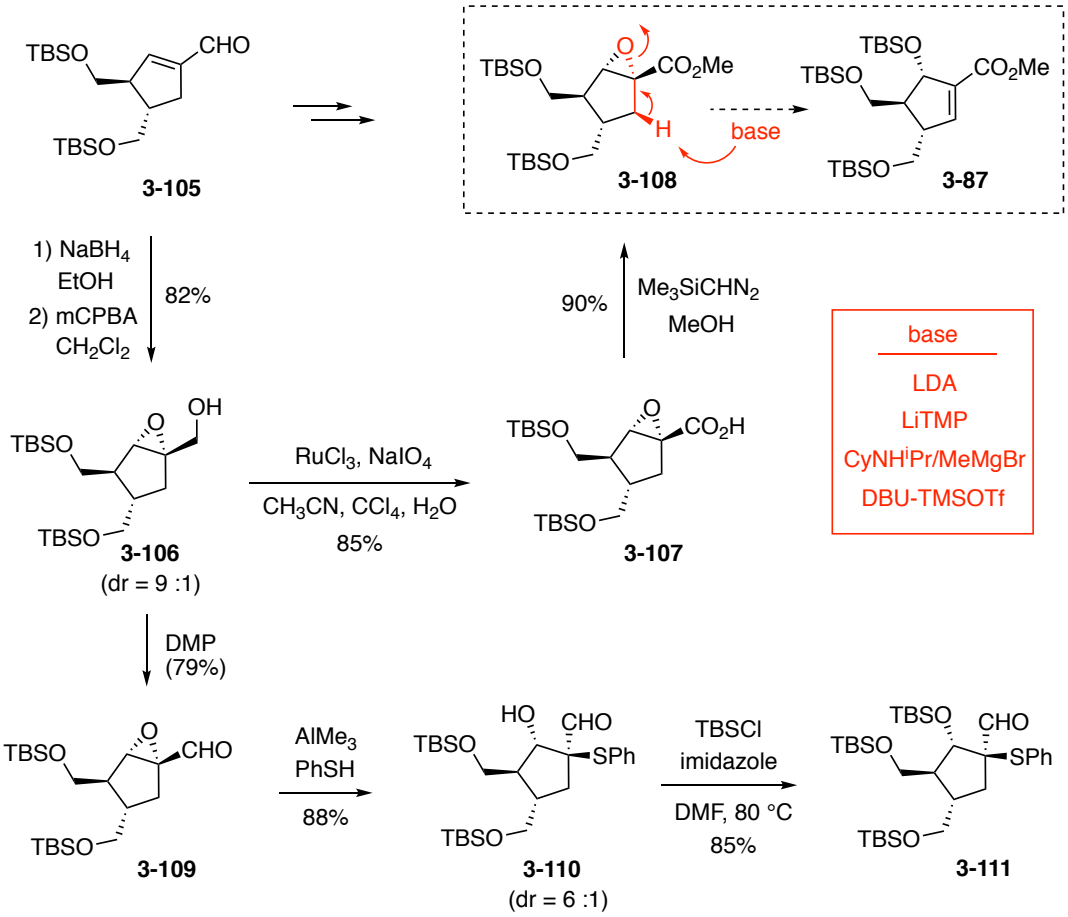

The oxidation of phenylthio group installed on the α-carbon of the aldehyde[34] **3-111** to the corresponding sulfoxide **3-112** followed by its elimination to generate unsaturated aldehyde **3-113** was investigated under various oxidation conditions (**Table 3.2**). While treating **3-111** with $NaIO_4$ in aqueous MeOH[35] returned the starting material untouched (entry 1), with H_2O_2 catalyzed by scandium triflate[36] led to complete decomposition (entry 2). Typical mCPBA

condition under different temperature and solvents did afford the desired sulfoxide with a moderate diastereoselectivity (3:1–5:1). Unfortunately, however, in the subsequent elimination step, only the minor isomer could be eliminated to provide **3-113** and the major sulfoxide isomer remained intact even after an extended reaction time or at a higher temperature (entries 3 and 4). To our delight, it was found that treating **3-111** with H_2O_2[37] in an acidic medium furnished sulfoxide **3-112** with an excellent diastereoselectivity (>19:1), which underwent smooth elimination upon heating in the presence of $P(OMe)_3$ to deliver **3-113** in 76% yield over 2 steps (entry 5).

Table 3.2. Oxidation of the phenylsulfide and its elimination

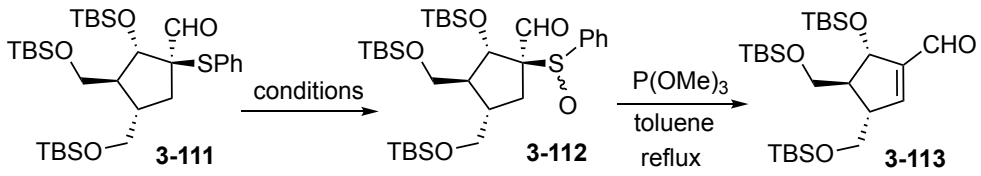

entry	conditions	dr of **3-112**	result
1	$NaIO_4$, aq MeOH, rt	—	Recovering starting material
2	$Sc(OTf)_3$, H_2O_2, CH_2Cl_2/EtOH	—	Complex reaction mixture
3	mCPBA, CH_2Cl_2, $-_{78}$ °C to rt	1:3	Only the minor isomer eliminated
4	mCPBA, MeOH, 0 °C	1:5	Only the minor isomer eliminated
5	H_2O_2, AcOH/CH_2Cl_2, rt	>19:1	76% in 2 steps

The diastereomers of sulfoxide **3-112** showed drastic difference in their elimination behaviors, which can be explained by two proposed models **3-112**-R and **3-112**-U (**Figure 3.3**). It might be possible that peroxide is first reacted with an aldehyde and then transferred to sulfide to generate phenyl sulfoxide. Once two diastereomers formed, isomer **3-112**-R effortlessly undergoes facile elimination reaction, however, another diastereomer requires rotation in order to

adopt the reactive conformation **3-112**-U, which have close proximity between the sulfoxy moiety and the β-proton Ha for elimination. However, this conformation generates an unfavorable steric interaction between the bulky phenyl group and the CH_2OTBS group which can be explicated why only the other diastereomer undergoes the elimination reaction.[38]

Figure 3.3. Phenylsulfoxide elimination

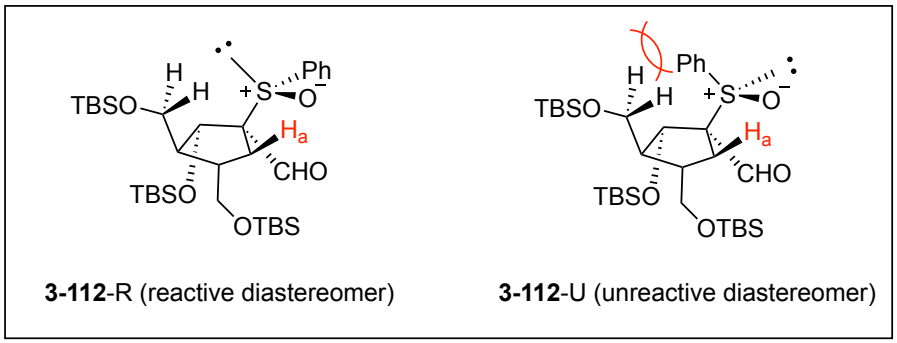

3.4.3.3. Completion of the carbocyclic core of massadine

To install the required α-amino-β-cyano group on cyclopentane carboxylate through a formal cycloaddition with LTMSD and a subsequent N–N bond cleavage the advanced aldehyde intermediate **3-111** was converted to **3-87** in 76% yield by treating with MnO_2 and MeOH (**Scheme 3.20**). Cyclopentanoate **3-87** was treated with LTMSD generated from *n*-BuLi and trimethylsilyldiazomethane at –78°C, installing Δ^2-pyrazoline in 85% yield as a single diastereomer. The following N–N bond cleavage was achieved by protonylitic N–N bond cleavage of Δ^2-pyrazoline with TsOH (2 equiv) in CH_2Cl_2 at 45 °C, affording primary amine-containing cyclopentane carboxylate **3-86** in 90% yield.

Scheme 3.20. The preparation of the carbocyclic core of massadine

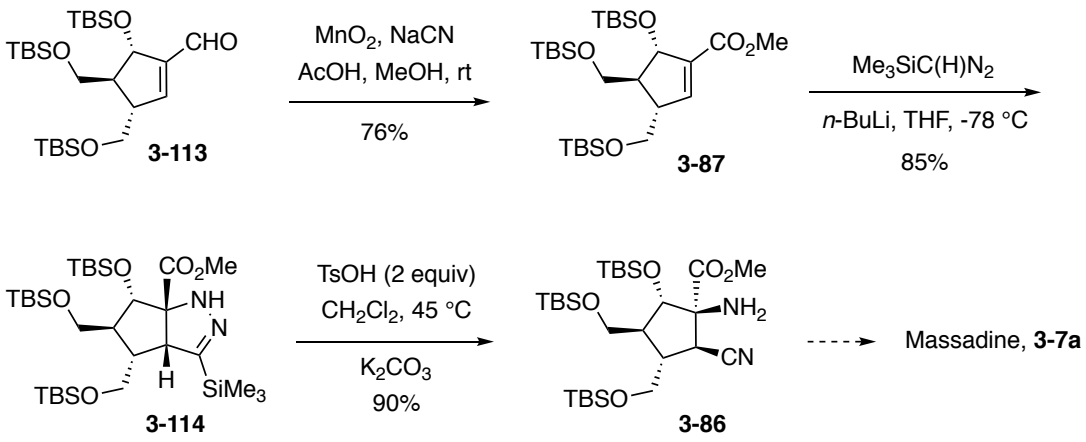

3.5. Enantioselective Synthesis of the Core Carbocycle of Massadine

3.5.1. Retrosynthetic Analysis

After the successful attempt to affect the dipolar [3+2] cyclization with LTMSD and α,β-unsaturated ester followed by N–N bond cleavage, forming the key framework, we turned our attention to the development of enantioselective synthetic route of the carbocycle core of massadine. Our asymmetric synthetic approach to the core is depicted in **Scheme 3.21**. Because [3+2] dipolar cycloaddition with LTMSD and unsaturated ester to generate α-amino-β-cyanated pentacyclic core **3-115** was successfully demonstrated, the corresponding asymmetric synthesis employed the same key transformation to set two critical stereogenic centers in **3-115**. It was anticipated that diene **3-117** could be prepared from cycloisomerization of enyne moiety **3-118**, which was obtained after reduction of lactone moiety of **3-119**. In turn, lactone **3-119** could be prepared from C_4-menthoxy butenolide **3-120**, which could be readily prepared from furfural **3-121** in the presence of rose Bengal and oxygen followed by condensation with D-menthol.

Scheme 3.21. Retrosynthetic analysis

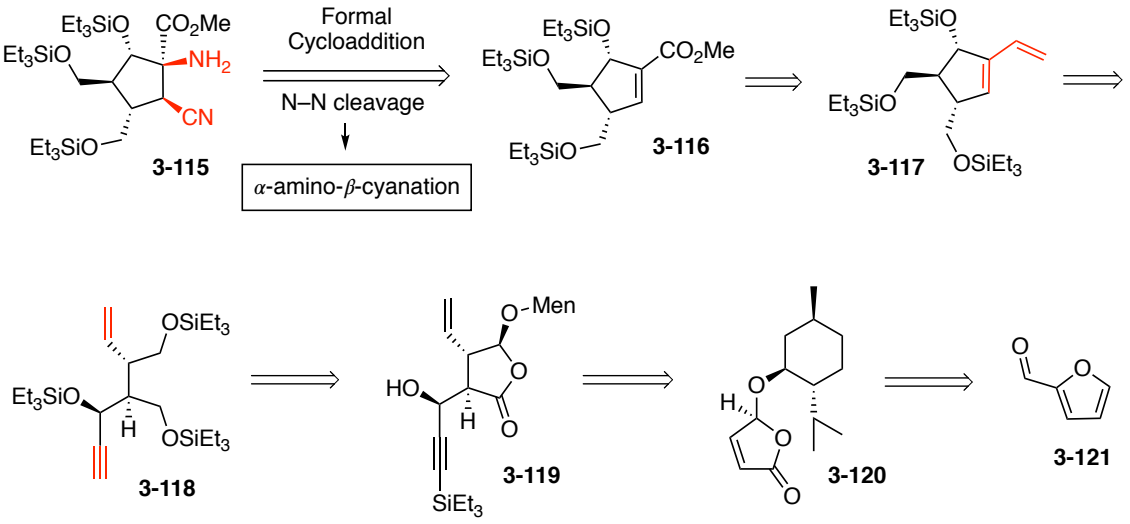

3.5.2. Synthesis of the Carbocycle Core of Massadine

Photolysis of furfural in the presence of rose Bengal and oxygen generated 5-hydroxy-2(5*H*)-furanone **3-122**, which was condensed with D-menthol to generate lactone **3-120** in 38% yield (**Scheme 3.22**).[39] 1,4-Addition of vinyl Grignard reagent in the presence of a stoichiometric amount of CuI followed by enolate trapping with triethylpropynal **3-124**, which was easily generated from the commercially available triethyl acetylene **3-123**, provided γ-lactone **3-119** in 48% yield.[40,41] Removal of the triethyl group from **3-119** followed by treatment with LAH yielded triols **3-125** in 80% yield. Protection of triols with TES-ethers gave 1,6-enyne **3-118**. Treating enyne **3-118** with the Grubbs second-generation catalyst under ethylene gas did not lead to full conversion to **3-117**. Therefore, cycloisomerization of the 1,6-enyne of **3-118** catalyzed by platinum chloride[43] was carried out to generate 1,3-diene **3-117** at room temperature in 76% yield. Increasing the reaction temperature led to decomposition of the enyne **3-118**.

Scheme 3.22. Synthesis of 1,6-enyne

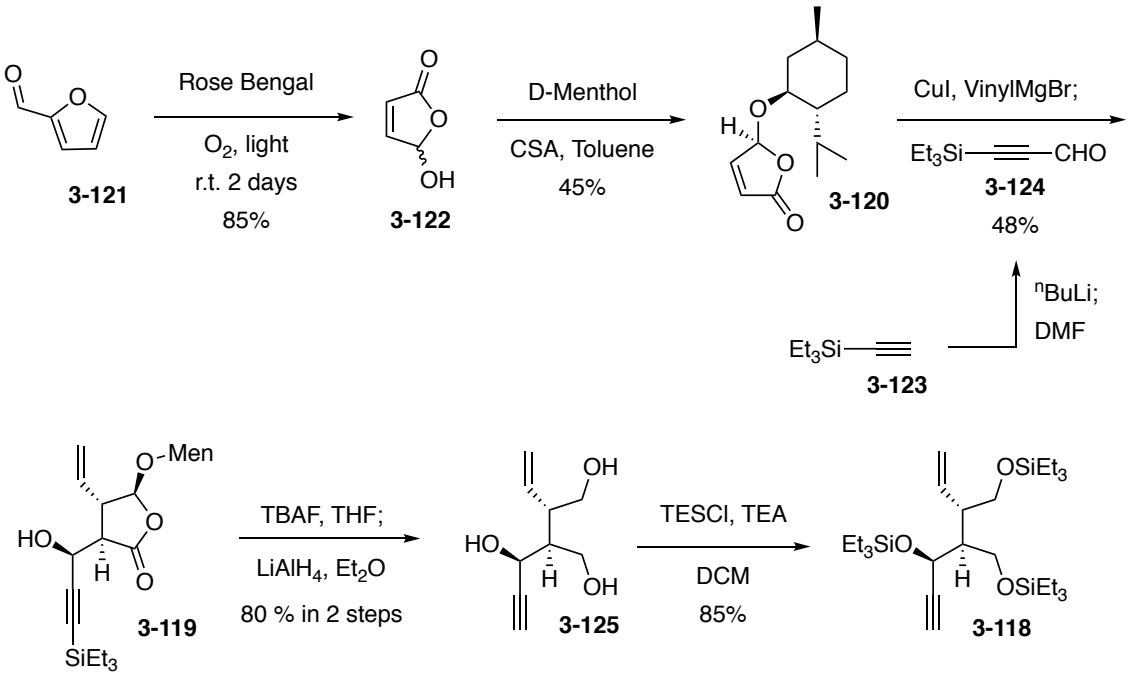

The next challenge was the oxidative cleavage of terminal alkene **3-117** (**Table 3.3**). The first attempt was to convert terminal alkyne **3-117** to a diol and then oxidative cleavage of the diol with $NaIO_4$ or $Pd(OAc)_2$.

Table 3.3. Oxidative cleavage of the terminal alkene

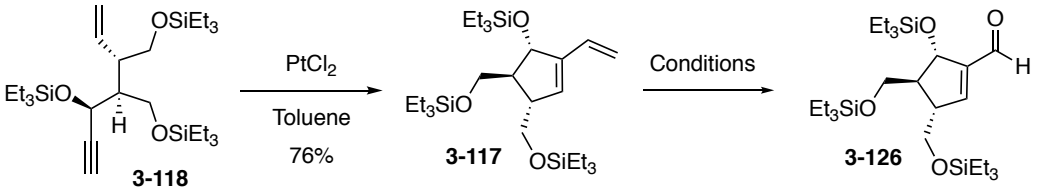

Entry	Condition	Yield (%)
1	OsO_4, NMO; $NaIO_4$	23
2	AD-mix-alpha; $Pb(OAc)_2$	33
3	AD-mix-alpha; $NaIO_4$	31
4	$RuCl_3$, $NaIO_4$	63

Treating **3-117** with a catalytic amount of OsO_4 and NMO (entry 1), or AD-mix-α (entry 2 and 3) generated the diol,[44] however, the subsequent cleavage of the diol with $NaIO_4$ or

$Pd(OAc)_2$ resulted in low yield. Ruthenium-catalyzed oxidative cleavage with $RuCl_3$ and $NaIO_4$ of **3-117** was found to be an efficient protocol[45] to generate aldehyde **3-126** in 63% yield. The reaction was carefully monitored by TLC and was quenched when 8% of the starting material remained in the reaction mixture. Because running the reaction for a long time formed more undesirable and unisolatable byproducts the reaction was stopped before full conversion to recycle the starting material **3-117** rather than waste it.

The endgame is the same as the earlier racemic synthesis. The enal **3-126** was subjected to a Corey–Ganem oxidation condition to prepare **3-115** (**Scheme 3.23**).

Scheme 3.23. The preparation of the carbocycle core of (–)-massadine

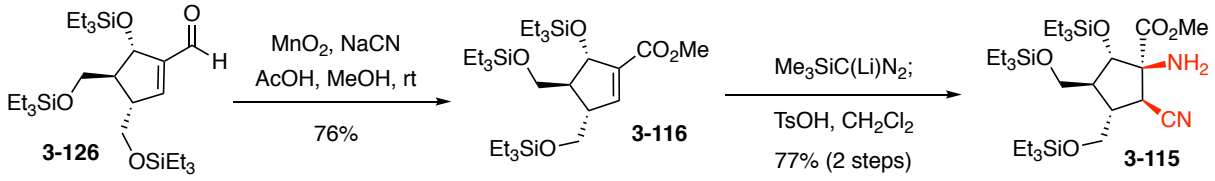

3.6. Construction of the Guanidine Fragment of Massadine

3.6.1. Model Study

We demonstrated efficient routes for preparing the carbocycle core of massadine. It was hypothesized that one of the guanidine moiety could be installed directly by trapping the lithium amide intermediate formed from the reaction between α,β-unsaturated ester and LTMSD with a suitable carbodiimide (**Scheme 3.24**). To test the feasibility of this one-pot construction of a guanidine moiety, we initially performed model studies with a simple α,β-unsaturated ester. We hypothesized that once LTMSD and methyl methacrylate undergo cycloaddition, the resultant lithium amide should be reactive enough to further react with carbodiimide to give the oxoguanidine moiety.

Scheme 3.24. Plan for cyclic guanidine installation

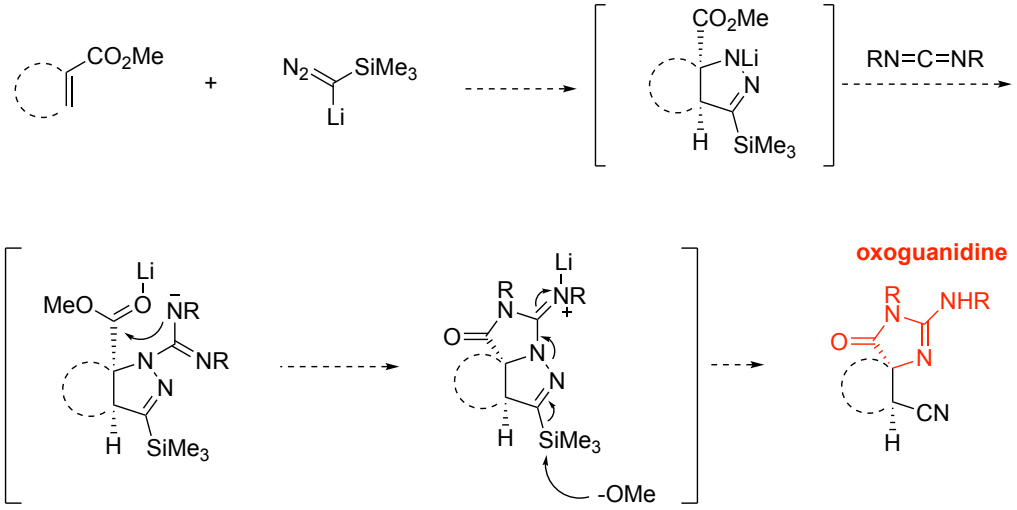

In the initial exploration, a commercially available dihexylcarbodiimide (DCC) was used and examined the effect of different additives (**Table 3.5**). In the presence of DMAP, monomer **3-127** primarily formed with **3-130** as a minor product. The reaction with 18-crown-6 as an additive generated pyrazoline dimer **3-129** and simple protonation product **3-127** in a 1:1 ratio. Gratifyingly, it was found that HMPA promoted the reaction of carbodiimide and subsequent cleavage of the N–N bond to furnish aminoimidazolone **3-131** with high efficiency (88%). Once we acquired this promising result with DCC, a removable group-containing carbodiimide such as dibenzylcarbodiimide was used for the model study with an expectation that the benzyl group can be removed in the total synthesis pursuit.

Dibenzylcarbodiimide was synthesized from thiourea, which is derived from benzylamine and carbon disulfide.[46] Under the conditions with HMPA, a mixture of the expected oxoguanidine **3-130** and its N–N bond cleavage product **3-131** in 3:4 ratio. The formation of the latter compound is the consequence of the in situ generated LiOMe to attack the trimethylsilyl

group. It was also found that **3-130** was readily converted to **3-131** with acid treatment.

Table 3.5. Formation of an oxoguanidine moiety (1)

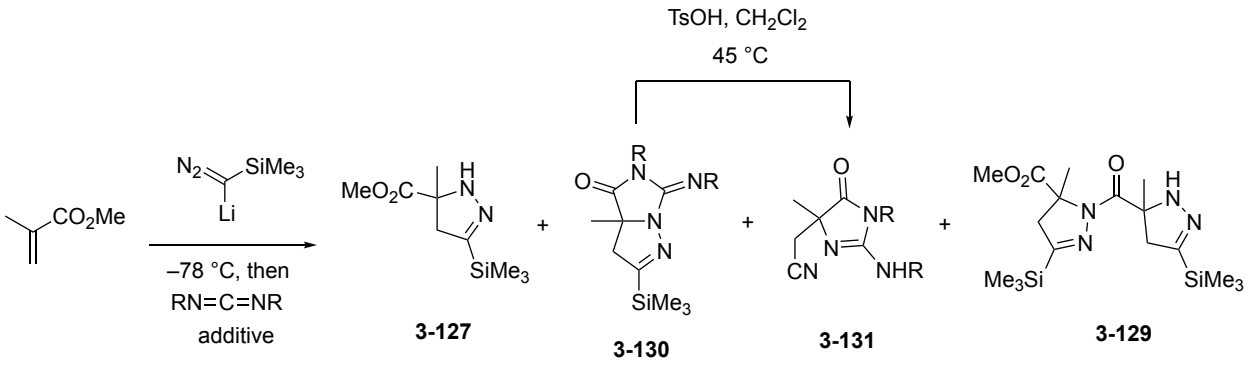

Entry	R	Additive	Result
1	Cyclohexyl	DMAP	**3-127**, 72%, **3-130**, 16%
2	Cyclohexyl	18-crown-6	**3-127**, 33%, **3-129**, 31%
3	Cyclohexyl	HMPA	**3-131**, 88%
4	Benzyl	HMPA	**3-130**, 34% with **3-131**, 45%

The above result is quite promising in that the oxoguanidine can be installed in one-pot. The other remaining task to be addressed to complete the synthesis is to extend a one-carbon unit from the cyano functionality. Based on a proposed synthetic route, one carbon will be extended at this stage after converting the resulting cyano group from **3-131** to α-bromoketone. We envisioned that replacing TMS-diazomethane with ethyl diazoacetate could solve this problem. Therefore, the Δ^2-pyrazoline cycloadduct from methyl methacrylate with ethyl diazoacetate in the presence of DIPEA under thermal condition was employed. However, attempts to form the oxoguanidine moiety from this compound with dibenxylcarbodiimide with various nucleophile/base, including *n*-BuLi, LDA and NaHMDS, did not form the desired product.

Table 3.6. Formation of an oxoguanidine moiety (2)

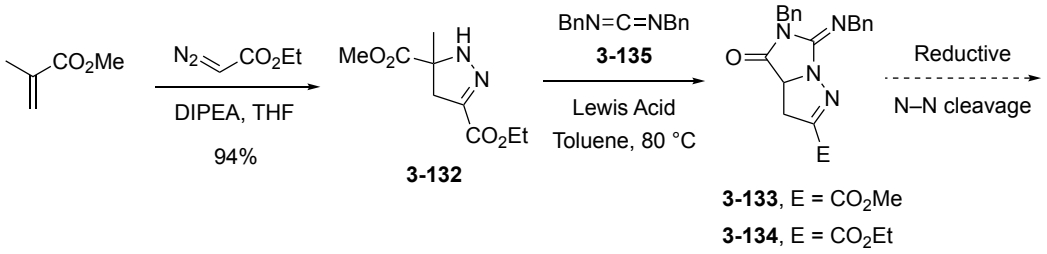

3-133, E = CO_2Me

3-134, E = CO_2Et

Lewis Acid	Time (hr)	Base	Yield (%)	Product
$PdCl_2$	5.5	none	38	**3-134**
$PtCl_3$	24	none	43	**3-133**
$AuCl_3$	18	none	57	**3-133:3-134** (1:7)
$Zn(OTf)_2$	24	none	58	**3-134**
$Cu(OTf)_2$	4	none	68	**3-134**
$ZnCl_2$	2.5	none	86	**3-133:3-134** (2:5)
$ZnCl_2$	2.5	Et_3N	86	**3-133:3-134** (2:5)

At this juncture, the anionic mode of the reaction was changed to cationic mode, thus several Lewis acids[47] were screened under a thermal condition in toluene to activate the carbodiimide. Gratifyingly, all Lewis acids examined promoted cyclization to form a mixture of oxoguanidine moiety-containing compound **3-133** and **3-134** in varying degrees of efficiency. $PtCl_3$, $PdCl_2$, $AuCl_3$, and $Zn(OTf)_2$ resulted in low yields with longer reaction duration. $Cu(OTf)_2$, and $ZnCl_2$ provided the desired product in relatively high yield. Without Lewis acids, the reaction did not proceed, and an addition of a base such as Et_3N has no effect on the result. The methyl ester of **3-133** is assumed to be the consequence of a transesterification by MeOH liberated from the initial ring closure step. Because both methyl and ethyl ester would serve the purpose in the later step, which is its conversion to an aldehyde via reduction, suppression of the transesterification was not pursued.

The possible mechanism for this Lewis acid-catalyzed oxoguanidine formation is commenced with the activation of dibenzylcarbodiimide followed by the first C–N bond

formation between a nitrogen of Δ^2-pyrazoline and carbon of carbodiimide (**Scheme 3.25**). The subsequent cyclization generated the cyclization product (**3-133** and **3-134**) and methanol.

Scheme 3.25. Lewis acid-catalyzed mechanism for oxoguanidine formation

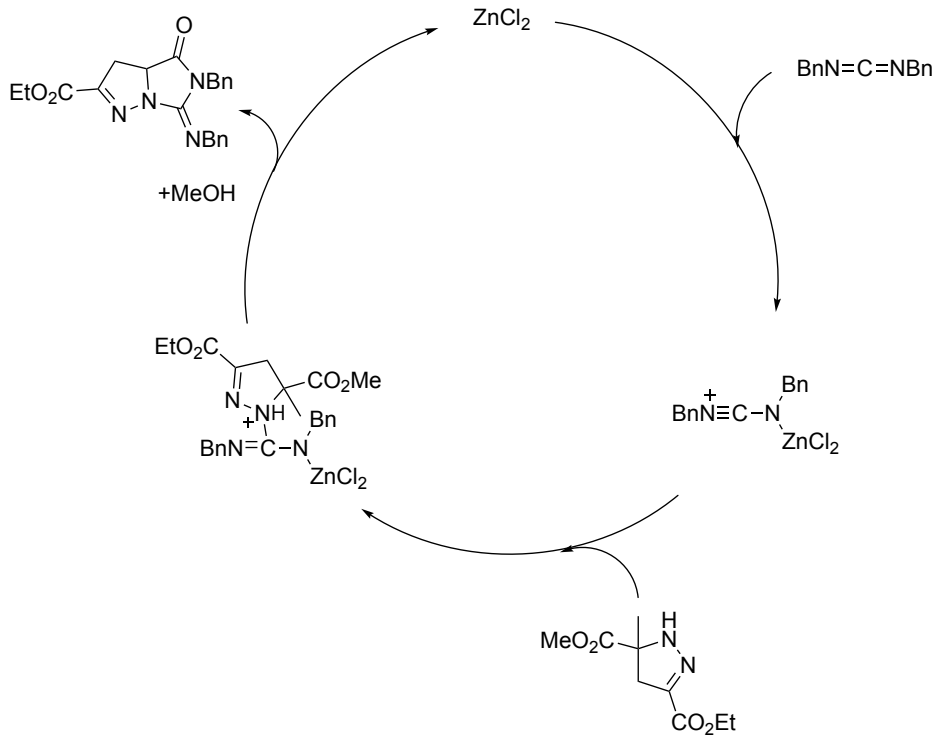

3.7. Conclusion and Future Directions

Both racemic and enantiomeric routes towards the highly substituted carbocyclic core of massadine have been developed. The synthesis featured the application of a formal [3+2] cycloaddition between LTMSD and α,β-unsaturated ester followed by N–N bond cleavage to construct α-amino-β-cyano functionality. The model studies demonstrated a high potential for the generation of the 2-aminoimidazole moiety via the formation of oxoguanidine intermediate with dibenzylcarbodiimide.

Scheme 3.26. Future study toward total synthesis of (–)-massadine

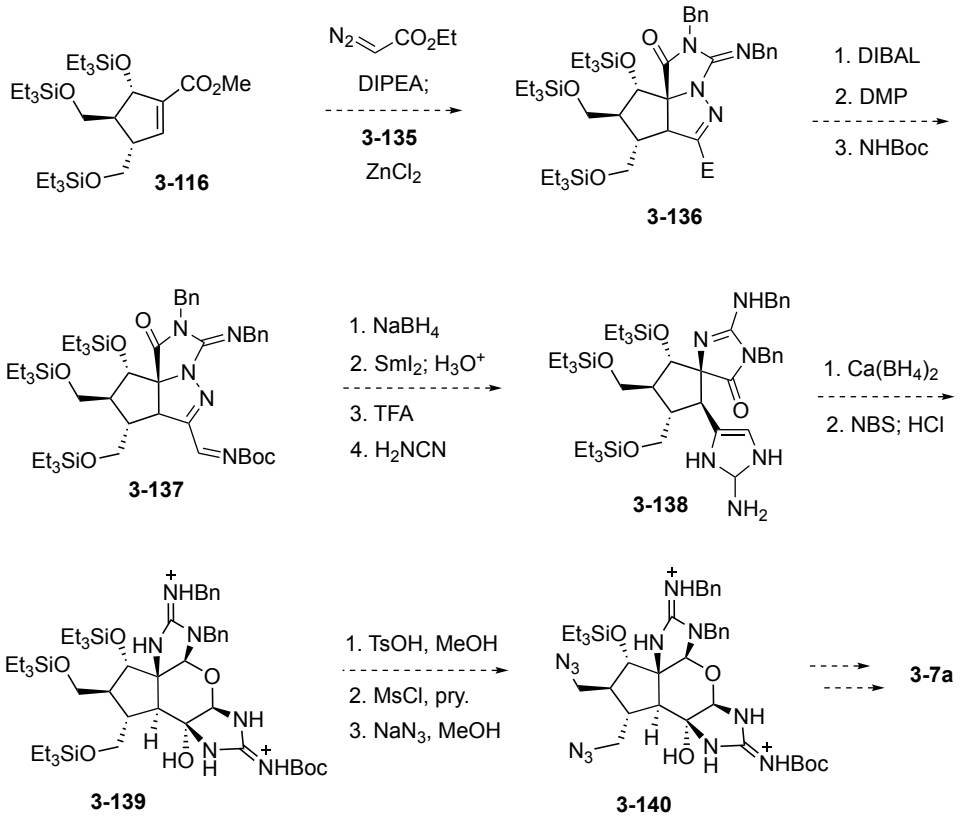

The future plan toward an efficient total synthesis of enantioselective massadine is depicted in **Scheme 3.26**. Cycloaddition between ethyl diazoacetate and **3-116** followed by the Lewis acid-catalyzed oxoguanidine formation with dibezlycarbodiimide **3-135** would give **3-136**. The ester group **3-136** would be converted to the imine **3-137** which would be adapted to α-aminoketone upon N–N bond cleavage with SmI_2, and then treating α-aminoketone with cyanamide generated the aminoimidazole **3-138**. In order to induce the ring closure, the carbonyl group would be reduced with $Ca(BH_4)_2$ followed by addition of NBS to provide **3-139** as the core skeleton of massadines. Two primary alcohols would be deprotected and then mesylated to transformation to azido groups **3-140** after being treated with sodium azide. The subsequent sequence to install the pyrrole moiety of massadine **3-7a** is well developed by many research groups including the Baran[12,16,19] and Chen groups.[22]

Other key transformations involve: a) aldol condensation of dial **3-104** which derived from cyclohexene **3-88**, b) 1,4-addtion of vinyl group followed by tapping enolate with propynal **3-124** to construct three stereogenic centers of **3-119** in one step, c) selective oxidative cleavage of diene **3-117**, d) zinc-catalyzed oxoguanidine formation with dibenzylcarbodiimide.

3.8. Experimental Procedure and Characterization data

3.8.1 General Information

Reactions were carried out in oven or flame-dried glassware unless otherwise noted. Compounds were purchased from Aldrich or Acros or TCI America unless otherwise noted. Toluene (C_7H_8) was distilled over calcium hydride under nitrogen atmosphere. CH_2Cl_2, THF, Et_2O were purified based on standard procedures. Tetrahydrofuran (THF) was distilled over sodium and benzophenone under nitrogen. Flash chromatography was performed using silica gel 60 Å (32−63 mesh) purchased from Silicycle Inc. Analytical thin layer chromatography (TLC) was performed on 0.25 mm E. Merck pre-coated silica gel 60 (particle size 0.040–0.063 mm). Yields refer to chromatographically and spectroscopically pure compounds unless otherwise stated. ^{1}H NMR and ^{13}C NMR spectra were recorded on a Bruker DR-500 spectrometer. Multiplicities are indicated by s (singlet), d (doublet), t (triplet), q (quartet), qn (quintet), sext (sextet), m (multiplet), b (broad), and app (apparent). ^{1}H NMR signals that fall within a ca. 0.3 ppm range are generally reported as a multiplet, with a single chemical shift value corresponding to the center of the peak. Coupling constants, *J*, are reported in Hz (Hertz). Electrospray ionization (ESI) mass spectra were recorded on a Waters Micromass Q-Tof Ultima in the University of Illinois at Urbana–Champaign. Electron impact (EI) mass spectra and Chemical Ionization (CI) mass spectra were obtained using a Micromass 70-VSE in the University of

Illinois at Urbana-Champaign.

3.8.2. Experimental procedures

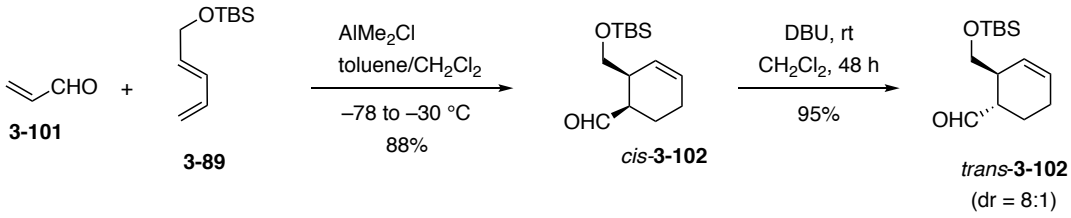

3-101 **3-89** *cis*-**3-102** *trans*-**3-102** (dr = 8:1)

To a solution of the **3-89** (1.98 g, 10 mmol) and acrolein **3-101** (90%, 1.56 g, 25 mmol) in 20 mL CH_2Cl_2/toluene (v/v = 1/3) at –78 °C was slowly added a solution of dimethylaluminum chloride solution (1.0 M in hexane, 15 mL, 15 mmol) over 30 min. The reaction mixture was slowly warmed up to –30 °C and stirred for an additional 3 h. Then the reaction mixture was poured onto the crushed ice and 20 mL of EtOAc was added followed by the addition of potassium sodium tartrate (20 mL). The mixture was warmed to room temperature. The layers were separated and the aqueous phase was extracted with ethyl acetate (10 mL x 3). The combined organic phase was dried over anhydrous $MgSO_4$, filtered, concentrated, and purified by silica gel column chromatography (Hex : EtOAc = 40 : 1) to give *cis*-**3-102** (2.23 g, 88%, 10 : 1 *dr*) together with a small amount of *trans*-**3-102**.

To the solution of a mixture of an inseparable diastereomeric **3-102** (2.23 g, 8.8 mmol) in CH_2Cl_2 (20 mL) was added DBU (2.0 g, 13.2 mmol) and the reaction was kept at room temperature for 48 hours. The solvent was removed under vacuum and the residue was purified by column chromatography (Hex : EtOAc = 40 : 1) to give *trans*-**3-102** (2.12 g, 95%, 8 : 1 *dr*)

together with a small amount of *cis*-**3-102**.

trans-**3-102** (colorless oil): ^{1}H NMR (500 MHz; $CDCl_3$) δ 6.68 (s, 1H), 5.80–5.76 (m, 1H), 5.55 (dq, J = 10.1, 2.3 Hz, 1H), 3.67–3.64 (m, 1H), 3.43 (dd, J = 9.7, 8.7 Hz, 1H), 2.71 (dt, J = 5.2, 2.6 Hz, 1H), 2.11–2.04 (m, 2H), 1.82 (dt, J = 13.0, 5.4 Hz, 1H), 1.71 (dt, J = 13.4, 6.9 Hz, 1H), 0.89 (s, 9H), 0.05 (d, J = 4.6 Hz, 6H); ^{13}C NMR (125 MHz; $CDCl_3$) δ 204.55, 128.50, 125.95, 66.10, 49.15, 38.40, 25.89, 23.70, 21.17, 18.28, –5.48; HRMS (ESI) calcd for $C_{14}H_{27}O_2Si$ $[M+H]^+$ 255.1780, found 255.1786.

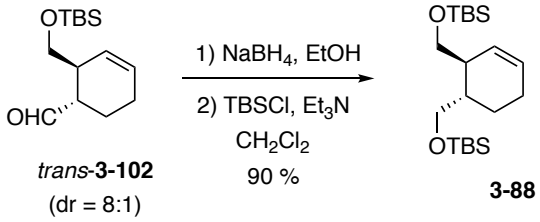

trans-**3-102** (dr = 8:1)

3-88

To a solution of *trans*-**3-102** (2.12 g, 8.36 mmol) in absolute EtOH (20 mL) was treated with $NaBH_4$ (318 mg, 8.36 mmol) at 0 °C and the reaction was stirred for 30 min and a solution of 5 wt% of aqueous citric acid was added dropwise until no gas evolution was observed. Then the reaction mixture was dried over anhydrous $MgSO_4$, filtered through a plug of celite, concentrated, and purified by column chromatography (Hex : EtOAc = 10 : 1) to give pure alcohol with a single diastereomer, which was dissolved in CH_2Cl_2 (20 mL) followed by the treatment of TBSCl (1.26 g, 8.36 mmol) and Et_3N (2.3 mL, 16.7 mmol) and the reaction was stirred at room temperature for 30 min and quenched by the addition of H_2O (20 mL). Then the organic layer was separated and the aqueous layer was extracted with CH_2Cl_2 (3 x 10 mL). The combined organic extract was dried over $MgSO_4$, filtered and concentrated in vacuum to afford the crude **3-88**, which was purified by column chromatography (Hex : EA = 40 : 1) to give pure **3-88** (2.78 g, 90 % over 2 steps).

3-88 (colorless oil): ^{1}H NMR (500 MHz; $CDCl_3$) δ 5.75–5.73 (m, 1H), 5.63 (dd, *J* = 9.7, 2.1 Hz, 1H), 3.64 (dd, *J* = 9.8, 5.6 Hz, 2H), 3.48 (ddd, *J* = 20.0, 9.8, 7.0 Hz, 2H), 2.08 (dd, *J* = 5.4, 2.7 Hz, 1H), 1.97 (m, 2H), 1.75 (dt, *J* = 9.7, 3.3 Hz, 1H), 1.68–1.66 (m, 1H), 1.48–1.43 (m, 1H), 0.90 (s, 18H), 0.06 (s, 12H); ^{13}C NMR (125 MHz; $CDCl_3$) δ 128.15, 127.91, 66.24, 65.82, 39.84, 37.22, 25.99, 23.55, 23.30, 18.36, –5.31; HRMS (ESI) calcd for $C_{20}H_{43}O_2Si_2$ $[M+H]^+$ 371.2802, found 371.2812.

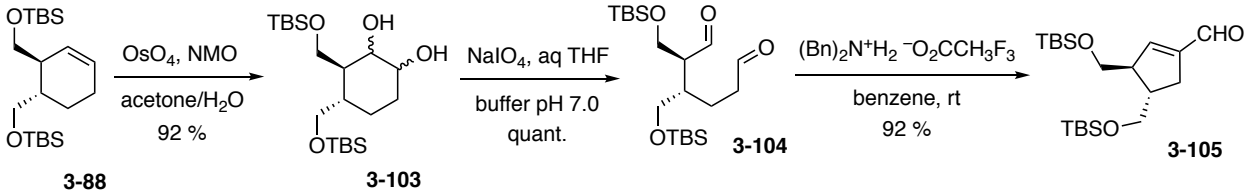

To a solution of **3-88** (2.78 g, 7.52 mmol) in 22 mL of acetone/H_2O (v/v, 10/1) was added NMO (1.32 g, 11.29 mmol) and a catalytic amount of OsO_4 (2.5 wt%, 0.2 mL) and the reaction was kept at room temperature for 2 hours until the TLC indicated the full consumption of the starting material. The reaction mixture was quenched with the addition of saturated aqueous $NaHSO_3$, stirred for 30 min and extracted with EtOAc (3 x 10 mL). The organic layer was dried over $MgSO_4$, filtered and the solvent was removed under vacuum to afford the crude **3-103**, which was purified by column chromatography (Hex : EA = 40 : 1) to give pure **3-103** (2.80 g, 92 %).

To a solution of **3-103** (2.80 g, 6.90 mmol) in 24 mL of acetone/buffer pH 7.0 (v/v, 5/1) was added $NaIO_4$ (2.21 g, 10.35 mmol) and the reaction was stirred at room temperature for about 2 hours with a frequent TLC monitoring until the TLC indication of the consumption of the starting material. THF was removed under vacuum and the residue was extracted with CH_2Cl_2 (3 x 10 mL). The combined organic extract was dried over $MgSO_4$, filtered and concentrated in vacuum to afford the crude **3-104**, which was used for the next step without any

further purification. The exposure of the **3-104** to the silica gel resulted in the decomposition of the compound.

To a solution of **3-104** in 20 mL of benzene was added dibenzylammonium trifluoroacetate salt (859 mg, 2.76 mmol) at room temperature and the reaction was kept for 3 h until the TLC indication of the consumption of the starting material. Benzene was removed under the vacuum and the residue was purified by column chromatography (Hex : EA = 40 : 1) to give pure **3-105** (2.44 g, 92 % over 2 steps).

3-105 (colorless oil) ^{1}H NMR (500 MHz; $CDCl_3$) δ 9.74 (s, 1H), 6.76 (d, *J* = 1.7 Hz, 1H), 3.75 (dd, *J* = 9.7, 5.7 Hz, 1H), 3.55 (dt, *J* = 14.9, 9.0 Hz, 3H), 2.89 (m, 1H), 2.63 (d, *J* = 16.7 Hz, 1H), 2.25 (d, *J* = 16.7 Hz, 2H), 0.86 (s, 18H), 0.03 (d, *J* = 5.7 Hz, 12H) ^{13}C NMR (125 MHz; $CDCl_3$) δ 190.10, 153.39, 146.73, 65.79, 65.41, 52.52, 42.46, 31.16, 25.88, 18.26, –5.41; HRMS (ESI) calcd for $C_{20}H_{41}O_4Si_2$ $[M+OH]^+$ 401.2543, found 401.2546.

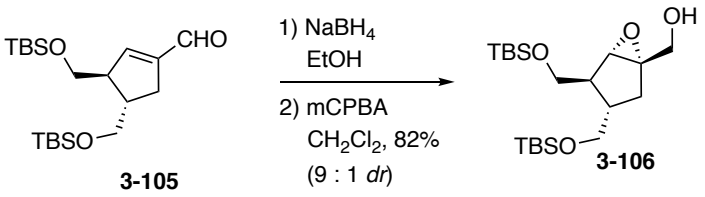

To a solution of **3-105** (420 mg, 1.09 mmol) in absolute EtOH (3 mL) was treated with $NaBH_4$ (41 mg, 1.09 mmol) at 0 °C and the reaction was stirred for 30 min and a solution of 5 wt% of aqueous citric acid was added dropwise until no gas evolution was observed. Then the reaction mixture was dried over anhydrous $MgSO_4$, filtered through a plug of celite, concentrated, and directly used for the next step without further purification.

To a solution of alcohol in 3 mL of dry CH_2Cl_2 was added of NaH_2PO_4 (196 mg, 1.64 mmol) followed by of mCPBA (77%, 368 mg, 1.64 mmol). After 2 h, TLC indicated the

consumption of the starting material. The reaction mixture was concentrated under vacuum and purified by flash chromatography (Hex : EA = 10 : 1) to give crude **3-106** as the major isomer (395 mg, 90 % over 2 steps) with inseparable by-product from mCPBA.

3-106 (colorless oil) ^{1}H NMR (500 MHz; $CDCl_3$) δ 3.94 (d, *J* = 12.5 Hz, 1H), 3.80–3.75 (m, 2H), 3.68 (d, *J* = 9.4 Hz, 1H), 3.62 (s, 1H), 3.55 (d, *J* = 4.7 Hz, 2H), 2.09 (t, *J* = 5.3 Hz, 2H), 1.63–1.60 (m, 2H), 1.27 (s, 1H), 0.92 (s, 9H), 0.90 (s, *J* = 13.7 Hz, 9H), 0.09 (s, 6H), 0.04 (s, 6H); ^{13}C NMR (125 MHz; $CDCl_3$) δ 67.69, 64.52, 63.22, 62.73, 61.63, 45.44, 39.30, 31.19, 25.90, 18.34, –5.37; HRMS (ESI) calcd for $C_{20}H_{43}O_4Si_2$ $[M+H]^+$ 403.2700, found 403.2701.

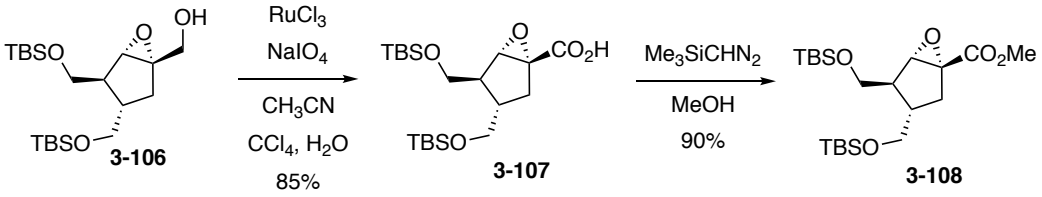

To a solution of **3-106** (395 mg, 0.98 mmol) in 3 mL of $CH_3CN/CCl_4/ H_2O$ (v/v/v, 2/2/1) was added of $NaIO_4$ (839 mg, 3.92mmol) and $RuCl_3•H_2O$ (20 mg, 0.10 mmol) and the reaction mixture was stirred at room temperature of 1 hour. The mixture was extracted with CH_2Cl_2 (3 x 3 mL). The combined organic extract was dried over $MgSO_4$, filtered and concentrated in vacuum to afford the crude acid **3-107** as dark oil, which was used for the next step without any further purification. To a solution of **3-107** in 3 mL MeOH was added trimethylsilyldiazomethane (2 M in Et_2O, 0.59 mL, 1.18 mmol) and the reaction was kept at room temperature for 1 h. The solvent was removed under vacuum and the residue was purified by column chromatography (Hex : EA = 20 : 1) to give pure **3-108** (347 mg, 85%).

3-108 (colorless oil): ^{1}H NMR (500 MHz; $CDCl_3$) δ 3.82 (s, 1H), 3.76 (s, 3H), 3.65–3.60 (m, 2H), 3.55 (d, *J* = 5.1 Hz, 2H), 2.21–2.09 (m, 3H), 1.54 (s, 1H), 0.90 (s, *J* = 7.1 Hz, 9H), 0.87

(s, 9H), 0.06 (s, 6H), 0.03 (s, 6H); ^{13}C NMR (125 MHz; $CDCl_3$) δ 169.78, 65.24, 64.15, 62.97, 62.23, 52.41, 45.72, 38.75, 30.35, 25.90, 18.29, –5.45; HRMS (ESI) calcd for $C_{21}H_{43}O_5Si_2$ $[M+H]^+$ 431.2649, found 431.2644.

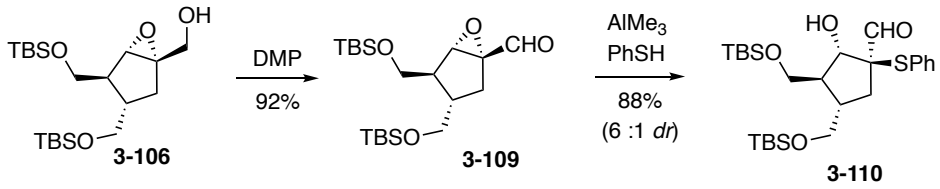

To a solution of the epoxy alcohol **3-106** in 3 mL of dry CH_2Cl_2 was added of $NaHCO_3$ (141 mg, 1.68 mmol) followed by of DMP (713 mg, 1.68 mmol). After about 1 h, TLC indicated the consumption of the starting material. CH_2Cl_2 was removed under vacuum and Et_2O was added and the suspension was filtered through a plug of celite. The filtrate was concentrated and purified by column chromatography (Hex : EA = 20 : 1) to give pure **3-109**. To a solution of PhSH (0.11 mL, 1.05 mmol) in CH_2Cl_2 (2 mL) was added $AlMe_3$ (2 M in Tol, 0.44 mL, 0.87 mmol) at 0 °C and was kept at that temperature for 20 min. Then the reaction was cooled to –78 °C and a solution of **3-109** (117 mg, 0.29 mmol) in CH_2Cl_2 (1 mL) was added. The reaction mixture was slowly warmed to room temperature in 2 hours and pour onto the crushed ice, and the aqueous layer was extracted with CH_2Cl_2 (3 x 2 mL). The combined organic extract was dried over $MgSO_4$, filtered and concentrated in vacuum to afford the crude **3-110**, purified by column chromatography (Hex : EA = 20 : 1) to give pure **3-110** (130 mg, 88%).

3-110: ^{1}H NMR (500 MHz; $CDCl_3$) δ 9.61 (s, 1H), 7.39–7.25 (m, 5H), 4.47 (d, J = 2.5 Hz, 1H), 4.03–3.99 (m, 2H), 3.88 (dd, J = 10.4, 5.8 Hz, 1H), 3.70–3.64 (m, 2H), 2.58–2.50 (m, 2H), 2.43–2.38 (m, 1H), 1.54 (dd, J = 14.4, 6.6 Hz, 1H), 0.91 (s, 9H), 0.89 (s, 9H), 0.08–0.06 (m, 12H); ^{13}C NMR (125 MHz; $CDCl_3$) δ 194.39, 135.85, 135.49, 129.25, 129.06, 80.73, 68.15,

65.60, 62.52, 46.40, 39.65, 30.71, 25.97, 25.82, 18.39, 18.11, –5.38, –5.54, –5.58; HRMS (ESI) calcd for $C_{26}H_{47}O_4SSi_2$ $[M+H]^+$ 511.2734, found 511.2716.

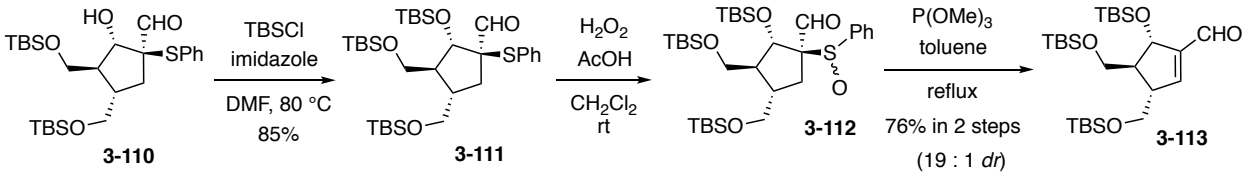

To a solution of **3-110** (590 mg, 1.16 mmol) in DMF (3 mL) was added TBSCl (696 mg, 4.64 mmol), imidazole (394 mg, 5.80 mmol) and a catalytic amount of DMAP. The reaction was stirred at 80°C for 2 h. Then the reaction was quenched by the addition of water (3 mL) and CH_2Cl_2 (3 mL) and the aqueous layer was extracted by CH_2Cl_2 (3 x 3 mL). The combined organic extract was dried over $MgSO_4$, filtered and concentrated in vacuum to afford the crude **3-111** which was purified by column chromatography (Hex : EA = 20 : 1) to give pure **3-111** (616 mg, 85%).

To a solution of **3-111** (39 mg, 0.06 mmol) in AcOH/ CH_2Cl_2 (v/v, 1/1, 2 mL) was added H_2O_2 (30 wt %, 0.008 mL) at 0 °C and the reaction was warmed to room temperature and kept at room temperature overnight. The aqueous layer was extracted with CH_2Cl_2 (3 x 1 mL). The combined organic extract was dried over $MgSO_4$, filtered and concentrated in vacuum to afford the crude **3-112** as a single diastereomer, which was subjected to the next reaction without further purification. The crude **3-112** was dissolved in toluene and treated with 2 drops of $P(OMe)_3$ and the reaction was stirred under reflux for 30 min. Solvent was removed under vacuum and the residue was purified by column chromatography (Hex : EA = 20 : 1) to give pure **3-113** (24 mg, 76% over 2 steps).

3-113: ^{1}H NMR (500 MHz; v) δ 9.78 (s, 1H), 6.91 (d, J = 2.5 Hz, 1H), 4.87 (d, J = 2.2

Hz, 1H), 3.78 (dd, J = 9.5, 6.9 Hz, 1H), 3.68 (dd, J = 9.4, 8.2 Hz, 1H), 3.60 (dd, J = 10.0, 6.2 Hz, 1H), 3.54 (t, J = 5.0 Hz, 1H), 2.73–2.69 (m, 1H), 2.03–1.99 (m, 1H), 0.93 (s, 9H), 0.90 (s, 10H), 0.88 (s, 10H), 0.15 (d, J = 9.5 Hz, 6H), 0.07 (d, J = 10.8 Hz, 12H); ^{13}C NMR (125 MHz; $CDCl_3$) δ 189.40, 154.07, 147.92, 75.00, 66.15, 65.87, 63.57, 53.07, 50.48, 40.35, 25.92, 18.31, 18.00, 15.30, –4.82, –5.35, –5.44; HRMS (ESI) calcd for $C_{26}H_{55}O_4Si_3$ $[M+H]^+$ 515.3408, found 515.3425.

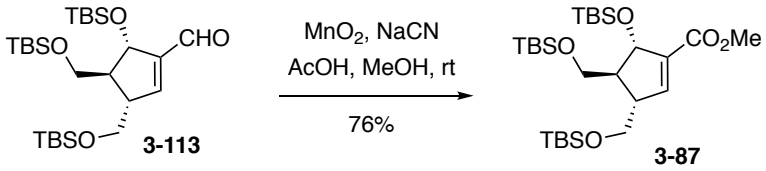

To a solution of **3-113** (149 mg, 0.29 mmol) in 3 mL of MeOH was added MnO_2 (501 mg, 5.77 mmol), NaCN (71 mg, 1.45 mmol) and AcOH (26 mg, 9.51 mmol) dropwise at room temperature. And the reaction was kept at room temperature overnight. The reaction mixture was poured onto a plug of celite and the solvent was removed under vacuum. The residue was purified by column chromatography (Hex : EA = 50 : 1) to give pure **3-87** (114 mg, 72 %).

3-87: ^{1}H NMR (500 MHz; $CDCl_3$) δ 6.85 (d, J = 2.0 Hz, 1H), 4.84 (s, 1H), 3.75 (s, 3H), 3.70–3.64 (m, 2H), 3.59 (dd, J = 9.9, 6.2 Hz, 1H), 3.49 (dd, J = 9.5, 7.4 Hz, 1H), 2.59–2.56 (m, 1H), 2.02–2.00 (m, 1H), 0.92 (s, 9H), 0.90 (s, 9H), 0.88 (s, 9H), 0.15 (s, 3H), 0.11 (s, 3H), 0.06 (s, 12H); ^{13}C NMR (125 MHz; $CDCl_3$) δ 165.13, 146.69, 138.49, 77.18, 66.39, 63.92, 52.73, 51.170, 50.26, 25.96, 25.93, 25.79, 18.35, 18.31, 17.98, –4.57, –4.83, –5.32, –5.38, –5.42; HRMS (ESI) calcd for $C_{27}H_{57}O_5Si_3$ $[M+H]^+$ 545.3514, found 545.3522.

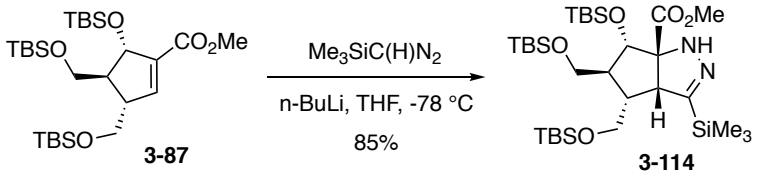

To a solution of trimethylsilyldiazomethane (2 M in Et_2O, 0.05 mL, 0.10 mmol) in 1 mL THF was treated with *n*-BuLi (2.5 M in Hex, 0.044 mL, 0.11 mmol) at –78 °C and the reaction was stirred at –78 °C for 30 min, followed by the slow addtion of **3-87** (50 mg, 0.09 mmol) in 1 mL of THF. Then the reaction mixture was slowly warmed up to room temperature in 1 h and quenched with 0.5 mL of saturated aqueous NH_4Cl and was dried over $MgSO_4$, filtered and concentrated in vacuum to afford the crude **3-114** which was purified by column chromatography (Hex : EA = 20 : 1) to give pure **3-114** as a single diastereomer (50 mg, 85 %).

3-114: ^{1}H NMR (500 MHz; $CDCl_3$) δ 6.68 (s, 1H), 4.21 (d, *J* = 5.6 Hz, 1H), 3.93 (d, *J* = 5.7 Hz, 1H), 3.82 (dd, *J* = 9.8, 6.3 Hz, 1H), 3.73 (s, 3H), 3.71 (dd, *J* = 9.8, 6.3 Hz, 1H), 3.57–3.49 (m, 2H), 2.15 (t, *J* = 5.6 Hz, 1H), 1.97 (t, *J* = 5.8 Hz, 1H), 0.95 (s, 9H), 0.89 (s, 9H), 0.87 (s, 9H), 0.23 (s, 9H), 0.10 (s, 6H), 0.08 (d, *J* = 3.8 Hz, 6H), 0.04 (d, *J* = 3.3 Hz, 6H); ^{13}C NMR (125 MHz; $CDCl_3$) δ 172.94, 161.38, 82.34, 80.95, 64.32, 61.29, 60.31, 45.60, 25.98, 25.70, 18.47, 18.32, 17.75, –1.49, –4.73, –4.84, –5.30, –5.36, –5.45; HRMS (ESI) calcd for $C_{31}H_{67}N_2O_5Si_4$ $[M+H]^+$ 659.4127, found 659.4132.

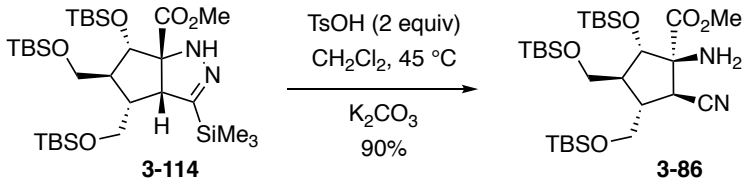

A solution of **3-114** (50 mg, 0.08 mmol) in 1 mL CH_2Cl_2 was treated with TsOH (22 mg, 0.12 mmol) and the reaction mixture was stirred under reflux until the TLC indicated the full

consumption of the starting material. The mixture was cooled back to room temperature and 1 mL of saturated aqueous $NaHCO_3$ solution was carefully added to neutralize the reaction. The organic layer was separated and the aqueous layer was extracted with CH_2Cl_2 (3 x 1 mL). The combined organic extract was dried over $MgSO_4$, filtered and concentrated in vacuum to afford the crude **3-86**, which was purified by column chromatography (Hex : EA = 5 : 1) to give 40 mg of pure **3-86** (90 %).

3-86: ^{1}H NMR (500 MHz; $CDCl_3$) δ 3.90 (s, 1H), 3.83 (dd, *J* = 10.9, 5.2 Hz, 1H), 3.80 (s, 3H), 3.80–3.76 (m, 2H), 3.73 (d, *J* = 11.2 Hz, 1H), 3.66 (dd, *J* = 10.9, 3.8 Hz, 1H), 2.70 (dd, *J* = 11.6, 6.0 Hz, 1H), 2.12–2.10 (m, 1H), 1.69 (bs, 2H), 0.94 (s, 9H), 0.88 (s, 9H), 0.86 (s, 9H), 0.12 (s, 6H), 0.08 (d, *J* = 5.1 Hz, 6H), 0.02 (d, *J* = 1.8 Hz, 6H); ^{13}C NMR (125 MHz; $CDCl_3$) δ 172.09, 118.88, 83.09, 69.90, 63.57, 61.91, 53.26, 52.82, 44.85, 37.04, 25.67, 25.42, 18.00, 17.60, 1.94, –2.92, –3.56, –4.63, –4. 46, –5.32; HRMS (ESI) calcd for $C_{22}H_{45}N_2O_5Si_2$ [M–$C_6H_{14}Si$+H]$^+$ 473.2867, found 473.2871.

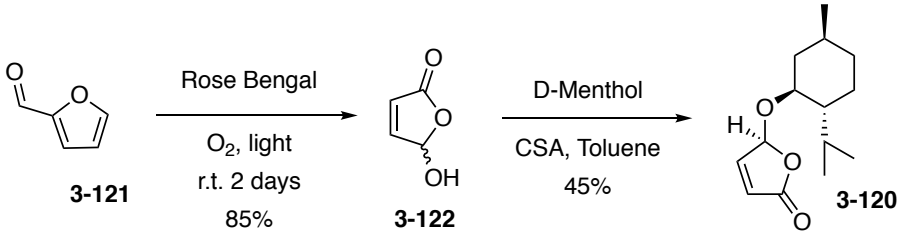

A solution of furfural **3-121** (8.58 g, 89.3 mmol) and rose Bengal (0.18 g, 0.18 mmol, 0.2 mol%) in dry methanol (45 mL) is placed in a photochemical reactor, with an appropriate water circulating outside of the vessel. The solution was bubbled with oxygen slowly while irradiated with a tungsten halogen lamp. In order to keep solvent loss, the reaction temperature is kept at or below 33 °C at all times with the water circulation cooling system. The reaction was monitored by TLC until no residual furfural is detected. About 48 h, the solution was transferred to a round bottom flask and solvent was concentrated under vacuum. The resulting dark pink solid was

washed with 7 mL x 3 of cold (–78 °C) chloroform through vacuum filtration, and orange crystal was dried under high vacuum to afford **3-122** (7.0 g, 85%).

3-122 (orange solid): ^{1}H NMR (500 MHz; DMSO-d_6) δ 7.81 (bs, 1H), 7.52–7.51 (d, J = 5.4 Hz, 1H), 6.31–6.30 (d, J = 5.4 Hz, 1H), 6.19 (s, 1H); ^{13}C NMR (125 MHz; DMSO-d_6) δ 171.6, 154.9, 123.6, 99.5.

A 250-mL, round-bottomed flask equipped with a magnetic stirring bar, 10 mL Dean-Stark trap, and reflux condenser is charged with D-menthol (10.21 g, 65 mmol), **3-122** (7.0 g, 69 mmol), D-(+)-camphorsulfonic acid (0.74 g, 32 mmol), and 30 mL of dry toluene. The stirred suspension is heated to reflux for about 2 hours and reaction was monitored by measuring the water amount in the Dean-Stark trap. When no further water trapped in the side of the Dean-Stark trap, the reaction is cooled in an ice bath. Once the solution was completely cooled, 15 mL of saturated aqueous solution of $NaHCO_3$ was added and the reaction mixture was stirred for 1 h at room temperature. The product is extracted with CH_2Cl_2 (30 mL) and the organic phase is washed with three portions of brine, dried over anhydrous $MgSO_4$, filtered and concentrated under vacuum to provide a 1:1 diastereomeric mixture of the menthyloxybutenolides. This mixture is recrystallized using hexanes and the crystal was collected by filtration to give the pure **3-120**. Another diastereomer which is liquid was recollected and treated with D-(+)-camphorsulfonic acid in refluxing CH_2Cl_2 to isomerize, followed by recrystallization to give **3-120** (7.39 g 45%).

3-120 (white needle crystal): ^{1}H NMR (500 MHz; $CDCl_3$) δ 7.15 (dd, J = 5.7, 1.1 Hz, 1H), 6.19 (dd, J = 5.7, 1.1 Hz, 1H), 6.07 (s, 1H), 3.64 (td, J = 10.7, 4.3 Hz, 1H), 2.16–2.06 (m, 2H), 1.69–1.63 (m, 2H), 1.40 (dddd, J = 12.2, 8.9, 6.2, 3.0 Hz, 1H), 1.24 (ddt, J = 12.6, 10.2, 2.7 Hz, 1H), 1.05–0.96 (m, 2H), 0.94 (d, J = 6.6 Hz, 3H), 0.87 (d, J = 6.6 Hz, 3H), 0.89–0.84 (m,

1H), 0.79 (d, J = 6.2 Hz, 3H). ^{13}C NMR (125 MHz; $CDCl_3$) δ 170.73, 150.92, 124.77, 100.47, 79.11, 47.79, 40.34, 34.22, 31.50, 25.36, 23.18, 22.23, 20.89, 15.81; HRMS (ESI) calcd for $C_{14}H_{22}O_3$ $[M+H]^+$ 239.1647 found 239.1654.

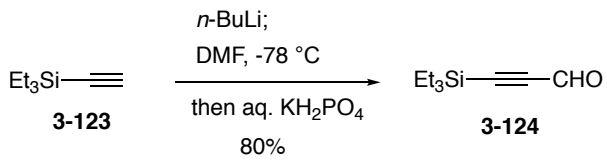

To a solution of **3-123** (3.0 g, 30.6 mmol) in dry Et_2O (60 mL) was added *n*-BuLi (2.5 M in Hex, 11.8 mL, 29.5 mmol) at –40 °C and the reaction was stirred for 30 min followed by the addition of DMF (4.27 mL, 61.2 mmol) and the reaction mixture was slowly warmed to room temperature in 3 h. The yellow solution was poured into a biphasic mixture of aqueous 10% KH_2PO_4 and Et_2O and the resulting mixture was extracted with Et_2O (3 x 50 mL), dried and concentrated at 0 °C carefully (the product is very volatile) to give **3-124** (6.17 g, 80%).

3-124 (colorless oil): ^{1}H NMR (500 MHz; $CDCl_3$) δ 9.14 (s, 1H), 0.96 (t, J = 7.8 Hz, 9H), 0.65 (q, J = 7.8 Hz, 6H); ^{13}C NMR (125 MHz; $CDCl_3$) δ 176.5, 103.6, 101.1, 7.2, 3.8.

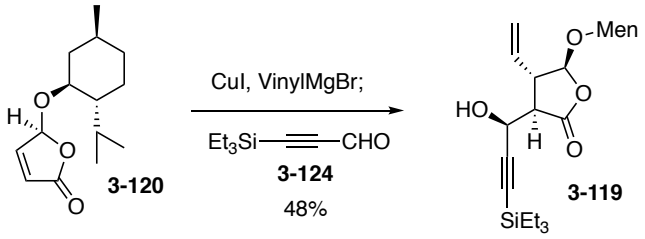

Vinylmagnesium bromide (1 M in THF, 1.63 mL, 1.63 mmol) was added over 15 min to a suspension of CuI (310 mg, 1.63 mmol) in THF (10 mL) at –78 °C and the resulting mixture stirred for 15 min and then a solution of compound **3-120** (242 mg, 1.0 mmol) in THF (3 mL) was added over the course of 5 min. Once the addition was complete, enolate was trapped by

adding propynal **3-124** (253 mg, 2.0 mmol) and the mixture slowly warmed to room temperature over the course of 3 h. The reaction was quenched with aq. sat. $NaHCO_3$, the aqueous layer extracted with EtOAc, the combined organic phases were dried and evaporated, and the residue purified by column chromatography (Hex : EA = 20 : 1) to give the pure **3-119** (188 mg, 48 %).

3-119 (yellow oil): ^{1}H NMR (500 MHz; $CDCl_3$) δ 5.84 (m, 1H), 5.37 (d, *J* = 6.1Hz, 1H), 5.30 (d, *J* = 17.2Hz, 1H), 5.24 (d, *J* = 11.1Hz, 1H), 4.81 (d, *J* = 6.1Hz ,1H), 3.48 (dt, *J* = 4.2Hz, *J* = 10.7Hz, 1H), 3.09 (m, 1H), 2.98 (s, 1H), 2.86 (dd, *J* = 6.2Hz, *J* = 10.0Hz, 1H), 2.15 (dtt, *J* = 2.3Hz, *J* = 7.1Hz, *J* = 14.5Hz, 1H), 1.99 (d, *J* = 12.1Hz, 1H), 1.62 (m, 1H), 1.34 (m, 2H), 0.96 (t, *J* = 7.9Hz, 9H), 0.91 (d, , *J* = 6.7Hz, 3H), 0.87 (d, *J* = 6.9Hz, 3H), 0.77 (d, *J* = 6.9Hz, 3H), 0.58 (q, *J* = 7.9Hz, 6H); ^{13}C NMR (125 MHz; $CDCl_3$) δ 173.6, 133.9, 119.4, 104.1, 79.1, 77.3, 77.0, 76.8, 75.5, 61.8, 51.7, 48.6, 47.6, 40.1, 34.2, 34.1, 31.4, 25.3, 23.0, 22.2, 20.9, 15.7.

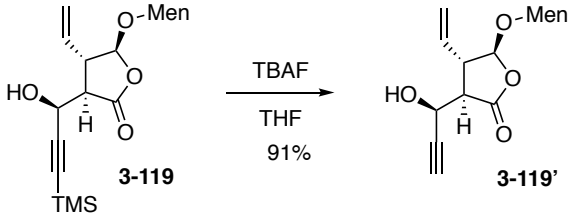

To a solution of **3-119** (150 mg, 0.59 mmol) in THF (2 mL) was added TBAF (1 M in THF, 0.71 mL, 0.71 mmol) at 0 °C and the reaction mixture was stirred for 1 hours. Solvent was removed under vacuum and the residue was purified by column chromatography (Hex : EA = 2 : 1) to give **3-119´** (97.2 mg, 91%).

3-119´ (colorless oil): ^{1}H NMR (500 MHz; $CDCl_3$) δ 5.82 (m, 1H), 5.39 (d, *J* = 5.8Hz, 1H), 5.32 (d, *J* = 17.1Hz, 1H), 5.27 (d, *J* = 10.4Hz, 1H), 4.77 (d, *J* = 5.1Hz, 1H) 3.50 (dt, *J* = 4.3Hz, *J* = 10.8Hz, 1H), 3.05 (m, 1H), 2.87 (dd, *J* = 6.2Hz, *J* = 9.5Hz, 1H), 2.55 (d, *J* = 1.9Hz,

1H), 2.16 (m, 1H), 2.01 (m, 1H), 1.64 (m, 2H), 1.34 (m, 1H), 1.01 (m, 1H), 0.92 (d, J = 6.5Hz, 3H), 0.88 (d, J = 7.0Hz, 3H), 0.78 (d, J = 6.9Hz, 3H); ^{13}C NMR (125 MHz; $CDCl_3$) δ 173.6, 133.9, 119.4, 104.1, 79.1, 77.3, 77.0, 76.8, 75.5, 61.8, 51.7, 48.6, 47.6, 40.1, 34.2, 34.1, 31.4, 25.3, 23.0, 22.2, 20.9, 15.7.

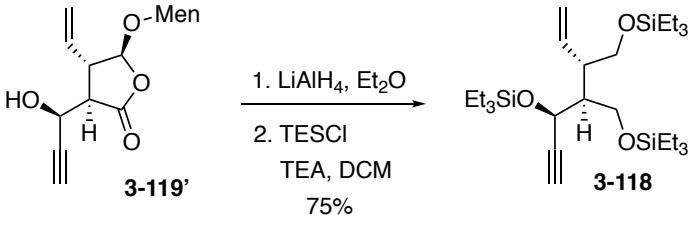

To a solution of $LiAlH_4$ (20.0 mg, 0.54 mmol) in EtO_2 (2mL) at 0 °C was added **3-119′** (97.2 mg, 0.54 mmol) in 1mL of EtO_2 dropwise over 3 min and the reaction was stirred overnight. The mixture was carefully quenched by the sequential addition of 0.1 mL H_2O, 0.2 mL 15 w/v% aq. NaOH, 0.4 mL H_2O and was then poured into 40 mL of Et_2O and stirred for 30 min. The crude material was dried over anhydrous $MgSO_4$, filtered through celite and the solvent was removed in vacuum.

To a solution of crude compound in 3mL of CH_2Cl_2 was treated with imidazole (128 mg, 1.89 mmol), TESCl (0.32 mL, 1.89 mmol) and a catalytic amount of DMAP. The reaction was refluxed for 2 h and solvent was removed under vacuum. The crude material was purified by silica gel column chromatography (Hex : EA = 70 : 1) to afford **3-118** (207 mg, 75% over 2 steps).

3-118 (colorless oil): ^{1}H NMR (500 MHz; $CDCl_3$) δ 5.92–5.88 (m, 1H), 5.10–5.07 (m, 2H), 4.69 (dd, J = 4.7, 2.0 Hz, 1H), 3.88 (ddd, J = 12.3, 10.4, 5.3 Hz, 2H), 3.77–3.71 (m, 2H), 2.68–2.67 (m, 1H), 2.42 (d, J = 2.0 Hz, 1H), 1.93 (t, J = 5.6 Hz, 1H), 1.01–0.96 (m, 27H), 0.71–

0.58 (m, 18H); ^{13}C NMR (125 MHz; $CDCl_3$) δ 139.59, 116.02, 85.02, 73.47, 64.36, 62.24, 61.25, 49.55, 46.24, 6.82, 4.91, 4.50, 4.46.

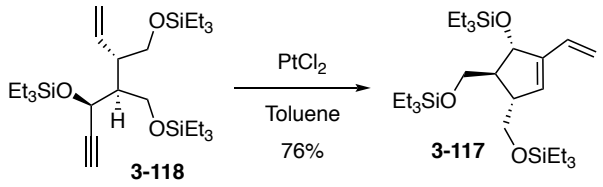

To a solution of **3-118** (207 mg, 0.40 mmol) in toluene (2 mL) was added $PtCl_2$ (5 mg, 5 mol%) and the reaction was stirred at room temperature until the TLC indicated the consumption of the starting material. Solvent was removed under vacuum and the residue was purified by column chromatography (Hex : EA = 60 : 1) to give **3-117** (156 mg, 76%).

3-117 (colorless oil): ^{1}H NMR (500 MHz; $CDCl_3$) δ 6.41 (dd, J = 17.7, 11.0 Hz, 1H), 5.85 (d, J = 2.2 Hz, 1H), 5.40 (d, J = 17.7 Hz, 1H), 5.14–5.12 (m, 1H), 4.83 (d, J = 1.7 Hz, 1H), 3.67–3.60 (m, 3H), 3.49 (dd, J = 9.6, 7.9 Hz, 1H), 2.45–2.42 (m, 1H), 2.05–2.02 (m, 1H), 1.01–0.92 (m, 27H), 0.72–0.67 (m, 6H), 0.65–0.59 (m, 12H); ^{13}C NMR (125 MHz; $CDCl_3$) δ 144.23, 132.96, 131.91, 115.20, 77.92, 66.96, 64.12, 53.01, 49.87, 6.96, 6.78, 5.20, 4.45, 4.36.

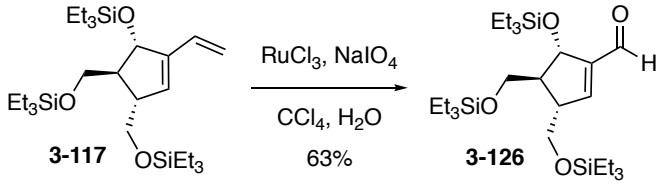

A solution of **3-117** (156 mg, 0.34 mmol) was added $RuCl_3$ and $NaIO_4$ in CCl_4/H_2O (v/v 1:1, 2mL) was stirred at room temperature. TLC checking frequently until a polar spot is showing on TLC. The reaction was quenched by the addition of solid sodium sulfite (15 mg) and extracted with ethyl acetate. The combined organic extracts were washed with water and brine, dried over

magnesium sulfate, filtered, and concentrated under vacuum. The residue was purified by column chromatography to give **3-126** (110 mg, 63 %)

3-126 (colorless oil): ^{1}H NMR (500 MHz; $CDCl_3$) δ 9.76 (s, 1H), 6.91 (d, J = 2.5 Hz, 1H), 4.88 (d, J = 2.3 Hz, 1H), 3.76 (dd, J = 9.4, 6.9 Hz, 1H), 3.66 (t, J = 8.9 Hz, 1H), 3.56 (dd, J = 9.9, 6.4 Hz, 1H), 3.50 (dd, J = 9.9, 6.8 Hz, 1H), 2.69–2.68 (m, 1H), 1.98 (dd, J = 6.3, 3.1 Hz, 1H), 0.95 (dt, J = 14.0, 6.2 Hz, 27H), 0.68–0.56 (m, 18H); ^{13}C NMR (125 MHz; $CDCl_3$) δ 189.40, 153.99, 147.84, 74.90, 65.93, 63.27, 53.39, 50.51, 6.77, 4.89, 4.41, 4.35.

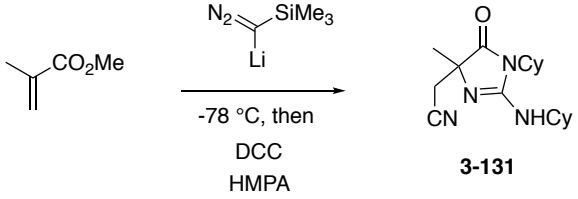

A solution of trimethylsilyldiazomethane (2.8 mL, 5.5 mmol, 2 M in Et_2O) in 10 mL THF was treated with nBuLi (2.4 mL, 6.0 mmol, 2.5 M in Hex) at –78 °C and the reaction was stirred at –78 °C for 30 min, followed by the slow addition of methyl methacrylate (501 mg, 5.0 mmol) in 5 mL of THF. Then the reaction mixture was stirred at that temperature for another 15 min and DCC (1.24 g, 6.0 mmol) in 5 mL THF was slowly added followed by a portion of the HMPA (1.34 g, 7.5 mmol). Then the reaction was slowly warmed up to room temperature in 2 h and kept at room temperature for another 2 h. The reaction was quenched with 1 mL of saturated aqueous NH_4Cl and was dried over $MgSO_4$, filtered and concentrated in vacuum. The crude material was purified by column chromatography (Hex : EA = 2 : 1) to give the pure **3-131** (1.39 g, 88%).

3-131 (yellow soild): ^{1}H NMR (500 MHz; $CDCl_3$) δ 7.40–7.29 (m, 6H), 7.09 (dd, J = 24.3, 6.8 Hz, 4H), 5.43 (d, J = 2.7 Hz, 2H), 4.40 (d, J = 6.7 Hz, 2H), 3.15 (d, J = 16.4 Hz, 1H),

2.94 (d, J = 16.4 Hz, 1H), 1.72 (s, 3H); ^{13}C NMR (125 MHz; $CDCl_3$) δ 195.1, 148.3, 137.5, 135.4, 129.3, 129.2, 128.5, 128.1, 126.3, 125.9, 117.8, 77.3, 77.1, 76.8, 60.3, 51.8, 47.6, 29.3, 26.2.

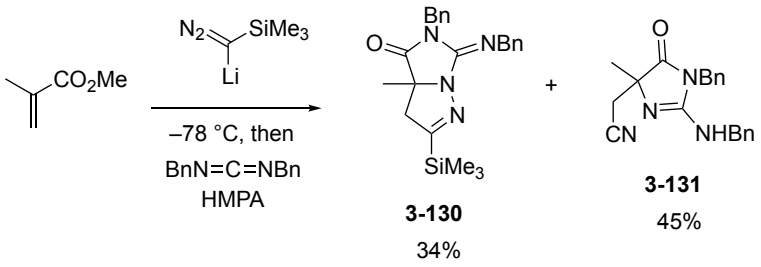

A solution of trimethylsilyldiazomethane (1.0 mL, 2.0 mmol, 2 M in Et_2O) in 4 mL THF was treated with nBuLi (0.88 mL, 2.2 mmol, 2.5 M in Hex) at –78 °C and the reaction was stirred at –78 °C for 30 min, followed by the slow addtion of methyl methacrylate (200 mg, 2.0 mmol) in 2 mL of THF. Then the reaction mixture was stirred at that temperature for another 30 min and dibenzylcarbodiimide (489 mg, 2.2 mmol) in 2 mL THF was slowly added followed by a portion of the freshly distilled HMPA (538 mg, 3 mmol). Then the reaction was slowly warmed up to room temperature in 2 h and kept at room temperature for another 2 h. The reaction was quenched with 1 mL of saturated aqueous NH_4Cl and was dried over $MgSO_4$, filtered and concentrated in vacuum. The residue was purified by column chromatography (Hex : EA = 6 : 1 to 1 : 1) to give the pure **3-130** (226 mg, 34%) and **3-131** (364 mg, 45%).

3-130 (yellow solid): ^{1}H NMR (500 MHz; $CDCl_3$) δ 7.37–7.29 (m, 6H), 7.24 (d, J = 6.9 Hz, 4H), 4.35 (s, 4H); ^{13}C NMR (125 MHz; $CDCl_3$) δ 141.31, 138.36, 128.63, 127.53, 127.52, 50.40.

3-131 (yellow solid): ^{1}H NMR (500 MHz; $CDCl_3$) δ 7.38–7.26 (m, 6H), 7.21–7.06 (dd, J = 16.7, 6.9 Hz, 4H), 5.43 (q, J = 13.2 Hz, 2H), 4.37 (d, J = 6.7 Hz, 2H), 3.15 (d, J = 17.2 Hz, 1H), 2.95 (d, J = 17.2 Hz, 1H), 1.72 (s, 3H); ^{13}C NMR (125 MHz; $CDCl_3$) δ 195.1, 148.3, 137.5,

135.4, 129.3, 129.2, 128.5, 128.1, 126.3, 125.9, 117.8, 77.3, 77.1, 76.8, 60.3, 51.8, 47.6, 29.3, 26.2.

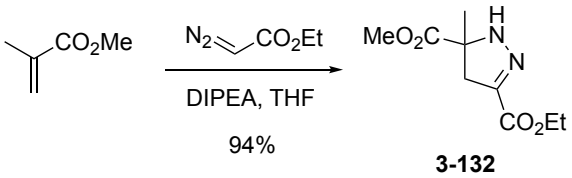

3-132

A solution of ethyl diazoacetate (0.42 mL, 4.0 mmol, 2 M in Et_2O) and methyl methacrylate (0.43 mL, 4 mmol) in 10 mL THF was treated with DIPEA (0.69 mL, 4.4 mmol) at 0 °C and the reaction was warmed up to room temperature and stirred for 6 h. Solvent was evaporated under vacuum and then the resulting product was directly purified by column chromatography (Hex : EA = 2: 1) to give the pure **3-132** (805 mg, 94%) as yellow oil.

3-132 (yellow oil): ^{1}H NMR (500 MHz; $CDCl_3$) δ 6.35 (s, 1H), 4.24 (q, J = 7.1 Hz, 2H), 3.71 (s, 3H), 3.45 (d, J = 17.5 Hz, 1H), 2.77 (d, J = 17.6 Hz, 1H) 1.50 (s, 3H), 1.29 (t, J = 7.1 Hz, 1H); ^{13}C NMR (125 MHz; $CDCl_3$) δ 174.2, 162.1, 142.4, 69.7, 61.2, 52.9, 41.2, 24.1, 14.2.

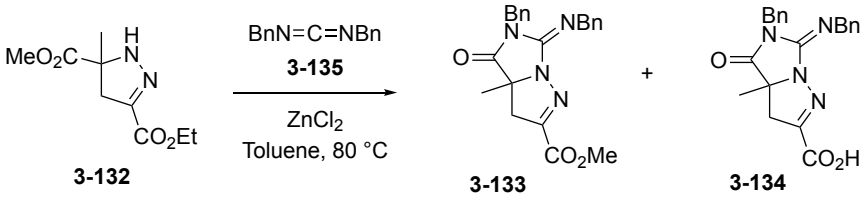

3-132 **3-133** **3-134**

To a solution of **3-132** (214 mg, 1.00 mmol) in toluene (2 mL) was added $ZnCl_2$ (6.81 mg, 5 mol%) and **3-128** and the reaction was heated up to 80 °C and stirred for 2 h at 80 °C. Solvent was removed under vacuum and the crude material was purified by column chromatography (Hex : EA = 4 : 1 to 3 : 1) to give **3-133** (94.1 mg, 25%) and **3-134** (238 mg, 61%).

3-133 (yellow oil): ^{1}H NMR (500 MHz; $CDCl_3$) δ 7.39 (m, 3H), 7.30 (td, J = 7.7Hz, J =

15.2Hz, 5H), 7.23 (t, *J* = 7.2Hz, 2H), 4.99 (d, *J* = 16.5Hz, 1H), 4.87 (d, *J* = 16.6Hz, 1H), 4.81 (d, J = 14.2Hz, 1H), 4.72 (d, J = 14.2Hz, 1H), 3.88 (s, 3H), 3.54 (d, *J* = 19.1Hz, 1H), 2.97 (d, *J* = 19.1Hz, 1H), 1.55 (s, 3H); ^{13}C NMR (125 MHz; $CDCl_3$) δ 174.4, 163.4, 160.8, 159.7, 151.7, 150.4, 146.8, 141.3, 140.9, 136.9, 136.1, 130.4, 128.8, 128.5, 128.1, 127.8, 127.4, 126.4, 121.6, 69.2, 64.4, 62.3, 54.1, 52.1, 51.2, 43.5, 42.6, 42.4, 31.9, 25.3, 14.6, 14.1, 10.4.

3-134 (yellow oil), ^{1}H NMR (500 MHz; $CDCl_3$) δ 7.41 (d, *J* = 7.3Hz, 2H), 7.38 (d, *J* = 7.5Hz, 2H), 7.30 (td, *J* = 7.7Hz, *J* = 15.2Hz, 3H), 7.23 (t, *J* = 7.2Hz, 2H), 4.93 (dd, *J* = 16.4Hz, *J* = 44.1Hz, 2H), 4.77 (dd, *J* = 14.2Hz, *J* = 44.6Hz, 2H), 4.33 (q, *J* = 7.1Hz, 2H), 3.53 (d, *J* = 19.1Hz, 1H), 2.96 (d, *J* = 19.1Hz, 1H), 1.55 (s, 3H), 1.36 (t, *J* = 7.1Hz, 3H); ^{13}C NMR (125 MHz; $CDCl_3$) δ 174.4, 161.3, 151.4, 146.7, 140.8, 136.0, 128.8, 128.5, 128.2, 127.8, 127.4, 126.4, 69.3, 62.3, 53.0, 52.0, 43.5, 42.3, 25.3.

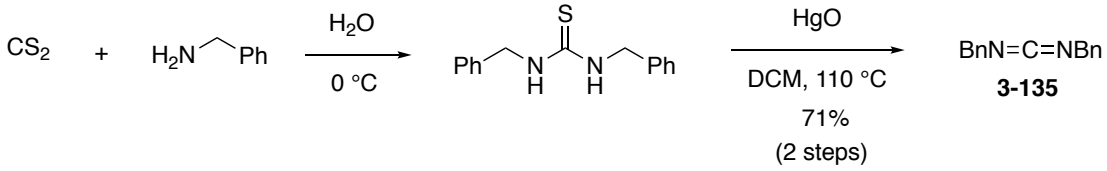

To a solution of CS_2 (1g, 13.1 mmol) in water at 0 °C was added benzylamine (2.8g, 26.3 mmol), the reaction was stirred at 0 °C for 1 h and then the white solid was filtered and dried under vacuum. DCM was added to the resulting thiourea and the reaction mixture was warm up to 80 °C. When temperature was reached to 80 °C, HgO (8.7g, 40 mmol) was added portion-wise over the course of 6 hours causing it dark brown from bright orange color. The reaction mixture was heated up to 110 °C and reflux another 6 hrs. Solvent was removed under vacuum and the residue filter though Celite only with hexanes (20 mL) to give pure dibenzylcarbodiimide **3-135** as colorless liquid (2.1g, 71%).

3-135, ^{1}H NMR (500 MHz; $CDCl_3$) δ 7.45–7.29 (m, 6H), 7.29–7.16 (m, 4H), 4.33 (s, 4H). ^{13}C NMR (125 MHz; $CDCl_3$) δ 141.3, 138.4, 128.7, 127.6, 127.5, 50.4. HRMS (ESI) calcd for $C_{15}H_{14}O_2$ $[M+H]^+$ 223.1235 found 223.1233.

3.9. References

1. pyrrole-imidazole alkaloids reviews: (a) Hoffmann, H.; Lindel, T. *Synthesis* **2003**, *1753*. (b) Jacquot, D. E. N.; Lindel, T. *Curr. Org. Chem*. **2005**, *9*, 1551. (c) Du, H.; He, Y.; Sivappa, R.; Lovely, C. J. *Synlett* **2006**, 965. (d) Köck, M.; Grube, A.; Seiple, I. B.; Baran, P. S. *Angew. Chem., Int. Ed*. **2007**, *46*, 6586. (e) Weinreb, S. M. *Nat. Prod. Rep*. **2007**, *24*, 931. (f) Arndt, H. D.; Riedrich, M. *Angew. Chem., Int. Ed.* **2008**, *47*, 4785. (g) Heasley, B. *Eur. J. Org. Chem*. **2009**, 1477. (h) Forte, B.; Malgesini, B.; Piutti, C.; Quartieri, F.; Scolaro, A.; Papeo, G. *Mar. Drugs*. **2009**, *7*, 705. (i) Gaich, T.; Baran, P. S. *J. Org. Chem*. **2010**, *75*, 4657. (j) Al-Mourabit, A.; Zancanella, M. A.; Tilvi, S.; Romo, D. *Nat. Prod. Rep*. **2011**, *28*, 1229. (k) Wang, X.; Ma, Z.; Wang, X.; De, S.; Ma, Y.; Chen, C. *Chem. Commun*. **2014**, *50*, 8628. (l) Lindel, T. *The Alkaloids* **2017**, *77*, 117.
2. (a) Catret, M.; Ivorra, M. D.; D'Ocón, M. P.; Anselmi, E. *J. Pharm. Pharmacol*. **1998**, *50*, 317. (b) Cipres, A.; O'Malley, D. P.; Li, K.; Finlay, D.; Baran, P. S.; Vuori, K. *ACS Chem. Biol*. **2010**, *5*, 195. (c) D'Ambrosio, M.; Guerriero, A.; Debitus, C.; Ribes, O.; Pusset, J.; Leroy, S.; Pietra, F. *Chem. Commun*. **1993**, 1305. (d) Rodriguez, R. A.; Steed, D. B.; Kawamata, Y.; Su, S.; Smith, P. A.; Steed, T. C.; Romesberg, F. E.; Baran, P. S. *J. Am. Chem. Soc*. **2014**, *136*, 15403. (e) Stout, E. P.; Choi, M. Y.; Castro, J. E.; Molinski, T. F. *J. Med. Chem*. **2014**, *57*, 5085.
3. Forenza, S.; Minale, L.; Riccio, R.; Fattorusso, E. *Chem. Commun*. **1971**, 1129

4. Garcia, E. E.; Benjamin, L. L.; Fryer, R. I. *J. Chem. Soc., Chem. Commun*. **1973**, 78.
5. (a) Burkholder, P. R.; Sharma, G. M. *Lloydia* **1969**, *32*, 466. (b) Sharma, G. M.; Burkholder, P. R. *J. Chem. Soc. Chem. Commun*. **1971**, 151.
6. Walker, R. P.; Faulkner, D. J.; Van Engen, D.; Clardy, J. *J. Am. Chem. Soc*. **1981**, *103*, 6772.
7. Grube, A.; Köck, M. *Org. Lett*. **2006**, 8, 4675.
8. Beniddir, M. A.; Evanno, L.; Joseph, D.; Skiredj, A.; Poupon, E. *Nat. Prod. Rep*. **2016**, *33*, 820.
9. (a) Stout, P. E.; Morinaka, B. I.; Wang, Y. G.; Romo, D.; Molinski, T. F. *J. Nat. Prod*. **2012**, *75*, 527. B) Stout, P. E.; Wang, Y. G.; Romo, D.; Molinski, T. F. *Angew. Chem., Int. Ed*. **2012**, *51*, 4877.
10. Kinnel, R. B.; Gehrken, H. P.; Swali, R.; Skoropowski, G.; Scheuer, P. *J. Org. Chem*. **1998**, *63*, 3281.
11. (a) Buchanan, M. S.; Carroll, A. R.; Quinn, R. J. *Tetrahedron Lett*. **2007**, *48*, 4573; (b) Grube, A.; Köck, M.; *Angew. Chem., Int. Ed.* **2007**, *46*, 2320. (c) Köck, M.; Grube, A.; Seiple, I. B.; Baran, P. S. *Angew. Chem., Int. Ed*. **2007**, *46*, 6586.
12. (a) Ma, Z.; Wang, X.; Wang, X.; Rodriguez, R. A.; Moore, C. E.; Gao, S.; Tan, X.; Ma, Y.; Rheingold, A. L.; Baran, P. S.; Chen, C. *Science* **2014**, *346*, 219. b) Wang, X.; Gao, Y.; Ma, Z.; Rodriguez, R. A.; Yu. Z. X.; Chen, C. *Org. Chem. Front*. **2015**, *2*, 978.
13. Schulte, G.; Scheuer, P. J.; McConnell, J. *Helv. Chim. Acta* **1980**, *63*, 159.
14. Lawwesson, S. O.; Nolde, C. *Tetrahedron* **1968**, *24*, 1051.
15. Birman, V. B.; Jiang, X. T. *Org. Lett*. **2004**, *6*, 2369.
16. Baran, P. S.; Zografos, A. L.; O'Malley, D. P. *J. Am. Chem. Soc*. **2004**, *126*, 3726.

17. Northrop, B. H.; O'Malley, D. P.; Zografos, A. L.; Baran, P. S.; Houk, K. N. *Angew. Chem., Int. Ed.* **2006**, *45*, 4126.

18. (a) O'Malley, D. P.; Yamaguchi, J.; Young, I. S.; Seiple, I. B.; Baran, P. S. *Angew. Chem., Int. Ed*. **2008**, *47*, 3581. (b) Yamaguchi, J.; Seiple, I. B.; Young, I. S.; O'Malley, D. P.; Maue, M.; Baran, P. S. *Angew. Chem., Int. Ed*. **2008**, *47*, 3578.

19. Su, S.; Rodriguez, R. A.; Baran, P. S. *J. Am. Chem. Soc*. **2011**, *133*, 13922.

20. Rodriguez, R. A.; Steed, D. B.; Kawamata, Y.; Su, S.; Smith, P. A.; Steed, T. C.; Romesberg, F. E.; Baran, P. S. *J. Am. Chem. Soc*. **2014**, *136*, 15403.

21. Ma, Z.; Wang, X.; Ma, Y.; Chen, C. *Angew. Chem., Int. Ed*. **2016**, *55*, 4763.

22. Wang, X.; Ma, Z.; Lu, J.; Tan, X.; Chen, C. *J. Am. Chem. Soc.* **2011**, *133*, 15350.

23. Dilley, A. S.; Romo, D. *Org. Lett*. **2001**. *3*, 1535.

24. Seiple, I. B.; Su, S.; Young, I. S.; Lewis, C. A.; Yamaguchi, J.; Baran, P. S. *Angew. Chem., Int. Ed*. **2010**, *49*, 1095.

25. Seiple, I. B.; Su, S.; Young, I. S.; Nakamura, A.; Yamaguchi, J.; Jørgensen, L.; Rodriguez, R. A.; O'Malley, D. P.; Gaich, T.; Köck, M.; Baran, P. S. *J. Am. Chem. Soc*. **2011**, *133*, 14710.

26. Namba, K.; Takeuchi, K.; Kaihara, Y.; Oda, M.; Nakayama, A.; Nakayama, A.; Yoshika, M.; Tanino, K. *Nat. Commun*. **2015**, *6*, 8731.

27. (a) Breder, A.; Chinigo, G. M.; Waltman, A. W.; Carreira, E. M. *Angew. Chem., Int. Ed*. **2008**, *47*, 8514. b) Breder, A.; Chinigo, G. M.; Waltman, A. W.; Carreira, E. M. *Chem. Eur. J*. **2011**, *17*, 12405.

28. O'Connor, M. J.; Sun, C.; Lee, D. *Angew. Chem., Int. Ed*. **2015**, *54*, 9963.

29. (a) Liu, H.; O'Connor, M.J.; Sun, C., Wink, D. J.; Lee, D. *Org. Lett*. **2013**, *15*, 2974. (b) Sun, C.; O'Connor, M. J.; Lee, D.; Wink, D. J.; Milligan, R. D. *Angew. Chem., Int. Ed*. **2014**, *53*, 3197.

30. Overman, L. E.; Taylor, G. F.; Jessup, P. J. *Tetrahedron Lett*. **1976**, *36*, 3089.

31. Gao, S.; Wang, Q.; Huang, L. J.; Lum, L.; Chen, C. *J. Am. Chem. Soc*. **2010**, *132*, 371.

32. (a) Birman, V. B.; Danishefsky, S. J. *J. Am. Chem. Soc*. **2002**, *124*, 2080. (b) Corey, E. J.; Danheiser, R. L.; Chandrasekaran, S.; Siret, P.; Keck, G. E.; Gras, J. L. *J. Am. Chem. Soc.* **1978**, *100*, 8031.

33. (a) Kühnel, E.; Laffan, D. D. P.; Lloyd-Jones, G. C.; Martínez del Campo, T.; Shepperson, I. R.; Slaughter, J. L. *Angew. Chem., Int. Ed.* **2007**, *46*, 7075. (b) Wakamatsu, K.; Kigoshi, H.; Niiyama, K.; Niwa, H.; Yamada, K. *Tetrahedron* **1986**, *42*, 5551.

34. Yasuda, A.; Takahashi, M.; Takaya, H. *Tetrahedron Lett*. **1981**, *22*, 2413.

35. Trost, B. M.; Salzmann, T. N. *J. Am. Chem. Soc*. **1973**, *95*, 6840.

36. Matteucci, M.; Bhalay, G.; Bradley, M. *Org. Lett*. **2003**, *5*, 235.

37. Holmgren, S. K.; Savage, P. B.; Desper, J. M.; Schladetzky, K. D.; Powell, D. R.; Gellman, S. H. *Tetrahedron* **1997**, *53*, 12249.

38. Bradshaw, B.; Etxebarria-Jardí, G.; Bonjoch, J. *J. Am. Chem. Soc.* **2010**, *132*, 5966.

39. Moradei, O. M.; Paquette, L. A. *Org. Synth*. **2003**, *80*, 66.

40. (a) Mulzer, J.; Riether, D. *Tetrahedron Lett*. **1999**, *40*, 6197. (b) Robertson, J.; Ménard, M.; Ford, R.; Bell, S. *Org. Biomol. Chem.* **2004**, *2*, 2988.

41. Frimpong, K.; Wzorek, J.; Lawlor, C.; Spencer, K.; Mitzel, T. *J. Org. Chem*. **2009**, *74*, 5861.

42. Diver, S. T.; Giessert, A. *Chem. Rev*. **2004**, *104*, 1317.

43. (a) Fürstner, A.; Stelzer, F.; Szillat, H. *J. Am. Chem. Soc*. **2001**, *123*, 11863. (b) Fürstner, A.; Szillat, H. Stelzer, F. *J. Am. Chem. Soc*. **2000**, *122*, 6785.

44. Sharpless, K. B.; Amberg, W.; Bennani, Y. L.; Crispino, G. A.; Hartung, J.; Jeong, K.-S.; Kwong, H. L.; Morikawa, K.; Wang, Z. M.; Xu, D.; Zhang, X. L. *J. Org. Chem*. **1992**, *57*, 2768.

45. Yang, D.; Zhang, C. *J. Org. Chem*. **2001**, *66*, 4814.

46. (a) Schanding, T.; Vogel, P. D.; Trommer, W. E.; Wiese, J.G. *Tetrahedron* **1996**, *52*, 5783. (b) Weith, W. *Ber. Dtsch. Chem. Ges*. **1873**, *6*, 1395.

47. Chi, Y.; Xu, L.; Du, S.; Yan, H.; Zhang, W. X.; Xi, Z. *Chem. Eur. J.* **2015**, *21*, 10369.

APPENDIX I: NMR Spectra

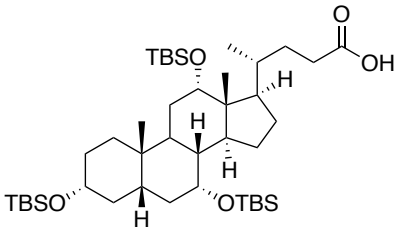

1-7

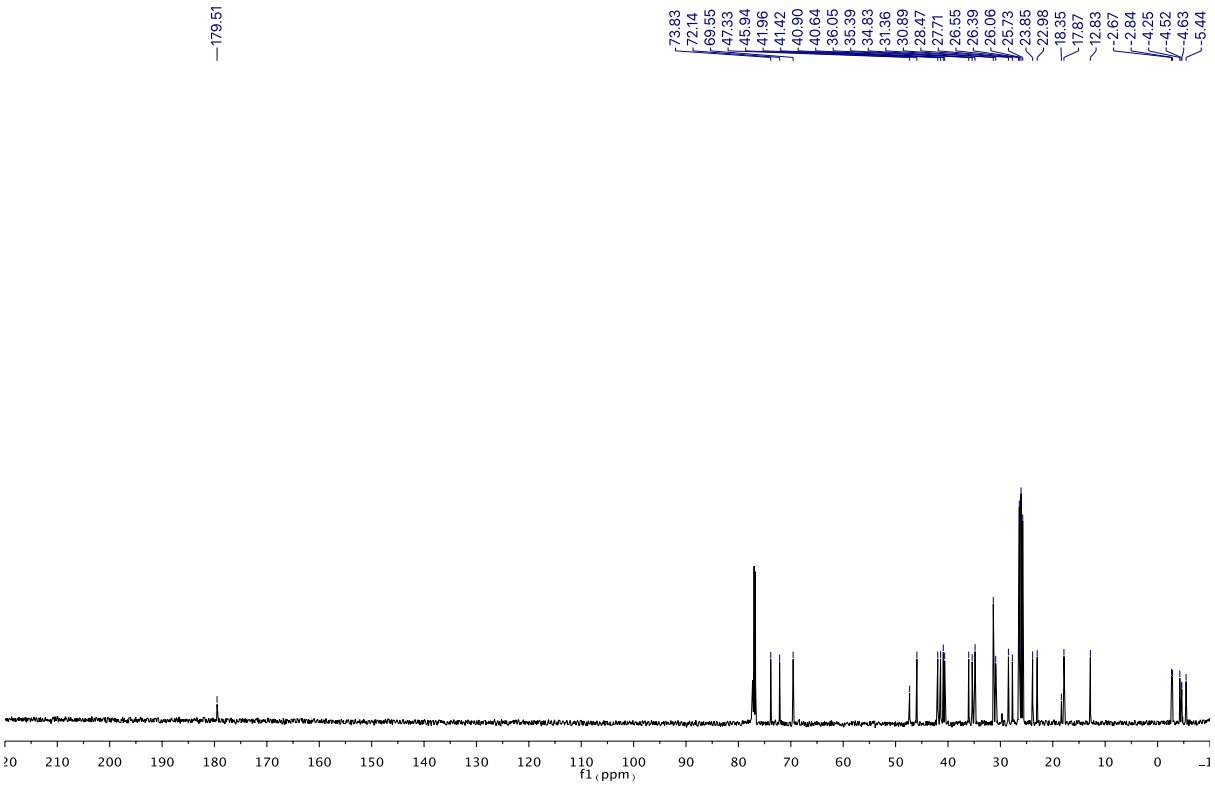
179.51
73.83
72.14
69.55
47.33
45.94
41.96
41.42
40.90
40.64
36.05
35.39
34.83
31.36
30.89
28.47
27.71
26.55
26.39
26.06
25.73
23.85
22.98
18.35
17.87
12.83
2.67
2.84
4.25
4.52
4.63
5.44
f1 (ppm)

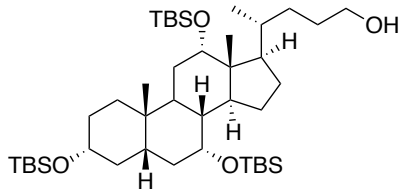
TBSO
OH
H
H
H
TBSO
OTBS
H

1-8

1.00
0.99
2.01
1.02
1.97
1.08
0.96
2.23
1.63
3.06
1.81
6.46
2.74
1.90
0.87
1.03
3.17
8.48
8.65
3.01
8.61
2.92
5.65
5.73
6.06
f1 (ppm)
73.88
72.14
69.59
63.66
47.28
46.07
41.97
41.40
40.91
40.65
36.37
35.39
34.85
32.01
31.36
29.98
29.71
28.48
27.91
26.55
26.40
26.07
25.73
23.89
22.98
18.30
12.82
-2.69
-2.86
-4.22
-4.52
-4.63
-5.43

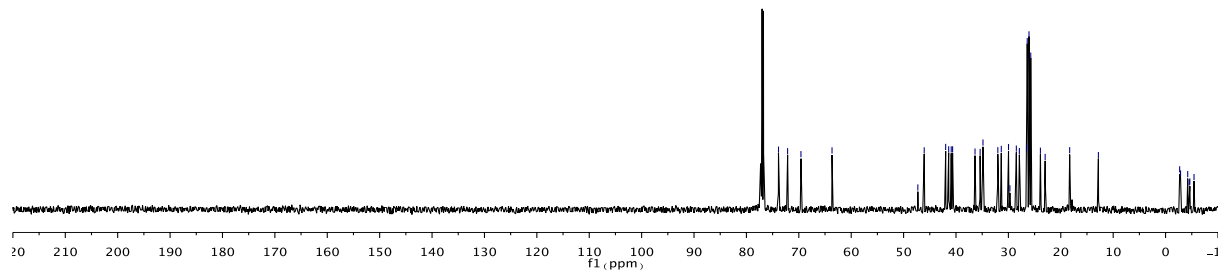
f1 (ppm)

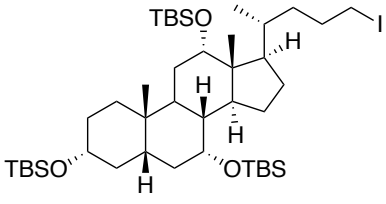
TBSO
I
H
H
H
TBSO
OTBS
H

1-9

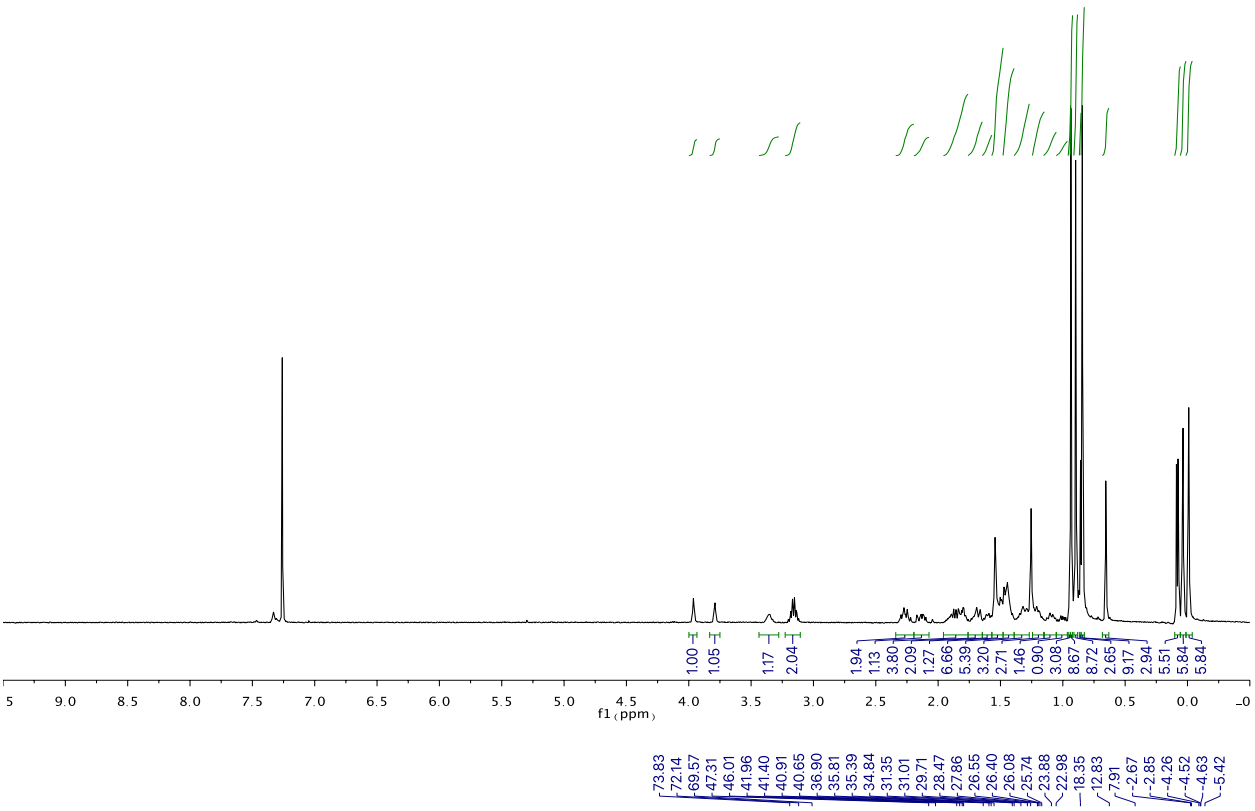
1.00
1.05
1.17
2.04
1.94
1.13
3.80
2.09
1.27
6.66
5.39
3.20
2.71
1.46
0.90
3.08
8.67
8.72
2.65
9.17
2.94
5.51
5.84
5.84
f1 (ppm)
73.83
72.14
69.57
47.31
46.01
41.96
41.40
40.91
40.65
36.90
35.81
35.39
34.84
31.35
31.01
29.71
28.47
27.86
26.55
26.40
26.08
25.74
23.88
22.98
18.35
12.83
7.91
-2.67
-2.85
-4.26
-4.52
-4.63
-5.42

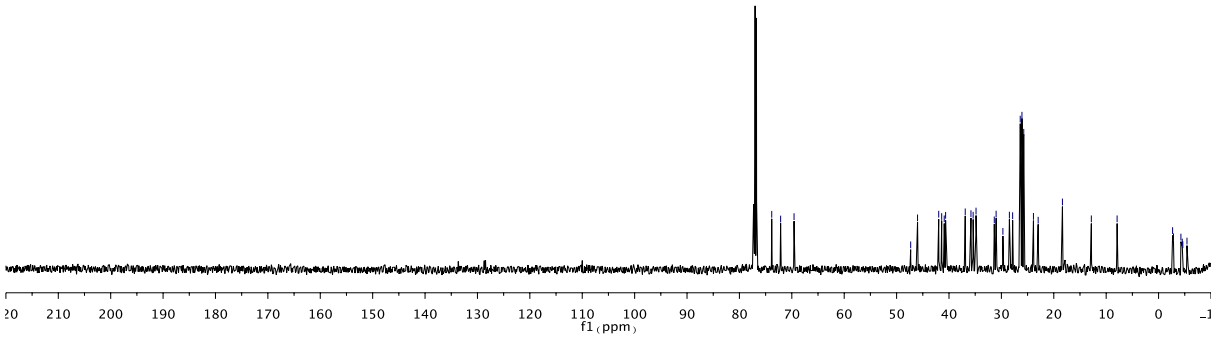
f1 (ppm)

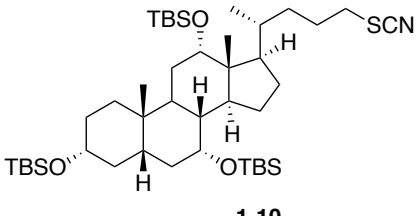
TBSO
SCN
H
H
H
TBSO
OTBS
H

1-10

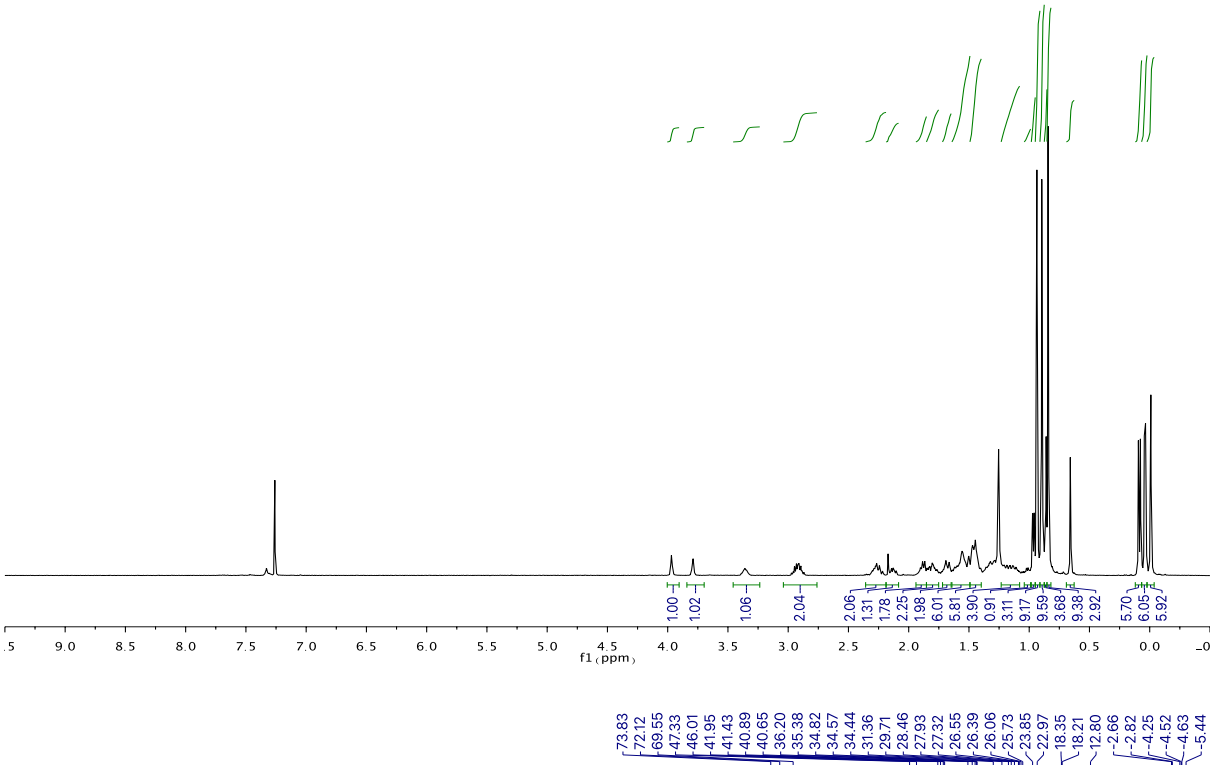
1.00
1.02
1.06
2.04
2.06
1.31
1.78
2.25
1.98
6.01
5.81
3.90
0.91
3.11
9.17
9.59
3.68
9.38
2.92
5.70
6.05
5.92
f1 (ppm)

73.83
72.12
69.55
47.33
46.01
41.95
41.43
40.89
40.65
36.20
35.38
34.82
34.57
34.44
31.36
29.71
28.46
27.93
27.32
26.55
26.39
26.06
25.73
23.85
22.97
18.35
18.21
12.80
-2.66
-2.82
-4.25
-4.52
-4.63
-5.44

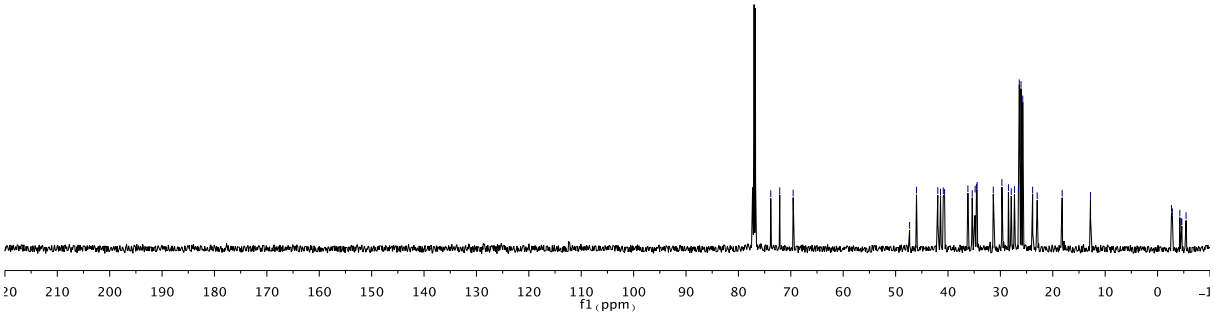
f1 (ppm)

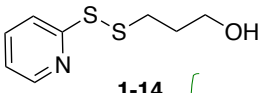
S
S
OH
N

1-14

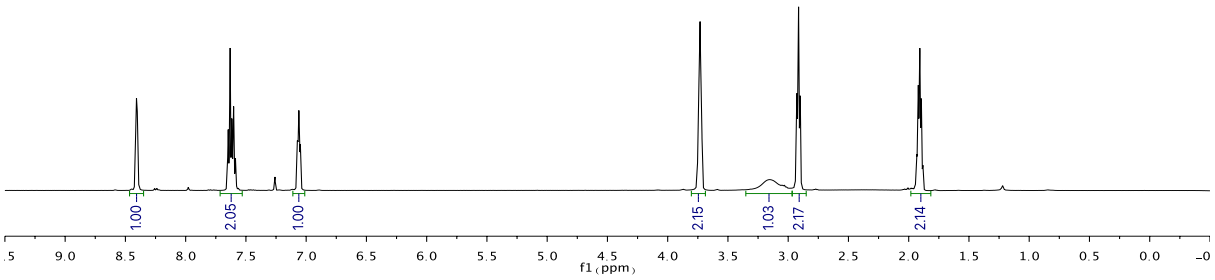
1.00
2.05
1.00
2.15
1.03
2.17
2.14
f1 (ppm)


159.93
149.61
137.06
120.82
120.19
60.69
35.74
31.37

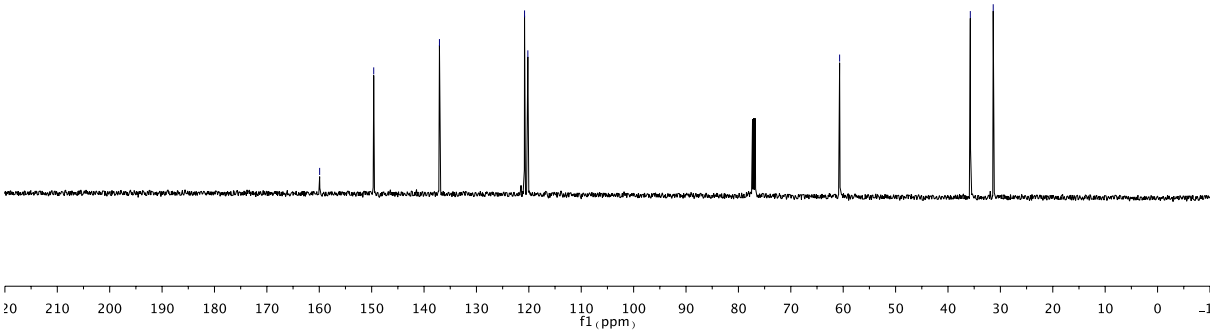
f1 (ppm)

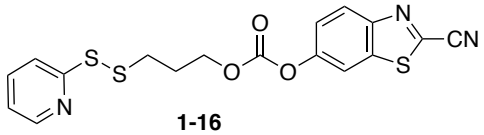
O
N
CN
S
S
O
O
S
S
N

1-16

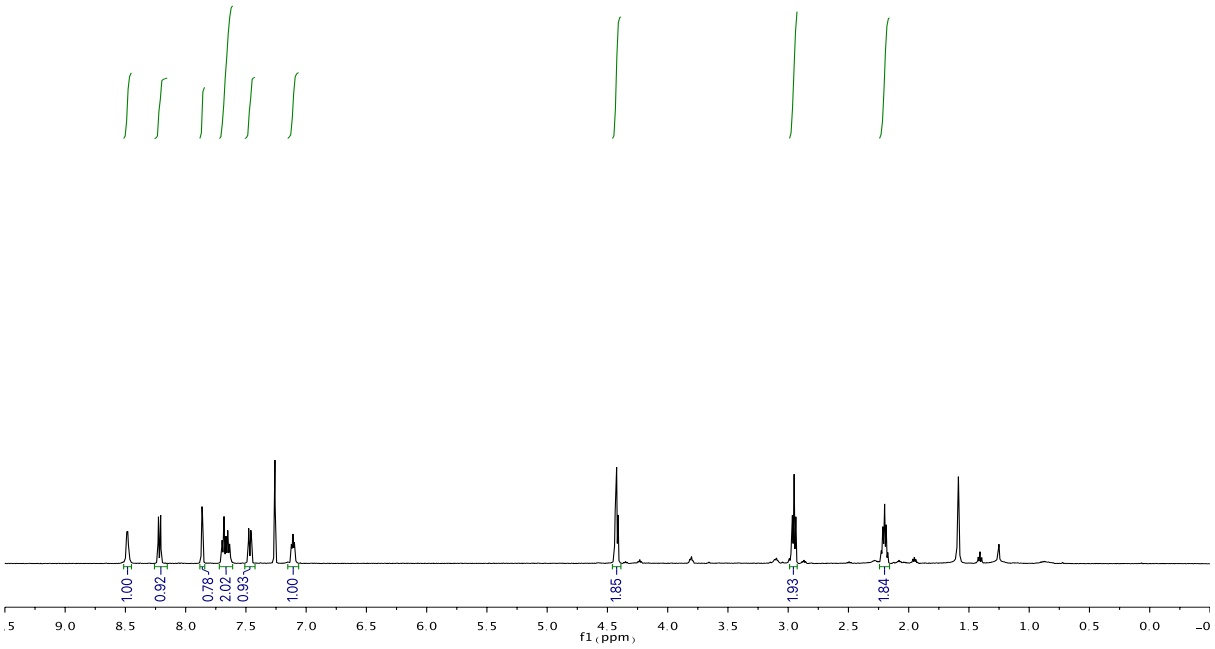
1.00
0.92
0.78
2.02
0.93
1.00
1.85
1.93
1.84
f1 (ppm)

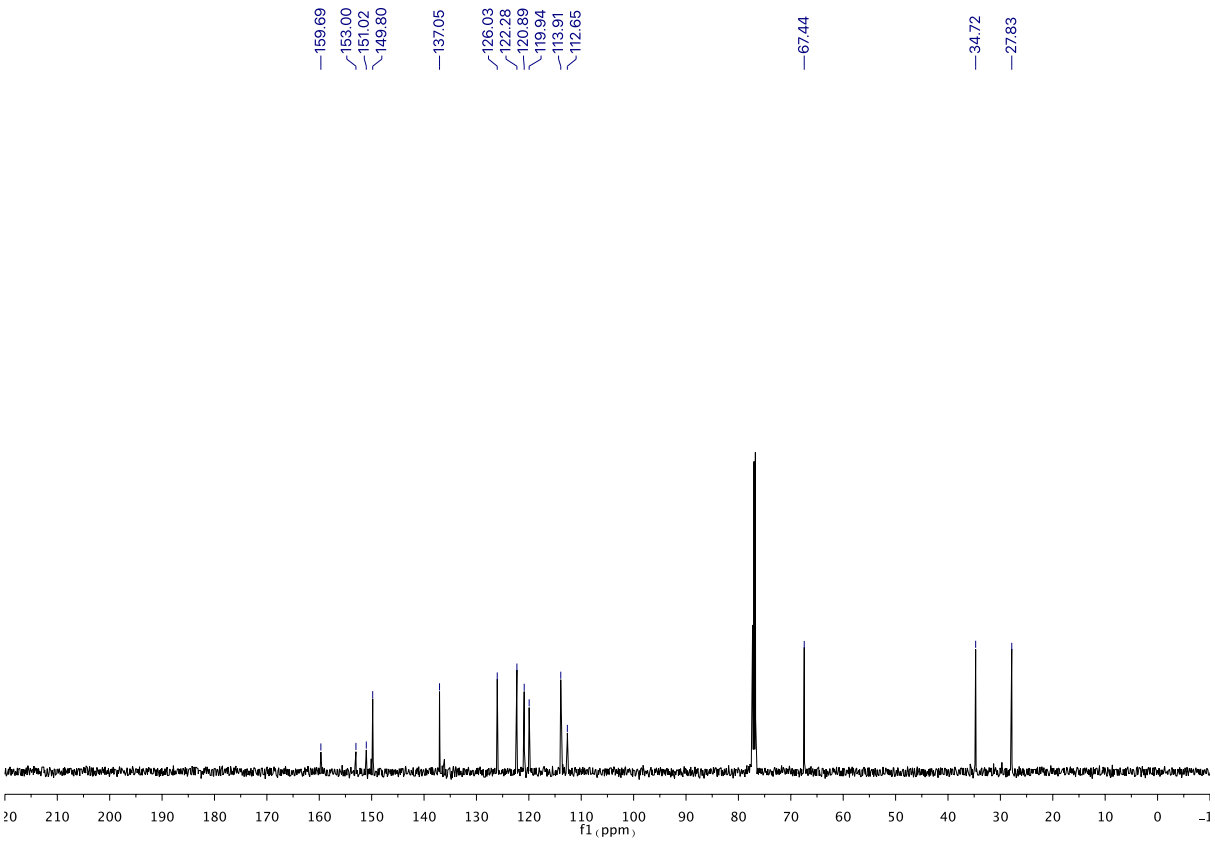
159.69
153.00
151.02
149.80
137.05
126.03
122.28
120.89
119.94
113.91
112.65
67.44
34.72
27.83
f1 (ppm)

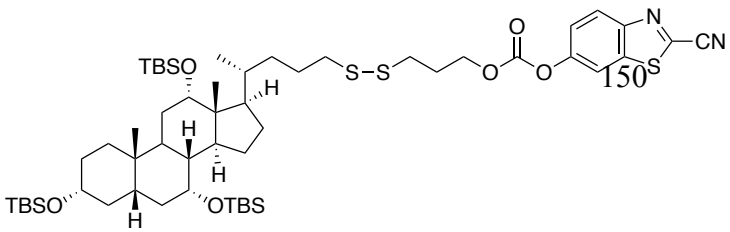
TBSO
H
S–S
O
O
O
N
CN
S
H
H
TBSO
OTBS
H

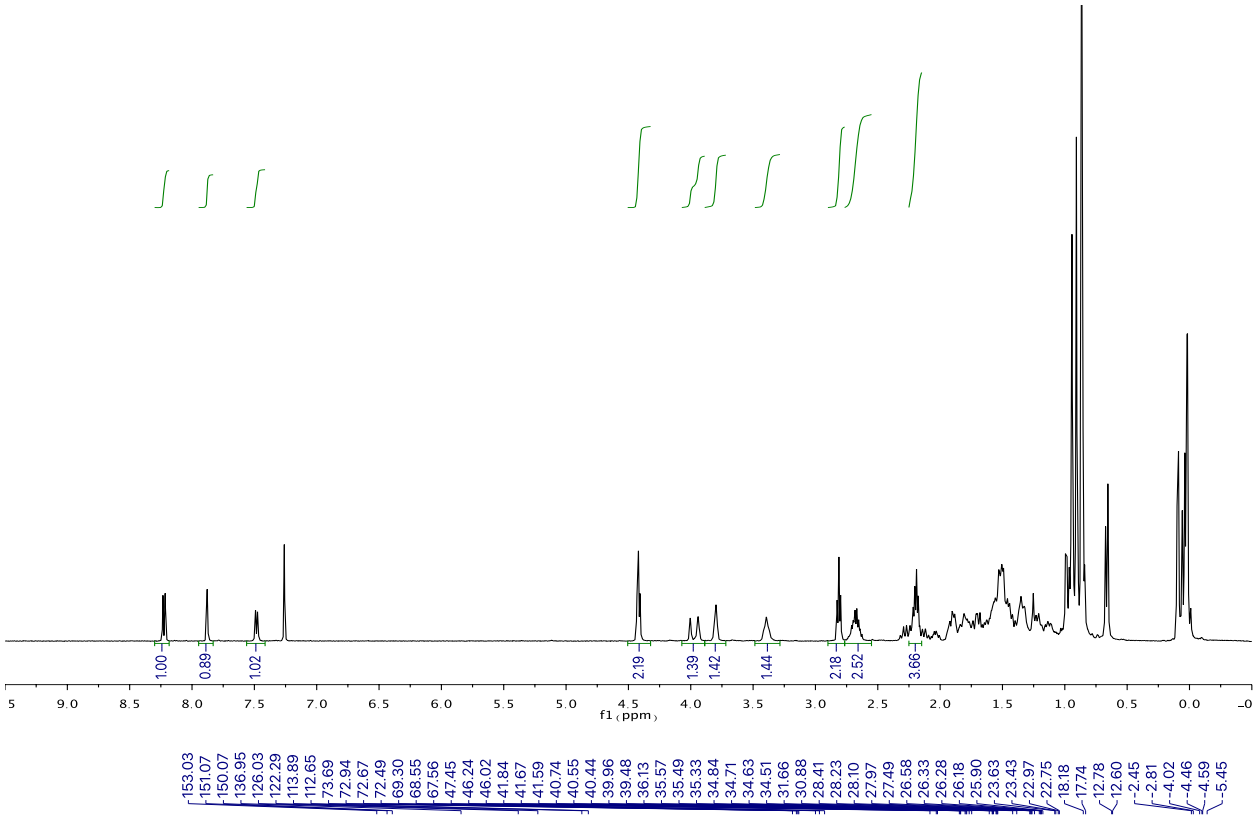
1.00
0.89
1.02
2.19
1.39
1.42
1.44
2.18
2.52
3.66
f1 (ppm)

153.03
151.07
150.07
136.95
126.03
122.29
113.89
112.65
73.69
72.94
72.67
72.49
69.30
68.55
67.56
47.45
46.24
46.02
41.84
41.67
41.59
40.74
40.55
40.44
39.96
39.48
36.13
35.57
35.49
35.33
34.84
34.71
34.63
34.51
31.66
30.88
28.41
28.23
28.10
27.97
27.49
26.58
26.33
26.28
26.18
25.90
23.63
23.43
22.97
22.75
18.18
17.74
12.78
12.60
-2.45
-2.81
-4.02
-4.46
-4.59
-5.45

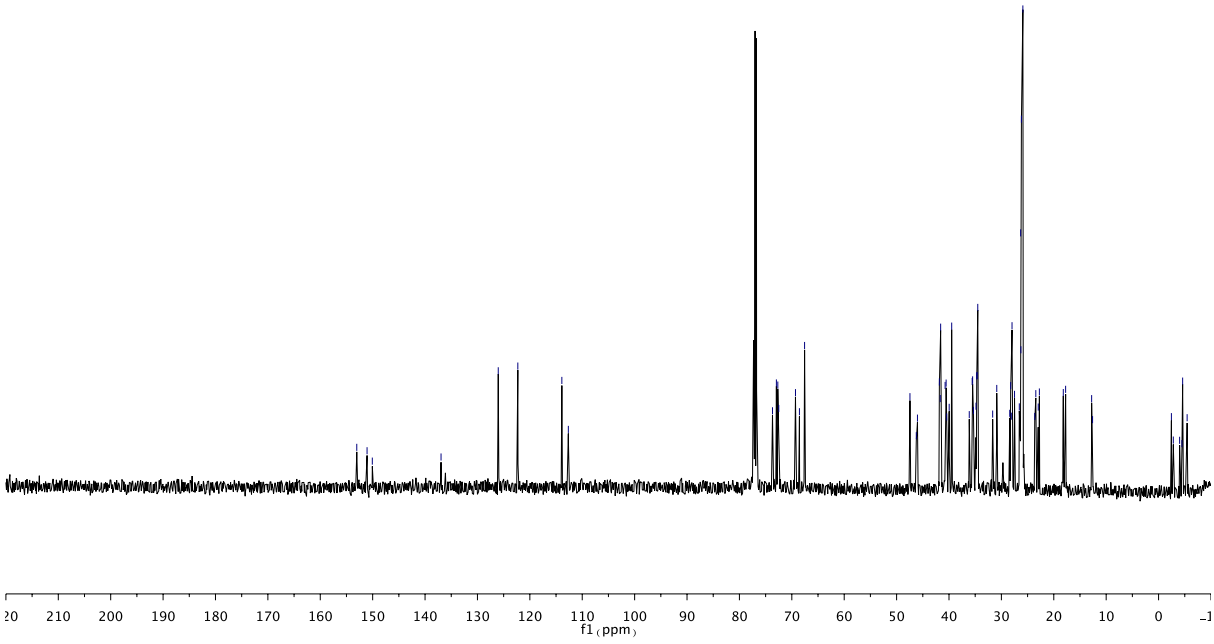
f1 (ppm)

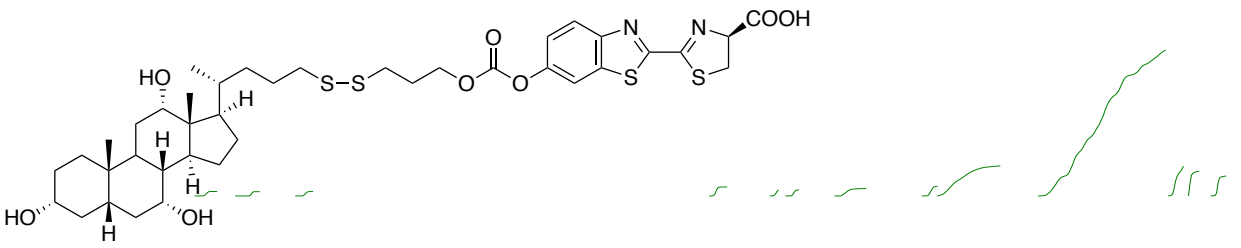

1-19

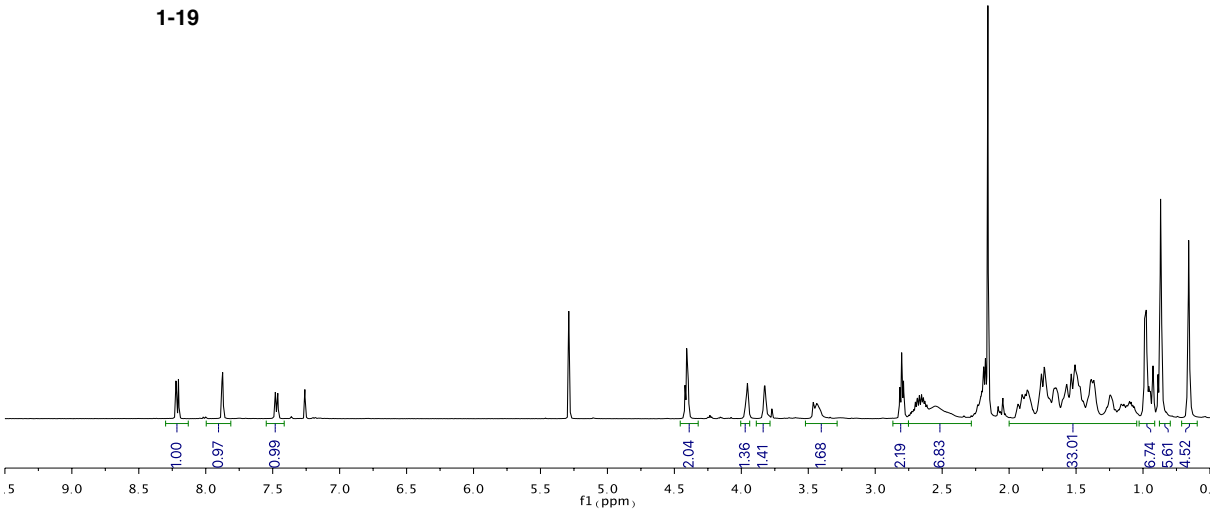

153.03
151.05
150.04
136.97
136.65
136.12
126.33
126.01
122.31
113.94
112.66
73.10
71.94
68.48
67.58
47.28
46.45
41.76
41.45
39.55
35.43
35.24
34.76
34.69
34.51
30.94
30.48
28.23
27.98
27.65
26.48
25.91
23.23
22.50
17.70
12.50

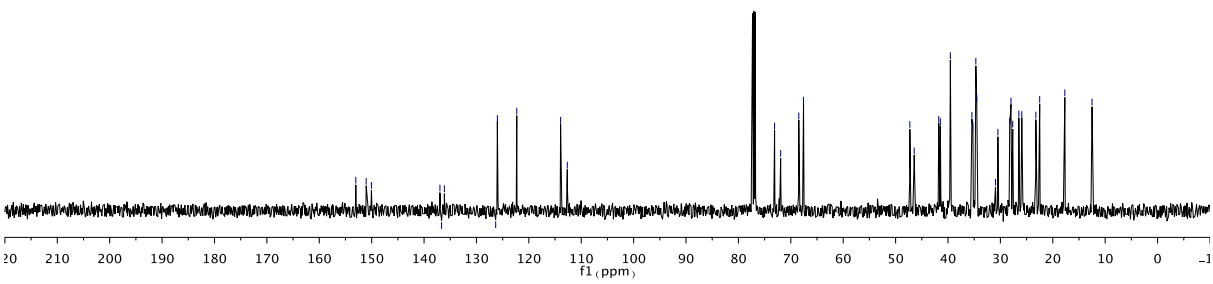

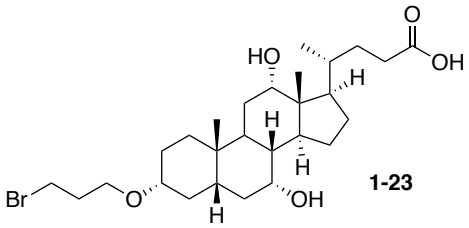
HO
O
OH
H
H
H
Br
O
OH
H

1-23

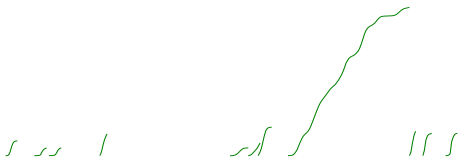

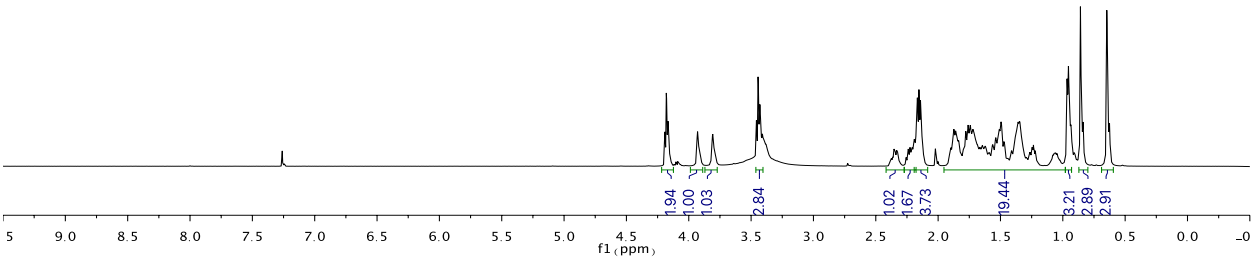
1.94
1.00
1.03
2.84
1.02
1.67
3.73
19.44
3.21
2.89
2.91
f1 (ppm)


174.20
73.08
71.84
68.44
61.98
46.97
46.41
41.57
41.49
39.45
35.35
35.29
34.78
34.68
31.71
31.24
30.92
30.31
29.49
28.13
27.55
26.28
23.23
22.46
17.30
12.48

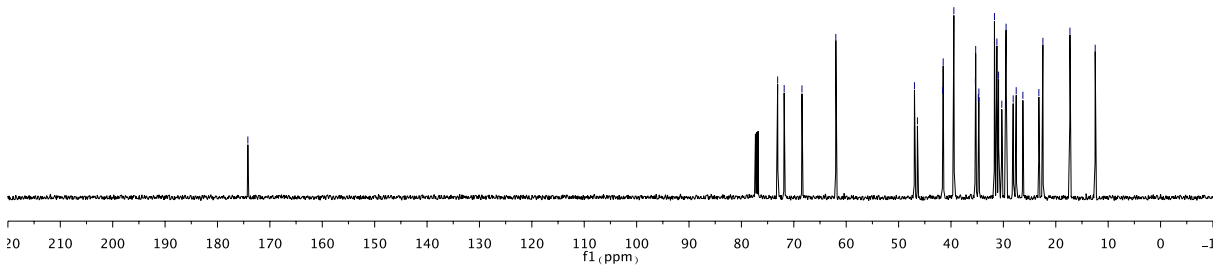
f1 (ppm)

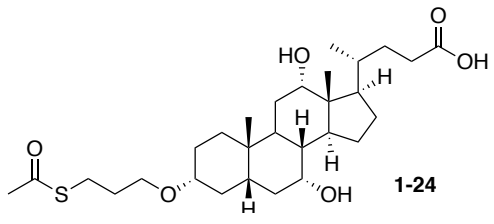
HO
O
OH
H
H
H
O
S
O
OH

1-24

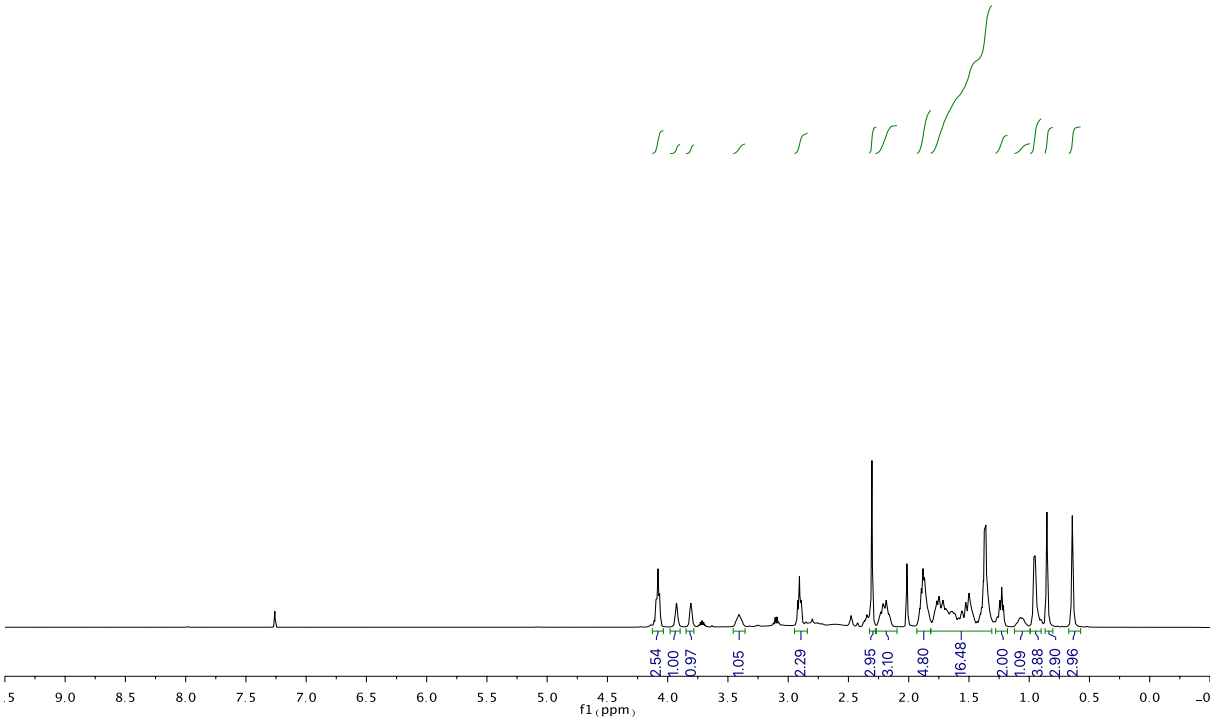
2.54
1.00
0.97
1.05
2.29
2.95
3.10
4.80
16.48
2.00
1.09
3.88
2.90
2.96
f1 (ppm)


195.56
174.27
73.05
71.85
68.43
62.62
47.00
46.44
41.66
41.48
39.50
35.28
34.77
34.70
31.24
30.88
30.63
30.41
28.69
28.19
27.52
26.37
25.70
23.23
22.47
17.31

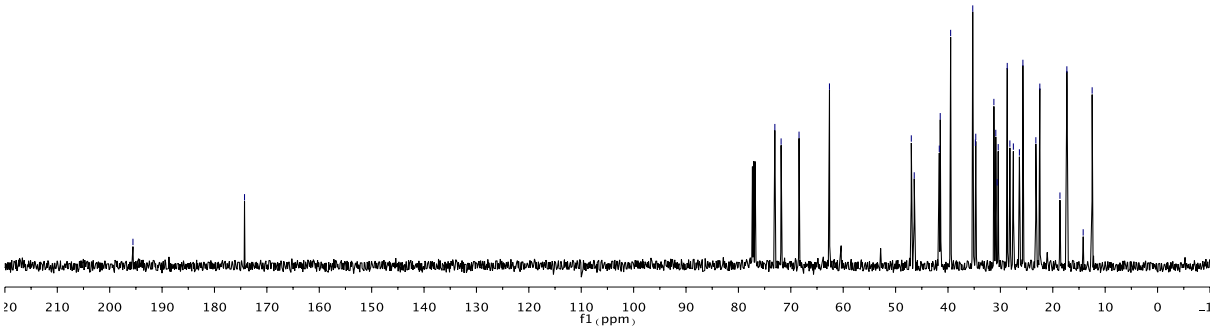
f1 (ppm)

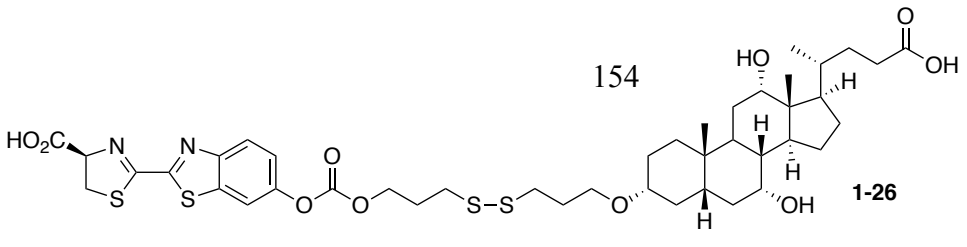
HO2C
N
S
N
S
O
O
O
S–S
O
HO
OH
H
H
H
OH
O
OH

1-26

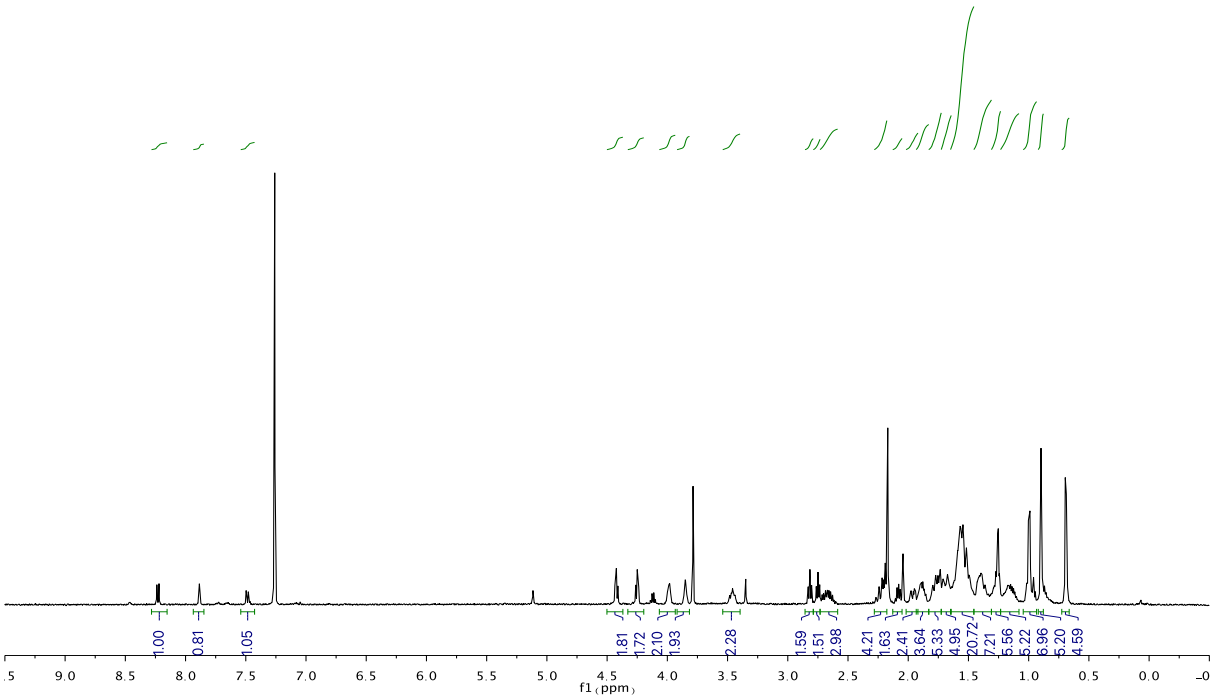
1.00
0.81
1.05
1.81
1.72
2.10
1.93
2.28
1.59
1.51
2.98
4.21
1.63
2.41
3.64
5.33
4.95
20.72
7.21
5.56
5.22
6.96
5.20
4.59
f1 (ppm)

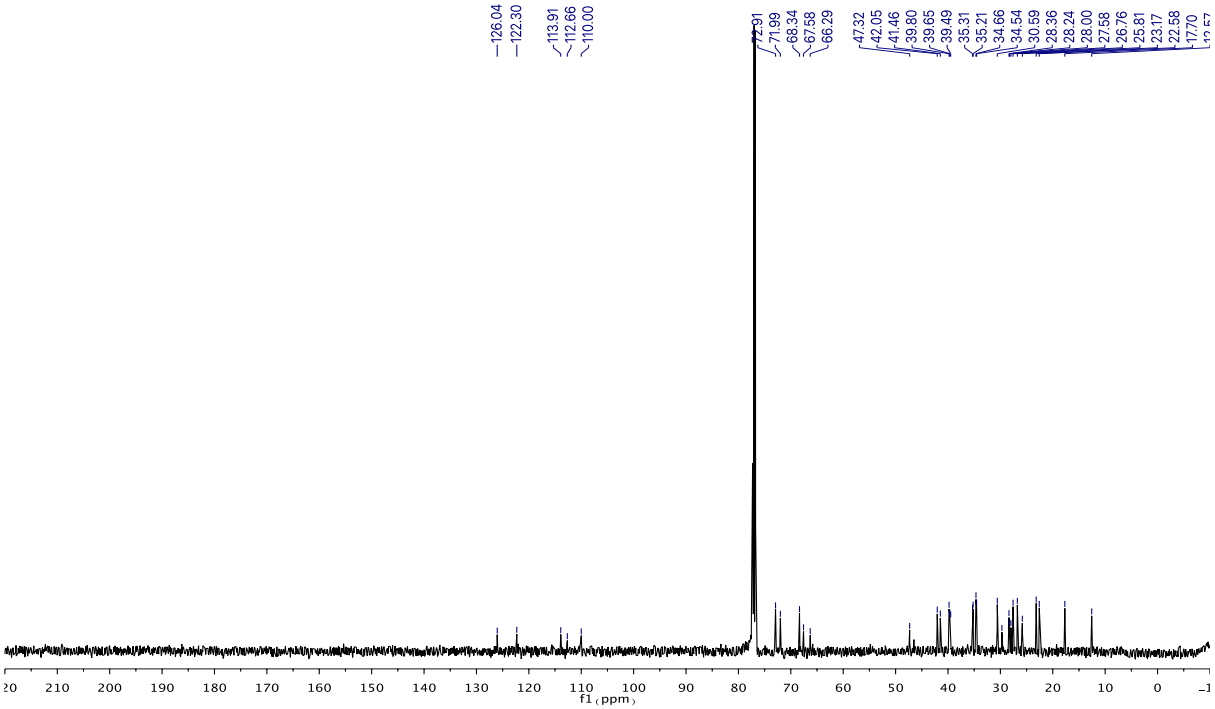
126.04
122.30
113.91
112.66
110.00
72.91
71.99
68.34
67.58
66.29
47.32
42.05
41.46
39.80
39.65
39.49
35.31
35.21
34.66
34.54
30.59
28.36
28.24
28.00
27.58
26.76
25.81
23.17
22.58
17.70
f1 (ppm)

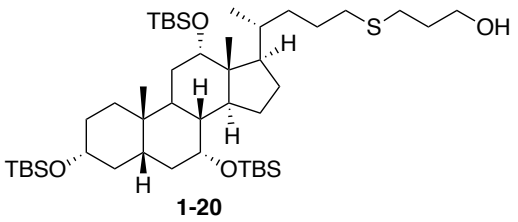
TBSO
H
S
OH
H
H
TBSO
OTBS
H

1-20

1.00
1.04
2.00
1.02
2.14
2.33
3.26
22.19
1.61
11.34
f1 (ppm)


73.67
72.96
72.68
72.50
69.30
68.55
61.94
47.53
47.46
46.23
46.04
41.85
41.68
41.57
40.74
40.54
40.41
39.95
36.09
35.54
35.49
35.33
35.26
35.15
34.88
34.73
34.63
34.49
32.60
31.93
31.65
30.86
28.89
28.40
28.18
28.03
27.47
26.57
26.48
26.31
26.27
26.17
25.90
23.62
23.43
22.97
22.75
18.35
18.22
17.76
12.77
12.61
-2.46
-2.83
-4.05
-4.41
-4.46
-4.60
-5.45

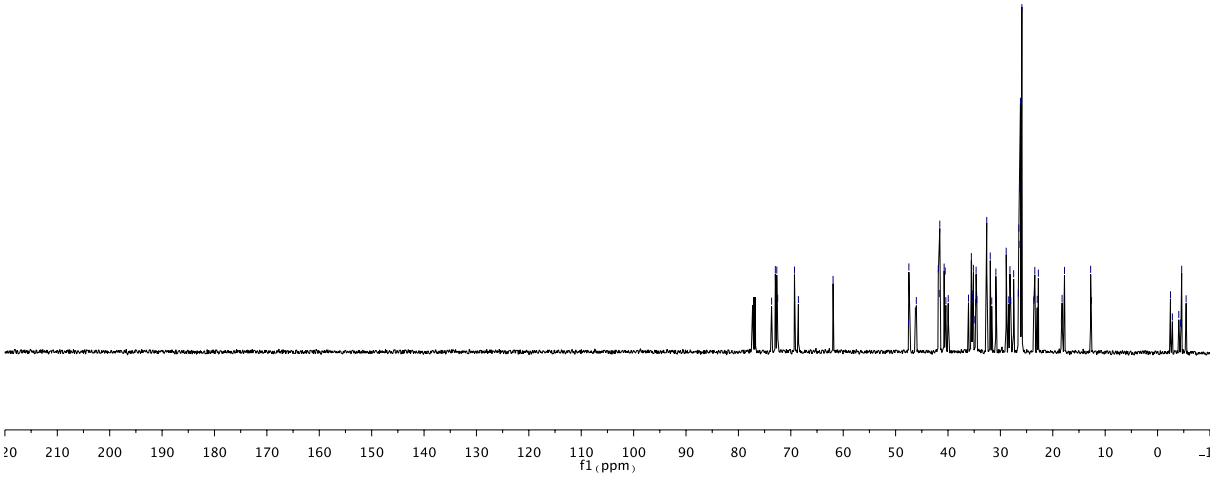
f1 (ppm)

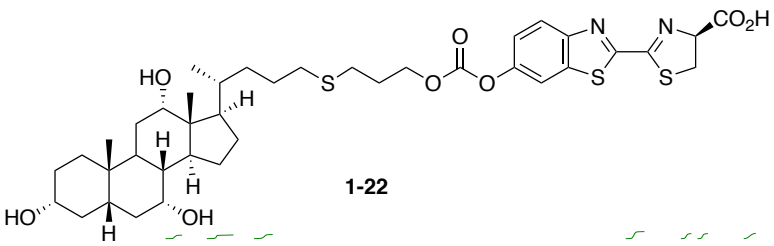
HO
H
H
H
HO
OH
S
O
O
O
N
S
N
S
CO2H

1-22

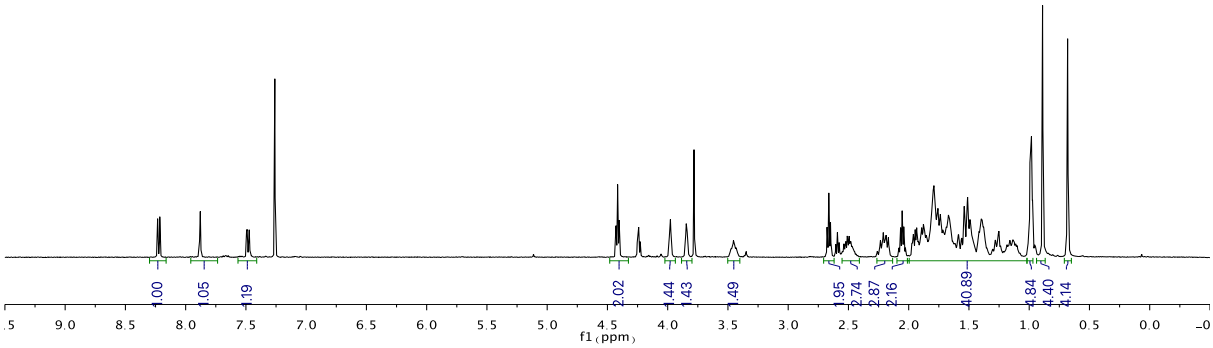
4.00
1.05
4.19
2.02
1.44
1.43
1.49
1.95
2.74
2.87
2.16
40.89
4.84
4.40
4.14
f1 (ppm)


126.01
123.76
122.31
114.47
113.90
113.50
112.65
109.98
73.01
72.36
71.96
71.61
68.41
68.13
67.97
67.56
66.67
55.69
47.32
46.57
46.48
44.70
41.93
41.68
41.45
41.02
39.73
39.61
37.22
35.34
35.23
35.10
34.98
34.70
34.61
32.90
32.73
32.21
30.55
28.99
28.76
28.50
28.30
27.96
27.59
27.21
26.65
26.43
26.22
23.91
23.20
22.98
22.54
19.21
17.74
14.46
12.54
4.80

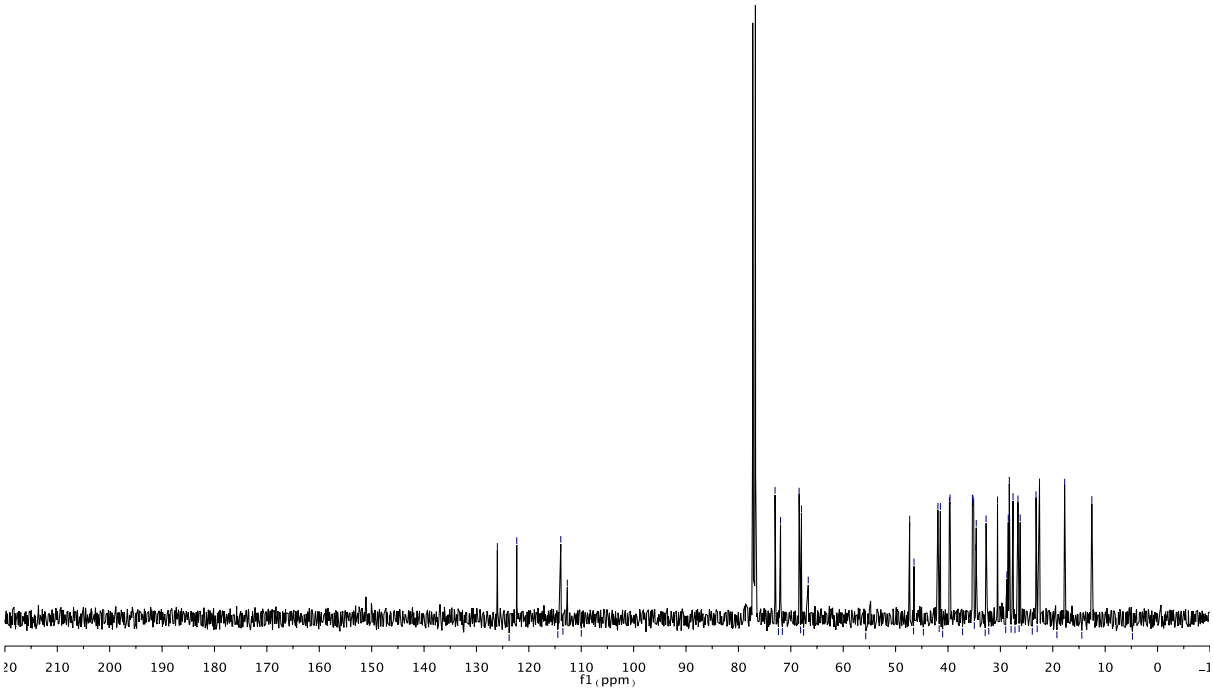
f1 (ppm)

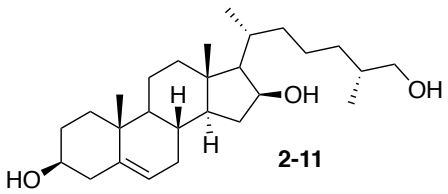
H
OH
OH
H
HO

2-11

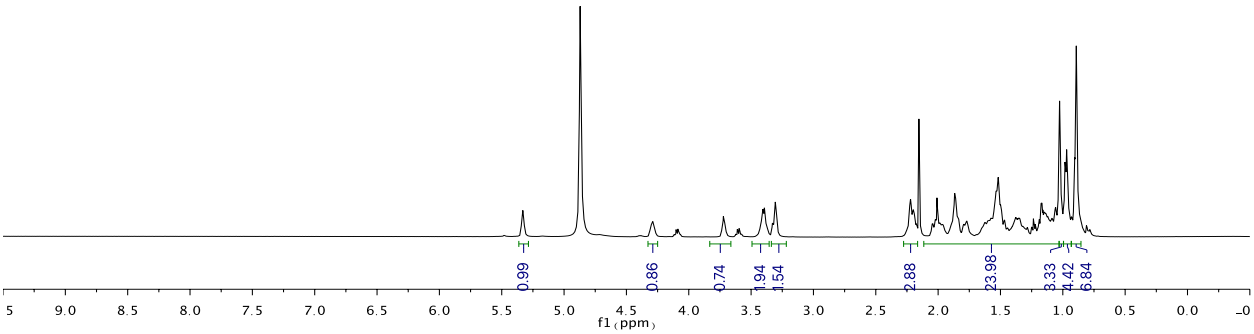
0.99
0.86
0.74
1.94
1.54
2.88
23.98
3.33
4.42
6.84
f1 (ppm)


140.91
120.94
71.30
71.02
67.23
61.57
54.42
50.31
48.01
47.84
47.67
47.50
47.33
42.00
41.63
39.97
37.14
36.63
36.33
35.97
35.50
33.36
31.62
31.47
30.90
29.86
23.60
20.54
18.59
17.53
15.77
12.19

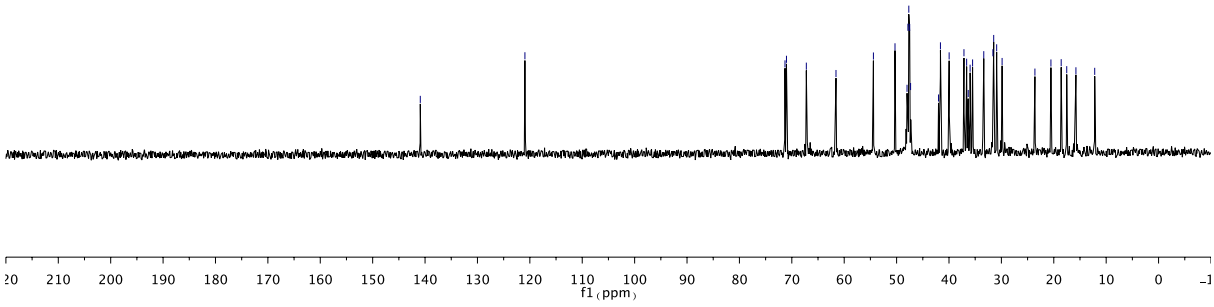
f1 (ppm)

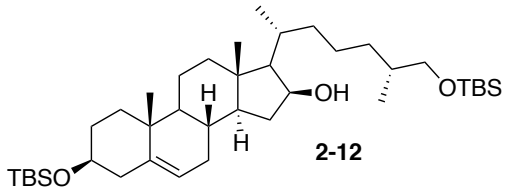
H
OH
OTBS
H
TBSO

2-12

1.00
0.85
2.06
1.09
27.73
25.99
13.42
f1 (ppm)


141.64
120.92
72.60
72.46
68.49
61.41
54.56
50.19
42.80
42.20
39.90
37.33
36.60
36.54
36.31
35.81
33.63
32.07
31.85
31.51
29.77
25.99
25.96
25.67
23.77
20.70
19.43
18.22
16.72
13.04
-4.56
-5.32

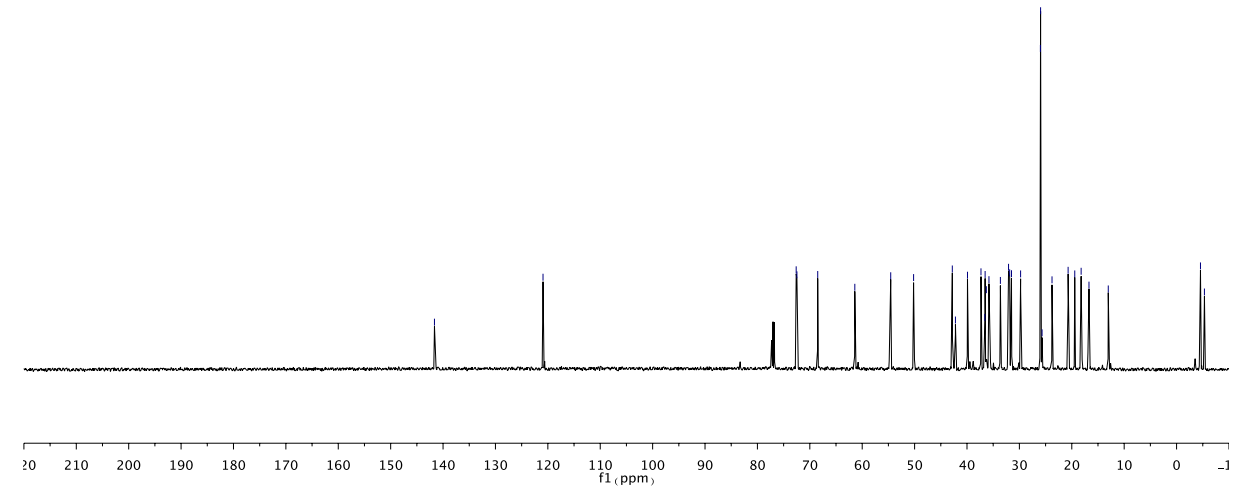
f1 (ppm)

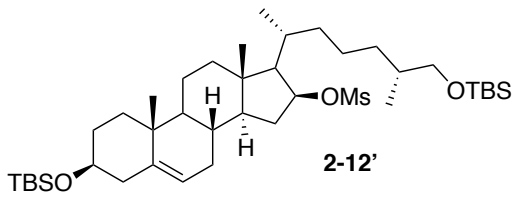
H
OMs
OTBS
H
TBSO

2-12'

1.00
0.73
1.90
0.94
2.49
23.80
22.23
11.29
f1 (ppm)


129.04
120.62
83.34
72.55
68.52
60.76
54.85
50.01
42.76
39.44
38.83
37.30
35.84
35.51
34.96
33.51
32.03
31.63
31.35
30.10
25.99
25.95
24.07
20.67
19.41
18.02
16.68
12.60
-4.57
-5.32

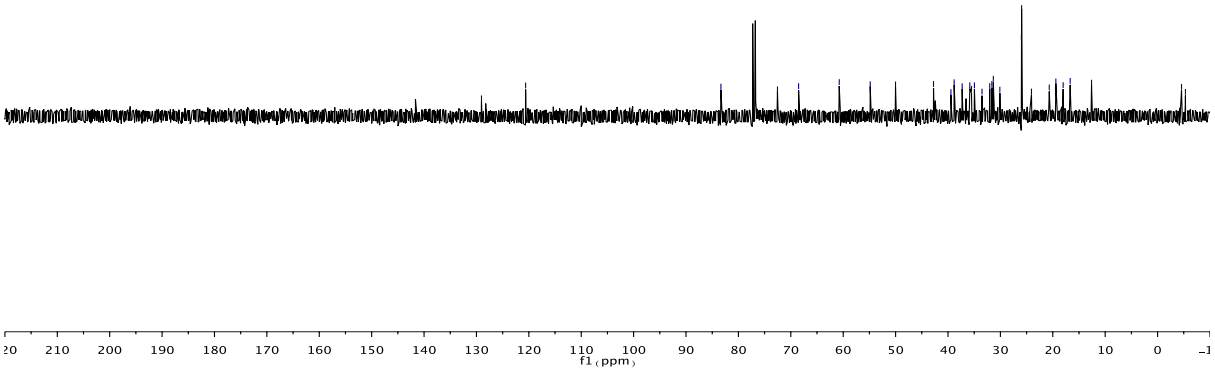
f1 (ppm)

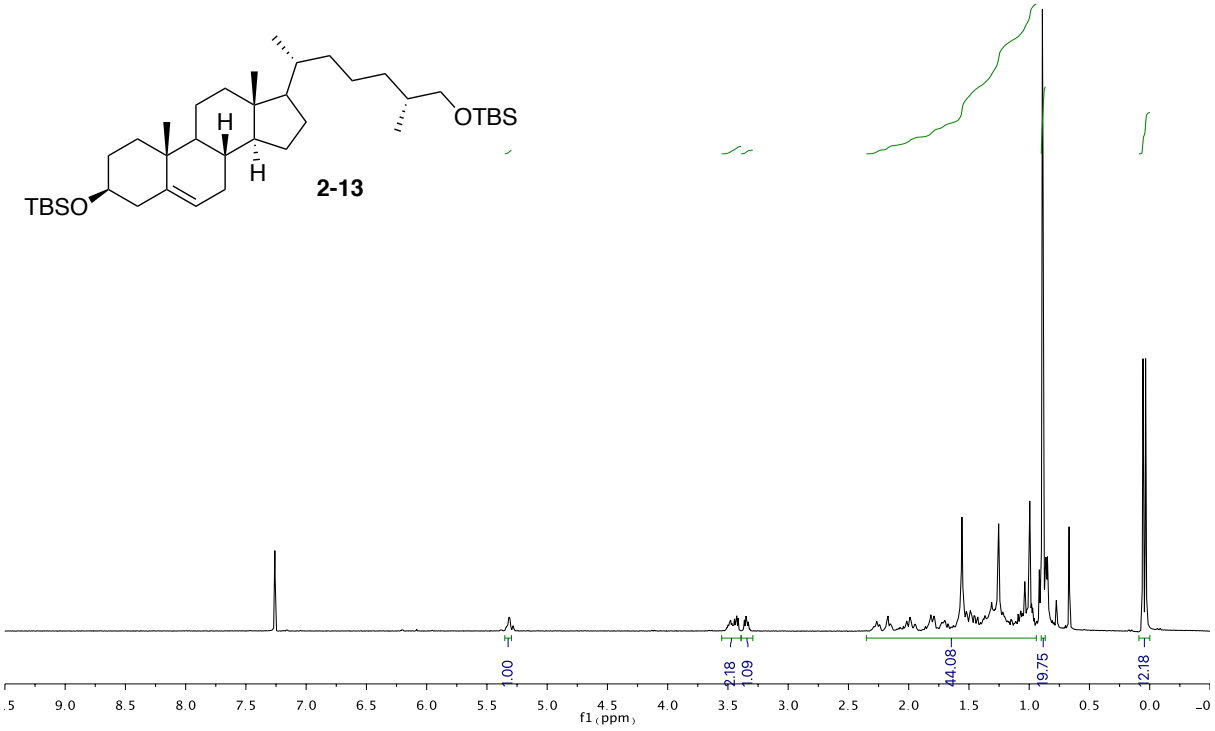
OTBS
H
H
TBSO
2-13
1.00
2.18
1.09
44.08
19.75
12.18
f1 (ppm)

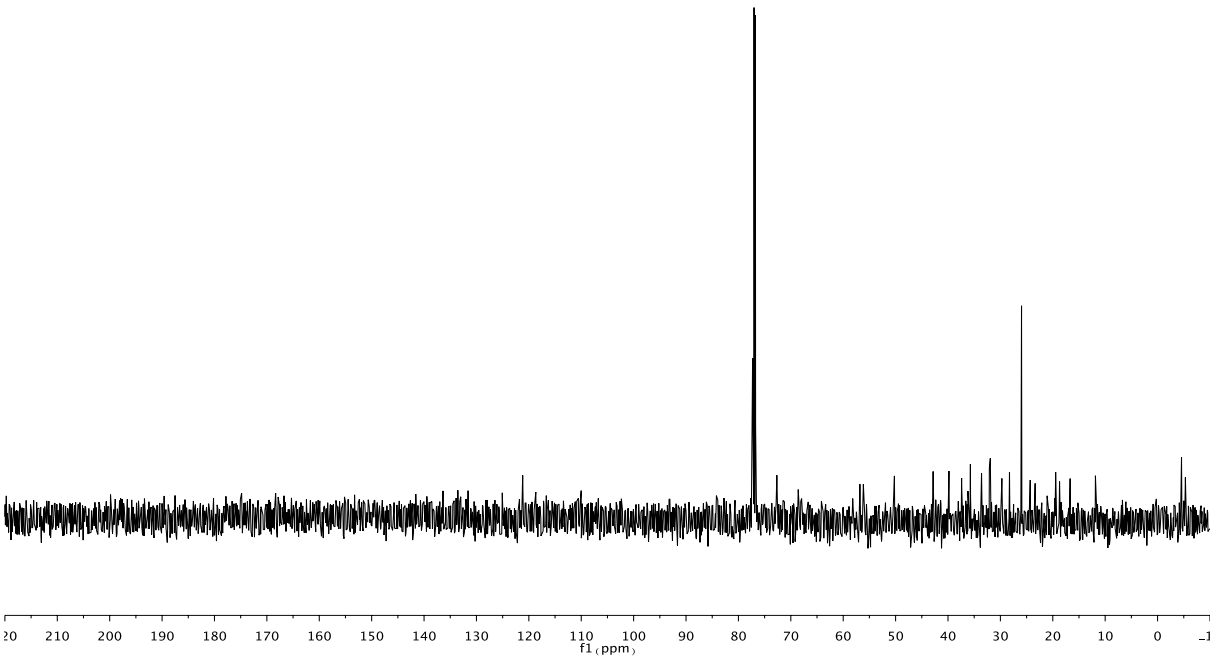
f1 (ppm)

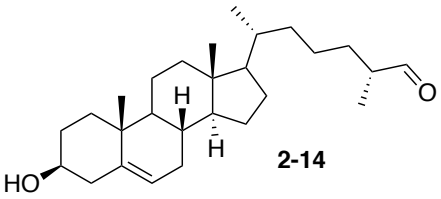
H
H
O
HO

2-14

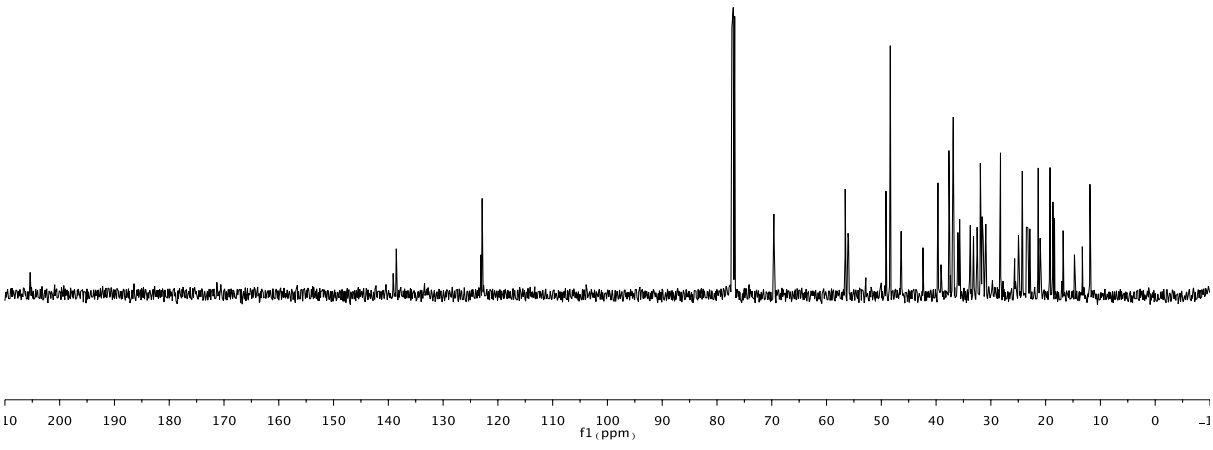
10
200
190
180
170
160
150
140
130
120
110
100
90
80
70
60
50
40
30
20
10
0
f1 (ppm)

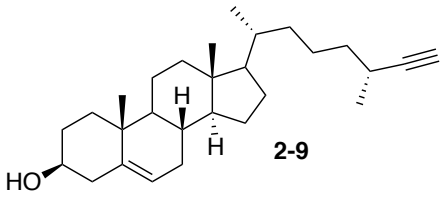
H
H
HO

2-9

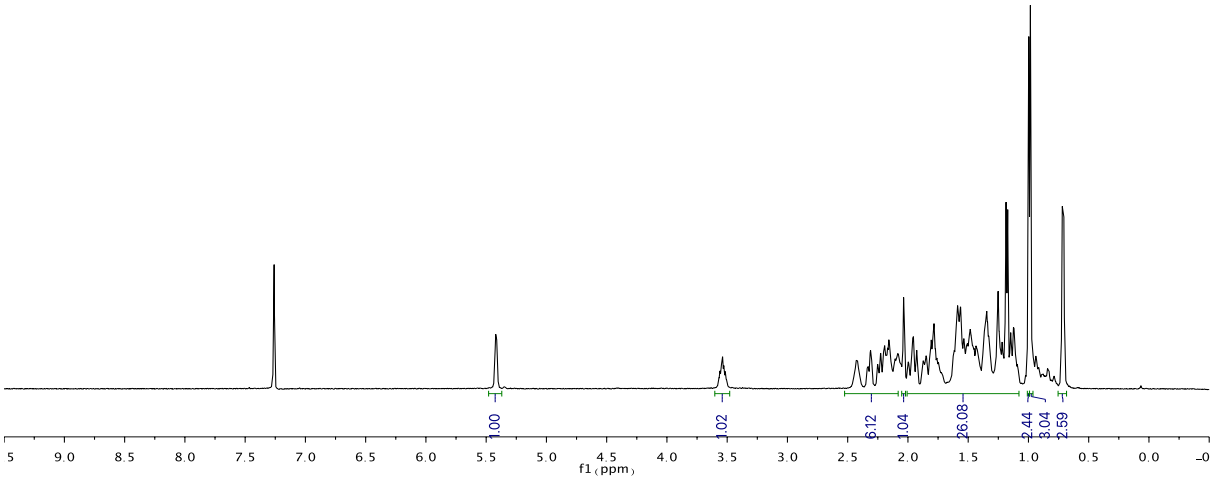
1.00
1.02
6.12
1.04
26.08
2.44
3.04
2.59
f1 (ppm)


141.36
121.97
72.05
68.05
67.99
49.24
42.19
39.26
37.16
37.06
33.10
31.66
31.52
31.32
31.18
30.96
26.02
25.75
24.98
23.26
22.98
20.93

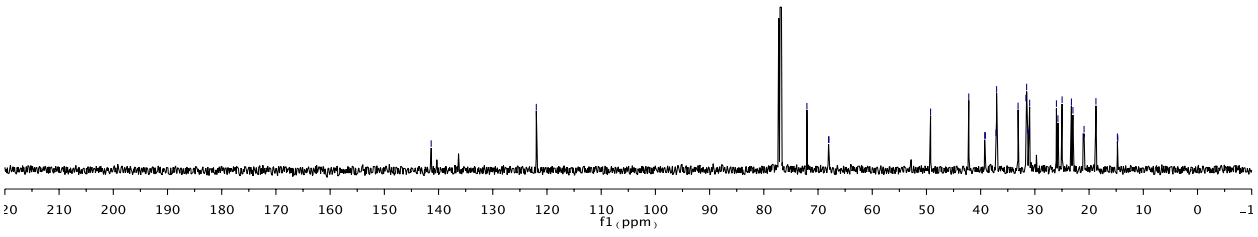
f1 (ppm)

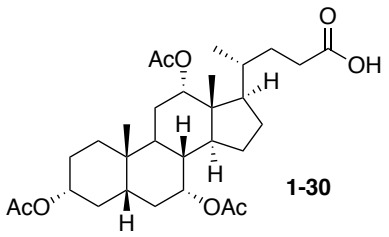
O
AcO
OH
H
H
H
AcO
OAc
H

1-30

1.00
1.02
1.02
1.02
1.09
2.98
2.94
8.37
22.49
3.04
2.99
8.01
f1 (ppm)


179.75
170.61
170.55
170.44
75.40
74.11
70.74
47.34
45.07
43.39
40.92
37.74
34.68
34.61
34.54
34.33
31.24
30.84
30.53
28.88
27.16
26.88
25.57
22.79
22.55
21.61
21.48
21.41
17.48
12.23

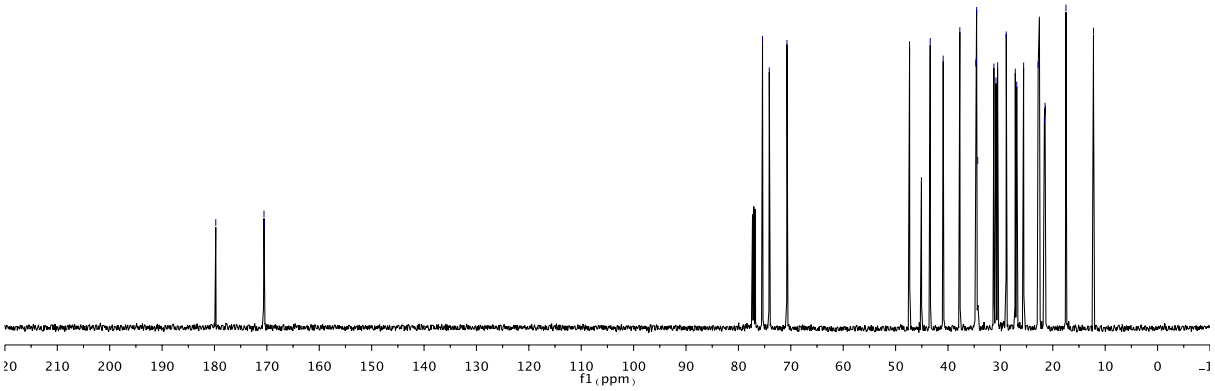
f1 (ppm)

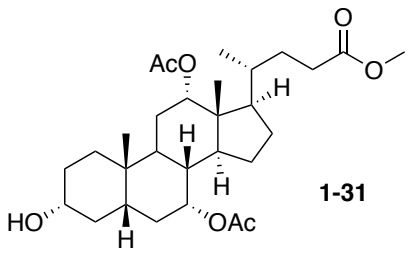
AcO
O
O
H
H
H
HO
OAc
H

1-31

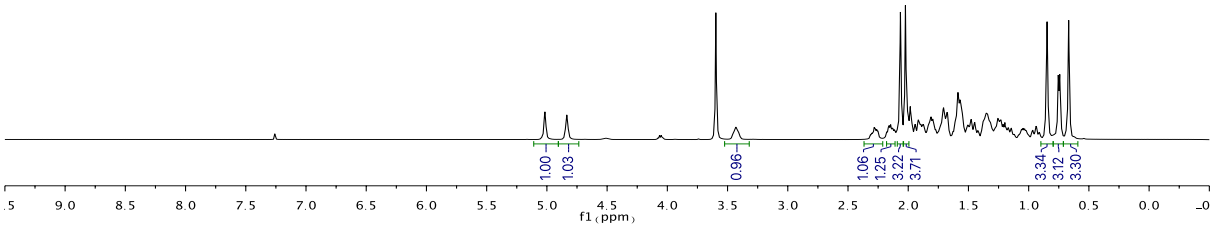
1.00
1.03
0.96
1.06
1.25
3.22
3.71
3.34
3.12
3.30
f1 (ppm)


174.49
170.59
75.39
71.56
70.83
51.47
47.29
43.36
41.01
38.62
37.73
34.85
34.55
34.26
31.32
30.83
30.73
30.43
28.90
27.14
25.52
22.77
22.55
21.61
21.42
17.46

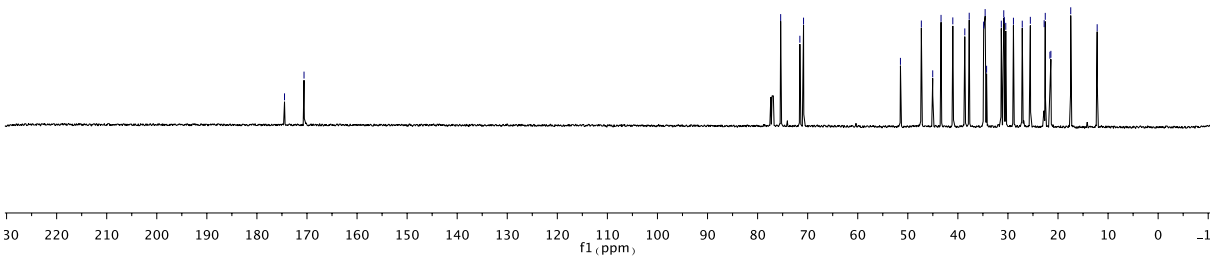
f1 (ppm)

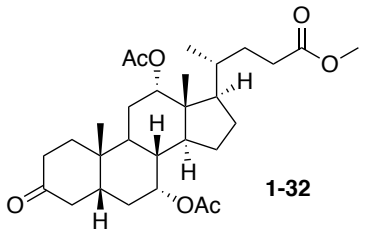
AcO
O
O
H
H
H
O
OAc
H

1-32

1.00
0.98
0.96
1.11
3.91
4.06
3.06
2.92
2.87
3.12
f1 (ppm)


211.99
174.43
75.20
70.55
60.33
47.35
44.54
43.26
42.14
37.73
36.60
36.11
34.56
30.89
30.83
30.71
29.79
27.11
25.81
22.79
21.63
21.45
21.29
17.50

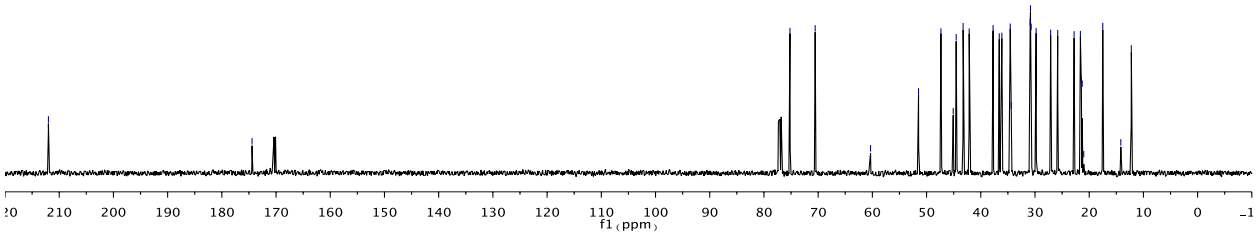
f1 (ppm)

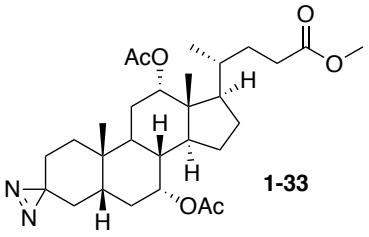
AcO
O
O
H
H
H
N
N
H
OAc

1-33

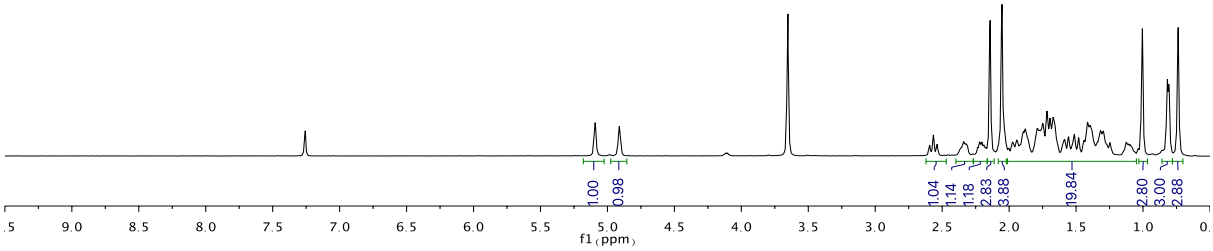
1.00
0.98
1.04
1.14
1.18
2.83
3.88
19.84
2.80
3.00
2.88
f1 (ppm)


174.49
170.48
170.22
75.34
70.63
51.52
47.37
45.09
43.31
40.25
37.71
34.62
34.49
33.78
30.90
30.77
28.76
27.16
26.46
25.65
22.84
22.48
21.57
21.38
17.53
12.24

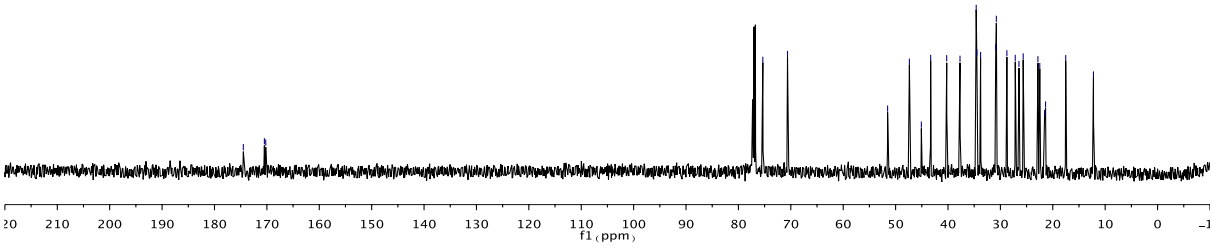
f1 (ppm)

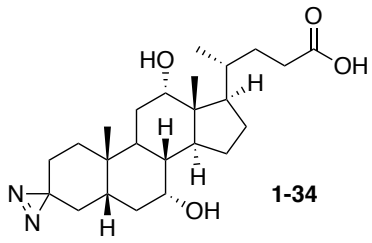
HO
O
OH
H
H
H
N
N
OH
H

1-34

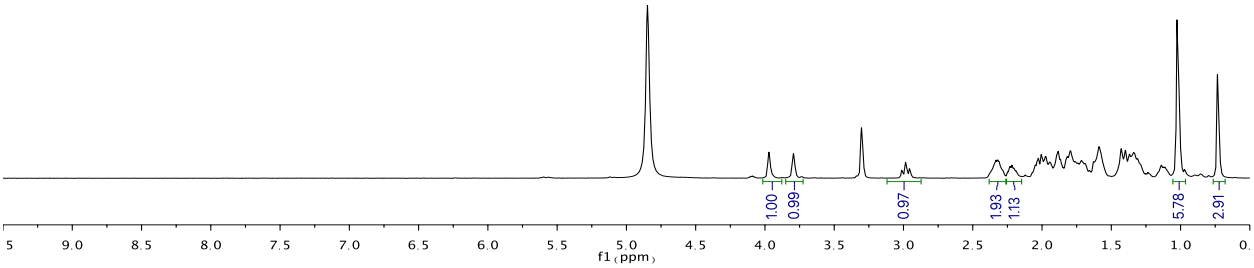
1.00
0.99
0.97
1.93
1.13
5.78
2.91
f1 (ppm)


176.85
72.54
67.46
46.66
46.15
41.58
41.00
39.56
35.37
34.83
34.57
34.34
33.61
30.93
30.63
28.33
27.25
26.35
26.03
22.81
21.69
16.22
11.61

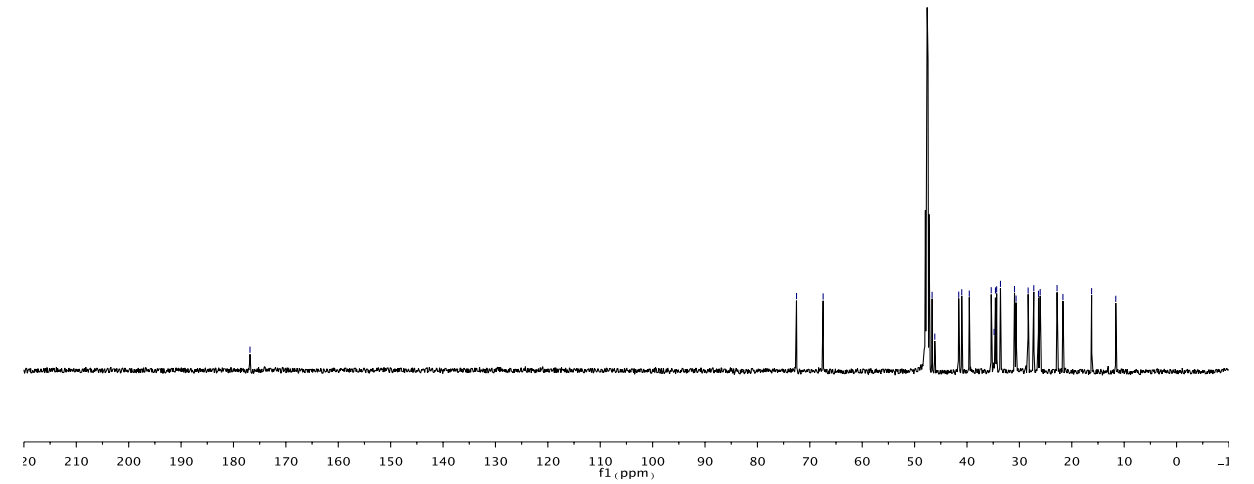
f1 (ppm)

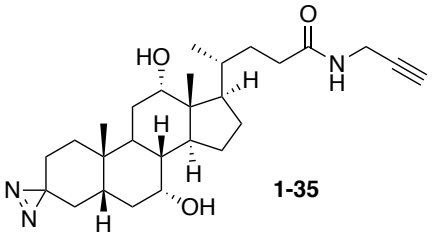
HO
O
N
H
H
H
H
N
N
H
OH

1-35

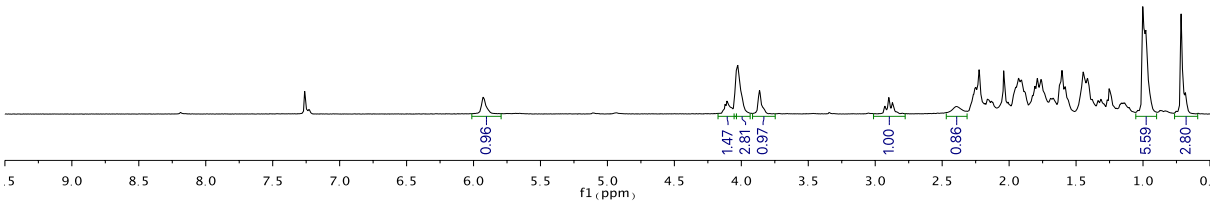
0.96
1.47
2.81
0.97
1.00
0.86
5.59
2.80
f1 (ppm)

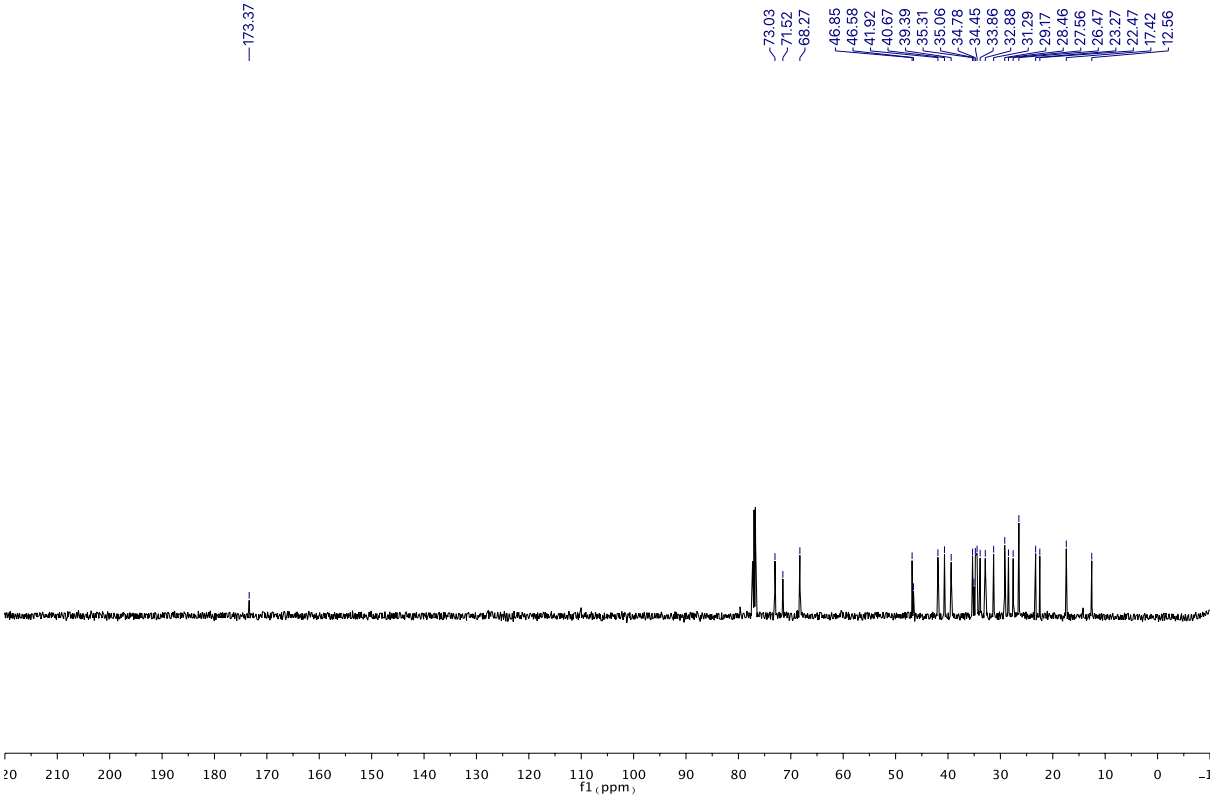
173.37
73.03
71.52
68.27
46.85
46.58
41.92
40.67
39.39
35.31
35.06
34.78
34.45
33.86
32.88
31.29
29.17
28.46
27.56
26.47
23.27
22.47
17.42
12.56
f1 (ppm)

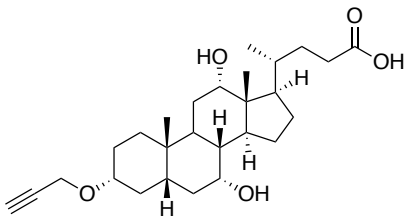
O
HO
OH
H
H
H
O
OH
H

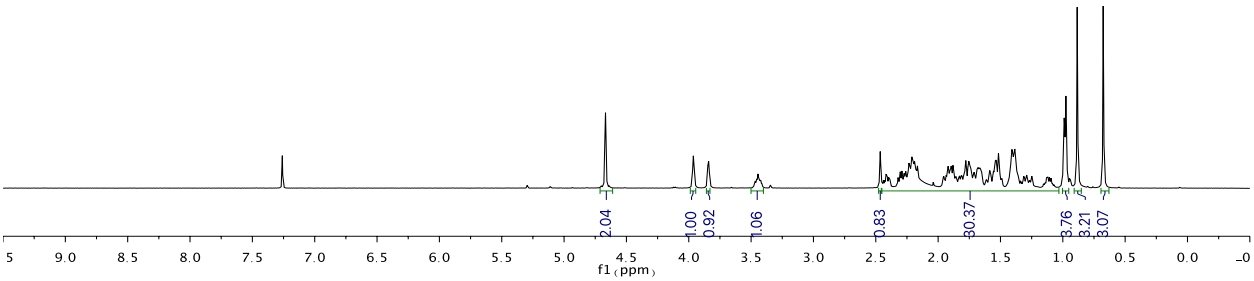
2.04
1.00
0.92
1.06
0.83
30.37
3.76
3.21
3.07
f1 (ppm)


173.39
74.71
73.01
71.94
68.44
51.78
47.07
46.50
41.81
41.47
39.65
39.56
35.25
35.16
34.74
34.65
31.01
30.75
30.51
28.28
27.47
26.52
23.21
22.51
17.32
12.52

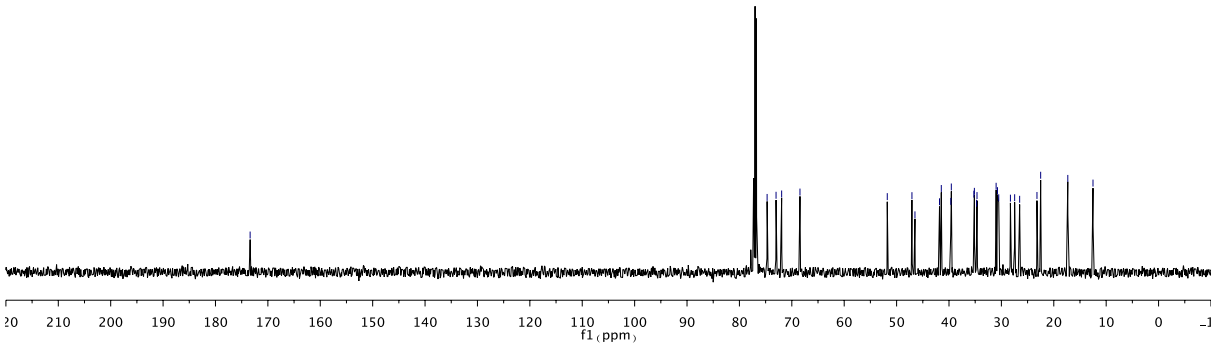
f1 (ppm)

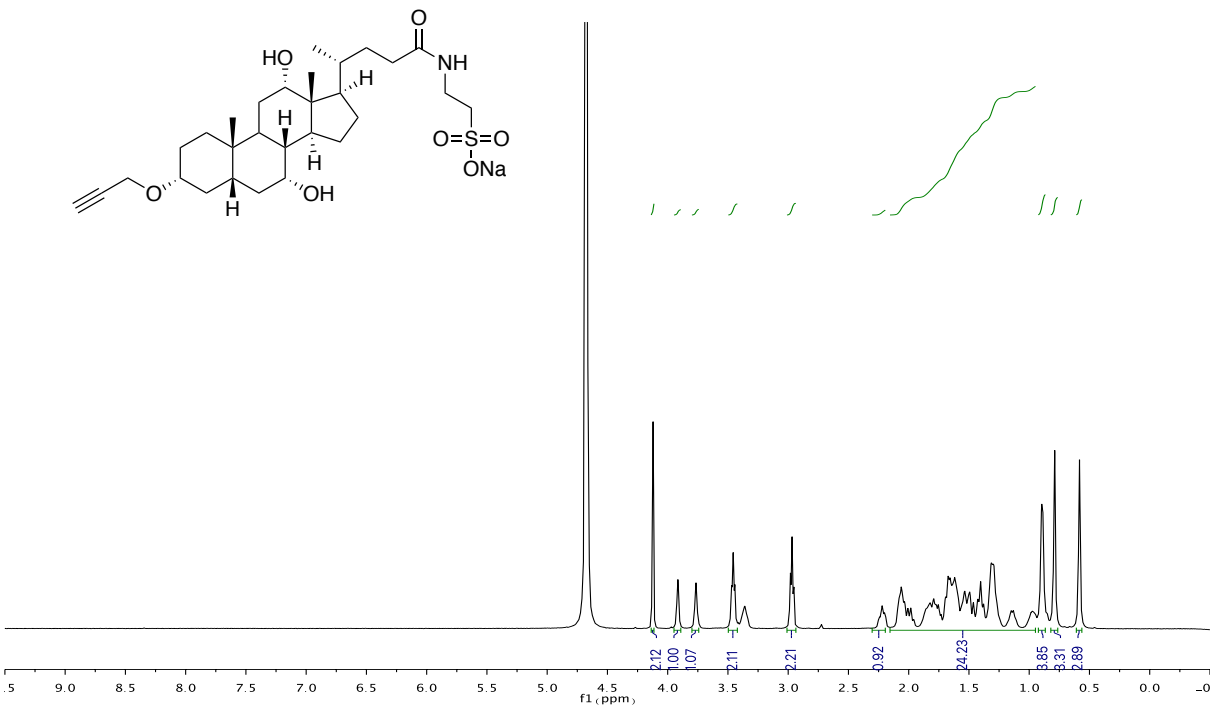
HO
H
H
H
H
O
O
NH
O=S=O
ONa
OH
2.12
1.00
1.07
2.11
2.21
0.92
24.23
3.85
3.31
2.89
f1 (ppm)

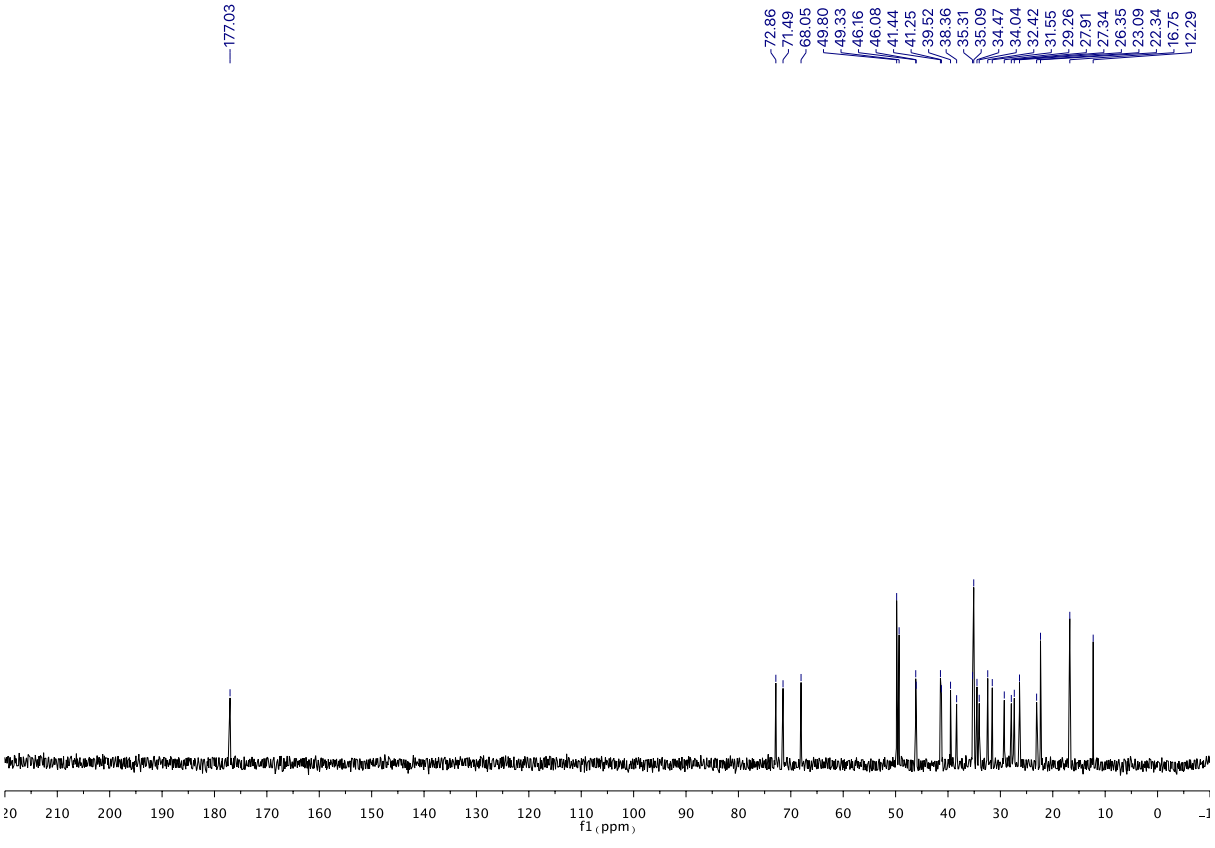
177.03
72.86
71.49
68.05
49.80
49.33
46.16
46.08
41.44
41.25
39.52
38.36
35.31
35.09
34.47
34.04
32.42
31.55
29.26
27.91
27.34
26.35
23.09
22.34
16.75
12.29
f1 (ppm)

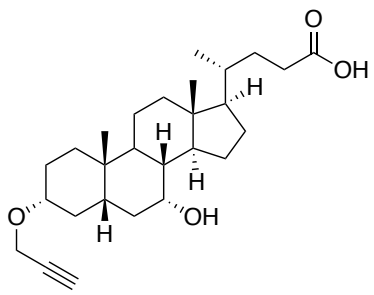
O
OH
H
H
H
O
OH
H

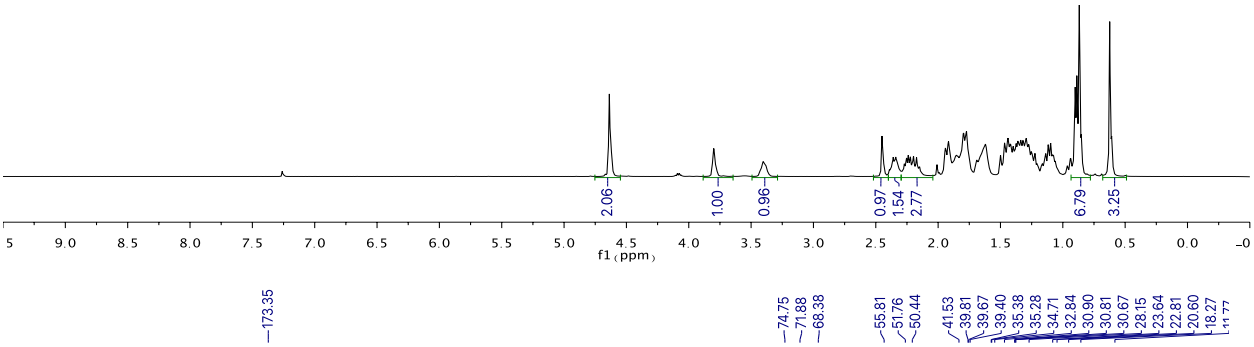
2.06
1.00
0.96
0.97
1.54
2.77
6.79
3.25
f1 (ppm)

173.35
74.75
71.88
68.38
55.81
51.76
50.44
41.53
39.81
39.67
39.40
35.38
35.28
34.71
32.84
30.90
30.81
30.67
28.15
23.64
22.81
20.60
18.27

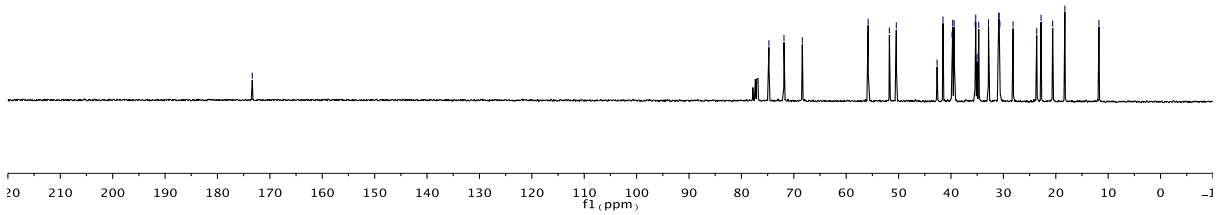
f1 (ppm)

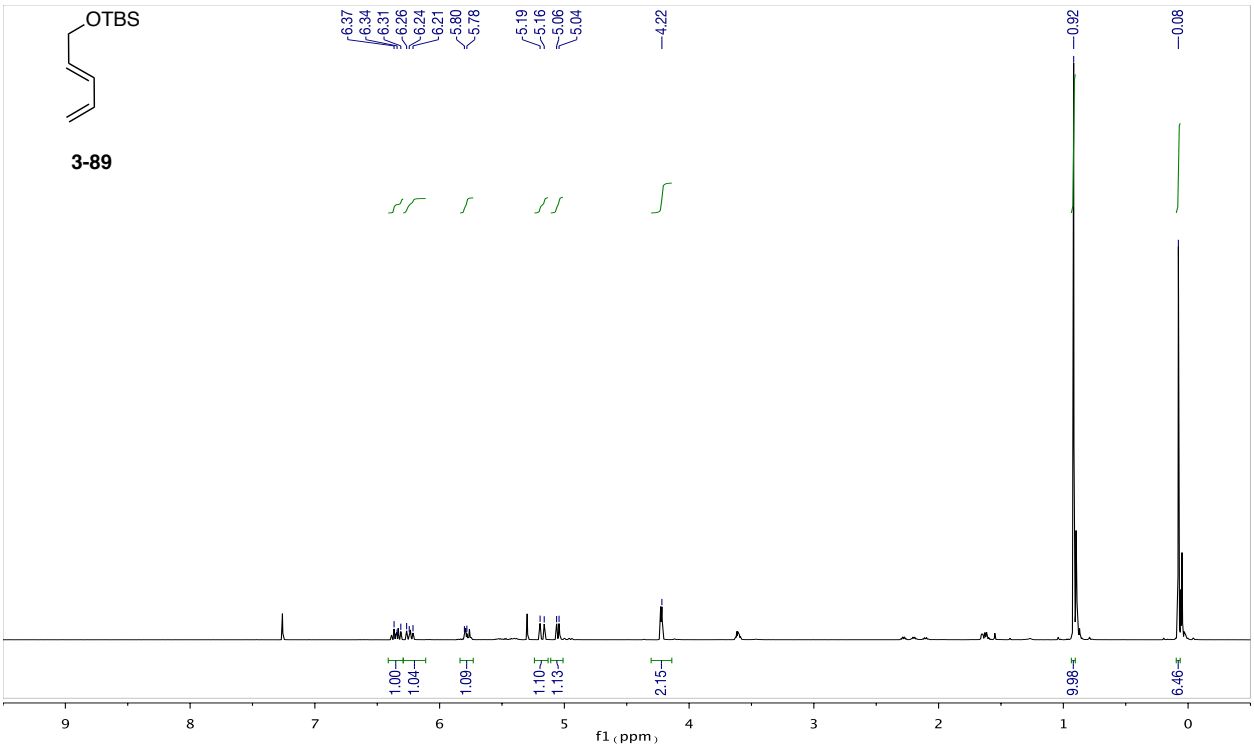
OTBS
3-89
6.37
6.34
6.31
6.26
6.24
6.21
5.80
5.78
5.19
5.16
5.06
5.04
4.22
0.92
0.08
1.00
1.04
1.09
1.10
1.13
2.15
9.98
6.46
f1 (ppm)

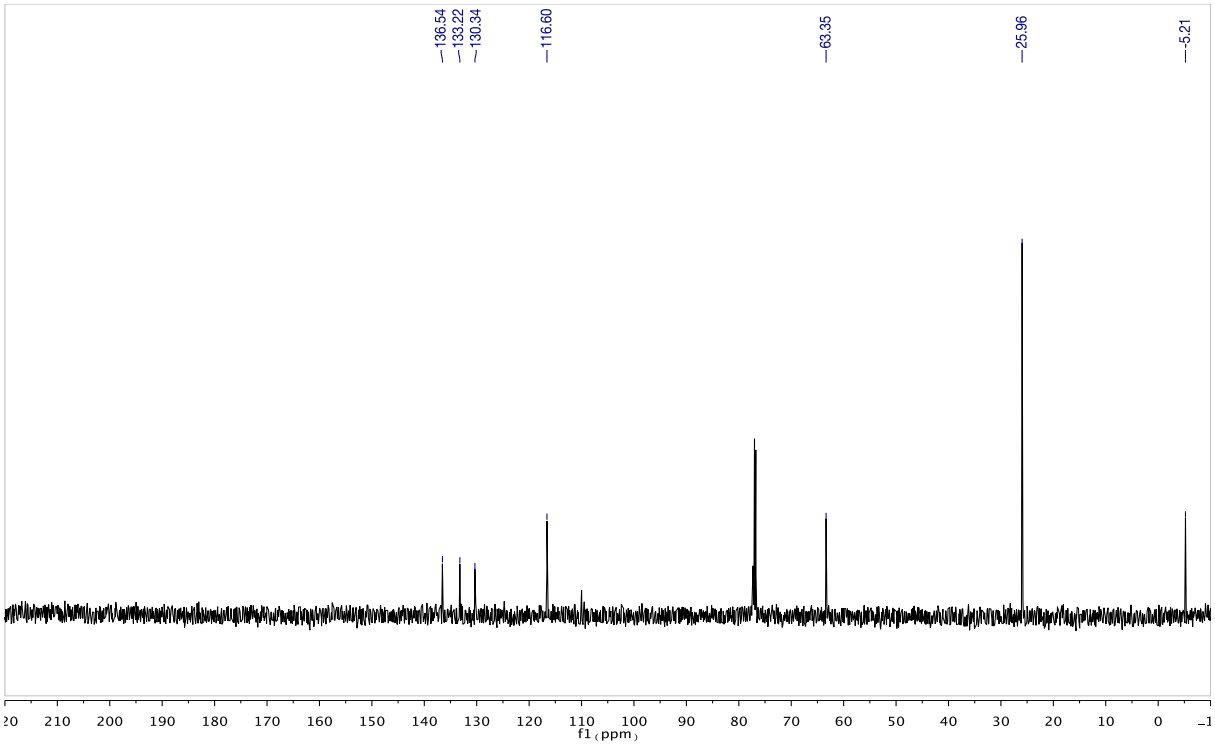
136.54
133.22
130.34
116.60
63.35
25.96
-5.21
f1 (ppm)

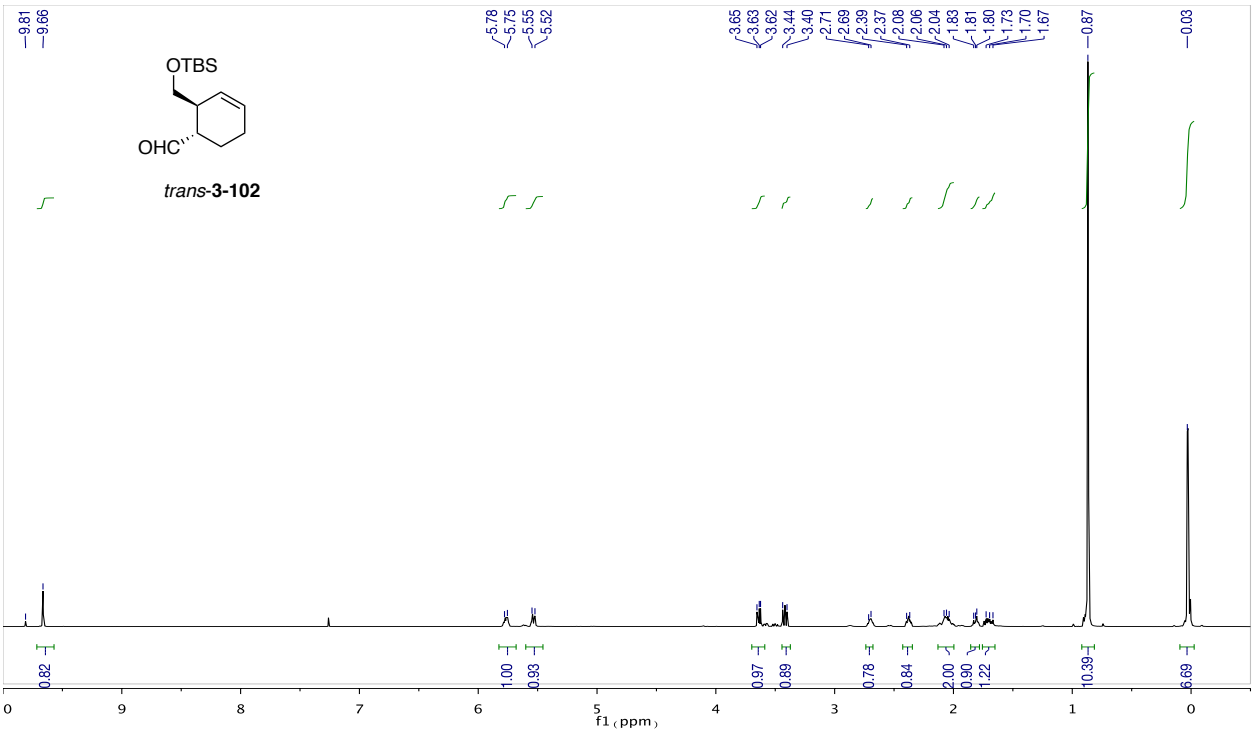
OTBS
OHC
trans-3-102
9.81
9.66
5.78
5.75
5.55
5.52
3.65
3.63
3.62
3.44
3.40
2.71
2.69
2.39
2.37
2.08
2.06
2.04
1.83
1.81
1.80
1.73
1.70
1.67
0.87
0.03
0.82
1.00
0.93
0.97
0.89
0.78
0.84
2.00
0.90
1.22
10.39
6.69
f1 (ppm)

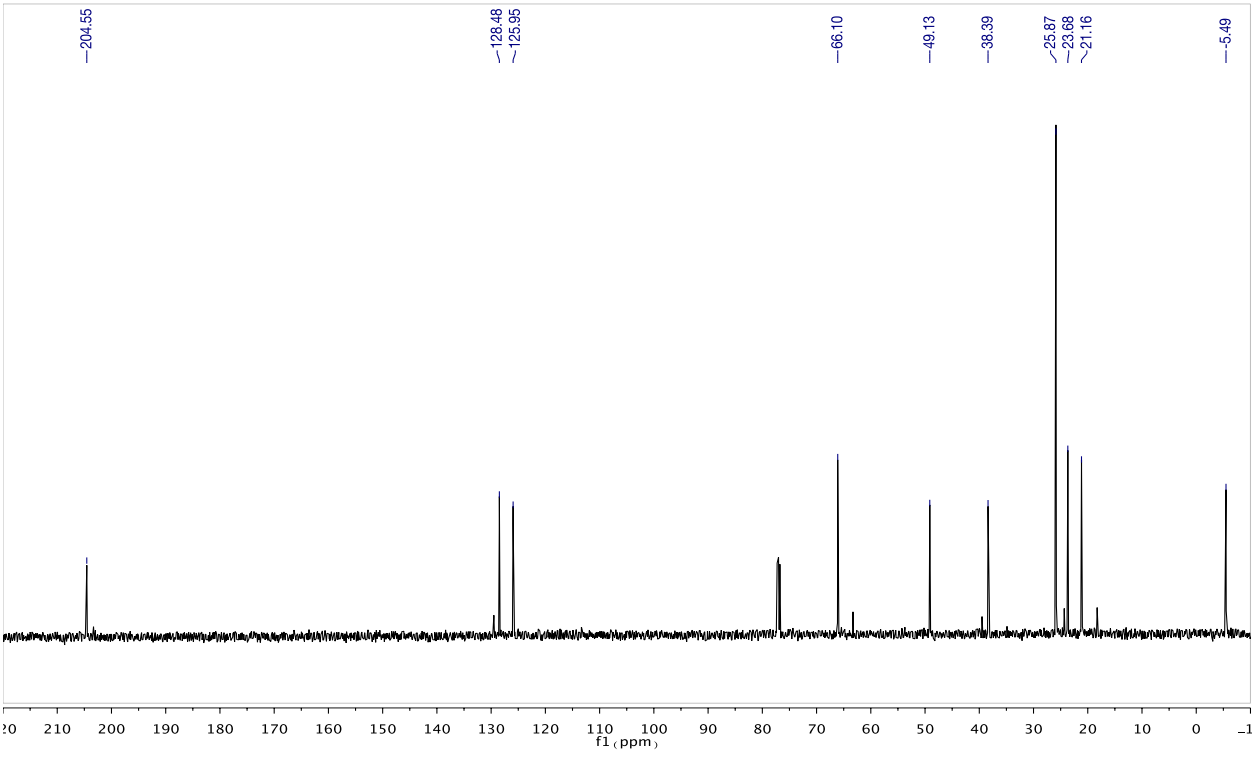
204.55
128.48
125.95
66.10
49.13
38.39
25.87
23.68
21.16
-5.49
f1 (ppm)

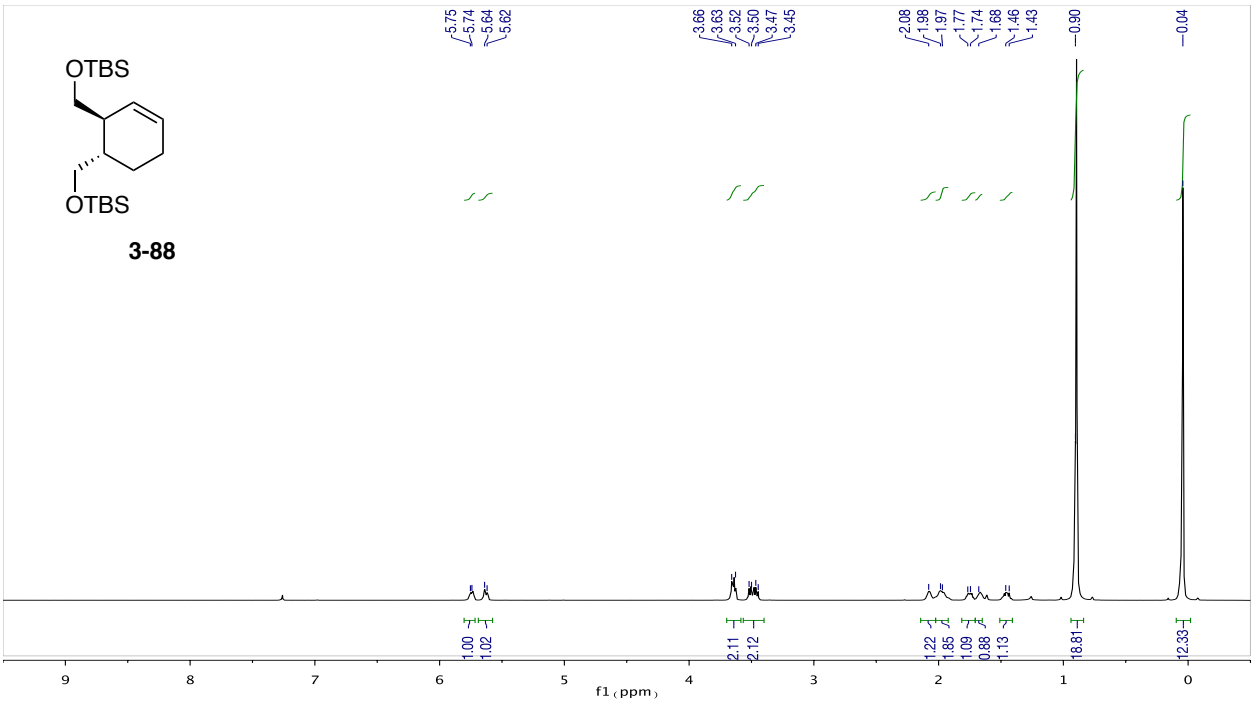
OTBS
OTBS
3-88
5.75
5.74
5.64
5.62
3.66
3.63
3.52
3.50
3.47
3.45
2.08
1.98
1.97
1.77
1.74
1.68
1.46
1.43
0.90
0.04
1.00
1.02
2.11
2.12
1.22
1.85
1.09
0.88
1.13
18.81
12.33
f1 (ppm)

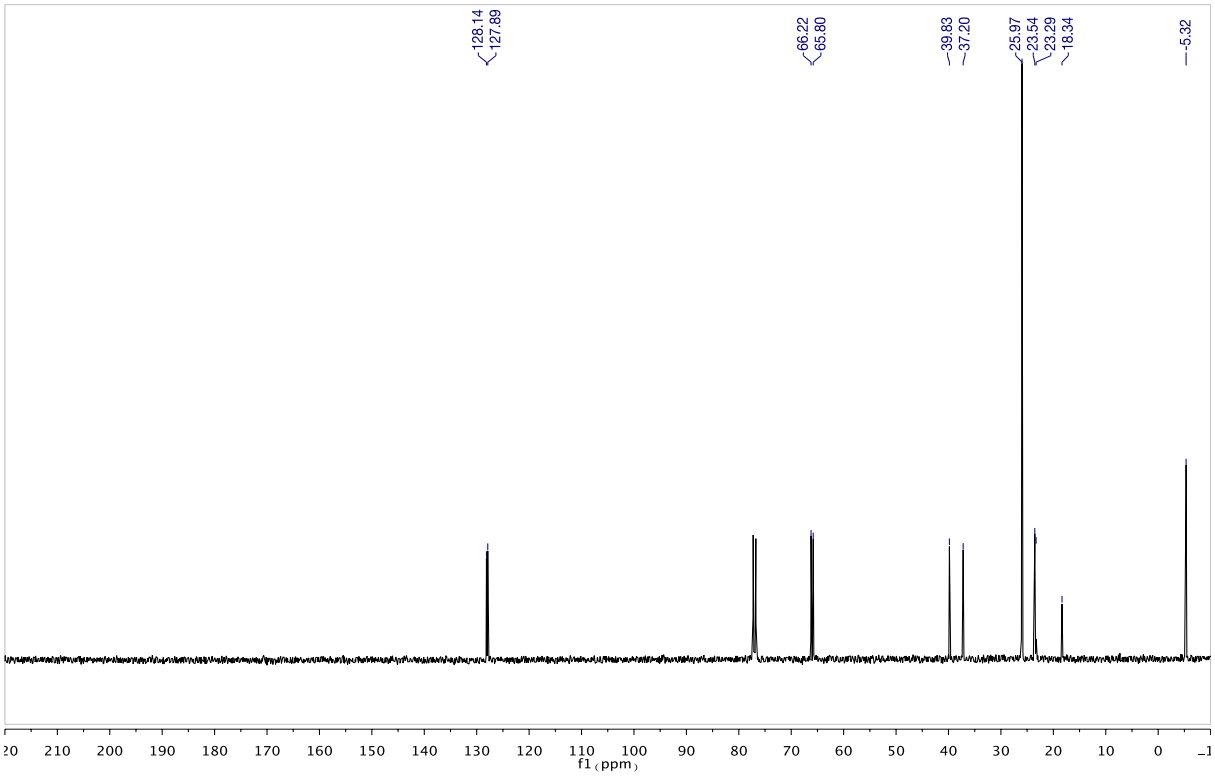
128.14
127.89
66.22
65.80
39.83
37.20
25.97
23.54
23.29
18.34
-5.32
f1 (ppm)

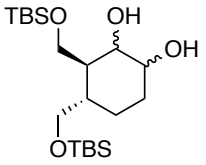
TBSO
OH
OH
OTBS

3-103

1.00
1.01
1.94
2.08
0.99
1.01
1.04
2.07
18.02
6.91
5.89
f1 (ppm)

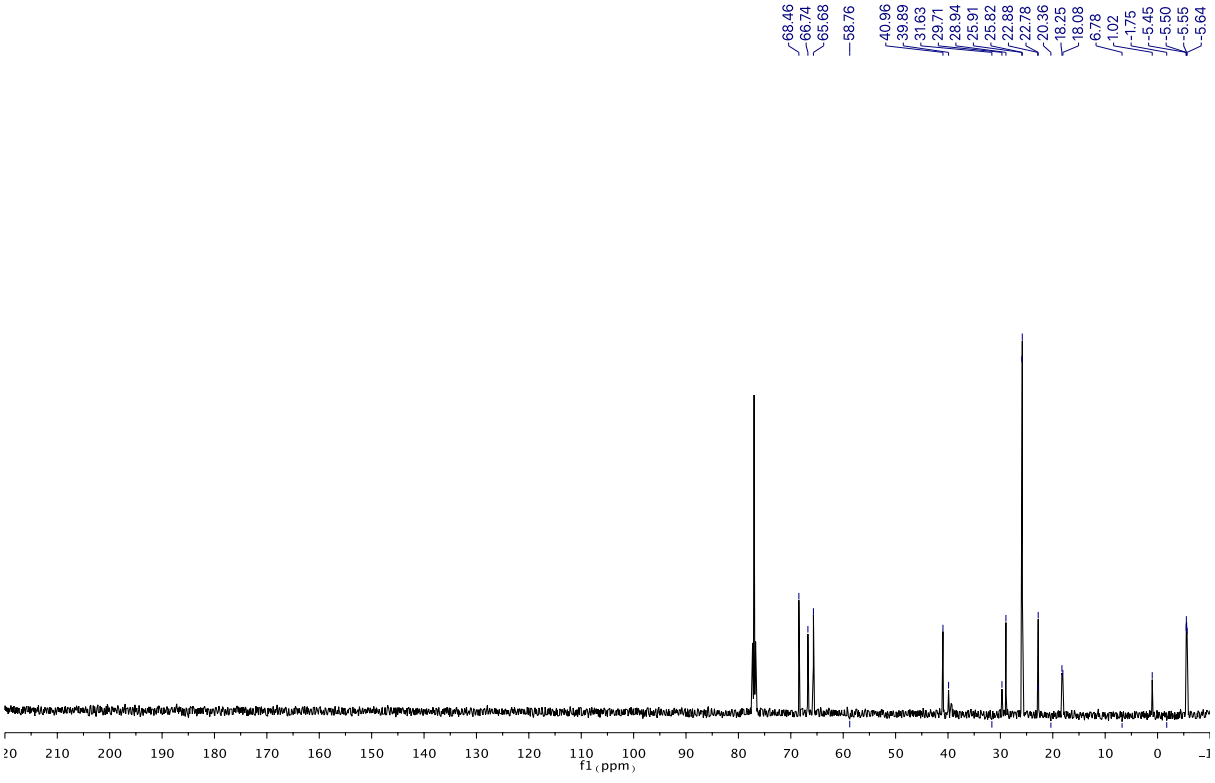
68.46
66.74
65.68
58.76
40.96
39.89
31.63
29.71
28.94
25.91
25.82
22.88
22.78
20.36
18.25
18.08
6.78
1.02
-1.75
-5.45
-5.50
-5.55
-5.64
f1 (ppm)

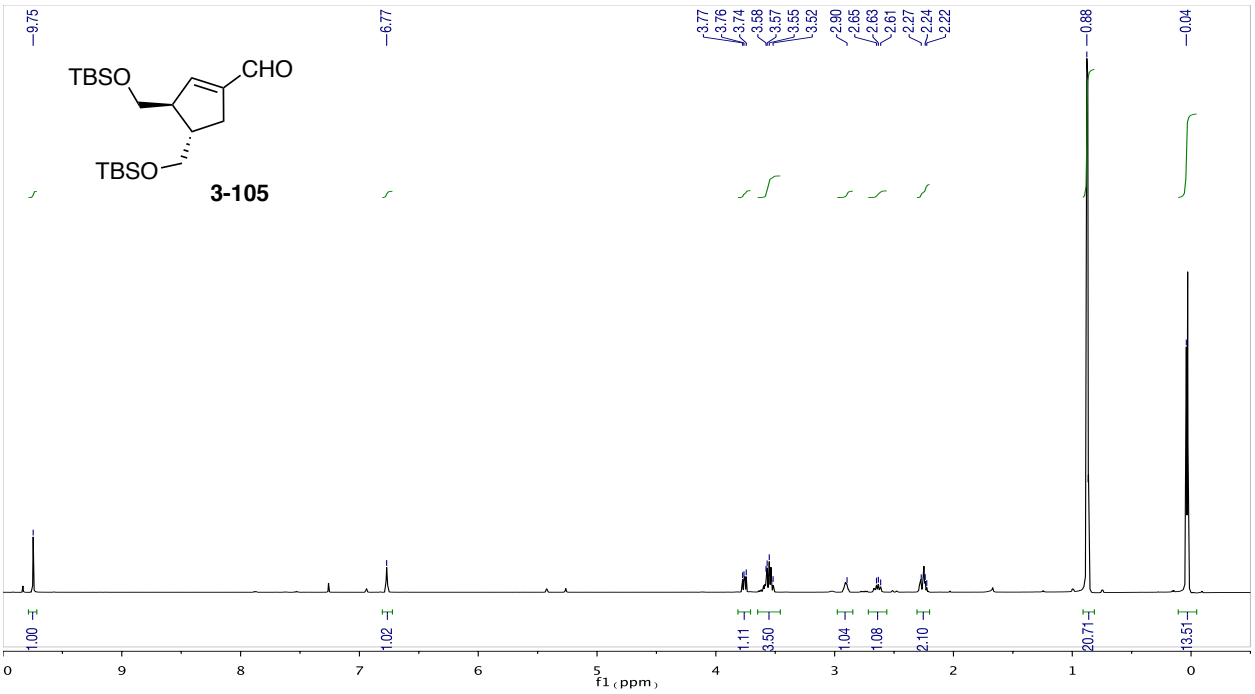
9.75
6.77
3.77
3.76
3.74
3.58
3.57
3.55
3.52
2.90
2.65
2.63
2.61
2.27
2.24
2.22
0.88
0.04
TBSO
CHO
TBSO
3-105
1.00
1.02
1.11
3.50
1.04
1.08
2.10
20.71
13.51
f1 (ppm)

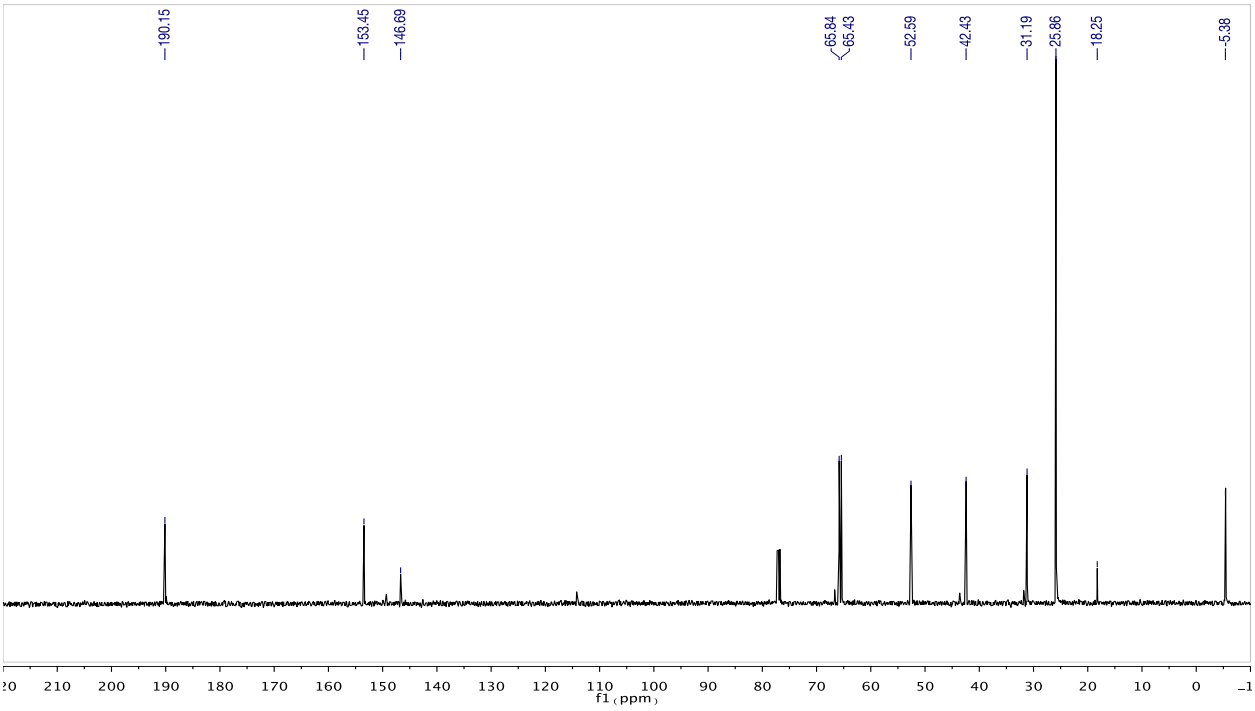
190.15
153.45
146.69
65.84
65.43
52.59
42.43
31.19
25.86
18.25
-5.38
f1 (ppm)

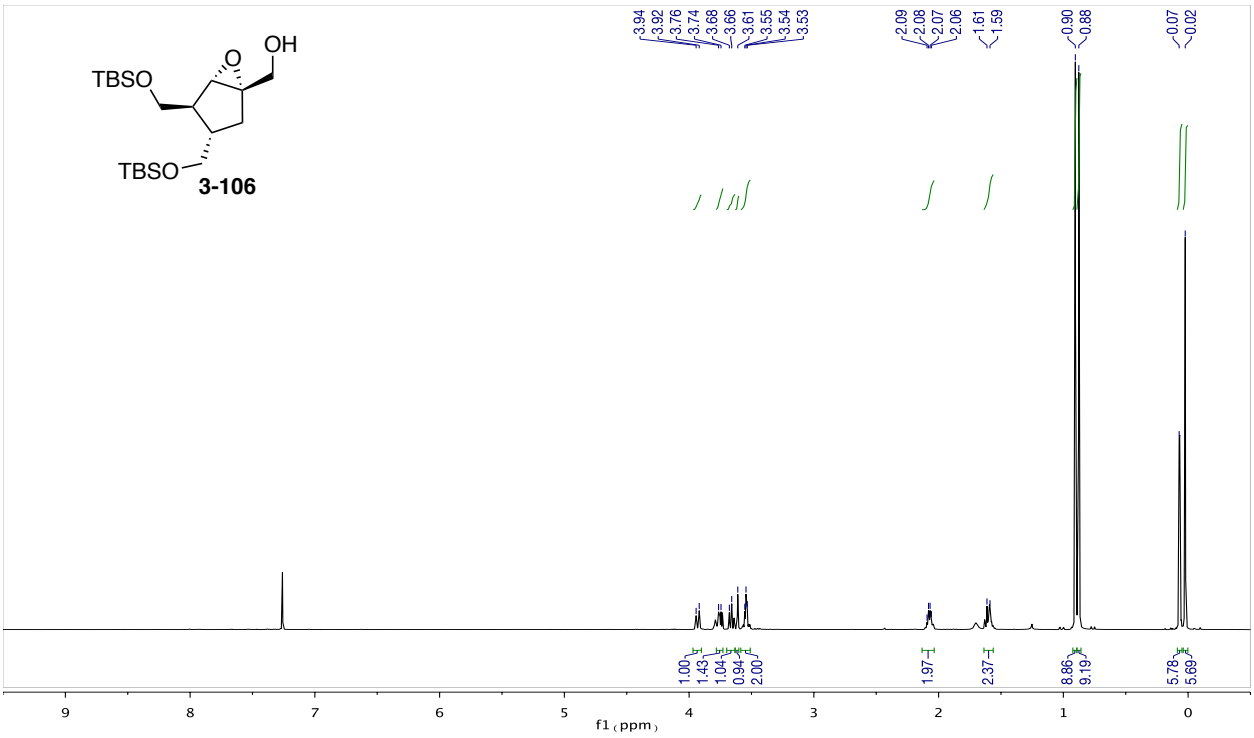
TBSO
OH
O
TBSO
3-106
3.94
3.92
3.76
3.74
3.68
3.66
3.61
3.55
3.54
3.53
2.09
2.08
2.07
2.06
1.61
1.59
0.90
0.88
0.07
0.02
1.00
1.43
1.04
0.94
2.00
1.97
2.37
8.86
9.19
5.78
5.69
f1 (ppm)

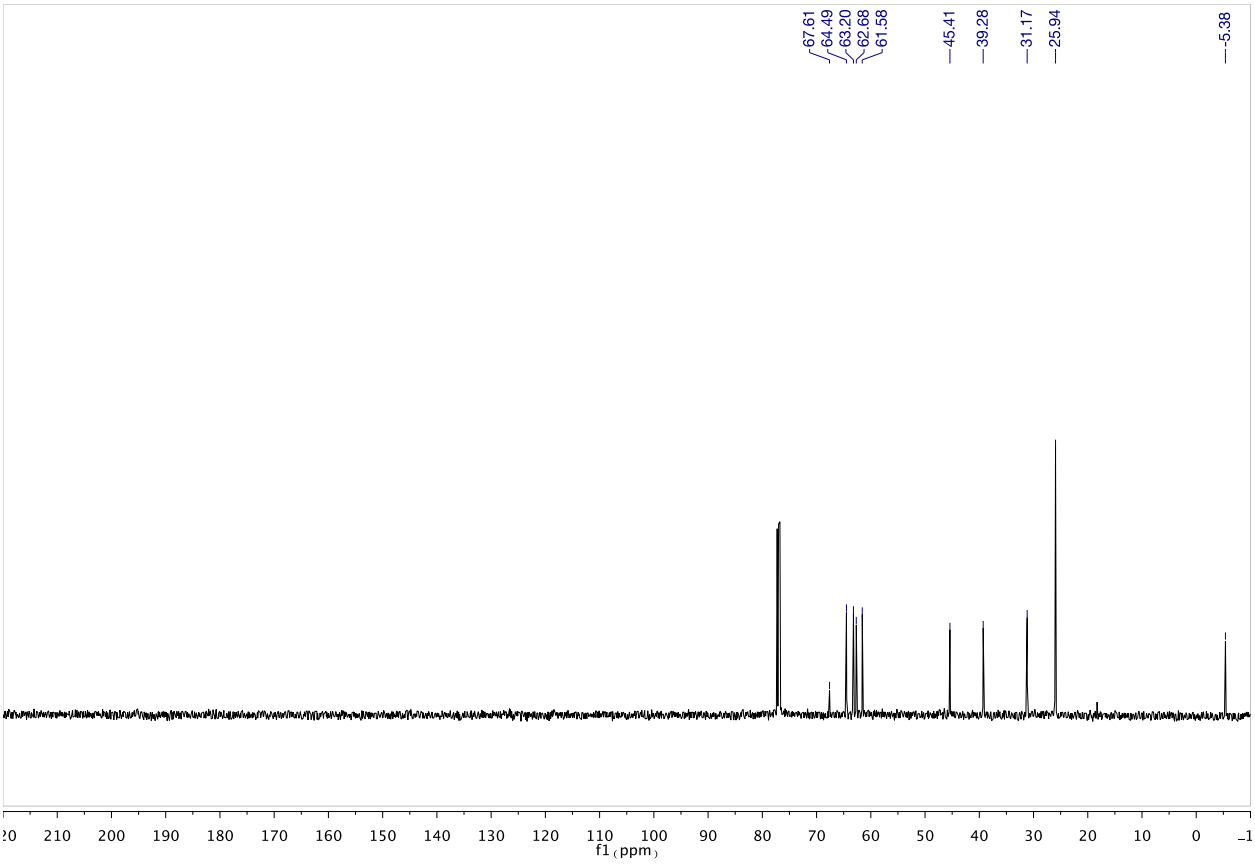
67.61
64.49
63.20
62.68
61.58
45.41
39.28
31.17
25.94
-5.38
f1 (ppm)

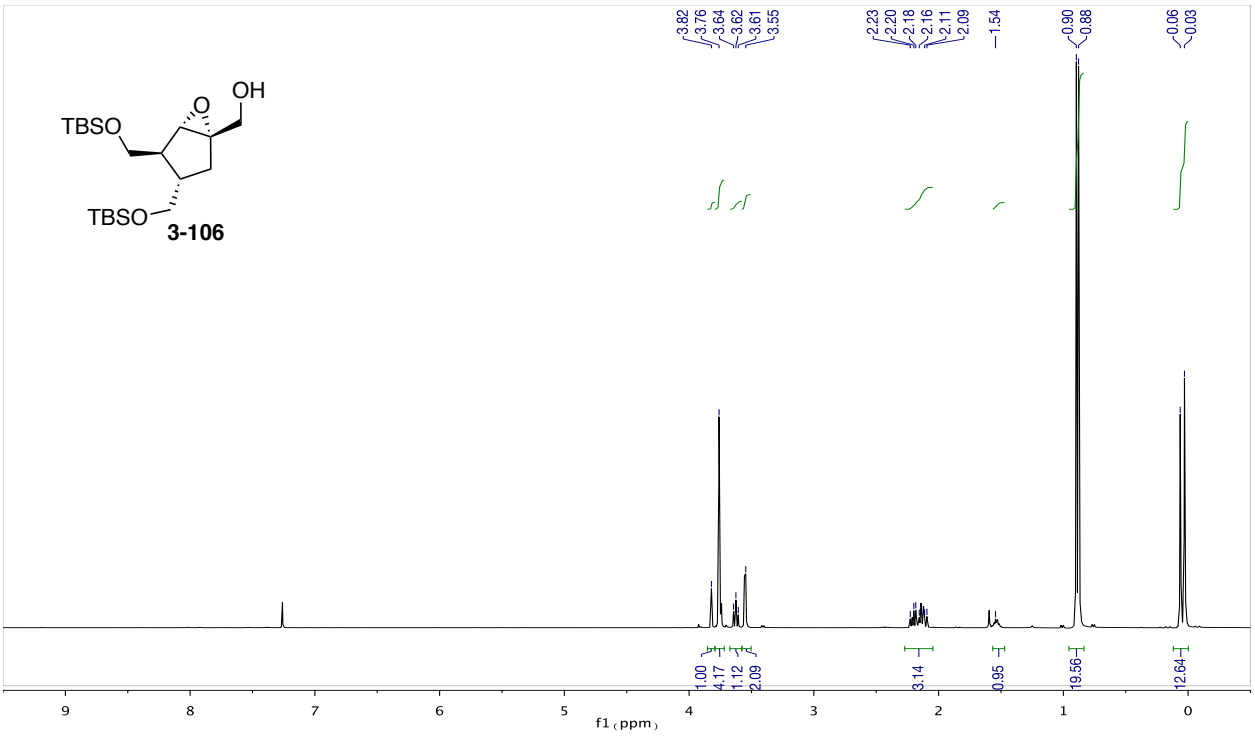
TBSO
O
OH
TBSO
3-106
3.82
3.76
3.64
3.62
3.61
3.55
2.23
2.20
2.18
2.16
2.11
2.09
1.54
0.90
0.88
0.06
0.03
1.00
4.17
1.12
2.09
3.14
0.95
19.56
12.64
f1 (ppm)

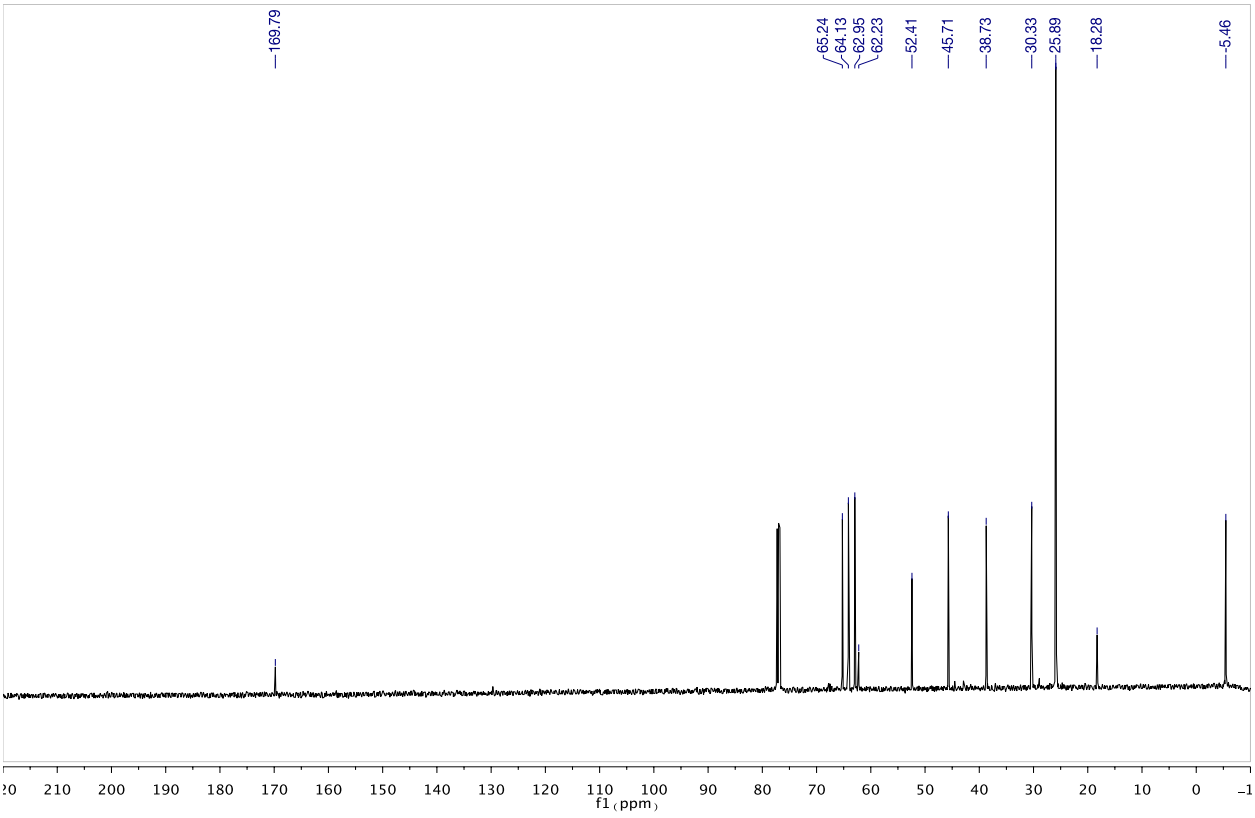
169.79
65.24
64.13
62.95
62.23
52.41
45.71
38.73
30.33
25.89
18.28
-5.46
f1 (ppm)

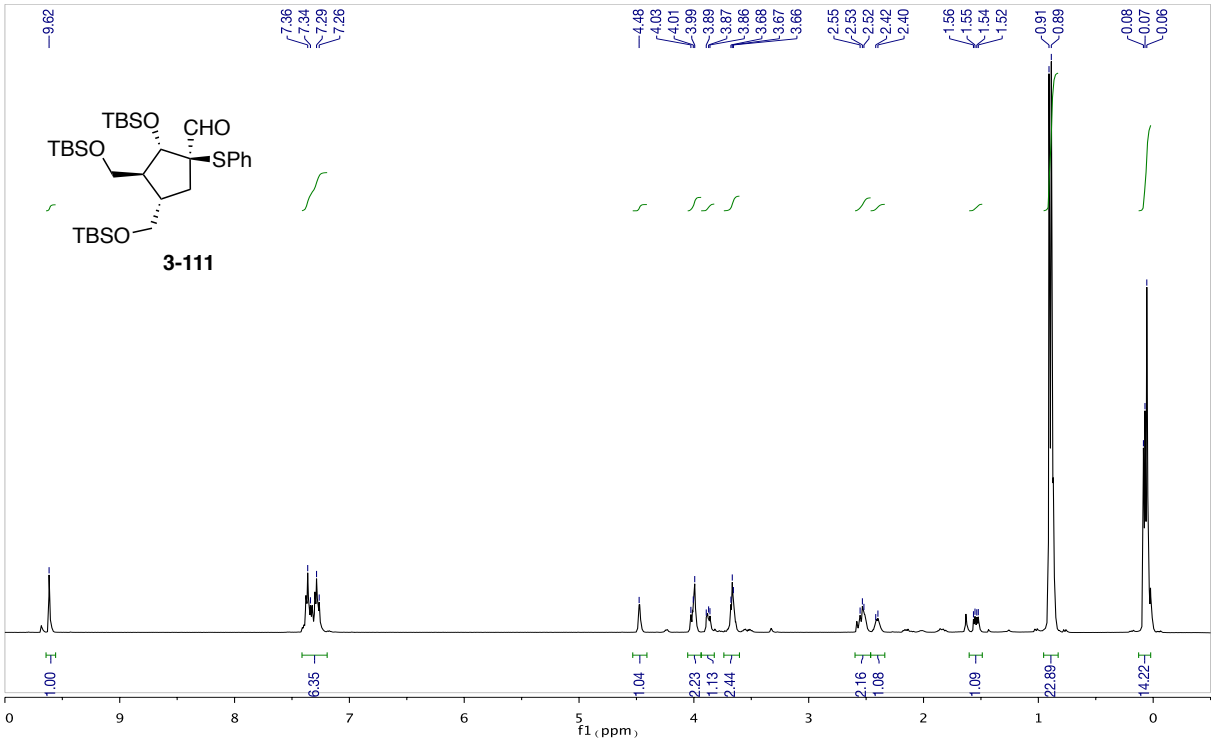
TBSO
CHO
TBSO
SPh
TBSO
3-111
f1 (ppm)

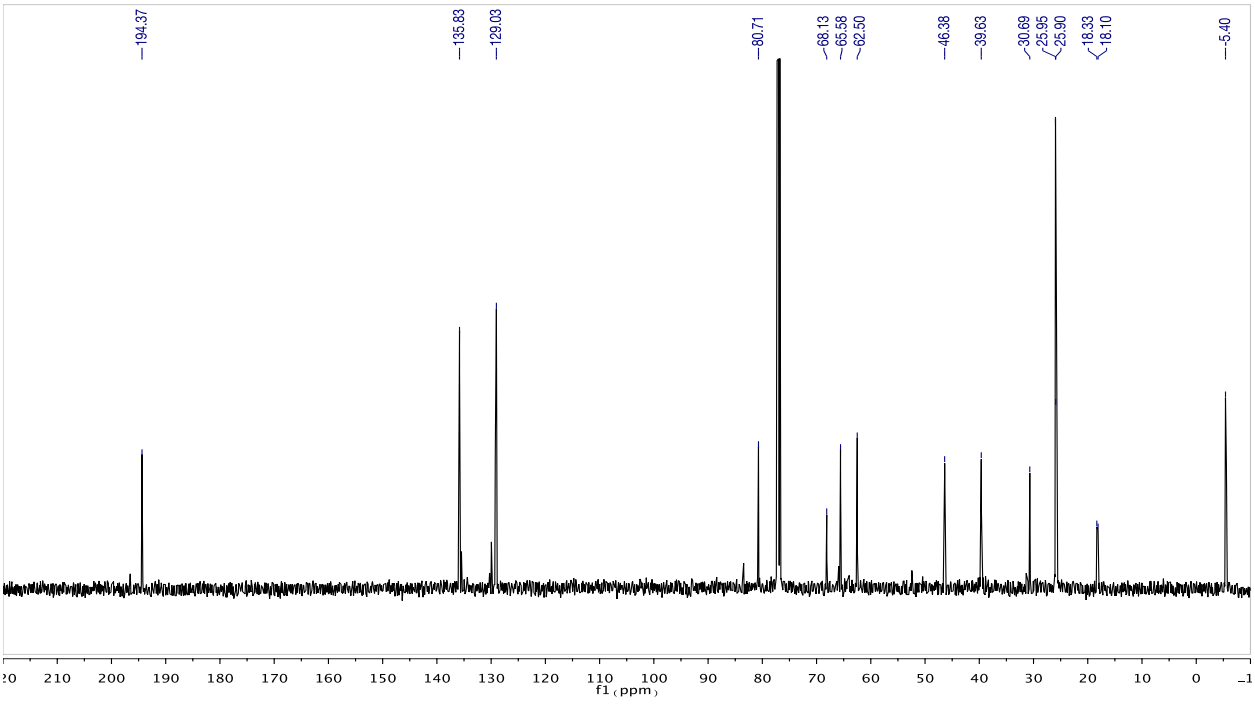
f1 (ppm)

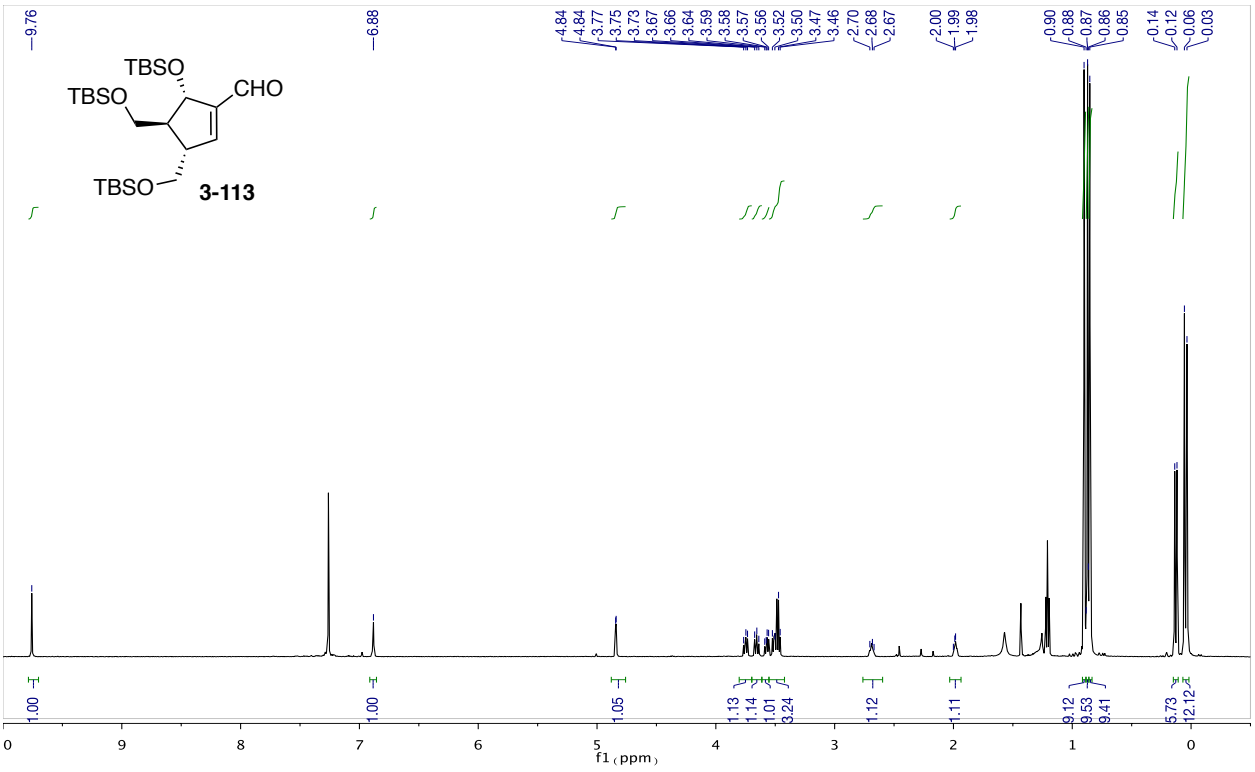
TBSO
TBSO
CHO
TBSO
3-113
f1 (ppm)

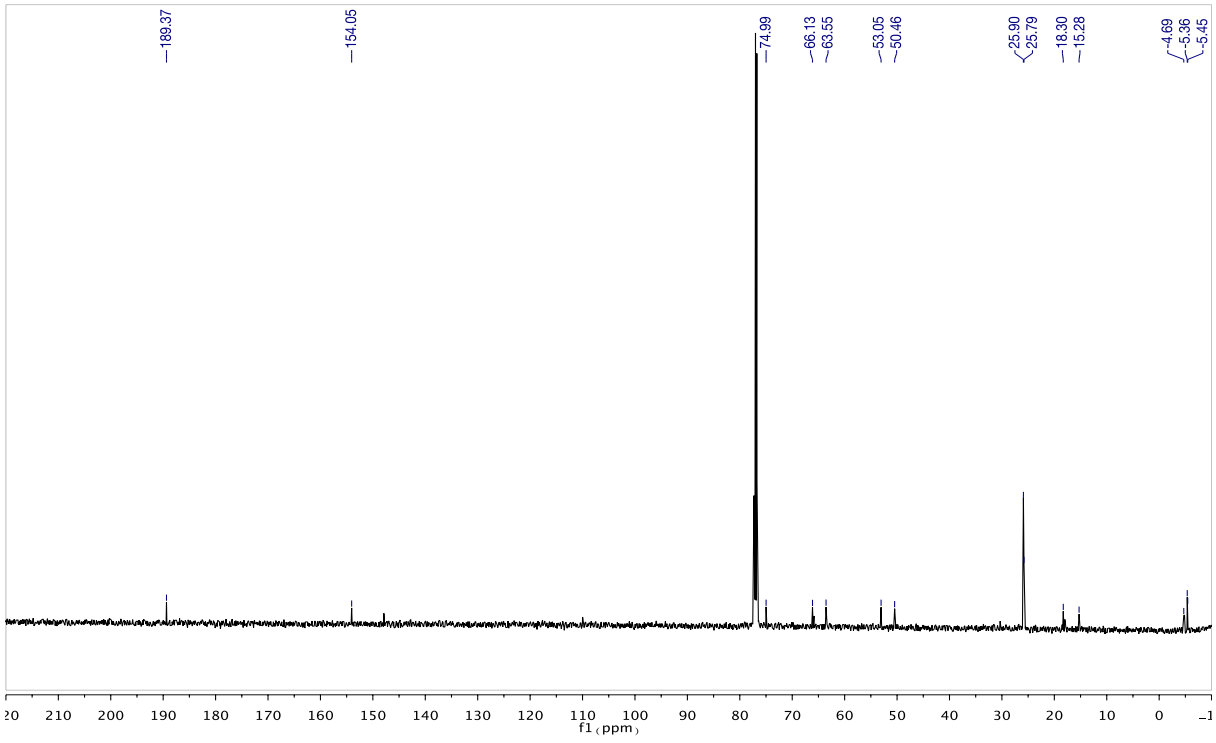
f1 (ppm)

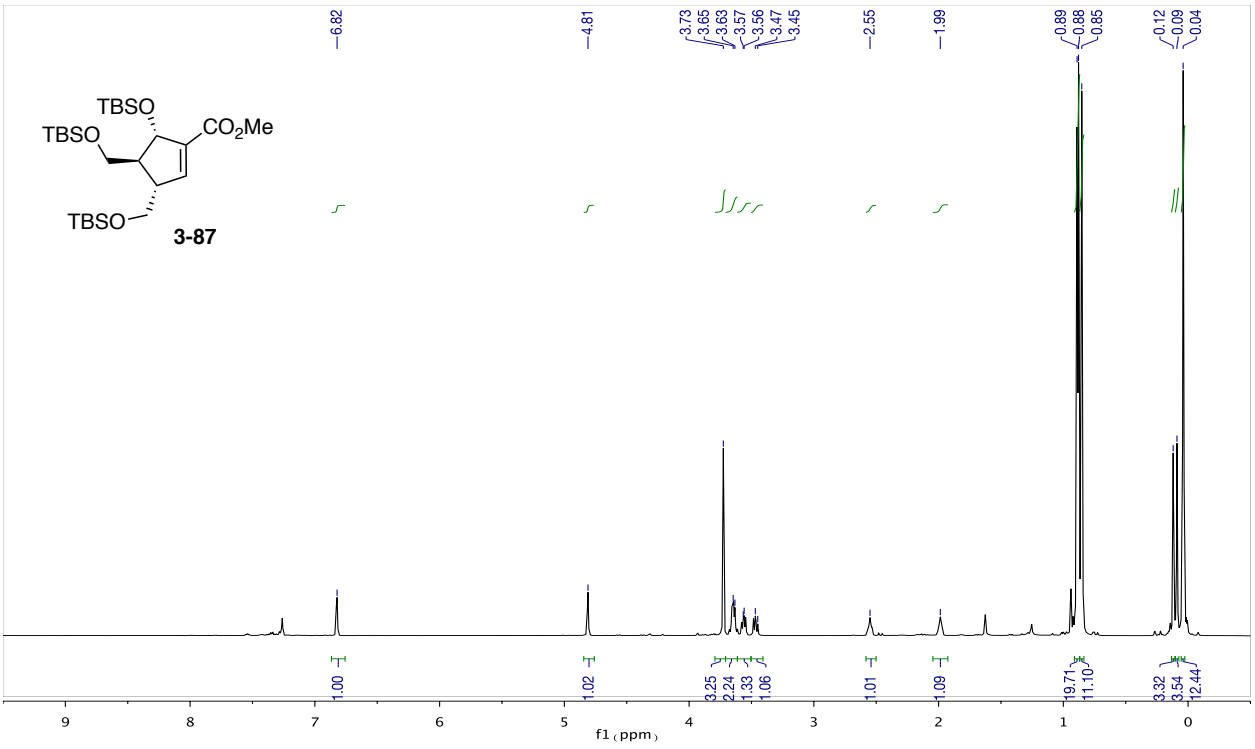
TBSO
TBSO
CO2Me
TBSO
3-87
6.82
4.81
3.73
3.65
3.63
3.57
3.56
3.47
3.45
2.55
1.99
0.89
0.88
0.85
0.12
0.09
0.04
1.00
1.02
3.25
2.24
1.33
1.06
1.01
1.09
19.71
11.10
3.32
3.54
12.44
f1 (ppm)

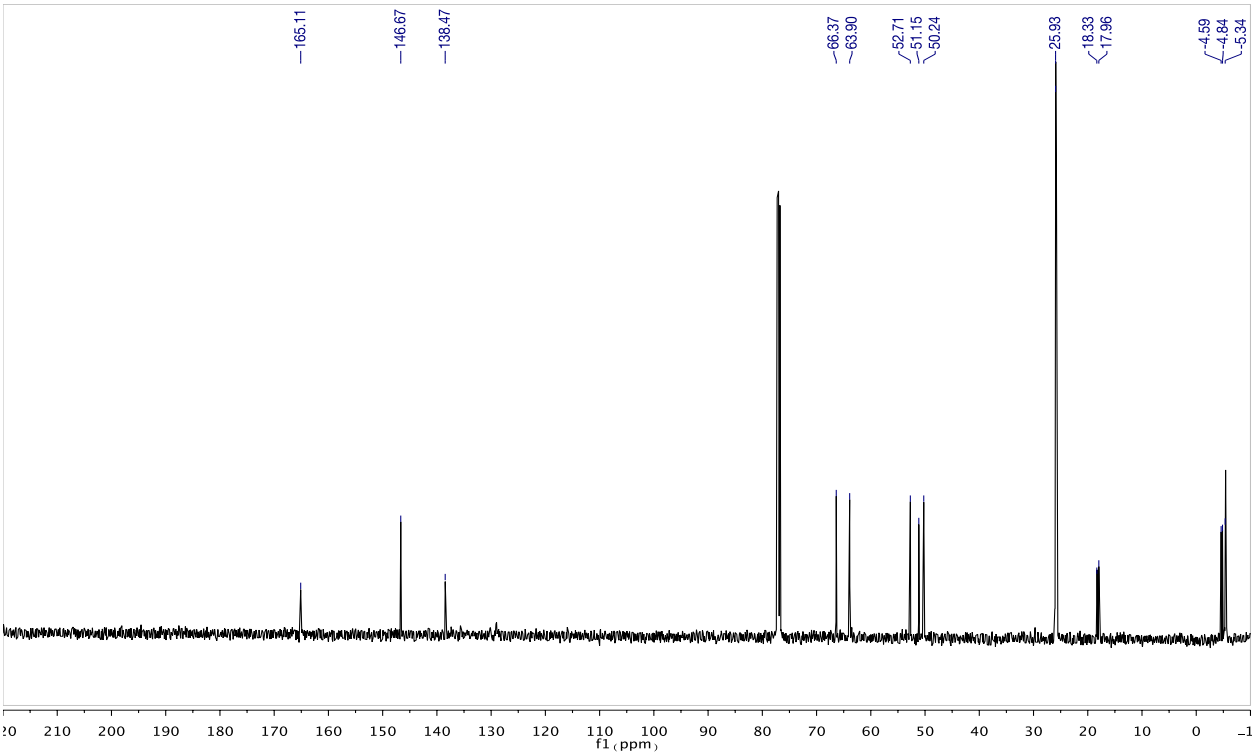
165.11
146.67
138.47
66.37
63.90
52.71
51.15
50.24
25.93
18.33
17.96
-4.59
-4.84
-5.34
f1 (ppm)

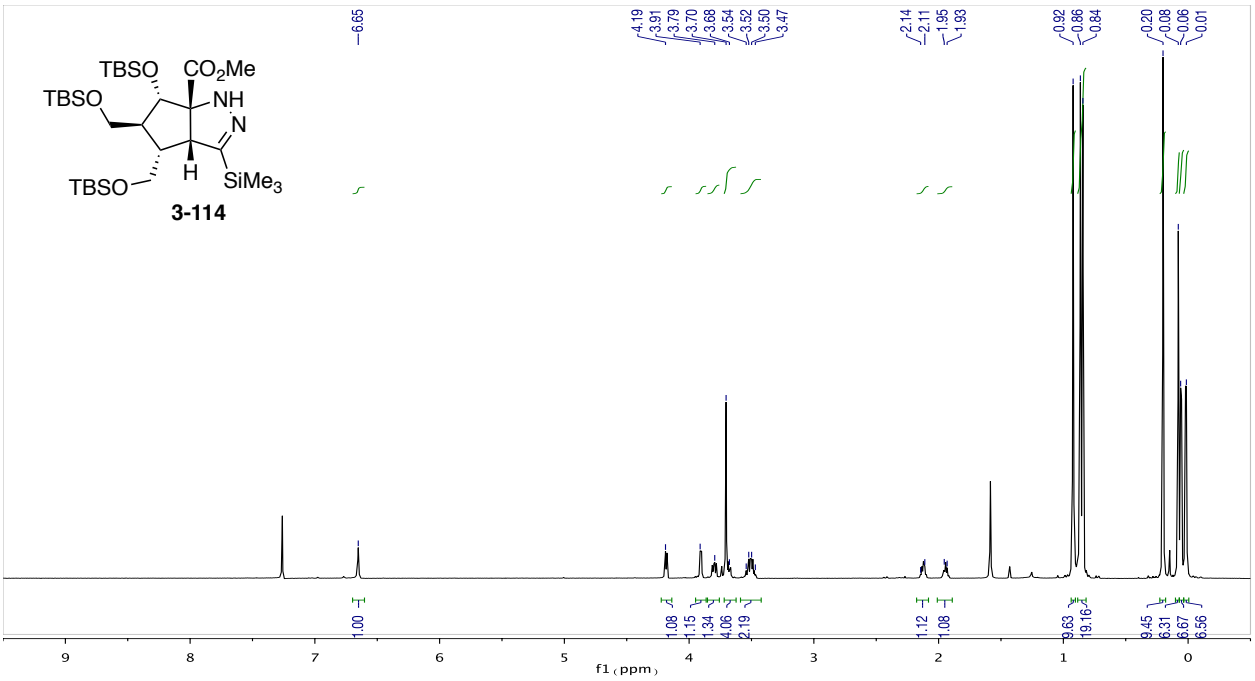
TBSO
CO2Me
TBSO
NH
N
H
SiMe3
TBSO
3-114
6.65
4.19
3.91
3.79
3.70
3.68
3.54
3.52
3.50
3.47
2.14
2.11
1.95
1.93
0.92
0.86
0.84
0.20
0.08
0.06
0.01
1.00
1.08
1.15
1.34
4.06
2.19
1.12
1.08
9.63
19.16
9.45
6.31
6.67
6.56
f1 (ppm)

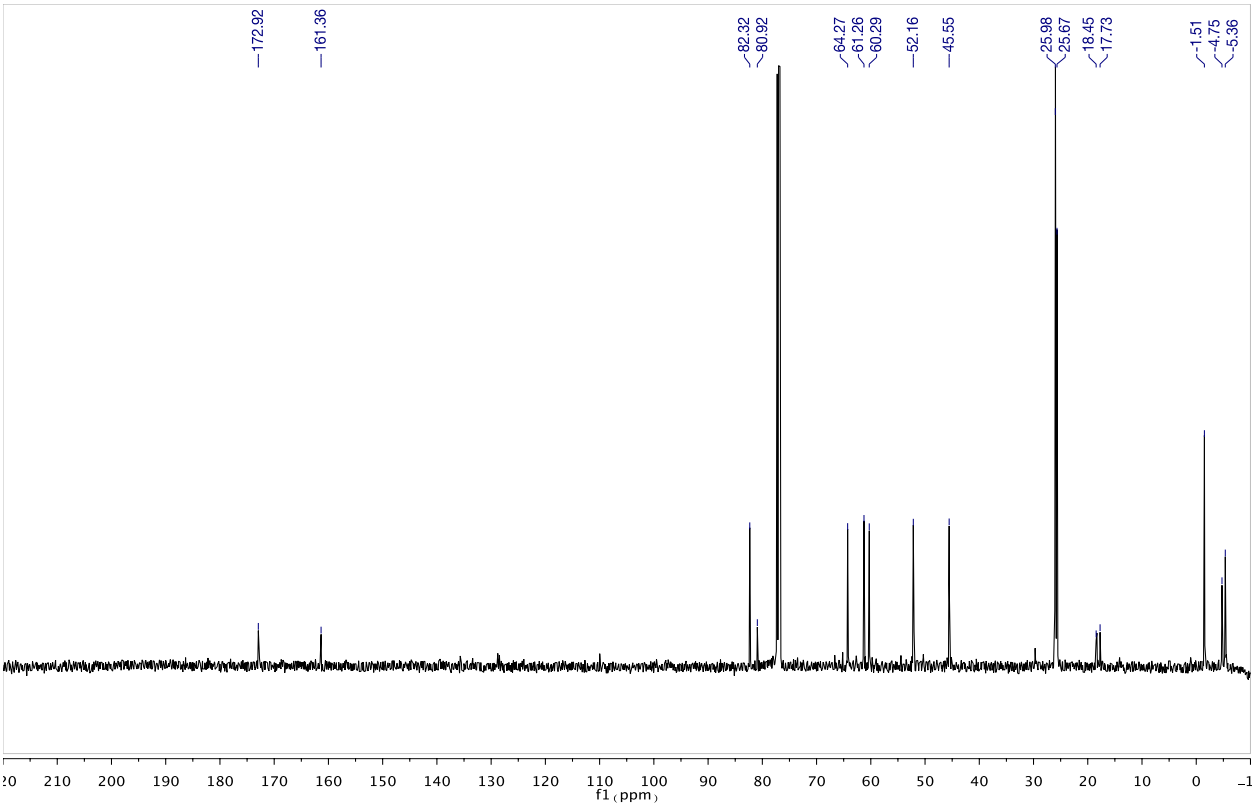
172.92
161.36
82.32
80.92
64.27
61.26
60.29
52.16
45.55
25.98
25.67
18.45
17.73
-1.51
-4.75
-5.36
f1 (ppm)

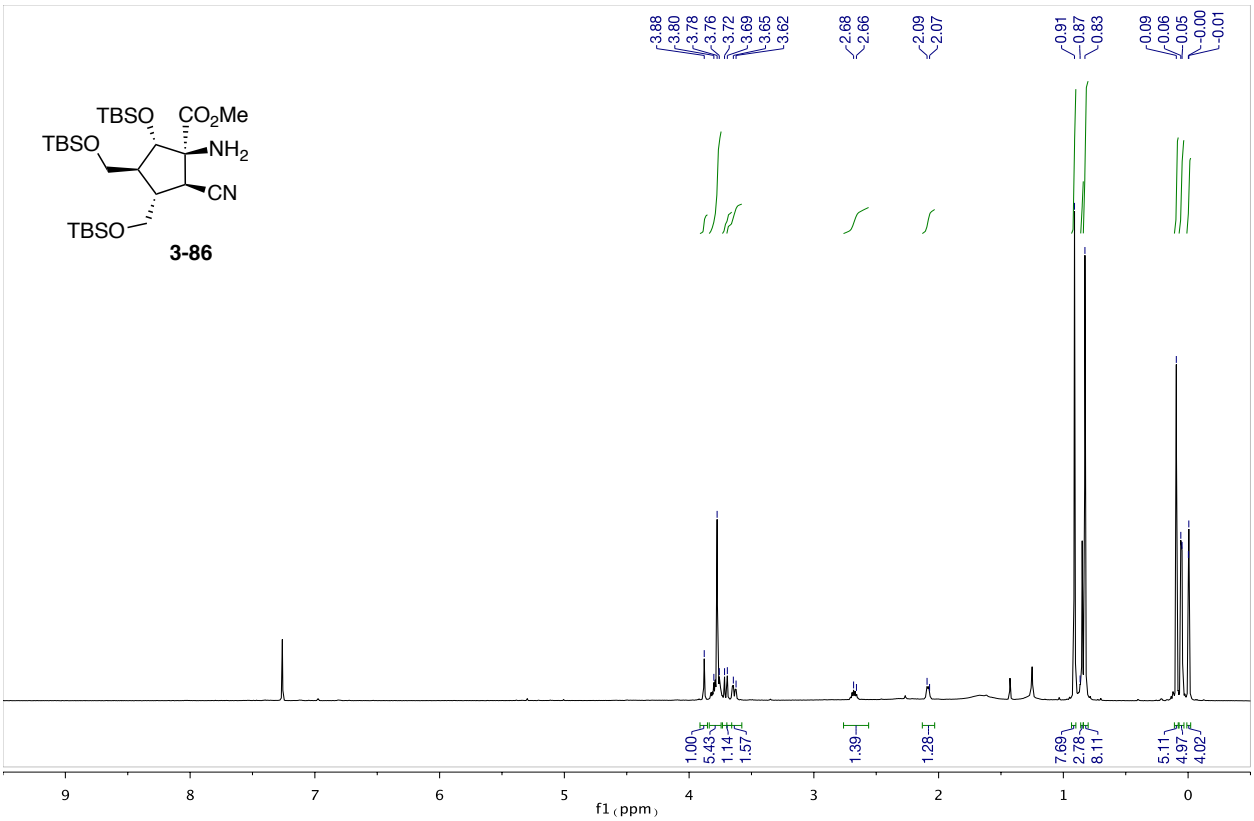
TBSO
CO2Me
TBSO
NH2
CN
TBSO
3-86
3.88
3.80
3.78
3.76
3.72
3.69
3.65
3.62
2.68
2.66
2.09
2.07
0.91
0.87
0.83
0.09
0.06
0.05
-0.00
-0.01
1.00
5.43
1.14
1.57
1.39
1.28
7.69
2.78
8.11
5.11
4.97
4.02
f1 (ppm)

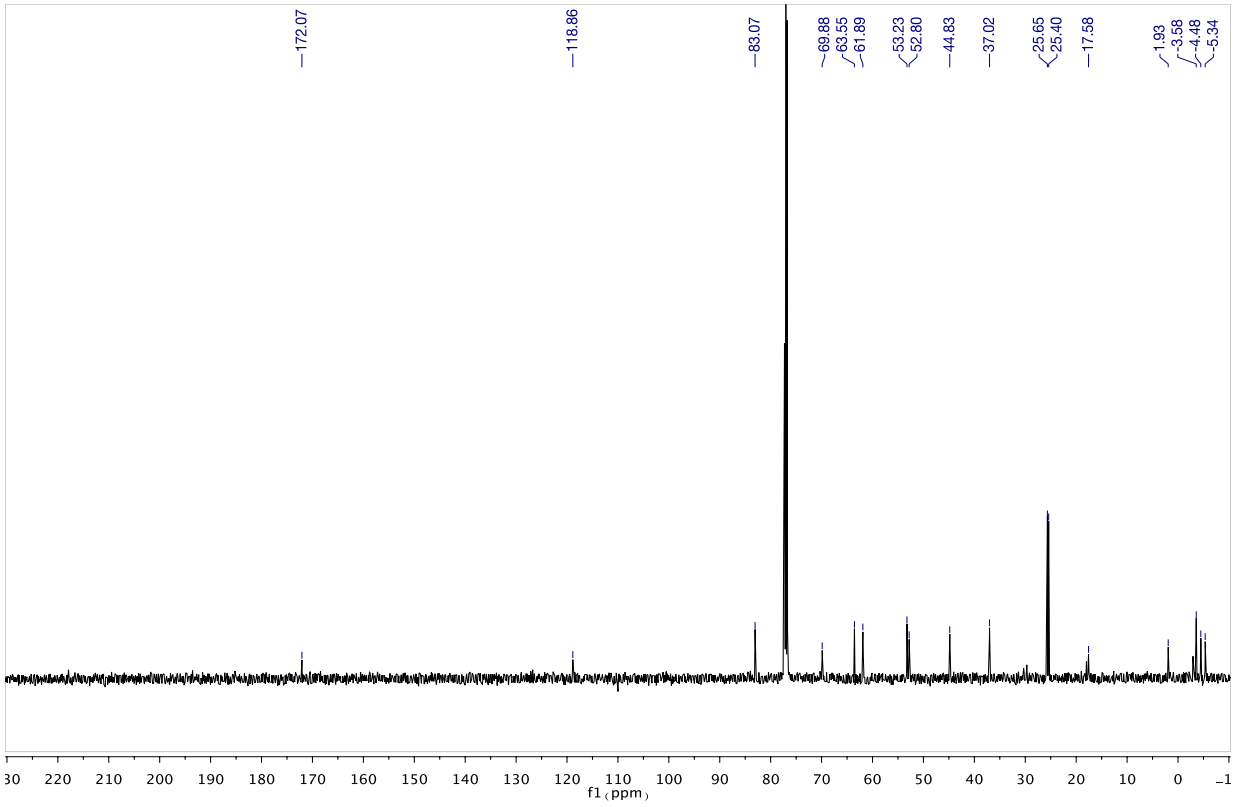
172.07
118.86
83.07
69.88
63.55
61.89
53.23
52.80
44.83
37.02
25.65
25.40
17.58
1.93
-3.58
-4.48
-5.34
f1 (ppm)

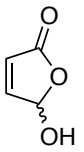

3-122

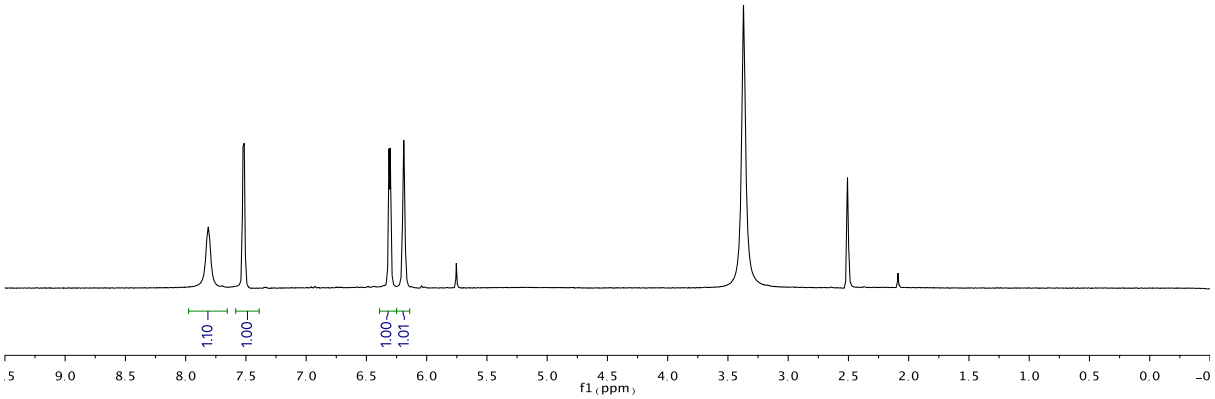

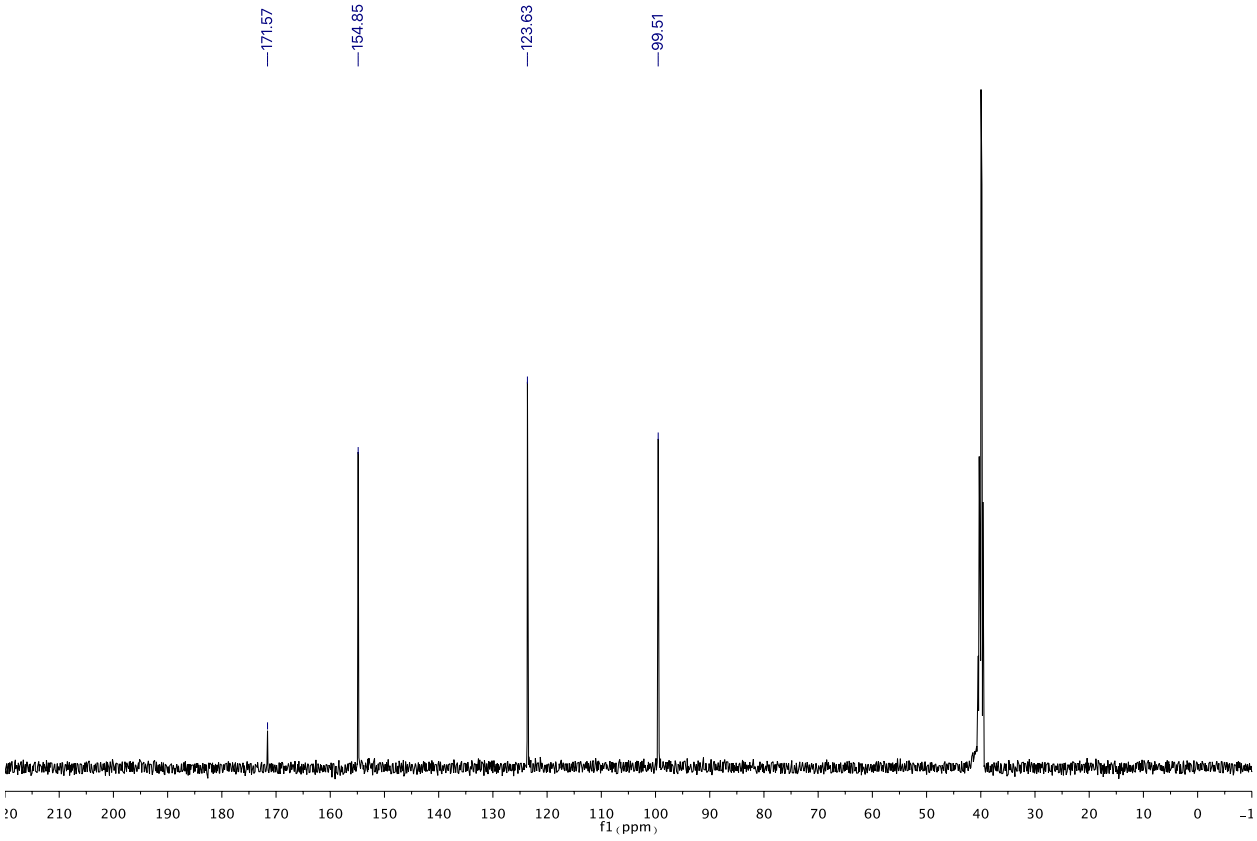

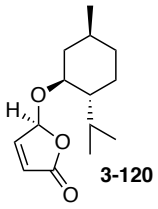
H
O
O
O
O

3-120

1.00
0.98
0.97
0.99
2.13
2.26
1.10
1.14
6.04
3.94
3.30
f1 (ppm)

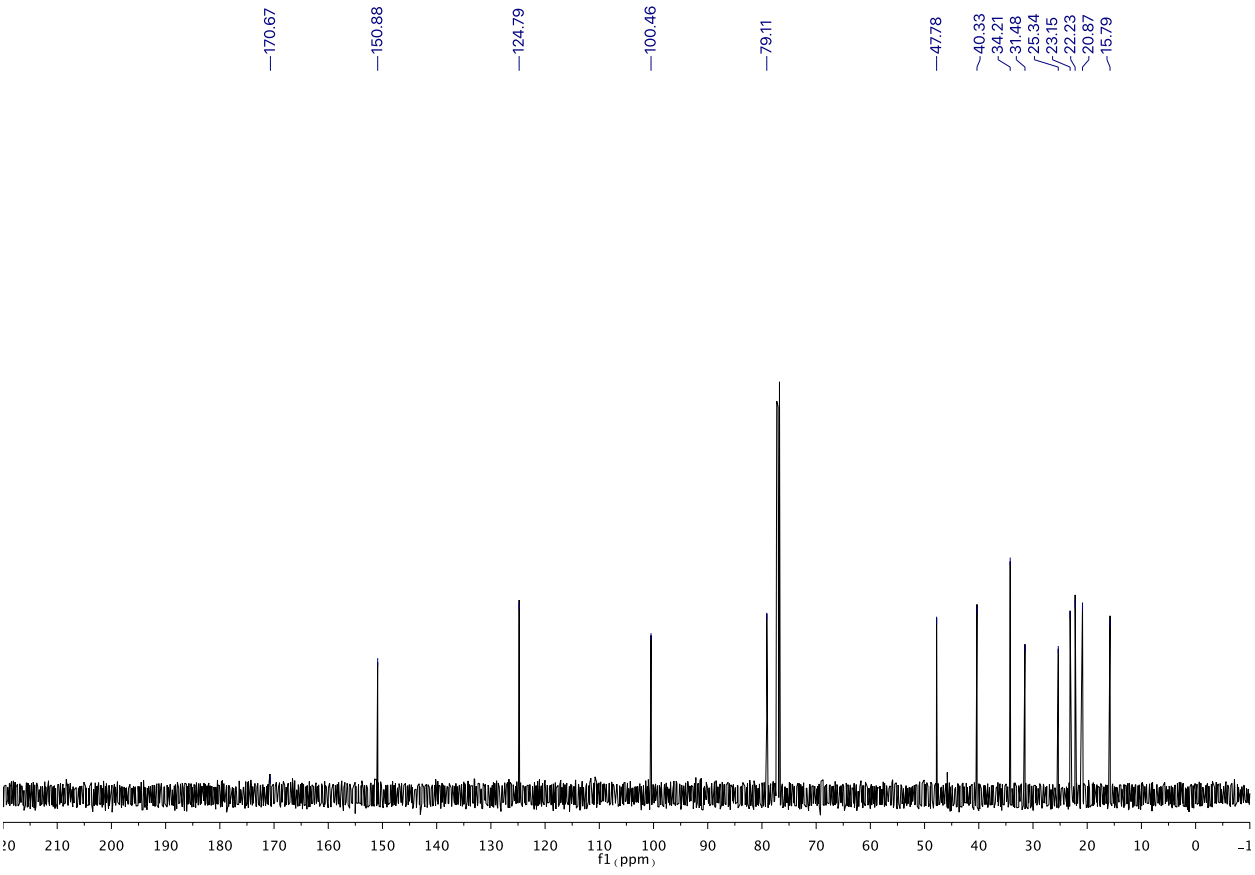
170.67
150.88
124.79
100.46
79.11
47.78
40.33
34.21
31.48
25.34
23.15
22.23
20.87
15.79
f1 (ppm)

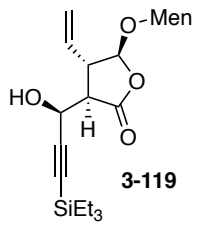
O-Men
HO
O
H
O
SiEt3

3-119

1.00
3.22
1.02
0.95
1.00
1.00
1.07
1.25
1.75
2.41
1.36
20.62
3.03
6.92
f1 (ppm)


172.21
134.86
117.54
103.49
103.05
92.14
78.60
63.02
53.17
47.70
47.66
40.05
34.29
31.40
25.21
23.06
22.26
20.95
15.75
6.71
4.74
-0.47

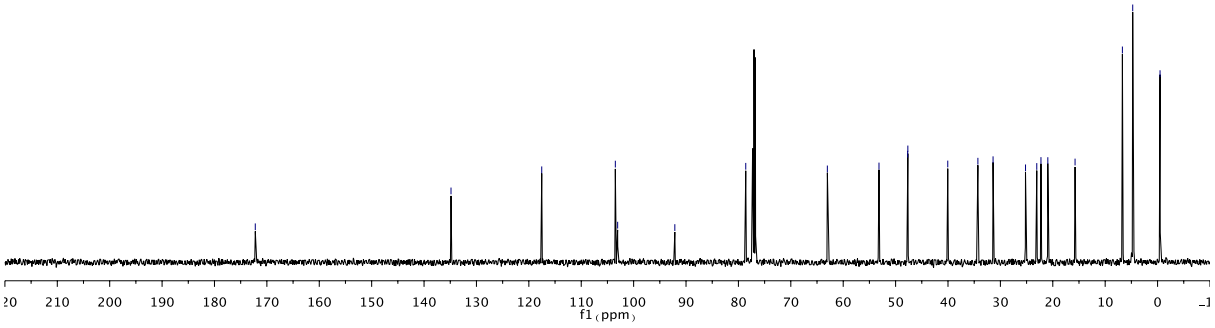
f1 (ppm)

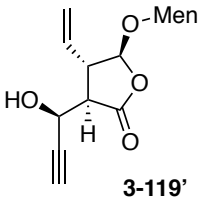
O-Men
HO
O
H
O

3-119'

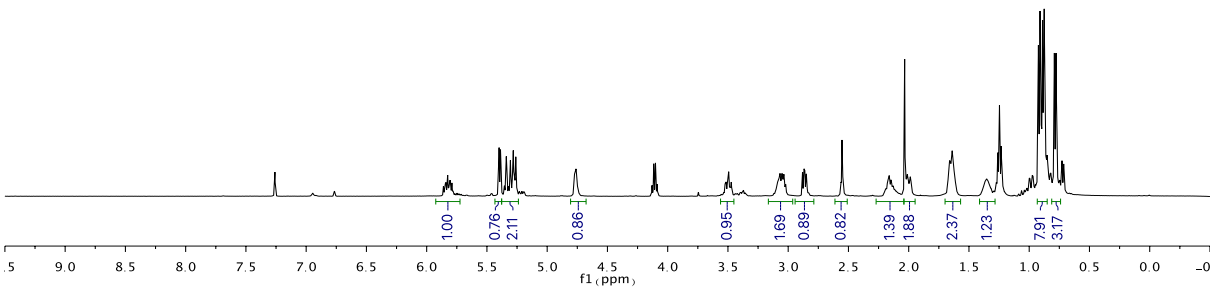
1.00
0.76
2.11
0.86
0.95
1.69
0.89
0.82
1.39
1.88
2.37
1.23
7.91
3.17
f1 (ppm)

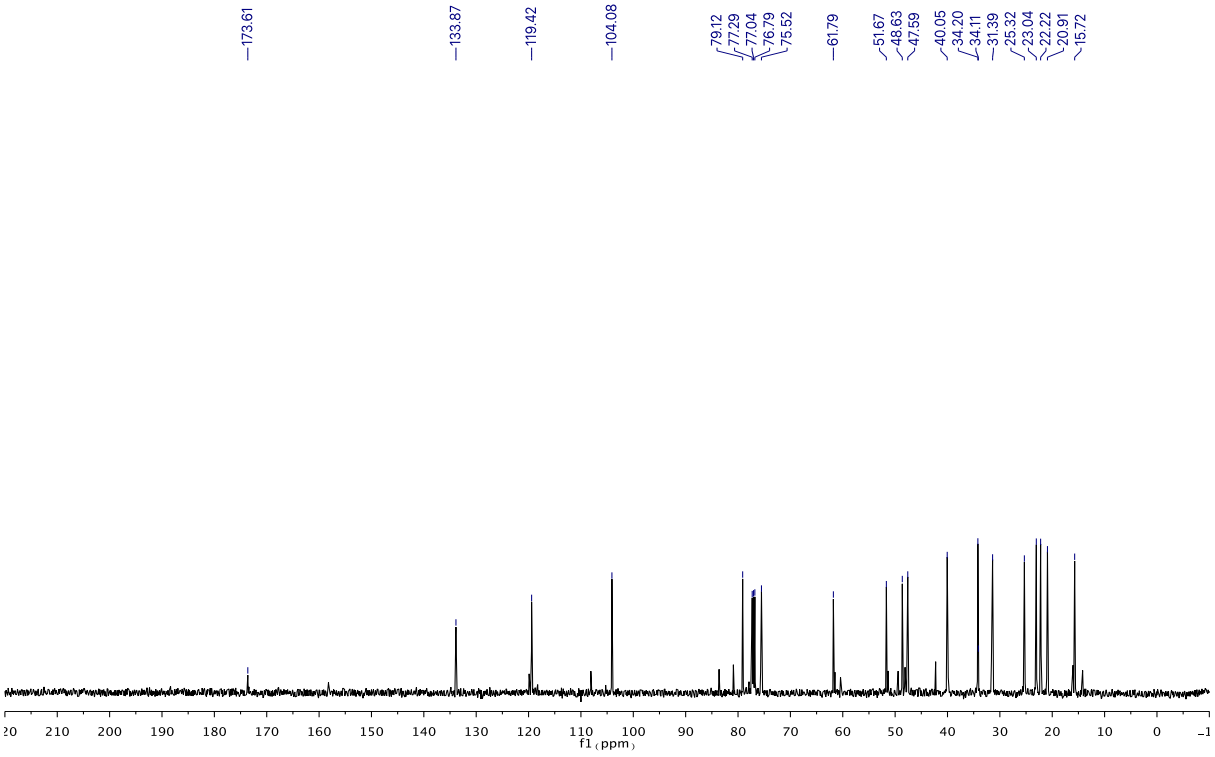
173.61
133.87
119.42
104.08
79.12
77.29
77.04
76.79
75.52
61.79
51.67
48.63
47.59
40.05
34.20
34.11
31.39
25.32
23.04
22.22
20.91
15.72
f1 (ppm)

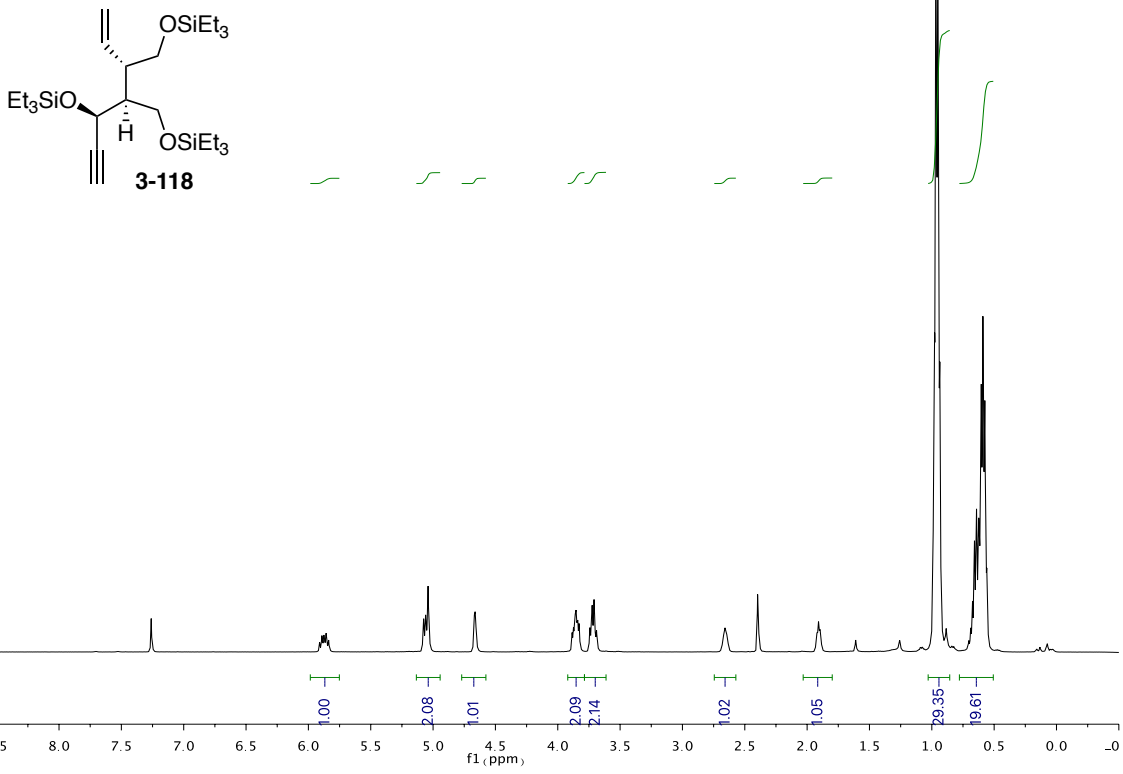
OSiEt3
Et3SiO
H
OSiEt3
3-118
1.00
2.08
1.01
2.09
2.14
1.02
1.05
29.35
19.61
f1 (ppm)

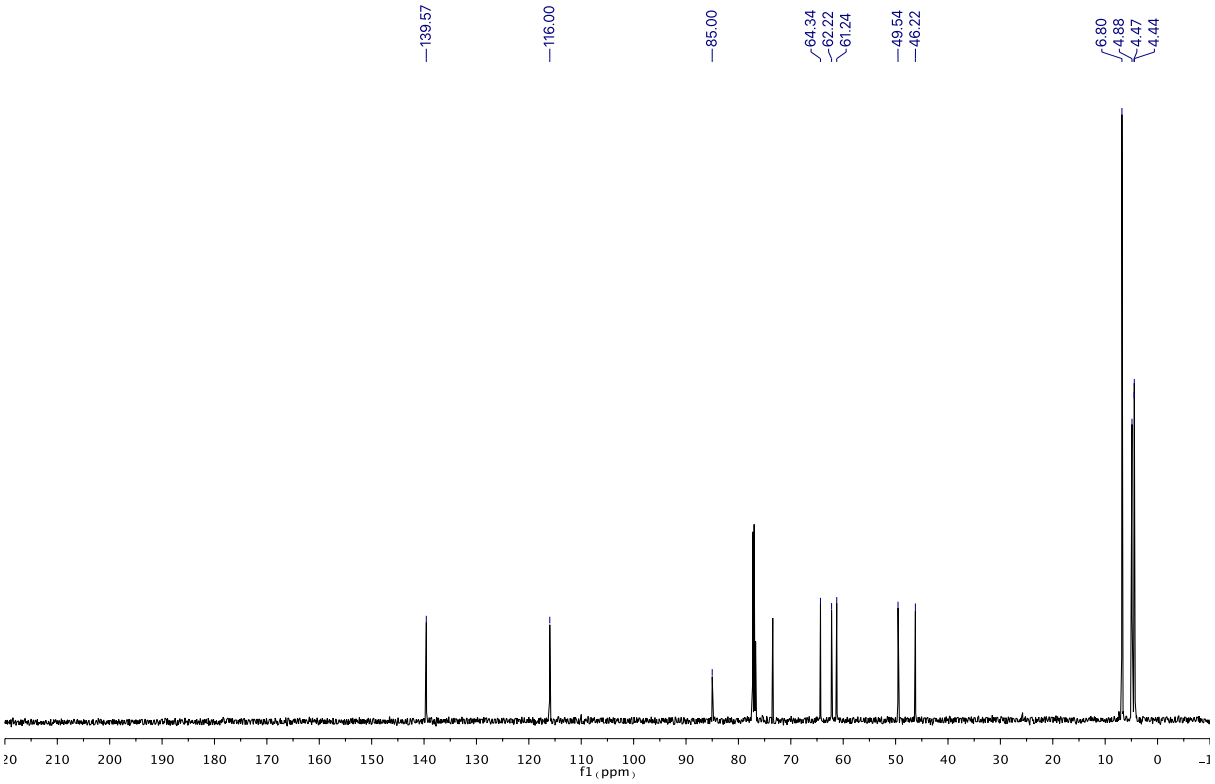
139.57
116.00
85.00
64.34
62.22
61.24
49.54
46.22
6.80
4.88
4.47
4.44
f1 (ppm)

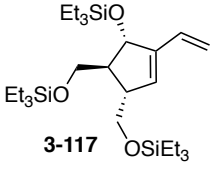
Et3SiO
Et3SiO
OSiEt3
3-117

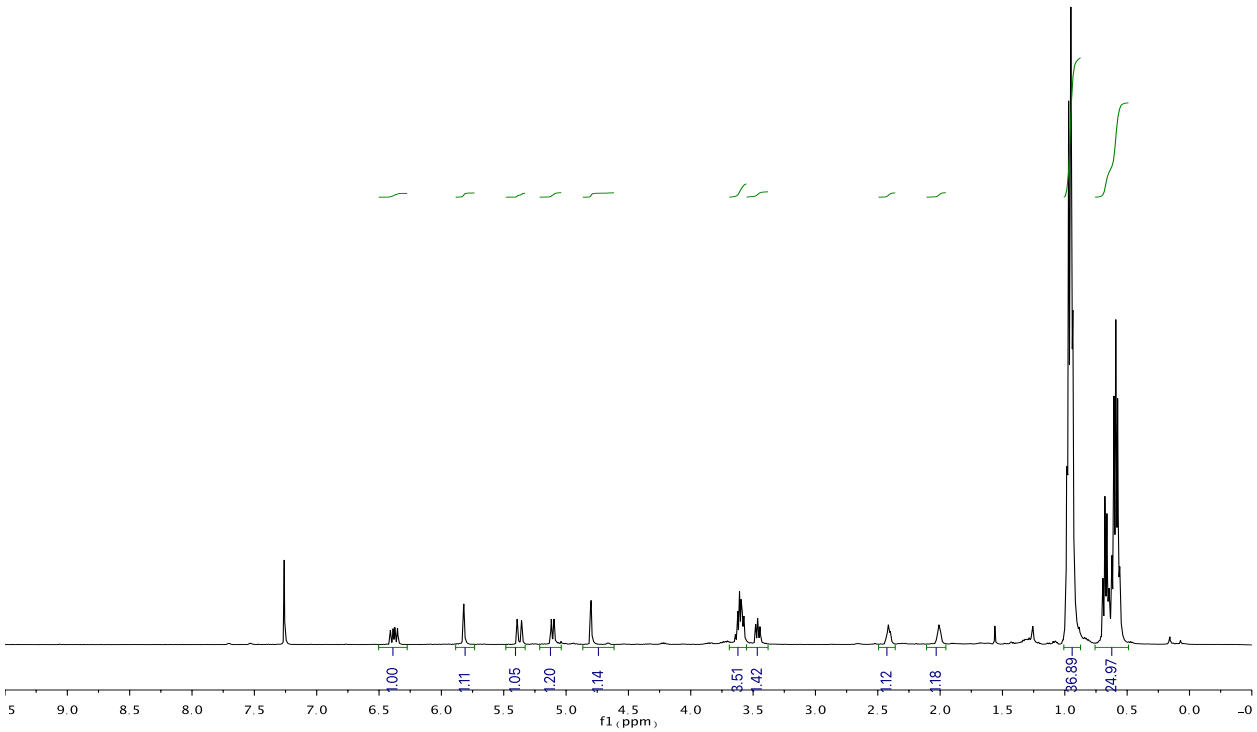
1.00
1.11
1.05
1.20
1.14
3.51
1.42
1.12
1.18
36.89
24.97
f1 (ppm)

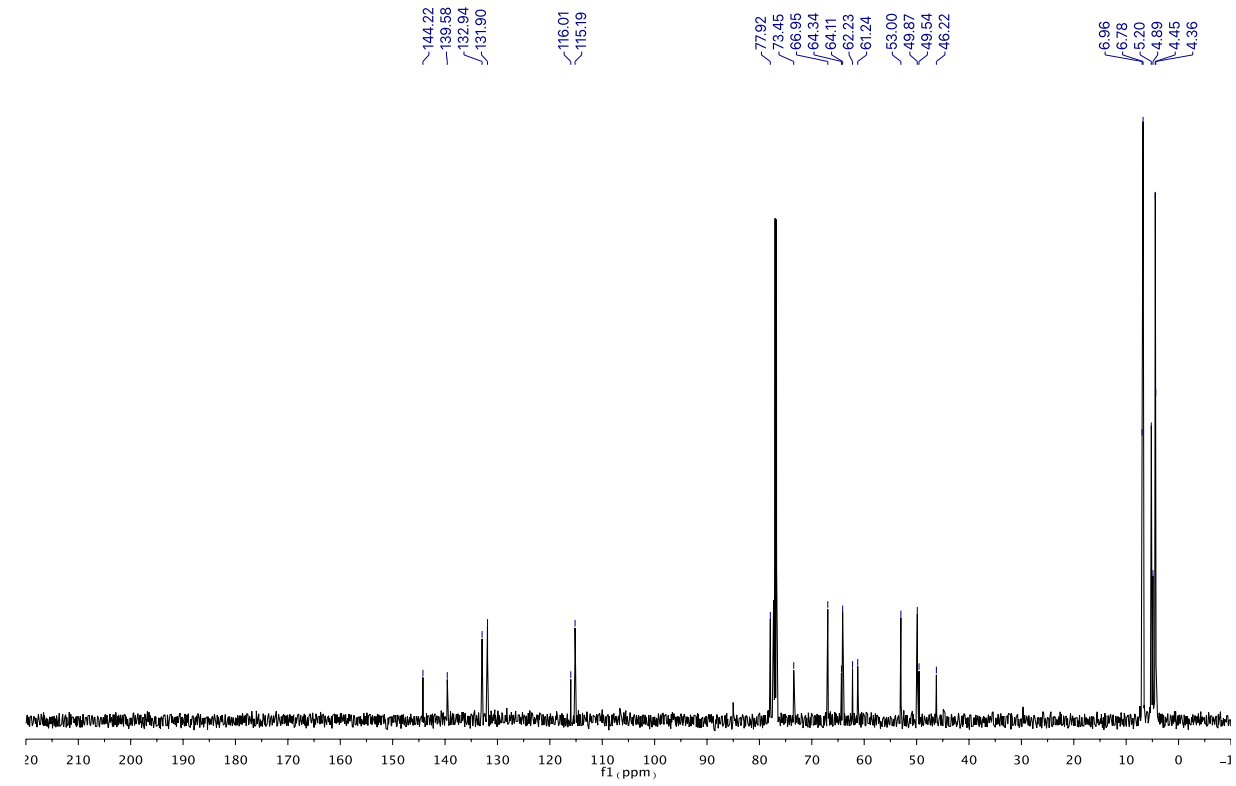
144.22
139.58
132.94
131.90
116.01
115.19
77.92
73.45
66.95
64.34
64.11
62.23
61.24
53.00
49.87
49.54
46.22
6.96
6.78
5.20
4.89
4.45
4.36
f1 (ppm)

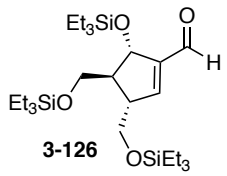
Et3SiO
O
H
Et3SiO
OSiEt3

3-126

1.00
1.04
1.06
1.09
1.06
2.30
1.05
1.08
27.39
18.90
f1 (ppm)

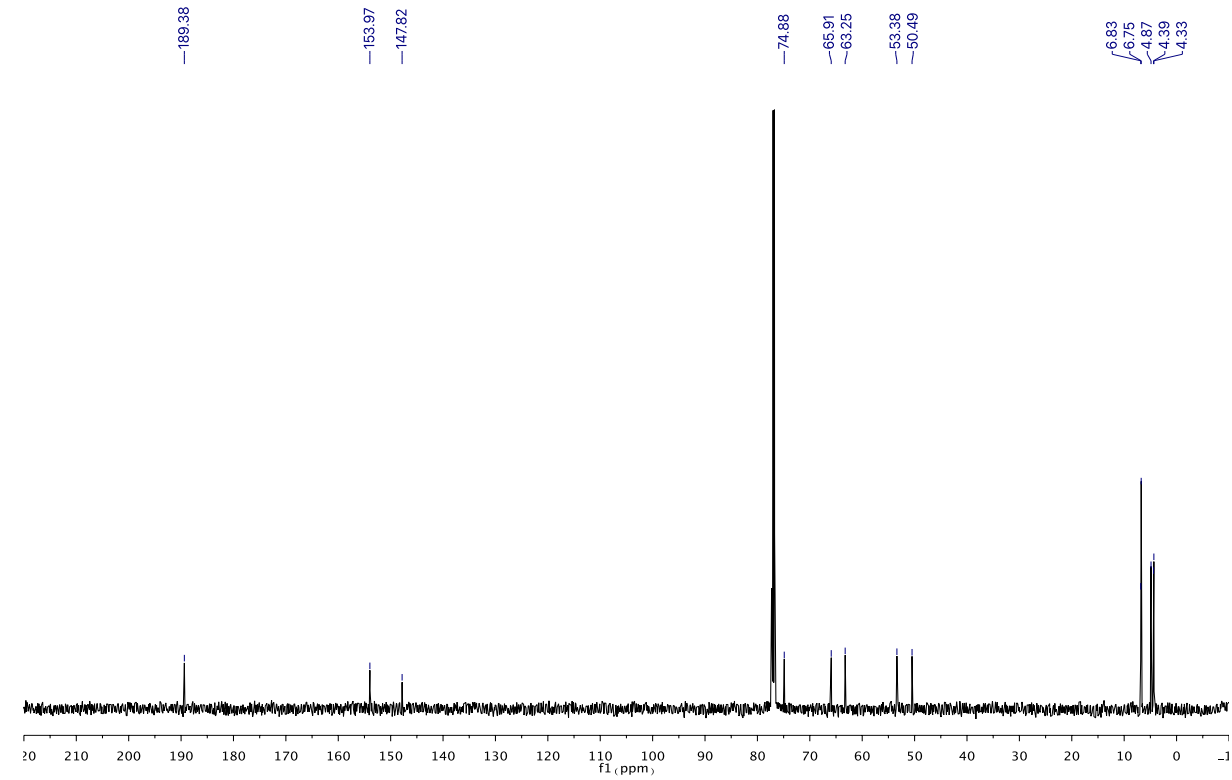
189.38
153.97
147.82
74.88
65.91
63.25
53.38
50.49
6.83
6.75
4.87
4.39
4.33
f1 (ppm)

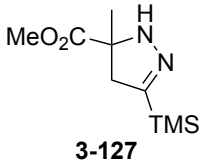
H
N
MeO2C
N
TMS

3-127

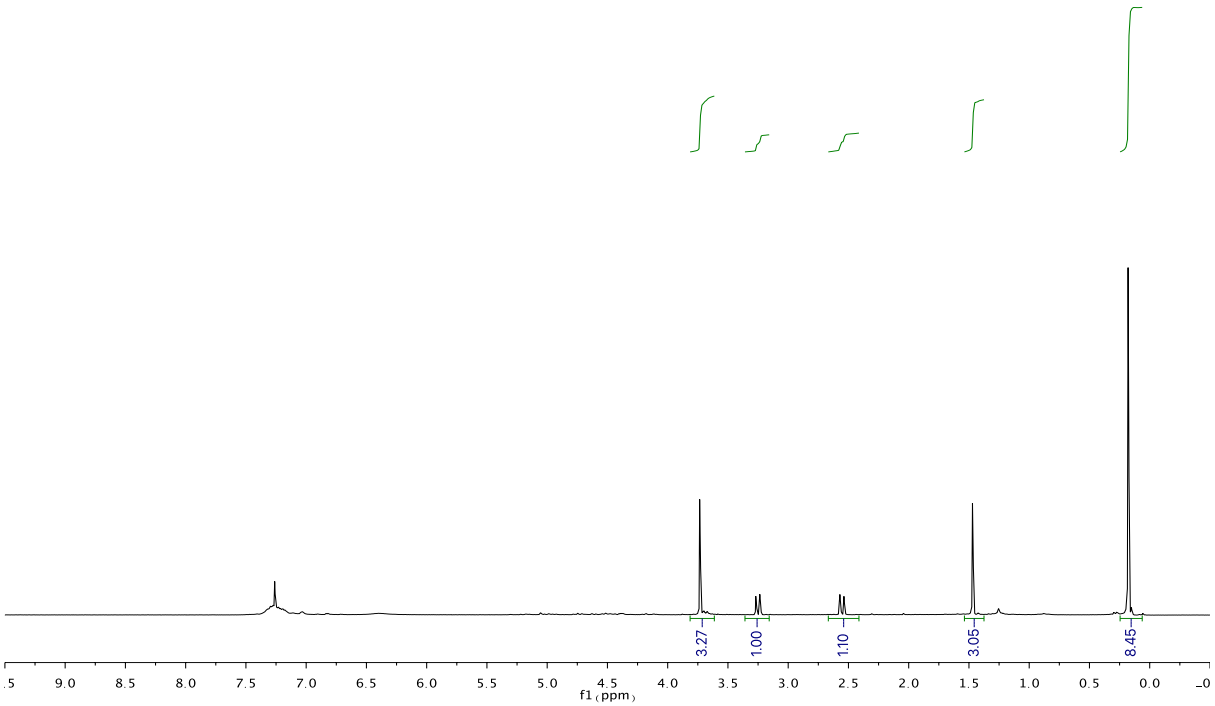
3.27
1.00
1.10
3.05
8.45
f1 (ppm)

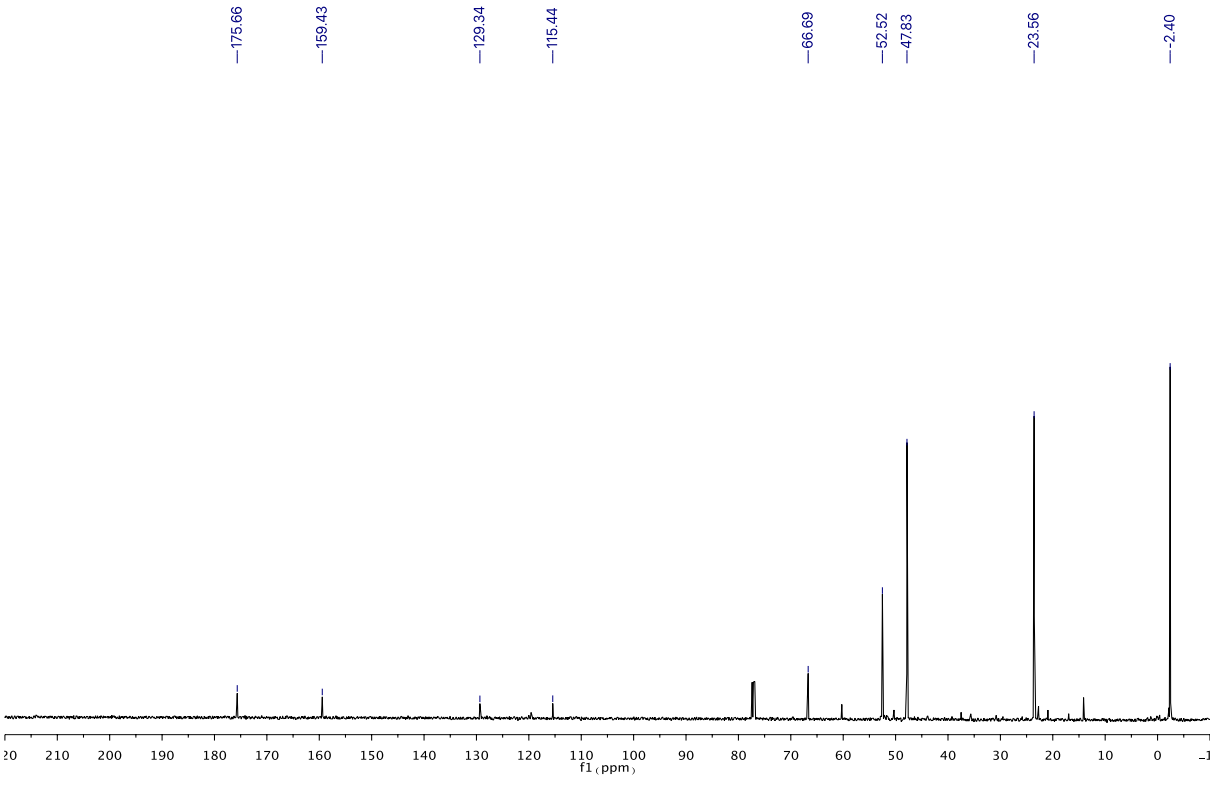
175.66
159.43
129.34
115.44
66.69
52.52
47.83
23.56
-2.40
f1 (ppm)

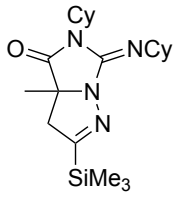
Cy
N
O
NCy
N
N
SiMe3

3-130

1.00
0.51
0.52
1.09
3.25
2.16
2.66
3.32
4.34
f1 (ppm)


176.18
167.33
146.51
65.73
56.68
52.21
48.39
34.80
34.54
28.57
28.26
26.06
25.96
25.87
25.26
25.10
24.66
24.60
-2.48

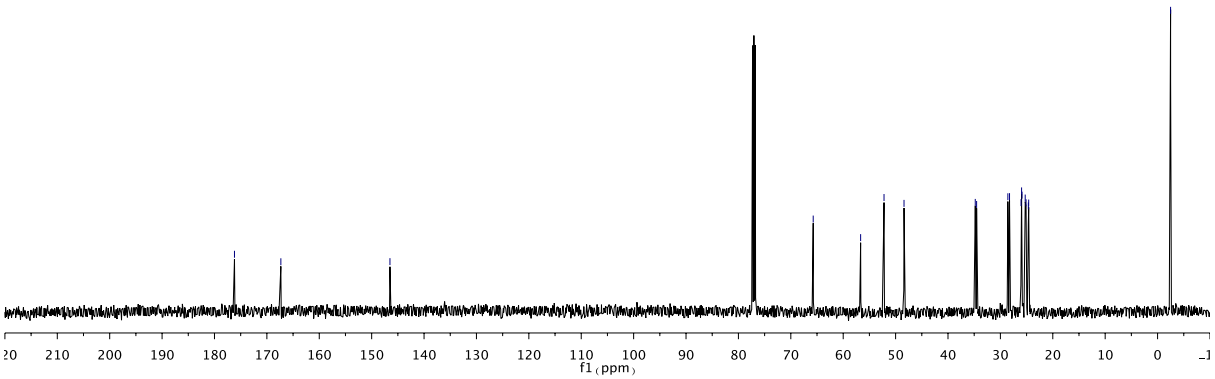
f1 (ppm)

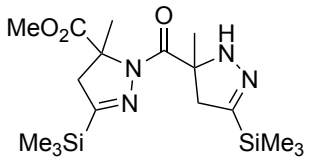
MeO2C
O
H
N
N
N
N
Me3Si
SiMe3

3-129

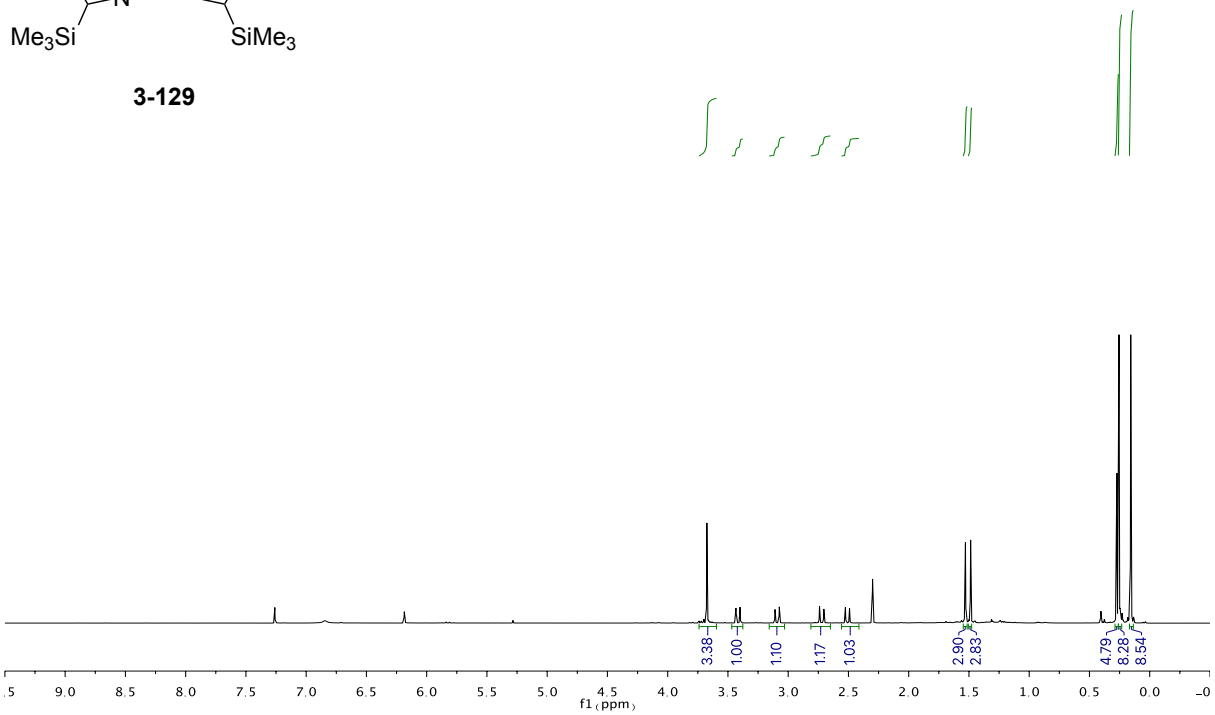
3.38
1.00
1.10
1.17
1.03
2.90
2.83
4.79
8.28
8.54
f1 (ppm)

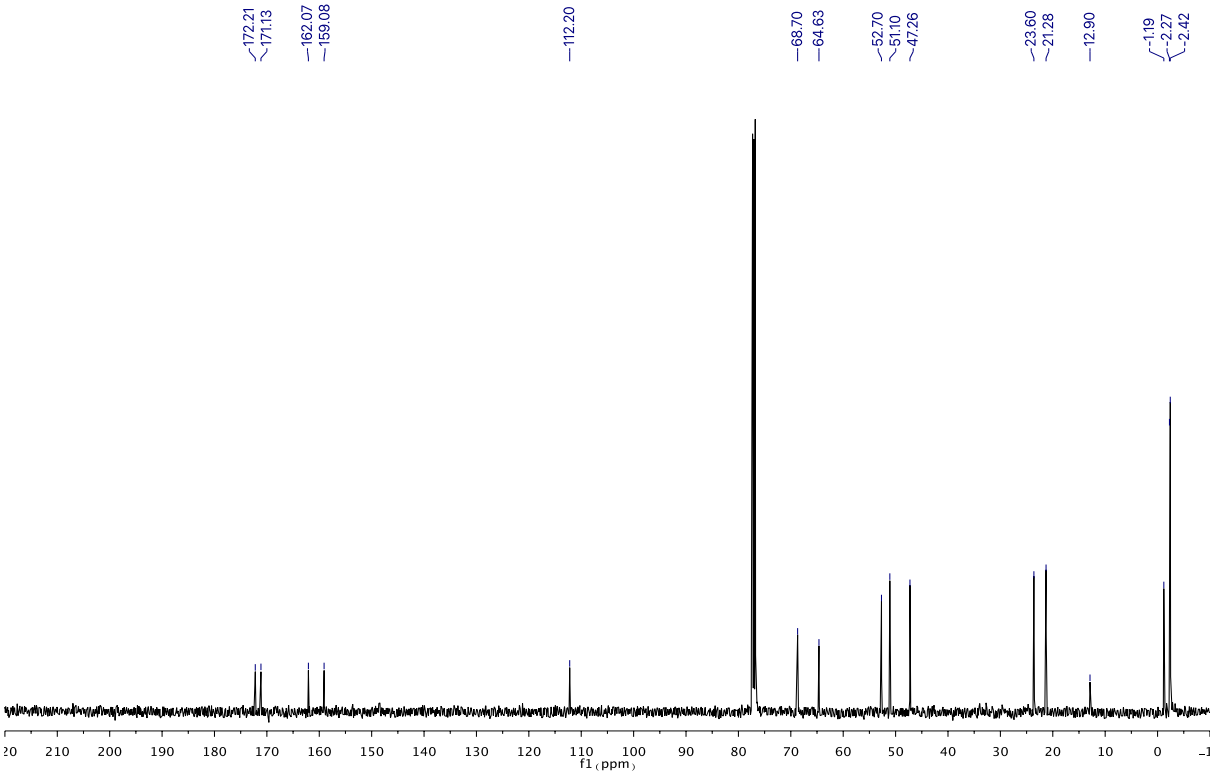
172.21
171.13
162.07
159.08
112.20
68.70
64.63
52.70
51.10
47.26
23.60
21.28
12.90
1.19
-2.27
-2.42
f1 (ppm)

BnN=C=NBn

3-128

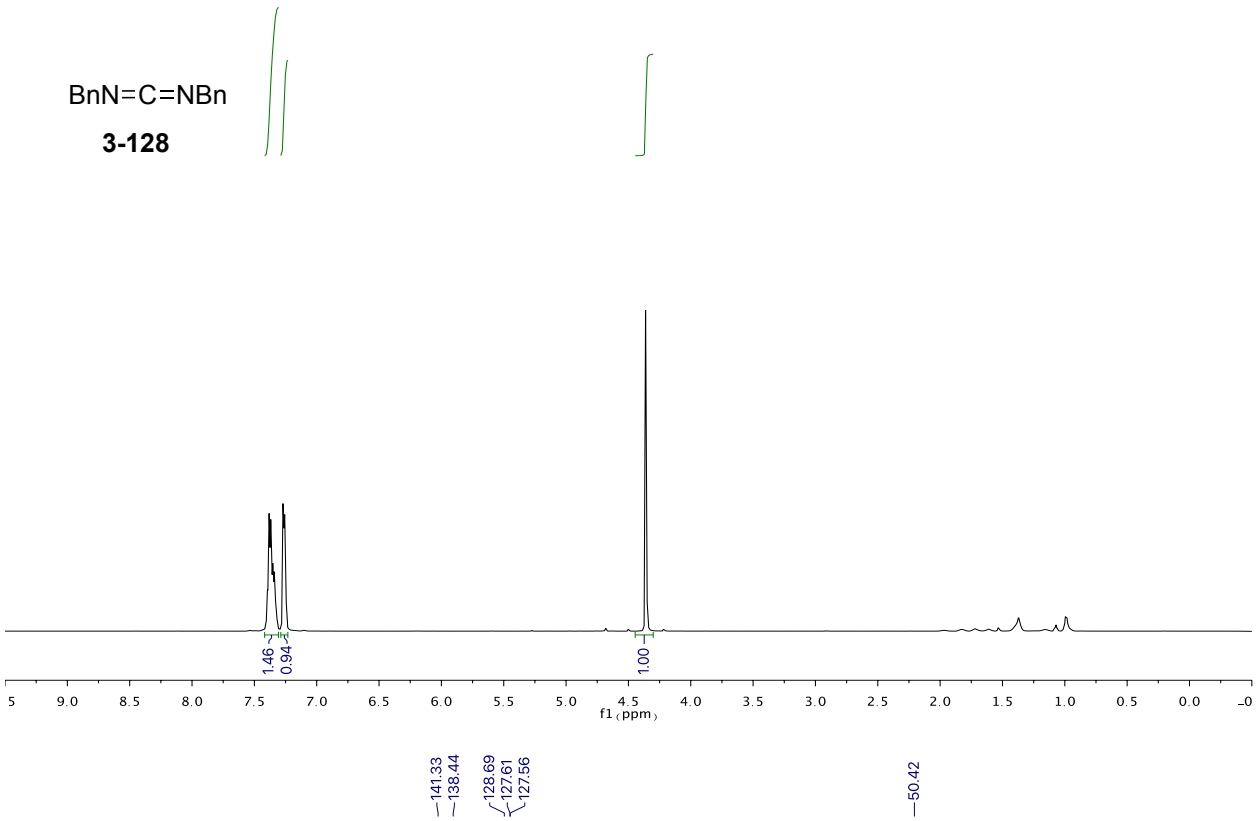

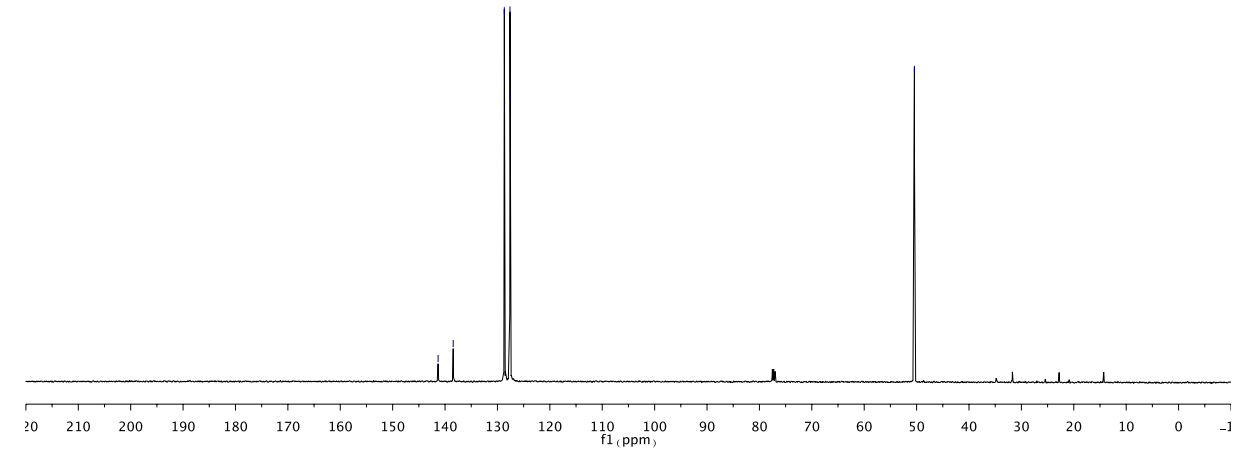

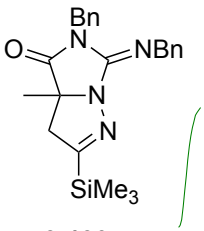
Bn
O
N
NBn
N
N
SiMe3

3-130

7.22
4.14
1.91
1.97
1.00
1.15
2.88
9.05
f1 (ppm)


196.18
159.36
147.90
137.68
135.53
129.21
129.10
128.40
128.01
127.47
126.25
125.99
71.40
51.68
47.64
46.85
25.15
2.22

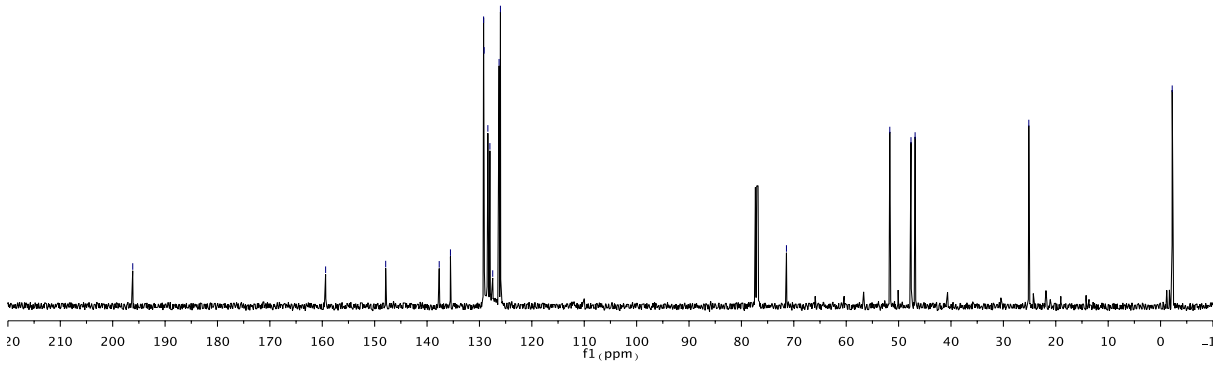
f1 (ppm)

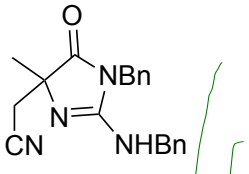
O
NBn
N
CN
NHBn

3-131

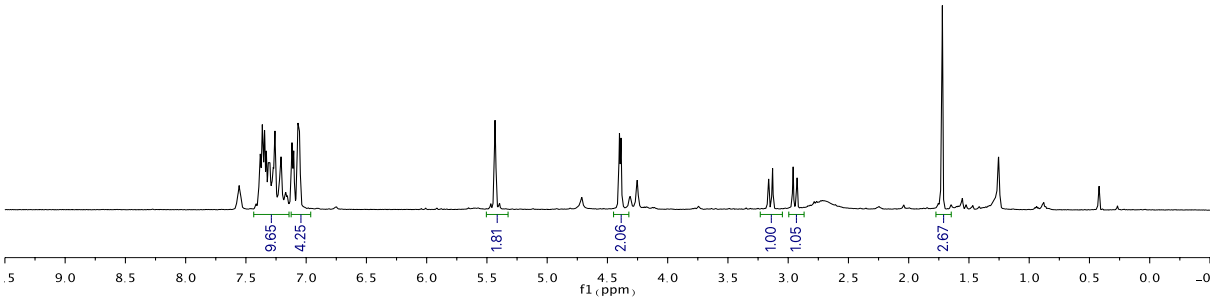
9.65
4.25
1.81
2.06
1.00
1.05
2.67
f1 (ppm)


195.11
148.27
137.47
135.40
129.29
129.19
128.78
128.60
128.49
128.12
127.76
127.35
127.05
126.27
125.94
117.79
60.30
51.79
49.70
47.62
44.84
29.71
29.32
26.17

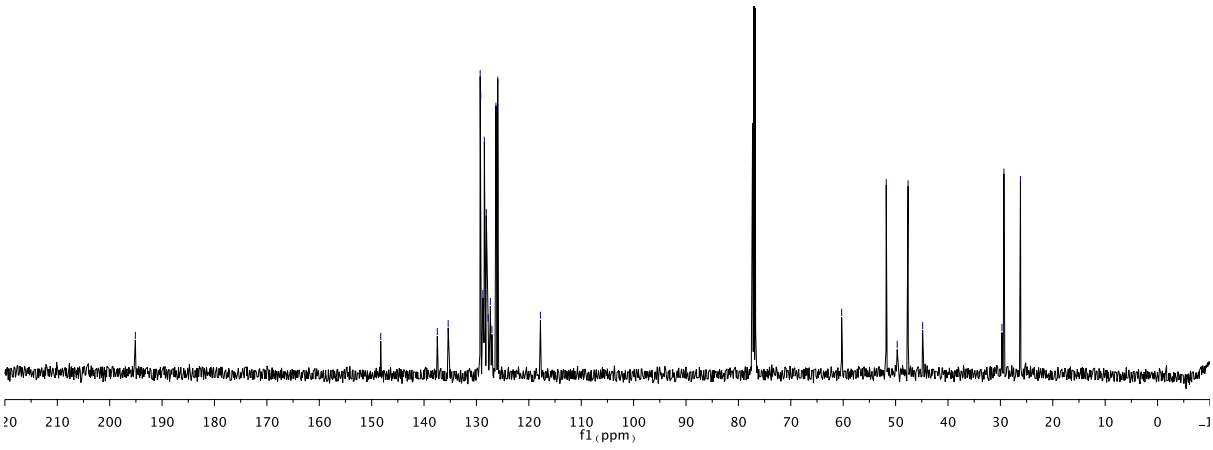
f1 (ppm)

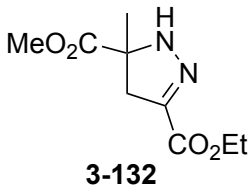
MeO2C
H
N
N
CO2Et

3-132

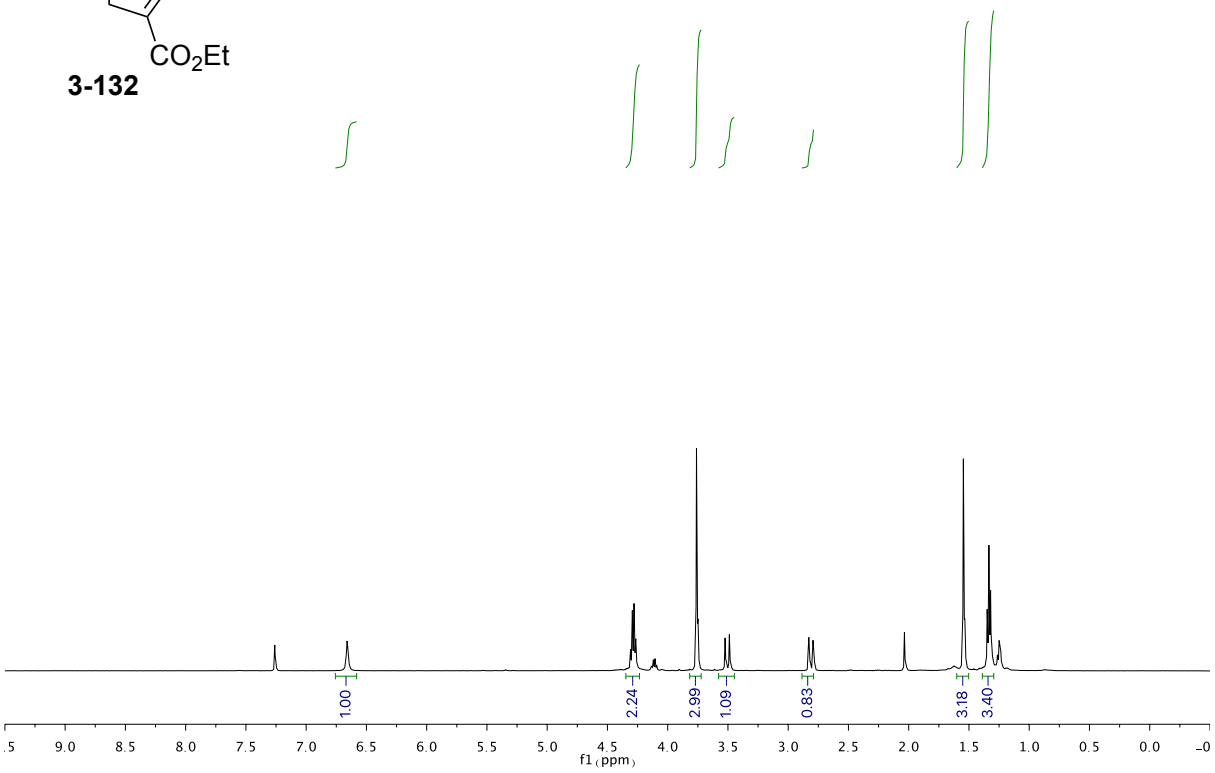
1.00
2.24
2.99
1.09
0.83
3.18
3.40
f1 (ppm)

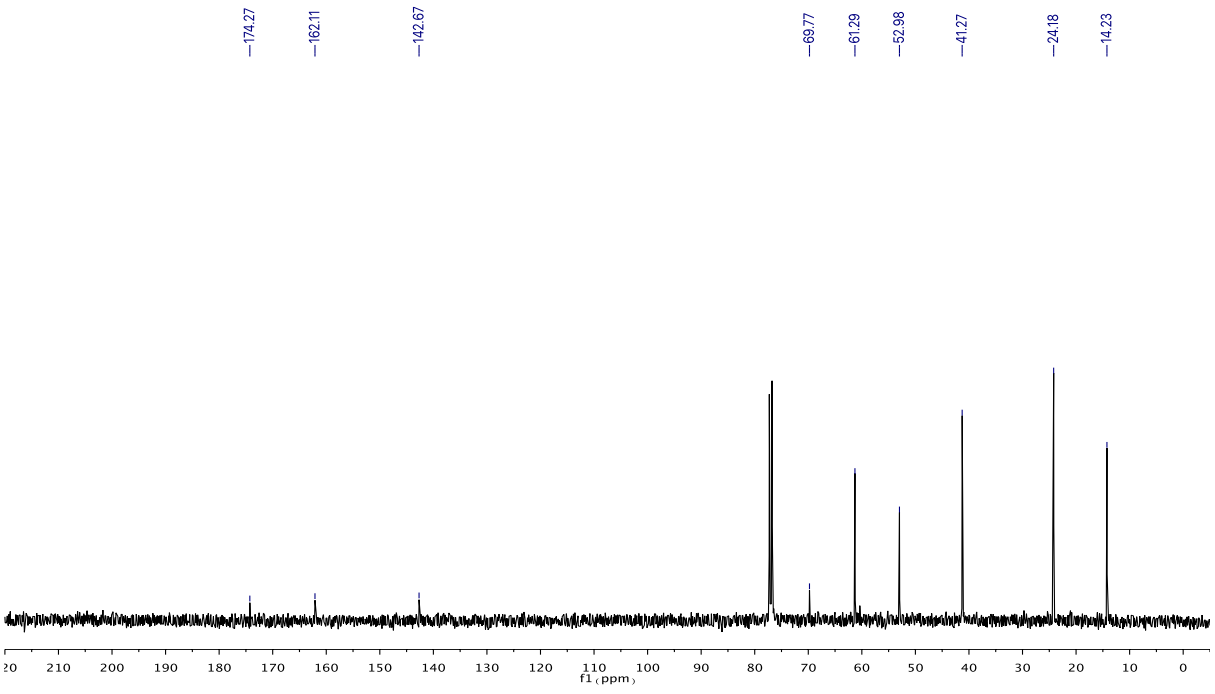
174.27
162.11
142.67
69.77
61.29
52.98
41.27
24.18
14.23
f1 (ppm)

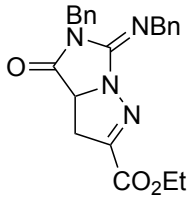
Bn
NBn
O
N
N
N
CO2Et

3-134

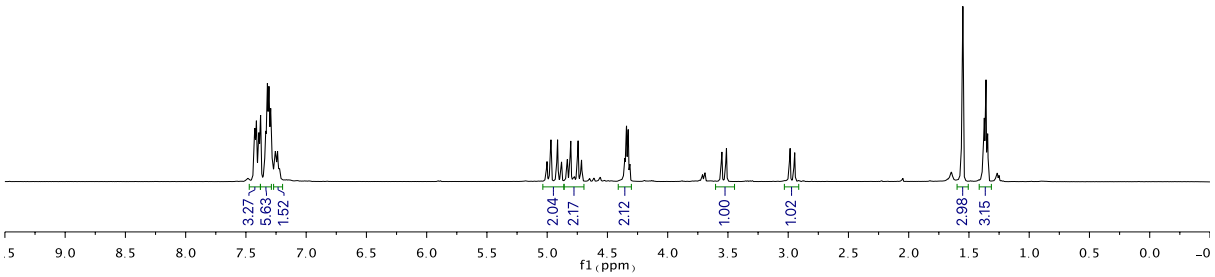
3.27
5.63
1.52
2.04
2.17
2.12
1.00
1.02
2.98
3.15
f1 (ppm)


174.45
160.84
151.70
146.79
140.86
136.06
129.09
128.79
128.54
128.15
127.80
127.44
126.39
69.24
62.29
52.09
43.53
42.39
26.16
25.30
14.12
9.55

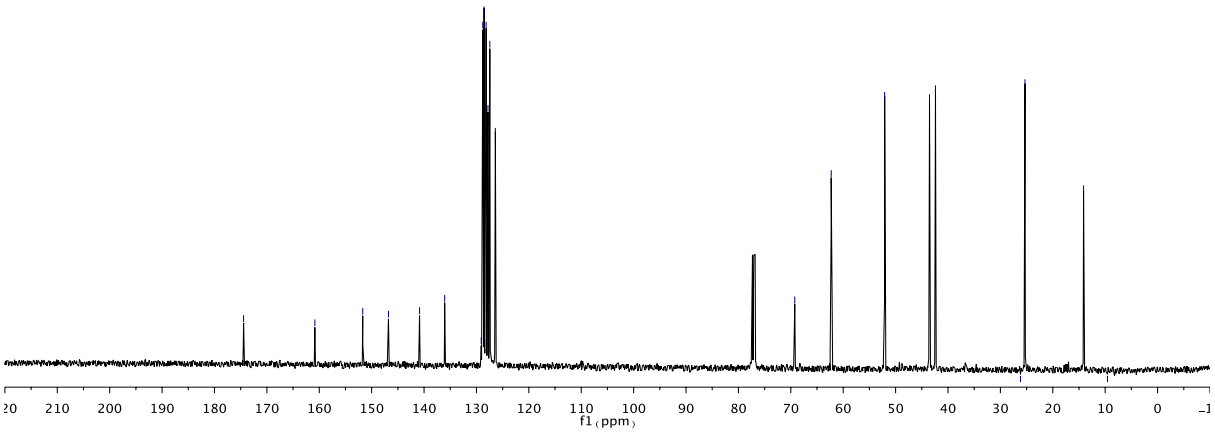
f1 (ppm)

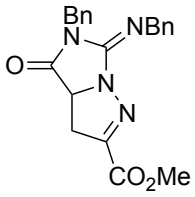
Bn
N
NBn
O
N
N
CO2Me

3-133

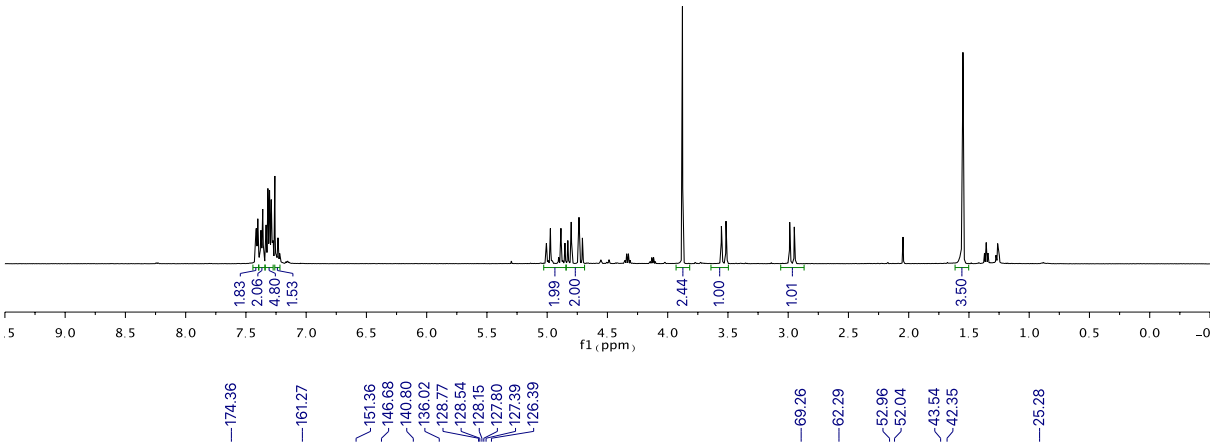
1.83
2.06
4.80
1.53
1.99
2.00
2.44
1.00
1.01
3.50
f1 (ppm)

174.36
161.27
151.36
146.68
140.80
136.02
128.77
128.54
128.15
127.80
127.39
126.39
69.26
62.29
52.96
52.04
43.54
42.35
25.28

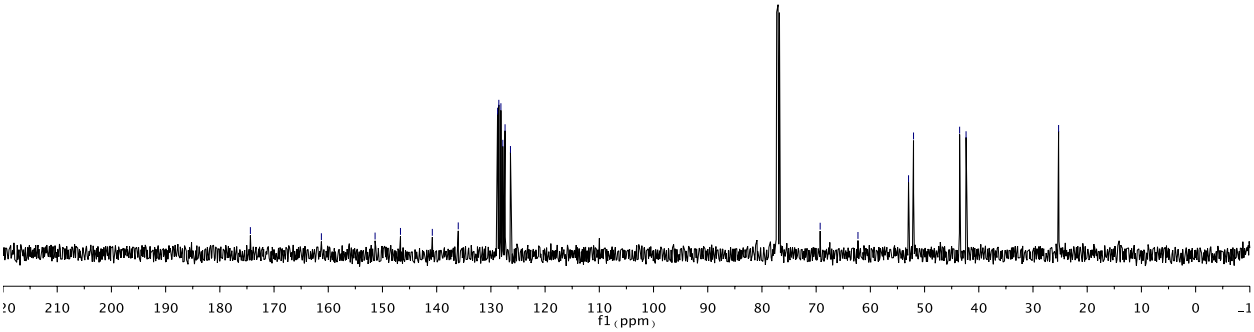
f1 (ppm)

APPENDIX II: Copyright Permissions

Chapter 1 original source:

Please note that, as the author of this Elsevier article, you retain the right to include it in a thesis or dissertation, provided it is not published commercially. Permission is not required, but please ensure that you reference the journal as the original source. For more information on this and on your other retained rights, please visit: https://www.elsevier.com/about/our-business/policies/copyright#Author-rights

Chapter 3 original source:

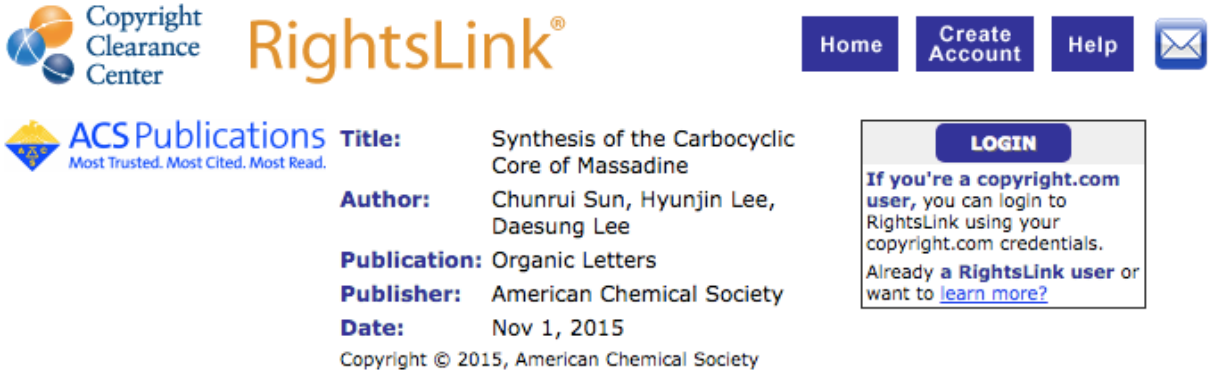

Copyright Clearance Center RightsLink®

Home | Create Account | Help

ACS Publications
Most Trusted. Most Cited. Most Read.

Title: Synthesis of the Carbocyclic Core of Massadine

Author: Chunrui Sun, Hyunjin Lee, Daesung Lee

Publication: Organic Letters

Publisher: American Chemical Society

Date: Nov 1, 2015

Copyright © 2015, American Chemical Society

LOGIN

If you're a copyright.com user, you can login to RightsLink using your copyright.com credentials.

Already **a RightsLink user** or want to learn more?

PERMISSION/LICENSE IS GRANTED FOR YOUR ORDER AT NO CHARGE

This type of permission/license, instead of the standard Terms & Conditions, is sent to you because no fee is being charged for your order. Please note the following:

- Permission is granted for your request in both print and electronic formats, and translations.
- If figures and/or tables were requested, they may be adapted or used in part.
- Please print this page for your records and send a copy of it to your publisher/graduate school.
- Appropriate credit for the requested material should be given as follows: "Reprinted (adapted) with permission from (COMPLETE REFERENCE CITATION). Copyright (YEAR) American Chemical Society." Insert appropriate information in place of the capitalized words.
- One-time permission is granted only for the use specified in your request. No additional uses are granted (such as derivative works or other editions). For any other uses, please submit a new request.

HYUNJIN LEE

845 W. Taylor St., Chicago, IL (708) 921-3692 | hlee121@uic.edu

EDUCATION

2013 – 2018 **Ph.D. Candidate in Organic Chemistry**, University of Illinois at Chicago
Advisor: Professor Daesung Lee

2012 **B.Sc. Chemistry**, Department of Chemical Science, University of Illinois at Urbana-Champaign

RESEARCH EXPERIENCE

2012 – present *Graduate Research Assistant***,** Organic Chemistry, Department of Chemistry, University of Illinois at Chicago, Advisor: Professor Daesung Lee

- Completed synthesis of core carbocyclic of Massadine
- Investigated of new reactivity of silyl- and alkyl substituted allens with various oxidants
- Developed an efficient thermal bicyclization reaction of ynamide-tethered 1,3,8-triynes to form structurally novel tetrahydropy-ranopyridines
- Synthesized of bioluminescent probes for bile acid transporters
- Accomplished synthesis of clickable photoreactive bile acid probes and alkyne cholesterolMaintained chemical inventory and laboratory equipment.

2012 – 2013 *Assistant Crystallographer,* G. L Clark X-ray Facility and 3M Material Laboratory

- Prepared chemical samples and maintain laboratory instruments
- Performed powder diffraction experiments by utilizing Bruker GADDS and analyze data with TOPAS and JADE
- Examined single crystal x-ray diffraction by operating Bruker Apex II (Cu and Mo) and process data with SHELXTL

2013 *Intern***,** Department of Brain and Cognition Science, Ehwa Women's University

- Isolated genomic DNA from mouse tails and ran a polymerase chain reaction (PCR)
- Extracted mice brains for immunoelectron microscopy and collected blood samples
- Injected target genes to mice's amygdala and nucleus accumbens regions and observed mice for depression behaviors
- Performed high performance liquid chromatography (HPLC) and analyzed HPLC data
- Investigated Literatures on effects of hypothalamic-pituitary-adrenal axis (HPA) on depression
- Carried out behavior tests: marble burying test, tail suspension test (TST), forced swim test (FST), light/dark box test

TEACHING EXPERIENCE

2012 – 2018 *Teaching Assistant,* Department of Chemistry, University of Illinois at Chicago

- General Chemistry, Organic Chemistry I, Organic Chemistry II, and Organic Chemistry Laboratory

HONORS AND AWARDS

April 2017 Chancellor's Student Service and Leadership Awards

AFFILIATIONS

2015 – Present **UIC Graduate Women in Chemistry**
Co-Founder & President

2015 – 2016 **UIC Chemistry Graduate Student Association**
Organic Chemistry Representative

PUBLICATIONS

- Ticho, A.; **Lee, H**.; L.; Gill, R. K.; Dudeja, P. K.; Saksena, S. Lee, D.; Alrefai, W. A. "A novel bioluminescence-based method to investigate cellular uptake of bile acids in living cell" *Am. J. Physiol. Gastrointest. Liver Physiol*. **2018**, doi: 10.1152/ajpgi.00133.2018. (Equally contributed first author)
- Sabbasani V., **Lee, H**.; Xie, D.; Lee, D**.** "Cyclization of Ynamide-Tethered 1,3,8-Triynes" *Chem. Eur. J*. **2017**, *23*, 8161. (Equally contributed first author)
- Sabbasani, V.; **Lee, H**.; Xia, Y.; Lee, D. "Complementary Iron-Catalyzed Oxidative Transformations of Allenes with Different Oxidants" *Angew. Chem., Int. Ed*. **2016**, *55*, 1151.
- Sun, S.; **Lee, H**.; Lee, D "Synthesis of the Carbocyclic Core of Massadine" *Org. Lett*. **2015**, *17*, 5348.

PRESENTATIONS

- **Lee, H.**; Chunrui, S.; Lee, D. "Synthesis of the Carbocyclic Core of Massadine", 8th Annual Chicago Organic Symposium, Univerisity of Illinois at Chicago, Chicago, IL, USA, September 30, 2017.
- **Lee, H.**; Sabbasani, V.; Lee, D. "Metal-Free Cyclization of Ynamide-based 1,3,8-Triynes", 7th Annual Chicago Organic Symposium, Loyola University, Chicago, IL, USA, October 1, 2016.